Sedimentology and basin context of the Numidian Flysch Formation; Sicily and Tunisia

A thesis submitted to The University of Manchester for the degree of Doctor of Philosophy in the Faculty of Engineering and Physical Sciences

2011

Myron Francis Hubert Thomas
School of Earth, Atmospheric and Environmental Sciences

Contents list.

Appendices

Total word count: 75,176
Paragraph text only: 51,129

List of figures.

List of tables.

Sedimentology and basin context of the Numidian Flysch Formation; Sicily and Tunisia

Myron Francis Hubert Thomas

The University of Manchester. Submitted for the degree of Doctor of Philosophy, July 2011.

The Numidian Flysch Formation is a regionally extensive series of deep marine sandstones and mudstones which crop out in Spain, Morocco, Algeria, Tunisia, Sicily, and southern mainland Italy. The formation is dated as Oligocene to mid Miocene and represents an approximately linear series of submarine fans characterised by a quartz rich petrofacies. Their unique regional extent is nearly twice the length of the Angolan margin although issues surrounding provenance and basin context have hampered understanding. The Numidian Flysch Formation was deposited into the Maghrebian Flysch Basin (MFB) which was a foreland basin remnant of the neo-Tethys ocean in the western portion of the present day Mediterranean Basin. The basin was bordered to the north by an active margin which consisted of a southward verging accretionary prism, underlain by European crustal blocks which rode above northwards subducting oceanic crust. To the south, the African margin formed a passive-margin to the basin.

The huge amount of geophysical and outcrop data which is becoming increasingly available suggests that submarine slope systems are more complex than previously thought, including topographically complex slopes, a wide variety of density flow types, and flow transformations. This thesis aims to review the sedimentology of the Numidian Flysch Formation in Sicily and Tunisia in light of these developments. Constraining the provenance and basin context of the formation is therefore of paramount importance, and this is also addressed.

Commonly used evidence for the provenance of Numidian Flysch sandstones include its quartz rich petrology, an Eburnian and Pan-African age detrital zircon suite, its structural position within the foreland fold and thrust belt, and complex palaeocurrent orientations. when reviewd in their entirety and placed in context of other basin successions, the Numidian Flysch is constrained to a depositional location in the south of the basin, with polycyclic sediment sourced from African basement. The Numidian Flysch Formation is therefore a ‘passive margin’ sequence as opposed to a flysch sensu stricto. The timing of Numidian Flysch deposition is also coincidental with uplift of the Atlas chain in North Africa, during a period of significantly wetter conditions. A switch from carbonate to clastic deposition results from these conditions, and the Numidian Flysch Formation is considered an offshore extension of this regional sedimentation.

Characterisation of outcrops in Sicily and Tunisia shows remarkably similar lithofacies and depositional elements. Sinuous upper slope channel complexes are entrenched within slope deposits to a depth of 100 m and occur within channel systems up to 5.7 km in width. They are filled predominantly with massive ungraded sandstones interpreted to aggrade through quasi-steady turbidity currents, interbedded with normally graded turbidites. Channel elements are subseismic in scale, are nested within complexes and show sinuosity. Coupled with lateral offset stacking, this strongly affects the architecture and facies heterogeneity of channel complexes. When compared to globally reviewed data, the thickness of channel elements as shown through their frequency distribution also suggests a fundamental control upon the degree of slope incision which is as yet unconstrained.

In lower slope settings, channel complexes stack aggradationally with a width of over 1000 m. They are also predominantly filled with massive sandstones in fining upwards cycles, and show heterogeneous margins and large scale slumping.

In central Sicily, large channel complexes are overlain by a stacked lobe complex, in turn overlain by a channel lobe transition zone. This progression coupled with palaeocurrent variability suggests intraslope deformation strongly impacts transiting flows through changes in flow capacity. Salt tectonics, present in Algeria and Tunisia is a possible forcing mechanism.

Taken in context, the sections in Sicily record a proximal to distal palaeogeographic trend which is reconstructed towards the north/northeast once well constrained tectonic rotations are taken into account. Given regional similarities, controls upon slope architecture are interpreted to be similar throughout the basin, and deposits in Sicily therefore provide a good analogue for the remainder of the basin. These results therefore allow for a better constrained fan architecture, along with the allogenic controls upon them. Given the continental extent of this formation, the Numidian Flysch Formation provides a unique opportunity to study controls upon fan architecture once provenance and intraslope topography is factored in.

Declaration

No portion of the work referred to in this thesis has been submitted in support of an application for another degree or qualification of this or any other university or other institute of learning.

Copyright statement

Acknowledgements

I would like to thank my supervisors Jonathan Redfern and Duncan Irving for starting this project and allowing me the scope to explore new ideas as it progressed. I have indeed been lucky to work in such a beautiful area as northern Sicily, and Dorik Stow is gratefully thanked for introducing me to the area during a reconnaissance trip in October 2006, along with the competitive world of the Numidian Flysch Formation. During the 9 weeks of fieldwork in Sicily many assistants have helped me and they are all thanked for their patience and support.

The ‘deep marine’ research community is a rapidly evolving area and I have also been lucky to have graced its fringes. Bill McCaffrey of the Turbidites Research Group at the University of Leeds has been kind in giving advice on various matters. Lorna Strachan at Auckland University has also been a great friend and support.

This PhD has been part time while also working as research assistant to the North Africa Research Group. I have also therefore had the opportunity to do fieldwork in Morocco and Libya and meet many wonderful people. Within the Basins group these have included Ruth, Nadine and Stefan from the first tranche of PhD students. Frank who started the same day as myself and has also been part time. Also Ivan, Vicky, Xavier, Laurent, Jonathan, Alanna, Ollie, Christophe, Rajasthmita and Debs who are of the second and third tranches. Lastly, the postdocs Stephane, Dorthe, Cat, Alvaro, Guy, Dina and Sebastian. They are all thanked for their friendship, rounds of beer and much stimulating discussion regarding North African geology, sedimentology, politics and religion, cultural differences and much much more. There are also many others from the department who have been good friends and colleagues over the years.

Many NARG sponsor company representatives have come and gone during the time of this project. In particular, I must thank Sebastian Luening (RWE) for his passion regarding North African Geology, and Stuart Marsh (Anadarko) for his interest in the Numidian Flysch Formation and his sense of humour which kept steering meetings lively.

North Africa (including Sicily!) is a wonderful place and I have met many extraordinary people. From Libya these include the Tuaregs Mohammed, Mohammed, Saleh, Mubarak and Abu Baka. Their understanding of the desert was truly remarkable and their friendship to Jonathan and myself was much appreciated. In Morocco, the staff of chez Jou jou were also great hosts. As this thesis is written, the Arab spring has been spreading through the region and into Arabia. Despots in Tunisia and Egypt have been deposed and those of Syria, Bahrain, Yemen and Saudia Arabia (among others) are killing their people as they revolt. Libya remains locked in a civil war, with no news of the above people. I therefore wish them well and hope that North Africa may soon become democratic and peaceful.

Finally of course my parents have remained as supportive as ever and encouraged me to enjoy the experience of the last few years. Hayley also has been there to remind me of the world outside of my head. Their support has been invaluable and immeasurable.

Chapter 1.

Introduction.

Chapter 1. Introduction

1.1 Aim of the thesis

The work presented in this thesis covers the sedimentology and basin context of the Numidian Flysch Formation of Sicily and Tunisia. The overall aim of the work has been to re-evaluate the sedimentology of the formation in light of current 'deep marine thinking', which recognises the complications associated with fan systems including intraslope topography and flow transformation. This has also required a better understanding of the basin context and in particular the provenance of Numidian Flysch Formation sandstones which has been an area of major controversy. A better understanding of the provenance and basin context is therefore an initial aim in itself, but also a prerequisite for the main aim. A background and context, covering both deep marine studies and previous work on the Numidian Flysch Formation, is presented below along with the rationale for pursuing these aims.

1.2 Background motivation for deep marine studies

Deep marine environments are intensely documented within modern literature with the use of outcrop studies, flume tank experiments, bathymetry and core data from modern systems, and seismic imaging. The boom in deep marine research began in the 1970's when hydrocarbon exploration began in earnest in deep water settings. An estimated 33% of the world's hydrocarbon deposits are contained in deep marine environments (*http://www.mcclatchydc.com/2007/12/01/22225/massive-deep-water-oil-find-in.html*) with major hydrocarbon discoveries including offshore West Africa, the Gulf of Mexico, and the North Sea. Interest has also come from the geohazard community, particularly due to the routine breaking of undersea communications cables during turbidity current events (e.g The Grand banks event, (Piper et al., 1999)). Flows also have the capacity to damage pipelines and other oil infrastructure and change the bathymetry of the seafloor over short timescales.

The increase in academic studies has primarily been due to industry funding and the advent of high quality 3D seismic, coupled with wells and cores, which has led to a huge amount of data with which to characterise submarine environments. New key outcrops have been heavily researched including the Permian Karoo basin succession (e.g the STRAT group, Liverpool University; Hodgson, 2009; Prélat et al., 2009), the Claire Formation of Ireland (Macdonald et al., 2011; Pyles, 2008), the Book Cliffs Formation of Utah, U.S (Pattison, 2005), and more recently the Cerro Torro Formation in Chile (Shultz et al., 2005). Bathymetry data and seismic data have similarly generated new insights into deepwater areas such as offshore western Africa and the Gulf of Mexico (Ercilla et al., 1998). Modelling of turbidites in flume tanks has also led to a new quantified understanding of the physics of such flows and the deposits they produce (e.g Pantin and Franklin, 2011).

With the exception of extensive outcropping systems, seismic and bathymetry studies provide the only opportunity to place observed depositional elements within the context of a larger fan or slope system (e.g Catterall et al., 2010; Saller et al., 2008). Modern seismic data is capable of resolving features greater than around 8 m thick, while facies are inferred from broadly spaced well control points. Outcrop studies however typically resolve details from the microscale to that of a few kilometres in extent, focussing upon facies and depositional element description. Slope context, and therefore the controls upon the system are often difficult to assess, except where exceptional outcrop exists (e.g the examples described above). The results of outcrop, seismic, and bathymetric studies are increasingly being compared to experimental results gained from flume tank modelling,

Figure 1.1.
Taken from Mutti et al. (2011). Calcarious flysch sequence from the Upper Cretaceous Monte Cassio Flysch Formation, northern Apennines of Italy.

in particular those facilities operated by industrial consortia such the Turbidites research Group at Leeds University. Flume tank studies currently provide the only opportunity to observe the physics of turbidity currents in action. Indeed, very few studies have succeeded in monitoring turbidity current events within their submarine environments due to their highly destructive nature (Vangriesheim et al., 2009). Outcrop studies of ancient turbidite systems therefore bridge an important gap in scale, generating high resolution models of turbidite systems, performing quality control for features observed in seismic data, and testing the predictions of experimental flume tank modelling.

1.2.1 The advancement of deep marine studies

The origin of deep marine studies lies in the 1940's and 50's with the mapping of alternating bands of sandstone and mudstone in the Alps, rocks that were termed 'flysch', and the 'flyschermen' who studied them (Ricci-Lucchi, 2003) (Figure 1.1). Migliorini (1943) was the first study to link turbulent processes with deep marine rocks in the Macigno Formation of the Italian Apennines. This was then widely applied, and a broad case study of deep marine environments was constructed (Mutti et al., 2009; Ricci-Lucchi, 2003). The Bouma classification scheme (Bouma, 1962) revolutionised the prediction of turbidity current deposits, with a facies scheme which essentially recognised a proximal to distal trend with decreasing flow velocity. A number of models then presented facies, facies stacking patterns and architectural elements within a downslope trend on a topographically simple slope (e.g Mutti, 1985; Mutti and Ricci Lucchi, 1978; Walker, 1978). It was during this phase that a majority of sedimentological studies were performed on the Numidian Flysch Formation, upon which this thesis focuses. Fascinating and complete reviews of this history are provided by Mutti et al. (2009) and Ricci-Lucchi (2003).

The advent and common use of geophysical data however allowed workers such as Bill Normark and David Piper to interpret large scale features of submarine fans, such as the Navy Fan offshore California, and place depositional elements within their context (Normark, 1970; Normark and Piper, 1972; Normark et al., 1979). The complexity of such systems was explored with recognition

of new depositional elements including mega-flutes, levees, and distributory channels. In more recent years, studies of modern systems using sidescan sonar, and recent or ancient systems using 3D seismic data, have enabled depositional elements in submarine fans to be mapped in very high resolution (e.g Deptuck et al., 2007; See figure 1.2) and new depositional elements, such as outer bank bars within sinuous submarine channels (Nakajima et al., 2009), are still being recognised. These datasets also allow submarine fans, and the structural or topographic controls upon them to be assessed (e.g Gee and Gawthorpe, 2006). Such studies have shown the complexity inherent resulting from mobile substrate, slope deformation and autocyclic effects. The interpretation of a topographically complex slope system in the Gulf of Mexico with an interpreted ponded-to-bypass evolution is one such example (e.g Prather et al., 1998). Work on modern systems such as the Agadir fan have also highlighted the importance of features such as Channel Lobe Transition Zones (CLTZ) which separate channel mouths from basin floor lobe deposits across a significant break of slope (See Wynn et al. (2002) and references therein). In outcrop studies, advancements have included the addition of many facies types. These include massive sandstones (Stow and Johansson, 2000), debris flows (Enos, 1977), and hybrid flow events which are neither fully turbulent nor fully laminar (Haughton et al., 2009). These concepts question the validity of topographically simple slope models and their associated facies predictions. The recognition of downslope flow transformations, including linked debrites (Haughton et al., 2009; Lowe and Guy, 2000) and the generation of debrite flows across Channel Lobe Transition Zones (Ito, 2008), mean that studying downslope variations in architecture and facies are of renewed importance. It is against the background of this huge volume of new concepts in deep marine sedimentology, that the Numidian Flysch Formation is evaluated for this thesis.

Figure 1.2.
Sea floor bathymetry data of the Niger delta submarine fan system, Nigeria. Taken from Deptuck et al. (2007). Two canyons with sinuous planforms are shown, the Benin major (bottom example) and Benin minor (upper example). Flow is to the left.

1.3 The Numidian Flysch Formation

The Numidian Flysch Formation is a regionally extensive series of deep marine sandstones and mudstones which crop out in Spain, Morocco, Algeria, Tunisia, Sicily, and southern mainland Italy (Figure 1.3). The formation is dated as Oligocene to mid Miocene and represents an approximately linear series of submarine fans characterised by a quartz rich petrofacies (Wezel, 1969; Wezel, 1970). Their unique regional extent is nearly twice the length of the Angolan margin for example, which is an area of prolific submarine channel systems, many of which are rich in hydrocarbons

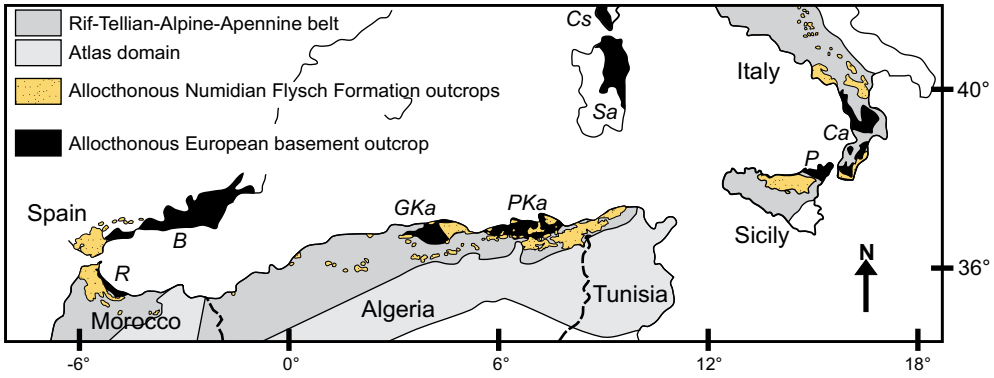

Figure 1.3.
Map of the western Mediterranean highlighting the extent of Numidian Flysch Formation oucrop. The Alpine aged fold and thrust belt and the Atlas fold and thrust belt are shown along with outcrop of European basement (B=Betic, R=Rif, GKa=Grand Kabylie, PKa=Petit Kabylie, P=Peloritani, Ca=Calabrian) which were thrust onto the African foreland.

(Fraser et al., 2005; Gee et al., 2007).

The Numidian Flysch Formation was deposited into the Maghrebian Flysch Basin (MFB) which was a foreland basin remnant of the neo-Tethys ocean in the western portion of the present day Mediterranean Basin (Figures 1.3 and 1.4) (Thomas et al., 2010b). The basin was bordered to the north by an active margin which consisted of a southward verging accretionary prism, underlain by European crustal blocks which rode above northwards subducting oceanic crust (Golonka, 2004; Guerrera et al., 1993) (Figure 1.4.). To the south, the African margin formed a passive-margin to the basin.

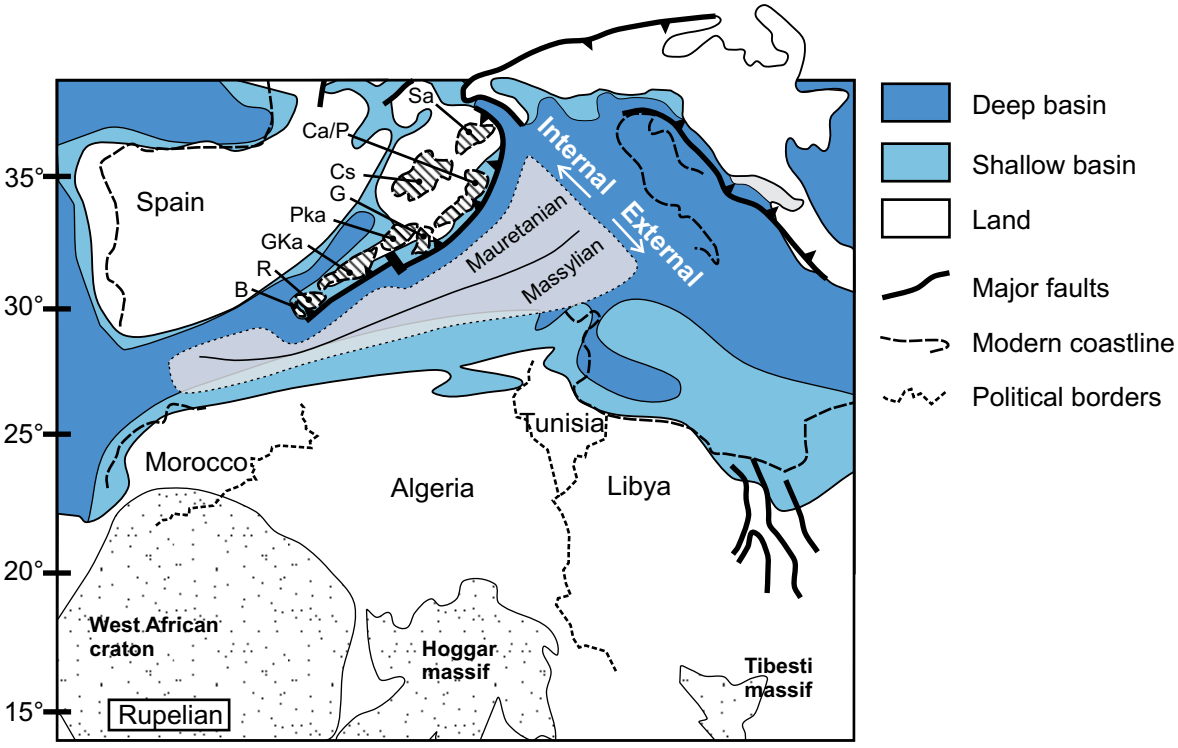

Figure 1.4.
Oligocene (Rupelian) palaeogeographic map of the western Mediterranean highlighting the location of the Maghrebian Flysch Basin (MFB) and commonly used basin nomenclature. Map redrawn from Meulenkamp and Sissingh (2003) (Peri-Tethys project). Suggested African and European source areas for Numidian Flysch Formation sandstones are highlighted, including African cratonic basement and blocks of the European AlKaPeCa domain. AlKaPeCa block abbreviations are: B=Betic; R,=Riff; Cs=Corsica; Sa=Sardinia; Ca/P= Calabria and Peloritan; G=Galite block; Pka=Petit Kabylie; Gka=Grand Kabylie.

African margin foreland sequences consist of thick Mesozoic to Cenozoic age platform carbonates and shallow marine clastic deposits (Thomas et al., 2010b, their figure 4). Units derived from the northern margin and thrust on to the African margin, consist of European derived crustal blocks (i.e the Kabylie, Galite, Peloritani and Calabrian blocks) transgressed by continental conglomerates, shallow marine limestones and very coarse grained turbidite sequences including canyon confined deposits (Bonardi et al., 1980; Gery, 1983; Mazzoleni, 1991; Patterson et al., 1995).

As the foreland basin closed in the mid to late Miocene (de Capoa et al., 2004; Thomas et al., 2010b), units from within the basin were thrust southwards onto the African foreland through a combination of thick and thin skinned deformation (Avellone et al., 2010; Roure et al., 1990). These units include thick mudstone sequences and prolific deep marine clastic deposits which transgress them. Two distinct clastic petrofacies are recognised, comprising an immature heterolithic series (Mauretanian deposits) and a quartzarenite Numidian series (Massylian deposits) (de Capoa et al., 2002; Guerrera et al., 1993; Thomas et al., 2010b).

In Tunisia, the Numidian was initially described as a shallow marine fluvial succession (Gottis, 1953) and grouped with the Fortuna delta Formation. The first substantial study which described it as a deep marine succession was performed by F.C Wezel in 1969 (Wezel, 1969) in which the formation was mapped in northern Sicily. A continental rise environment was interpreted and formalised in a publication to Nature (Wezel, 1970). More recent studies in Sicily, Tunisia, Algeria and southern mainland Italy have interpreted depositional lobes, large sandstone channels and a variety of density flow deposits (Carbone et al., 1987; Johansson et al., 1998; Vila et al., 1995).

1.3.1 Hydrocarbon occurrences

The Numidian Flysch Formation has been explored for hydrocarbons primarily in Tunisia and Sicily. A single field, the Gagliano field, produces gas and gas condensate in central Sicily (>700 Bcf gas, 20 million bbl condensate) at depths of 2,800 to 3000 m (Vercellino and Rigo, 1970). Bitumen seeps have also been observed in northern Tunisia associated with large sandstone bodies and direct hydrocarbon indicators have also been observed in 2D seismic data from offshore northern Tunisia (Wolden and Jones, 2005). The Numidian Flysch Formation therefore contains an active petroleum system. There are several difficulties in exploiting this knowledge however. Offshore North Africa the Numidian Flysch can be seismically imaged in 2D data. It lies beneath thick Messinian evaporites and seismic energy is highly attenuated as a result (pers.comms Stuart Marsh). Its incorporation into steeply dipping nappes also creates a complicated structural setting and similarly attenuates seismic energy resulting in generally poor quality imaging. The establishment of this project within the North Africa Research Group (NARG) was championed primarily by Anadarko Petroleum and Petrocanada, both of whom were actively exploring offshore northern Tunisia at that time. Statoil continue to show interest however, primarily as an analogue for injectite affected submarine channels in the North Sea (pers.comm. Jamie Vinnels, 2009).

1.3.2 Current sticking points in Numidian Flysch Formation studies

Placing the many sedimentological studies within the context of the basin and resolving further details about slope and fan architecture has been problematic. This results from several key issues which are outlined below.

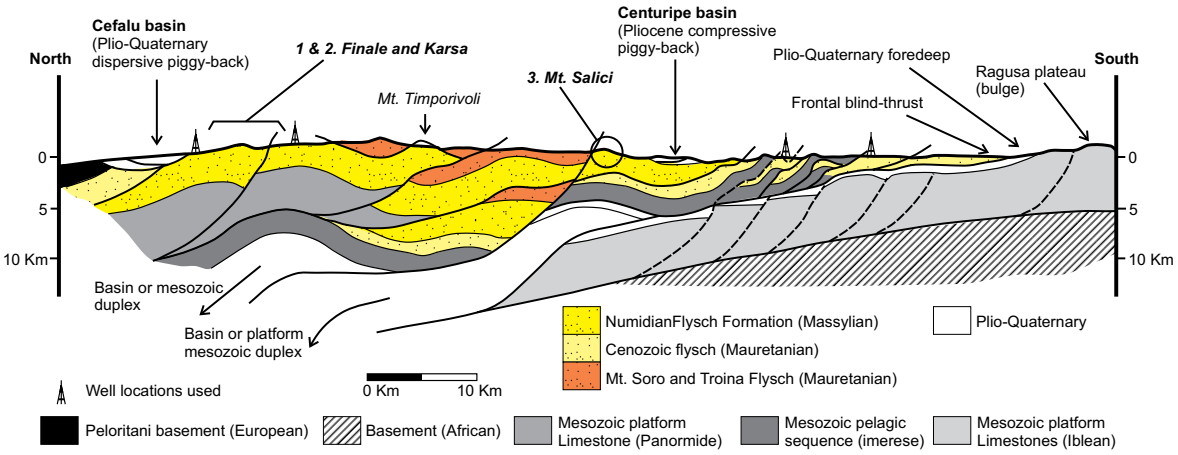

Figure 1.5.
Schematic cross section through the Sicillian fold and thrust belt (redrawn from Roure et al., 1990). The section includes areas of study within this thesis, labelled 1 to 3 (Finale, Karsa and Mt. Salici respectively).

1.3.2.1 Tectonics

Numidian Flysch Formation sections crop out within an Alpine aged fold-and-thrust-belt which includes the Betic, Rif, Tellian and Apennine mountain chains (Figure 1.1). In Sicily, deposits form steeply dipping nappes often with hanging wall anticline geometries which verge southwards (Figure 1.5) (Roure et al., 1990). In northern Sicily, the formation transgresses platform carbonates of the Panormide domain (Carbone et al., 1990) (Figure 1.5) while in central Sicily, the formation transgresses thick mudstone sequences of the Imerese domain (Lentini et al., 1974) (Figure 1.5). The basement domains upon which the fold-and-thrust-belt lies also underwent significant rotations, prior to and during stacking of nappes (Oldow et al., 1990) (Figure 1.6). In Tunisia, the outcrop belt suffers from further complications with intrusion from Triassic evaporittes (Ben Slama et al., 2009). The relationship between sections of the Numidian Flysch Formation and the substrate is therefore complicated and reconstructing the palaeogeographic location of deposition is extremely difficult.

1.3.2.2 Relationship to Mauretanian domain deposits

The relationship between the Numidian (Massylian) and Mauretanian petrofacies (see section 1.3) has been much debated. Mixing of these distinct petrofacies also occurs although only in specific locations (e.g Belayouni et al., 2010). Debate has therefore focussed upon whether they represent contemporaneous turbidite systems sourced from different source areas (e.g European and African) or switches in sediment type from a single source region (e.g, a European source).

1.3.2.3 Petrology and dating of Numidian deposits

The quartzarenite character of the Numidian Flysch Formation is a defining feature of the formation (Wezel, 1970). The uniformity of this character is interesting but also unhelpful in that key marker beds, as used for long distance correlation in the Apennines basins for example, are lacking. Furthemore biostratigraphic dating results are generally poor with the exception of Tunisia (see Riahi et al. (2010) and Torricelli and Biffi (2001) for example) and correlation across nappes is often not possible.

1.3.2.4 Analogue foreland basin turbidite sequences

Perhaps the most infamous issue surrounding the Numidian Flysch Formation is the provenance of

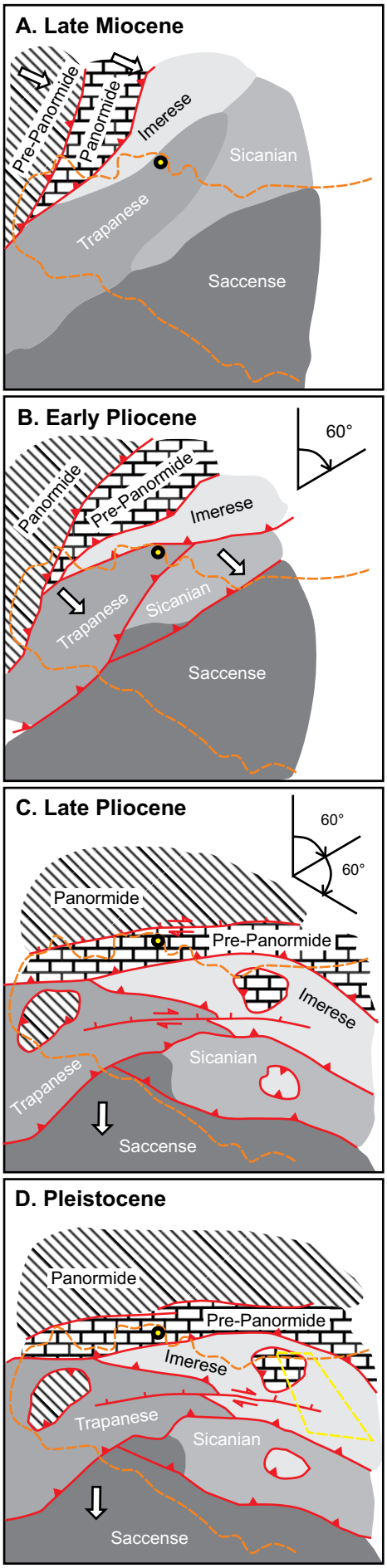

Figure 1.6.
Palinspastic reconstruction of the basement domains which form Sicily (redrawn from Oldow et al., 1990). An outline of western Sicily is shown overlain. The approximate location of the Sicilian study area is shown in the Pleistocene reconstruction, as is the location of Palermo (the capital of Sicily) with a yellow dot. The reconstruction highlights the complex clockwise rotations associated with basin closure and continental collision.

its quartz rich sandstones with proponents arguing variously for a European (northern margin) source and an African (southern margin) source (Thomas et al., 2010b). There are several reasons for this debate including those outlined above. Perhaps the simplest reason however is that when other foreland basin turbidite systems are described (for example, those of the Italian Apennines, the Alps, and the Magellanes basin of Chile), prolific turbidite sedimentation into the foredeep occurs via flows sourced from the uplifting orogenic wedge (accretionary prism) at the active margin of the basin (the northern, European margin in the case of the MFB) (Catuneanu, 2004; DeCelles and Giles, 1996; Hubbard et al., 2008; Ricci-Lucchi, 2003; Sinclair, 1997). This is logical given the high uplift rates associated with a rapidly growing accretionary prism, and associated volcanic activity (Catuneanu, 2004; de Capoa et al., 2002; DeCelles and Giles, 1996). In comparison, uplift on the cratonic edge of a foreland basin (the African margin in the case of the MFB) may be in the order of only 15 m through generation of forebulge uplift (DeCelles and Giles, 1996). The problem of provenance has meant that allogenic controls upon the system are poorly understood.

1.4 Thesis aims and structure

In light of the developments (section 1.2.1) and complications (section 1.2.2) outlined above, the general aim of this thesis is to re-evaluate the sedimentology and slope architecture of the Numidian Flysch formation of Sicily and Tunisia. To this end, four key questions are addressed which build on from each other. These are;

1. Can the Numidian provenance and basin setting be better constrained, so that Numidian Flysch fan architectures and their associated controls can be reconstructed?
2. What depositional elements and lithofacies are recognised within deposits of the Numidian Flysch Formation (with emphasis placed on Sicily and Tunisia)?
3. Following from questions 1 and 2, can conclusions be

drawn about slope and fan architectures within the Numidian Flysch?

4. What can the slope processes recorded within the Numidian Flysch Formation contribute to the wider discussion about deep marine sedimentology, particularly given its unique regional extent?

To answer these questions, the thesis is divided into four research chapters. **Chapter 2** attempts to address question 1 and places the Numidian Flysch Formation within a basin context. Evidence regarding the palaeogeography and in particular the provenance of Numidian Flysch clastic material throughout the entire basin is discussed and assessed. The timing of Numidian Flysch deposition is also placed within context of the basin evolution, and major tectonic, climatic and eustatic events, such that controls upon deposition are discussed. This chapter has previously been published within the journal Earth Science Reviews;

A constrained African craton source for the Cenozoic Numidian Flysch: Implications for the palaeogeography of the western Mediterranean basin. M.F.H. Thomas, S. Bodin, J. Redfern, D.H.B. Irving. Earth Science Reviews 101. pp1-23.

There have been several publications in recent years which discuss the provenance of the Numidian Flysch Formation clastic material. A discussion of these is included within chapter 2. The study by Fildes et al. (2010) was published during revision of the Thomas et al. (2010b) manuscript however, and a separate comment article was written in order to discuss the implications of their new data. This comment (Thomas et al., 2010a) and their subsequent reply (Stow et al., 2010) are included in the appendix section of this thesis (appendix 1 and 2 respectivley).

Chapter 3 attempts to characterise the sedimentology of the Numidian Flysch Formation in Sicily through three key outcrops. Lithofacies and depositional architectures are described in order to address question 2. While the incorporation of Numidian Flysch deposits into a series of nappes throughout the entire basin has complicated slope reconstructions (see section 1.3.2.1), the sections described are placed within a proximal to distal trend. A topographically complex slope and a preserved channel lobe transition zone are recognised. The former has not previously been recognised within the Numidian Flysch Formation and as such has important implications regarding slope architecture (question 3). Channel lobe transition zones however are not often documented in ancient deep marine systems. Its impact upon transiting flows is therefore of interest to the wider community of deep marine sedimentology and contributes to addressing question 4.

Chapter 4 focuses upon the Finale locality within the Numidian Flysch Formation of northern Sicily. This section contains excellent examples of channel complexes within a seismic scale channel system. A hierarchical methodology is applied to characterise the channel system and provide a high resolution study of Numidian Flysch Formation slope processes. This methodology enables the evolution of the section to be quantified in order to assess temporal controls upon slope deposition. Question 3 regarding Numidian Flysch slope architecture, and question 4 regarding the wider applications of this study, are therefore discussed with regard to this specific locality. This chapter is currently in press with Marine and Petroleum Geology in a special issue publication which resulted from a Geological Society of London conference called “Internal Architecture, Bedforms and Geometry of Turbidite Channels” (20-21st June 2011).

Chapter 5 describes the sedimentology of Numidian Flysch sections from northern Tunisia. The depositional architectures and lithofacies are compared to sections from Sicily and southern mainland Italy in order to compare and contrast the sedimentology of the Numidian Flysch Forma-

tion over approximately 1000 km of lateral slope system. Despite the 2000 km outcrop belt being classified as a single formation, the recognition of similarities and differences are important when considering controls upon the system (e.g local or regional controls upon deposition). This chapter therefore addresses lateral variability in slope processes and the controls upon them (question 3).

Finally, a **synthesis chapter** (chapter 6) draws these discussions together. A depositional model is presented which is intended to account for the observations made in chapters 3, 4 and 5 and this is placed within the framework of an updated basin palaeogeography which was established in chapter 2. The wider implications of this depositional model are discussed. Regionally they include controls upon Numidian Flysch Formation deposition throughout the basin, and hydrocarbon exploration issues (reservoir architectures, connectivity, and trap styles). More generically these include the role of intraslope topography upon transiting density flows, and the benefits of characterising and quantifying depositional element hierarchies within slope channel systems.

References.

Avellone, G., Barchi, M.R., Catalano, R., Morticelli, M.G. and Sulli, A., 2010. Interference between shallow and deep-seated structures in the Sicilian fold and thrust belt, Italy. Journal of the Geological Society of London, 167(1): 109-126.

Belayouni, H. et al., 2010. La Galite Archipelago (Tunisia, North Africa): Stratigraphic and petrographic revision and insights for geodynamic evolution of the Maghrebian Chain. Journal of African Earth Sciences, 56(1): 15-28.

Ben Slama, M.M., Masrouhi, A., Ghanmi, M., Ben Youssef, M. and Zargouni, F., 2009. Albian extrusion evidences of the Triassic salt and clues of the beginning of the Eocene atlasic phase from the example of the Chitana-Ed Djebs structure (N.Tunisia): Implication in the North African Tethyan margin recorded events, comparisons. Comptes Rendus Geoscience, 341(7): 547-556.

Bonardi, G. et al., 1980. Osservazioni sull'evoluzione dell'Arco Calabro-Peloritano nel Miocene inferiore: la Formazione di Stilo-Capo d'Orlando. Bollettino Della Societa Geologica Italiana, 99: 365-393.

Bouma, A.H., 1962. Sedimentology of some Flysch deposits;: A graphic approach to facies interpretation. 168 pp: Elsevier.

Carbone, S., Catalano, S., Grasso, M., Lentini, F. and Monaco, C., 1990. Carta Geologica Della Sicilia Centro-Orientale (1: 50,000) Instituto di Scienze della Terra.

Carbone, S., Lentini, F., Sonnino, M. and De Rosa, R., 1987. Il flysch numidico di Valsinni (Appennino lucano): Translated Title: The numidic flysch of Valsinni, Lucanian Apennines. Bollettino Della Societa Geologica Italiana, 106(2): 331-345.

Catterall, V., Redfern, J., Gawthorpe, R., Hansen, D. and Thomas, M., 2010. Architectural style and quantification of a submarine channel-levee system located in a structurally complex area: Offshore Nile delta. Journal of Sedimentary Research, 80(11-12): 991-1017.

Catuneanu, O., 2004. Retroarc foreland systems - evolution through time. Journal of African Earth Sciences, 38(3): 225-242.

de Capoa, P., Di Staso, A., Guerrera, F., Perrone, V. and Tramontana, M., 2004. The age of the oceanic accretionary wedge and onset of continental collision in the Sicilian Maghrebian Chain. Geodinamica Acta, 17(5): 331-348.

de Capoa, P. et al., 2002. The Lower Miocene volcaniclastic sedimentation in the Sicilian sector of the Maghrebian Flysch Basin: geodynamic implications. Geodinamica Acta, 15(2): 141-157.

DeCelles, P.G. and Giles, K.A., 1996. Foreland basin systems. Basin Research, 8(2): 105-123.

Deptuck, M.E., Sylvester, Z., Pirmez, C. and O'Byrne, C., 2007. Migration-aggradation history and 3-D seismic geomorphology of submarine channels in the Pleistocene Benin-major Canyon, western Niger Delta slope. Marine and Petroleum Geology, 24: 406-433.

Enos, P., 1977. Flow regimes in Debris flows. Sedimentology, 24(1): 133-142.

Ercilla, G. et al., 1998. Origin, sedimentary processes and depositional evolution of the Agadir turbidite system, central eastern Atlantic. Journal of the Geological Society, 155: 929-939.

Fildes, C. et al., 2010. European provenance of the Numidian Flysch in northern Tunisia. Terra Nova, 22(2): 94-102.

Fraser, A.J. et al., 2005. Angola Block 18; a deep-water exploration success story. Petroleum Geology of Northwest Europe: Proceedings of the ... Conference, 6: 1199-1216.

Gee, M.J.R. and Gawthorpe, R.L., 2006. Submarine channels controlled by salt tectonics: Examples from 3D seismic data offshore Angola. Marine and Petroleum Geology, 23(4): 443-458.

Gee, M.J.R., Gawthorpe, R.L., Bakke, K. and Friedmann, S.J., 2007. Seismic geomorphology and evolution of submarine channels from the Angolan continental margin. Journal of Sedimen-

tary Research, 77(5-6): 433-446.

Gery, B., 1983. Age and Tectonic Situation of the Allochthonous Sedimentary Formations in Northern Grande Kabylie - an Example in the Djebel Aissa-Mimoun. Comptes Rendus De L Academie Des Sciences Serie Ii, 297(9): 729-&.

Golonka, J., 2004. Plate tectonic evolution of the southern margin of Eurasia in the Mesozoic and Cenozoic. Tectonophysics, 381(1-4): 235-273.

Gottis, C., 1953. Stratigraphie et tectonique du « flysch » numidien en Tunisie septentrionale. Compte Rendus Hebdomadaires des Seances de l'Academie des Sciences, Paris, 236: 1059-1061.

Guerrera, F., Martinalgarra, A. and Perrone, V., 1993. Late Oligocene-Miocene Syn-/-Late-Orogenic Successions in Western and Central Mediterranean Chains from the Betic Cordillera to the Southern Apennines. Terra Nova, 5(6): 525-544.

Haughton, P., Davis, C., McCaffrey, W. and Barker, S., 2009. Hybrid sediment gravity flow deposits - Classification, origin and significance. Marine and Petroleum Geology, 26(10): 1900-1918.

Hodgson, D.M., 2009. Distribution and origin of hybrid beds in sand-rich submarine fans of the Tanqua depocentre, Karoo Basin, South Africa. Marine and Petroleum Geology, 26(10): 1940-1956.

Hubbard, S.M., Romans, B.W. and Graham, S.A., 2008. Deep-water foreland basin deposits of the Cerro Toro Formation, Magallanes basin, Chile: architectural elements of a sinuous basin axial channel belt. Sedimentology, 55(5): 1333-1359.

Ito, M., 2008. Downfan transformation from turbidity currents to debris flows at a channel-to-lobe transitional zone: The lower Pleistocene Otadai Formation, Boso Peninsula, Japan. Journal of Sedimentary Research, 78(9-10): 668-682.

Johansson, M., Braakenburg, N.E., Stow, D.A.V. and Faugeres, J.C., 1998. Deep-water massive sands: facies, processes and channel geometry in the Numidian Flysch, Sicily. Sedimentary Geology, 115(1-4): 233-265.

Lentini, F., Vezzani, L., Carveni, P., Copat, B. and Grasso, M., 1974. Carta Geologica della Madonie (Sicilia Centro - Settentrionale) (1:50,000). Instituto di Geologia dell'Universitá di Catania.

Lowe, D.R. and Guy, M., 2000. Slurry-flow deposits in the Britannia Formation (Lower Cretaceous), North Sea: a new perspective on the turbidity current and debris flow problem. Sedimentology, 47(1): 31-70.

Macdonald, H.A., Peakall, J., Wignall, P.B. and Best, J., 2011. Sedimentation in deep-sea lobe-elements: implications for the origin of thickening-upward sequences. Journal of the Geological Society, 168(2): 319-332.

Mazzoleni, P., 1991. Porphyric rocks in the basal conglomerate from the Stilo-Capo d'Orlando Formation: Le rocce profiriche nel conglomerato basale della formazione di Stilo-Capo d'Orlando. Memorie della Societa Geologica Italiana, 47: 557-565.

Migliorini, C.I., 1943. Sul modo di formazione dei complessitipo macigno. Bollettino Della Societa Geologica Italiana, 62: 48-49.

Mutti, E., 1985. Turbidite systems and their relations to depositional sequences. NATO ASI series C: Mathematical and physical sciences, 148(Provenance of Arenites): 65-93.

Mutti, E., Bernoulli, D., Lucchi, F.R. and Tinterri, R., 2009. Turbidites and turbidity currents from Alpine 'flysch' to the exploration of continental margins. Sedimentology, 56(1): 267-318.

Mutti, E. and Ricci Lucchi, F., 1978. Turbidites of the northern Apennines: introduction to facies analysis. International Geology Review, 20(2): 125 - 166.

Nakajima, T., Peakall, J., McCaffrey, W.D., Paton, D.A. and Thompson, P.J.P., 2009. Outer-bank bars; a new intra-channel architectural element within sinuous submarine slope channels. Journal of Sedimentary Research, 79(12): 872-886.

Normark, W.R., 1970. Growth patterns of deep-sea fans. The American Association of Petroleum Geologists Bulletin, 54(11): 2170-2195.

Normark, W.R. and Piper, D.J.W., 1972. Sediments and growth pattern of Navy deep-sea fan, San Clemente Basin, California borderland. Contributions - University of California, San Diego, Scripps Institution of Oceanography, 42, Part 2(80): 1094-1119.

Normark, W.R., Piper, D.J.W. and Hess, G.R., 1979. Distributary channels, sand lobes, and meso-topography of Navy Submarine Fan, California Borderland, with applications to ancient fan sediments. Sedimentology, 26(6): 749-774.

Oldow, J.S., Channell, J.E.T., Catalano, R. and D, A.B., 1990. Contemporaneous thrusting and large-scale rotations in the western Sicilian fold and thrust belt. Tectonics, 9(4): 661-681.

Pantin, H.M. and Franklin, M.C., 2011. Improved experimental evidence for autosuspension. Sedimentary Geology, 237(1-2): 46-54.

Patterson, R.T., Blenkinsop, J. and Cavazza, W., 1995. Planktic Foraminiferal Biostratigraphy and Sr Isotopic Stratigraphy of the Oligocene-to-Pleistocene Sedimentary Sequence in the Southeastern Calabrian Microplate, Southern Italy. Journal of paleontology, 69(1): 7-20.

Pattison, S.A.J., 2005. Isolated highstand shelf sandstone body of turbiditic origin, lower Kenilworth Member, Cretaceous Western Interior, Book Cliffs, Utah, USA. Sedimentary Geology, 177(1-2): 131-144.

Piper, D.J.W., Cochonat, P. and Morrison, M.L., 1999. The sequence of events around the epicentre of the 1929 Grand Banks earthquake: initiation of debris flows and turbidity current inferred from sidescan sonar. Sedimentology, 46(1): 79-97.

Prather, B.E., Booth, J.R., Steffens, G.S. and Craig, P.A., 1998. Classification, lithologic calibration, and stratigraphic succession of seismic facies of intraslope basins, deep-water Gulf of Mexico. Aapg Bulletin-American Association of Petroleum Geologists, 82(5): 701-728.

Prélat, A., Hodgson, D.M. and Flint, S.S., 2009. Evolution, architecture and hierarchy of distributary deep-water deposits: a high-resolution outcrop investigation from the Permian Karoo Basin, South Africa. Sedimentology, 56(7): 2132-2154.

Pyles, D.R., 2008. Multiscale stratigraphic analysis of a structurally confined submarine fan: Carboniferous Ross Sandstone, Ireland. Aapg Bulletin, 92(5): 557-587.

Riahi, S. et al., 2010. Stratigraphy, sedimentology and structure of the Numidian Flysch thrust belt in northern Tunisia. Journal of African Earth Sciences, 57(1-2): 109-126.

Ricci-Lucchi, F., 2003. Turbidites and foreland basins: an Apenninic perspective. Marine and Petroleum Geology, 20(6-8): 727-732.

Roure, F., Howell, D.G., Muller, C. and Moretti, I., 1990. Late Cenozoic Subduction Complex of Sicily. Journal of Structural Geology, 12(2): 259-266.

Saller, A. et al., 2008. Characteristics of Pleistocene deep-water fan lobes and their application to an upper Miocene reservoir model, offshore East Kalimantan Indonesia. AAPG Bulletin, 92(7): 919-949.

Shultz, M.R., Fildani, A., Cope, T.D. and Graham, S.A., 2005. Deposition and stratigraphic architecture of an outcropping ancient slope system; Tres Pasos Formation, Magallanes Basin, southern Chile. In: M. Hodgson David and S. Flint Stephen (Editors), Submarine slope systems; processes and products. Geological Society of London. London, United Kingdom. 2005.

Sinclair, H.D., 1997. Tectonostratigraphic model for underfilled peripheral foreland basins: An Alpine perspective. Geological Society of America Bulletin, 109(3): 324-346.

Dorrik Stow, Christine Fildes, Sami Riahi, Mohamed Soussi, Urval Patel, J. Andy Milton and Stuart Marsh. 2010. Reply to comment on ‘European provenance of the Numidian Flysch in northern Tunisia’. Terra Nova, Vol 22, No. 6, 504–505

Stow, D.A.V. and Johansson, M., 2000. Deep-water massive sands: nature, origin and hydrocarbon implications. Marine and Petroleum Geology, 17(2): 145-174.

Thomas, M.F.H., Bodin, S. and Redfern, J., 2010a. Comment on 'European provenance of the Numidian Flysch in northern Tunisia' by Fildes et al. (2010). Terra Nova, 22(6): 501-503.

Thomas, M.F.H., Bodin, S., Redfern, J. and Irving, D.H.B., 2010b. A constrained African craton source for the Cenozoic Numidian Flysch: Implications for the palaeogeography of the western Mediterranean basin. Earth-Science Reviews, 101(1-2): 1-23.

Torricelli, S. and Biffi, U., 2001. Palynostratigraphy of the Numidian Flysch of northern Tunisia (Oligocene-early Miocene). Palynology, 25: 29-55.

Vangriesheim, A., Khripounoff, A. and Crassous, P., 2009. Turbidity events observed in situ along the Congo submarine channel. Deep Sea Research Part II: Topical Studies in Oceanography, In Press, Corrected Proof.

Vercellino, J. and Rigo, F., 1970. Geology and exploration of Sicily and adjacent areas. Memoir - American Association of Petroleum Geologists, 14: 388-398.

Vila, J.M. et al., 1995. The Sandy Uppermost Oligocene Channel and the Miocene of Sidi-Affif Area in Their East Algerian Structural Setting - the Saharan Origin of the Numidian and the Calendar of the Miocene Overthrusts. Comptes Rendus De L Academie Des Sciences Serie Ii, 320(10): 1001-1009.

Walker, R.G., 1978. Deep-water sandstone facies and ancient submarine fans - models for exploration for stratigraphic traps. Aapg Bulletin-American Association of Petroleum Geologists, 62(6): 932-966.

Wezel, F.C., 1969. Lineamenti Sedimentologico Del Flysch Numidico Della Sicilia Nord-Orientale. Memorie Degli Instituti Di Geologia e Mineralogia Del L'Universita Di Padova, 26.

Wezel, F.C., 1970. Numidian Flysch - an Oligocene - Early Miocene Continental Rise Deposit Off the African Platform. Nature, 228(5268)

Wolden, T. and Jones, M.S., 2005. Offshore Northern Tunisia MC2D - La Galite Block (N1). -.

Wynn, R.B., Kenyon, N.H., Masson, D.G., Stow, D.A.V. and Weaver, P.P.E., 2002. Characterization and recognition of deep-water channel-lobe transition zones. Aapg Bulletin, 86(8): 1441-1462.

Chapter 2.

A constrained African-craton source for the Cenozoic Numidian Flysch: Implications for the palaeogeography of the western Mediterranean basin.

Chapter 2. A constrained African-craton source for the Cenozoic Numidian Flysch: Implications for the palaeogeography of the western Mediterranean basin

Abstract

The provenance of the Numidian Flysch in the western Mediterranean remains a controversial subject which hinders understanding of this regionally widespread depositional system. The Numidian Flysch is a deep marine formation dated as Oligocene to Miocene which outcrops throughout the Maghreb and into Italy. Evidence that is widely used for provenance analysis has not previously been reviewed within the context of the Maghrebian Flysch Basin as a whole. The structural location within the Alpine belt indicates deposition proximal to the African margin, while the uniformity of the Numidian Flysch petrofacies suggests a single cratonic source, in stark contrast to heterolithic and immature flysch formations from the north of the basin. Detrital zircon ages constrain a source region with Pan-African and Eburnian age rocks, unaffected by either Hercynian or Alpine tectonic events, which precludes the European basement blocks to the north of the basin. Palaeocurrent trends which suggest a northern source are unreliable given foreland basin analogues and observed structural complications. An African craton source remains the only viable option once these data are reviewed in their entirety, and the Numidian Flysch therefore represents a major Cenozoic drainage system on the North African margin. Deposition is concurrent with regional Atlas uplift phases, and coincidental with globally cooling climates and high sea levels. The Numidian Flysch is therefore interpreted to represent a highstand passive margin deposit, with timing of deposition controlled primarily by hinterland uplift and climatic fluctuations.

2.1. Introduction

The Cenozoic Numidian Flysch is a foreland basin deposit representing the most widespread tectono-stratigraphic unit in the western Mediterranean (Wezel, 1970a; Dejong, 1975) (Figure 2.1). Numidian Flysch sediments were fed into the east-west oriented foreland basin (Mahgrebian Flysch Basin (MFB)) which resided in the western palaeo-Tethys realm between a growing accretionary prism to the north and the passive African margin to the south (Elter et al., 2003; Guerrera et al., 2005). Facies include hemipelagic mudstones and a variety of density flow deposits both unconfined and confined within channel bodies (Vila et al., 1995; Johansson et al., 1998) (Figure 2.2). Depositional environment is assigned to both the slope and basin floor environments within a deep marine setting (e.g. Wezel, 1969; Johansson et al., 1998; Riahi et al., 2007). Displaying a seemingly continuous ultramature quartzarenite petrofacies throughout the western Mediterranean, the Numidian Flysch has been a formation of great controversy regarding its provenance since the 1950's (Gottis, 1953; Wezel, 1970a; Caire and Duée, 1971). Attempts to reconcile this fundamental problem have been hampered by its homogeneous nature and the complexity of its allocthonous emplacement. Its vast regional extent (>2000 km) has also lead some authors to promote it as a facies rather than a single formation (Magné and Raymond, 1972; Giunta, 1985; Moretti et al., 1991). Its source region has ultimately been described as being northern, from European terrains and the foreland basin orogenic wedge; southern from the African craton; or a mixture of both. Evi-

dence has focused upon its structural position relative to other units within the basin, petrology of the clastic fraction, ages of detrital zircons, and palaeocurrent orientations. Progress has stagnated in recent years with heated debate over palaeocurrent orientations giving no obvious conclusion (see Johansson et al., 1998; Parize et al., 1999; Stow et al., 1999). More recently, work has spread to provenance analysis of mudstones rather than the clastic fraction which has failed to resolve the debate so far (Barbera et al., 2009). The lack of a definitive source area has hampered understanding of the Numidian Flysch system as a whole, and little evidence exists concerning either basin architecture or controls upon deposition. The duration and large regional extent of Numidian Flysch deposition potentially offers an insight into the palaeogeography and drainage in the entire western Mediterranean once these problems are addressed. Here we present the first integrated critical review of the published evidence on provenance, together with additional field and petrological data, in order to constrain the source of the Numidian Flysch and place it within a palaeogeographic framework of the western Mediterranean during the Cenozoic.

2.2 Geological setting

The Mahgrebian Flysch Basin (MFB) represents a major Meso-Cenozoic domain of the Alpine orogenic belt (Guerrera et al., 2005) which today marks the northern extent of the African margin from Morocco to southern Italy (Wezel, 1970a) (Figure 2.1). The basin, a remnant of the neo-Tethys ocean, lay to the north of the African margin and trended approximately east-west, linking the Atlantic and eastern Mediterranean domains (Piqué et al., 2002; Guerrera et al., 2005) (Figure 2.3). The original oceanic basin was initiated through the northwards separation of Eurasia from Gondwana during the Jurassic breakup of Pangea (Golonka, 2004). An east-west trending group of continental microplates, variously termed the Meso-Mediterranean Terrain (MMT (Guerrera et al., 1993; de Capoa et al., 2004; Zaghloul et al., 2007) or AlKaPeCa domain (Al=Alboran block, Ka=Kabylie block, Pe=Peloritan block, Ca=Calabrian block (sensu Bouillin et al., 1986) formed the northern border of the Mahgrebian basin (Figures 2.1 and 2.3), also rifted from the Eurasian plate in the Jurassic (Cohen, 1980; Guerrera et al., 1993). Basement lithologies of the AlKaPeCa domain include phyllites, amphibolite facies rocks, mica-shists, granites and volcanics (Trombetta et al., 2004; Festa et al., 2006; Hammor et al., 2006). African oceanic crust, basement to the MFB, was subducted to the north beneath the AlKaPeCa domain from the Eocene (Lentini et al., 2002; Golonka, 2004) such

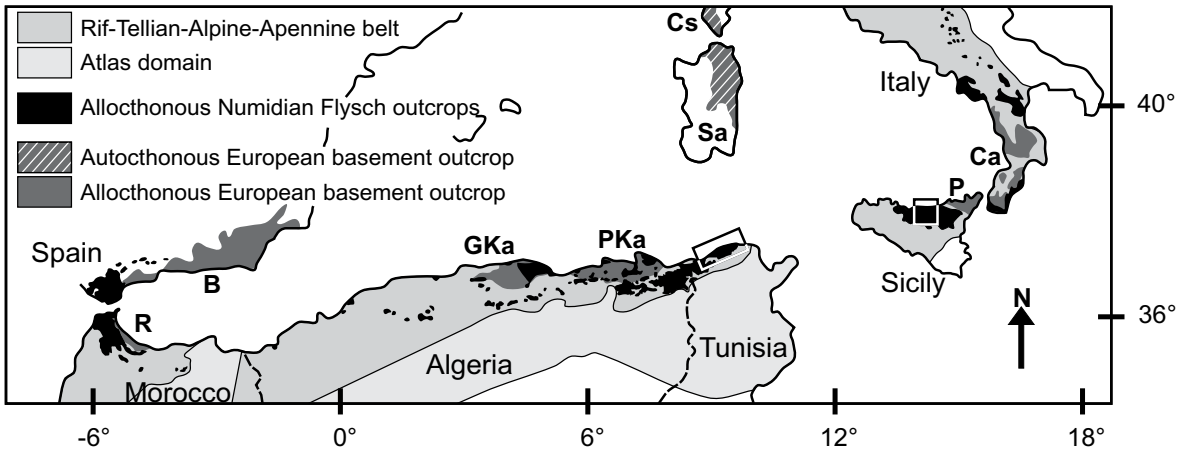

Figure 2.1.
Numidian Flysch outcrops and their relation to the Alpine and Atlas fold and thrust belts. European basement blocks from the AlKaPeCa domain are; R, Riff; B, Betic; Gka, Grand Kabylie; Pka, Petit Kabylie; Cs, Corsica; Sa, Sardinia; P, Peloritan; Ca, Calabria. Numidian Flysch outcrops taken from Wezel (1970a). See text for other data. Sicilian and Tunisian field areas used for this study are boxed.

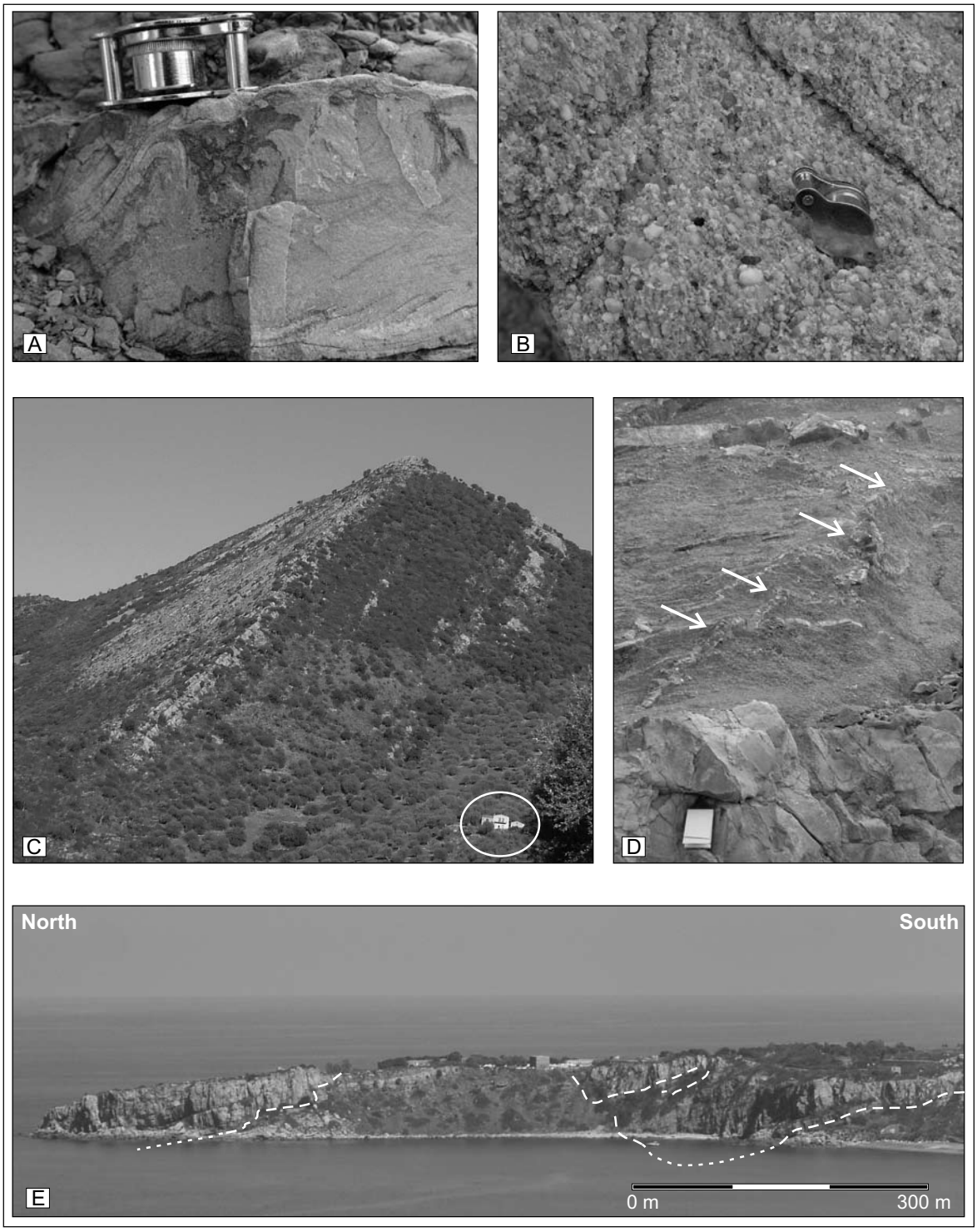

Figure 2.2.
Outcrop photographs of common Numidian Flysch facies and depositional architectures: A) Thin, medium grained turbidite deposit (Bouma Tc division) with dewatering structures at top. Finale village, northern Sicily. B) Matrix supported conglomerate from channel base, representing frictional debris flow deposit. Cap Serat, Tunisia. C) Sheet sandstones observed up to 750 m across. See house at bottom right for scale. Karsa district near San Mauro Castelverde, northern Sicily. D) Steeply inclined sandstone dyke sourced from unstructured medium grained sandstone bed at base. Tabarka. Tunisia. E) Coastal exposure of large scale incisional channel complexes. Finale village, northern Sicily.

that the MFB became a true foreland basin. The AlKaPeCa domain migrated southwards towards the African margin from the upper Oligocene (Puglisi, 2008), coincident with counter-clockwise rifting of Corsica and Sardinia from Europe, and the opening to their north of the Algerian basin (Mauffret et al., 2004). The rotation and southwards migration of the Sardinia/Corsica block, coupled with subduction-related slab roll-back were the main geodynamic controls upon the eastern sector of the MFB from the late Eocene (Cohen, 1980; Carminati et al., 1998; Mauffret et al., 2004). Portions of the AlKaPeCa domain also formed basement to a magmatic arc during migration, shedding volcaniclastic sediment to the MFB and possibly north to the Algerian basin (de Capoa et al., 2002; Mauffret et al., 2004).

With migration, the continental AlKaPeCa domain formed the basement to a growing south verging orogenic wedge, preceded to its south and east by thin-skinned thrust deformation (Knott, 1987; Putignano and Schiattarella, 2008). Figure 2.3 highlights the geographic terminology used within this review. Internal units from the north of the basin and proximal to the young accretionary wedge, were incorporated into thrust nappes relatively early within the Aquitanian (de Capoa et al., 2004; Guerrera et al., 2005; de Capoa et al., 2007). These units are found today structurally or conformably overlying the AlKaPeCa basement (de Capoa et al., 2002; Guerrera et al., 2005). External units conformably or structurally overlie both the African carbonate platform and Tellian units of the southern passive margin, and became structured in the latest Burdigalian (de Capoa et al., 2004). Deep marine 'flysch' units from the foredeep area of the basin define a flysch domain mid way between these internal and external areas. The flysch domain is in turn split into a northern Mauretanian subdomain which is characterised by a metamorphic/volcaniclastic rich petrofacies, and a southern Massylian subdomain characterised by a quarzose petrofacies (Gelard, 1969; Bouillin and

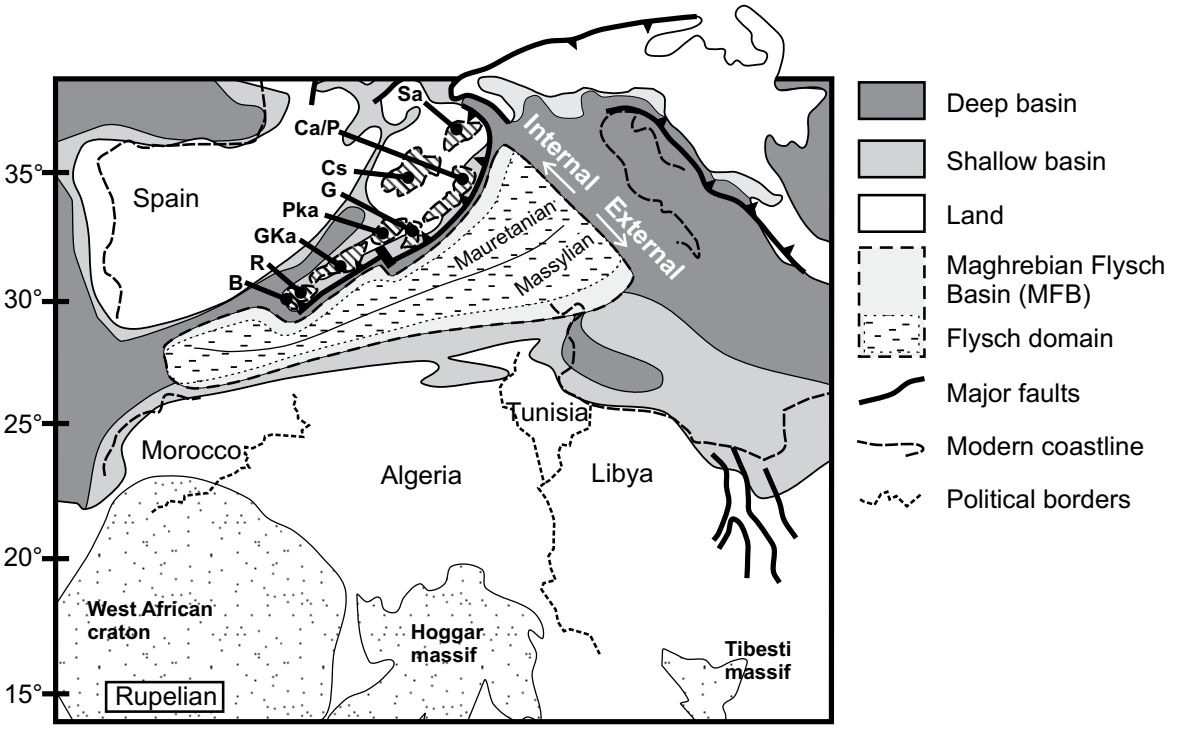

Figure 2.3.
Oligocene (Rupelian) palaeogeographic map of the western Mediterranean highlighting the location of the Maghrebian flysch basin and commonly used basin nomenclature. Map redrawn from Meulenkamp and Sissingh (2003) (Peri-Tethys project. See also Dercourt et al. (2000) and Gaetani et al. (2003). Suggested African and European source areas discussed within the text are highlighted, including African cratonic basement and blocks of the European AlKaPeCa domain. AlKaPeCa block abbreviations are: B, Betic; R, Riff; Cs, Corsica; Sa, Sardinia; Ca/P, Calabria and Peloritan; G, Galite block; Pka, Petit Kabylie; Gka, Grand Kabylie.

Glacon, 1973; de Capoa et al., 2004). So-called mixed successions which have characteristics of both Mauretanian and Massylian subdomains are described throughout the entire chain, and have been interpreted to be the result of mixing of the two petrofacies in the foredeep axis (Carmisciano et al., 1987; Fornelli, 1998).

Numidian Flysch deposits are unanimously regarded as having ages that span the Oligocene to early Miocene compressional foreland basin stage (Lahondére et al., 1979; Leblanc and Feinberg, 1982; Didon et al., 1984; Faugères et al., 1992; Torricelli and Biffi, 2001). Numidian Flysch deposits in Morocco, Algeria, Tunisia, and Italy are relatively well dated, however Sicilian deposits have not been well constrained. Unpublished biostratigraphic dating undertaken for this study in Sicily using planktonic and benthic foraminifera as well as radiolaria, have constrained the Sicilian deposits to an Aquitanian - Burdigalian age (Appendix 3).

On the African margin, the large Fortuna Delta system in Tunisia was contemporanous with the Numidian Flysch, and fed sediment east and south towards the Pelagian basin. The delta has been commonly cited as a potential Numidian Flysch input point in northern Tunisia (Vanhouten, 1980; Yaich et al., 2000). Closure of the MFB, resulting from southwards migration of the AlKaPeCa domain, occurred in the early to mid Miocene, and resulted in stacking of MFB deposits upon the African passive margin (Carr and Miller, 1979; de Capoa et al., 2004).

2.3 Evidence for the Numidian Flysch provenance

Since the earliest major works on the Numidian Flysch by Wezel (1969) and Wezel (1970b), the provenance of the numidian detrital supply has been contested. Studies concerned primarily with regional tectonics and stratigraphy have generally preferred the African craton as the most likely source region, and this has been supported by petrological studies which relate the rounded ultra-mature quartz pebbles to a cratonic source. There have also been some attempts to use zircon age dating to constrain the source region which have however met with little reaction from a majority of subsequent publications. Sedimentologists have tended to suggest a northern source however, prompted primarily by the orientation of sole marks on the base of density flow deposits (e.g. Parize et al., 1986; Yaich, 1992a). Foreland basin examples such as the Apennines and Alps also suggests that in foreland basin settings, a majority of flysch sediment is commonly sourced from the tectonically active accretionary prism, which in the MFB would be located at its northern margin. This division of ideas related to provenance, remains prevalent within the literature, with the two main protagonist groups maintaining their positions.

Possible northern source regions include continental basement from mainland Europe, or terrains rifted from it, such as the AlKaPeCa microplates, Corsica, and Sardinia (Figure 2.3). Specific source regions are rarely cited, although Sardinia (Caire and Duée, 1971) and the Kabylie blocks (Magné and Raymond, 1972; Ivaldi, 1977; Lahondére et al., 1979; Vila et al., 1995, Fildes et al., 2010) have been suggested. Supporters of a southern source have variously suggested the Continental Intercalaire (Lancelot et al., 1976; Ivaldi, 1977; Moretti et al., 1991) and Pharusian series (Moretti et al., 1991) of western and central Africa, the Nubian sandstone of the Sirt basin in Libya (Wezel, 1970a; Johansson et al., 1998) and Permo-Triassic and Ordovician continental sandstones of southern Tunisia (Gaudette et al., 1975; Gaudette et al., 1979).

Four key lines of evidence are therefore commonly used: The structural position of Numidian Flysch nappes constrains the depositional location of the Numidian Flysch and its palaeogeography

within the basin; petrological studies of the Numidian Flysch have allowed differentiation with flysch deposits of the Mauretanian subdomain, and comparison of its characteristics with those predicted from provenance models; palaeocurrent analysis has been used to determine the direction that density flows travel from source to depositional location, thereby assessing the source orientation; finally, zircon analysis has been used to constrain source rock ages. In general, these lines of evidence are discussed individually within a majority of publications. Here they are presented and reviewed sequentially, before being integrated together.

2.3.1. Structural position within Alpine nappes

The location of the Numidian Flysch within the Alpine thrust belt provides evidence as to its position relative to the AlKaPeCa domain and the North African passive margin. Early nappe emplacement and an internal/structurally high position within the nappe pile constrains units to a pre-allocthonous position proximal to the orogenic wedge and the north of the basin (Boyer and Elliott, 1982; de Capoa et al., 2002). Similarly, late stage nappe emplacement and an external/structurally low position within the nappe pile constrains units to a pre-allocthonous position to the south of the Mauretanian subdomain and proximal to the North African passive margin. This line of evidence is well established in Morocco, Sicily and Italy where the majority of work has been performed. A summary of the following tectonostratigraphic relationships is presented in figure 2.4.

2.3.1.1. The Sicilide basin of Sicily and southern Italy

Commonly grouped as the Sicilide basin, the sedimentological and tectonic evolution of both Sicily and southern Italy are very similar. The Numidian Flysch in northern Sicily, exposed in stacked south-verging nappes, lies conformably upon Eocene platform carbonates and Oligocene mudstones of the Imerese and Panormide carbonate platforms (Wezel, 1969; Faugères et al., 1992; Johansson et al., 1998). Structurally above and to the north of the Numidian Flysch, units of the Troina-Tusa nappes contain Oligocene to early Miocene volcaniclastic arenites (the Tusa Tuffite Fm) (Figure 2.4) unconformably overlain by the volcaniclastic Reitano flysch, of either Langhian or Serravallian age, which seals the nappes of the Mauretanian flysch domain (Cassola et al., 1995; de Capoa et al., 2000). The Troina Tusa Flysch (Troina Tusa nappe), a micaceous sandstone with volcaniclastic intervals is contemporaneous with the Numidian Flysch and crops out in northeast and central Sicily within the same succession (Lancelot et al., 1977; Barbera et al., 2009). The northern Numidian Flysch and its immediate substrate were detached in the Langhian and displaced southwards over more external carbonate domains in the early Tortonian (Catalano et al., 1995). In contrast, southern deposits which crop out in central Sicily lie conformably upon Oligocene to Aquitanian deep marine basinal mudstones of the Argille Varicolori Fm (Carbone et al., 1987; de Capoa et al., 2000). The European Peloritani basement massif (AlKaPeCa domain), largely submerged offshore northern Sicily, crops-out in the northeastern Peloritani mountains, unconformably overlain by porphyric clast turbidite deposits of the Upper Oligocene-Lower Miocene Stilo-Capo d'Orlando Formation (Bonardi et al., 1980; Mazzoleni, 1991; Patterson et al., 1995). Continental collision of the Peloritani block with Africa occurred in the Serravallian and was completed by the late Tortonian (de Capoa et al., 2004).

In southern Italy, east verging Numidian Flysch nappes directly overlie Oligocene to early Miocene carbonates and calcarenites of the Apulia margin (Cerchiara Fm) (Iannace et al., 2007). Structurally higher to the west lie nappes of varicoloured clays and the Tufiti di Tusa Fm as recognised in Sicily (Pescatore et al., 1992; Lentini et al., 2002) (Figure 2.4). Eastward continental collision of the Calabria block with the African Apulia margin took place in the late Miocene (Cello and Mazzoli, 1998;

Figure 2.4.

Table summarising the structural relationships of the internal, Mauretanian, Numidian/Massylian, and external domain nappes. Formations and units are not intended to be exhaustive. Horizontal dashed lines between formations/groups denote transgressive/conformable contacts. See section 2.3.1 for references and details.

Iannace et al., 2007).

2.3.1.2. Tunisia and Algeria

Less agreement exists about the structural evolution of the Alpine chain of northern Tunisia and Algeria. The Numidian Flysch crops out in the Alpine belt which strikes roughly parallel to the northern coastline, subsequently turning north at Ras el Koran to become submerged offshore in the Sicily channel (Catalano et al., 1996). South of the Alpine belt, units of the African Tellian domain represent continental and marine sediments, and debate in Tunisia has centred around the relationship of the Numidian Flysch to underlying Tellian units being either allocthonous, parautocthonous, or autocthonous. Recent work confirms them to be allocthonous through the use of biostratigraphy and the relationship of Numidian Flysch deposits to the underlying Tellian deposits (Riahi et al., 2007; Talbi et al., 2008; Boukhalfa et al., 2009) (Figure 2.4). Furthermore, biostratigraphic and palynostratigraphic dating of the Numidian Flysch series confirms the vertical superposition of three coeval members (the Zousa, Kroumerie and Babouche members) and their subsequent lateral juxtaposition to the external shallow marine Bejaoua Group (Torricelli and Biffi, 2001; El Euchi et al., 2004; Riahi et al., 2007; Boukhalfa et al., 2009). The Numidian Flysch is therefore stacked above the external Tellian units, which are in turn stacked upon the African foreland (Burollet, 1991; El Euchi et al., 2004; Boukhalfa et al., 2009).

The European basement Galite block (AlKaPeCa domain), a lateral equivalent to the Kabylies of northern Algeria, does not outcrop. It is interpreted, using marine 2D seismic surveys and dredged samples, to lie to the north of the Tunisian coast (Tricart et al., 1994), stacked upon Numidian Flysch nappes (Tricart et al., 1994; El Euchi et al., 1998; El Euchi et al., 2004) (Figure 2.4). Galite island, 50 km north of the Tunisian mainland also shows a juxtaposition of Numidian Flysch quartz rich sandstones, immature litharenite turbidites of the Galite Flysch and some stratigraphic intervals of mixed successions (Belayouni et al., 2010). Early Miocene arkosic turbidites have also been recovered in dredge samples from the offshore Galite area (Tricart et al., 1994).

The location of the Numidian Flysch in Algeria has fuelled a debate about where the Numidian Flysch basin lay with respect to the internal European Kabylie basement (AlKaPeCa domain). The Numidian Flysch outcrops throughout the width of the Alpine belt, thrust above African Tellian units in the south. In northern Algeria the Numidian Flysch lies above and to the north of the Kabylie blocks on the Algerian coastline (Magné and Raymond, 1972; Moretti et al., 1991). This relationship is contrary to that observed throughout the rest of the basin, and has prompted some authors to view the Numidian Flysch as conformable cover to the European Kabylie blocks rather than a deposit of the Massylian subdomain to the south (Coutelle, 1979; Laval, 1974; Laval, 1992) (Figure 2.4). In order to account for recorded Numidian Flysch palaeocurrent orientations and a position conformable with the Kabylie blocks, Laval (1992) proposed a hypothetical continental source to the north of the Kabylies which fed Numidian Flysch sand southwards. An alternative interpretation requires Miocene backthrusting of Numidian Flysch deposits and portions of the Tellian units to the north over the Kabylie block (Bouillin and Glacon, 1973; Vila, 1978; Moretti et al., 1991). Biostratigraphic dating and structural analysis of the Numidian Flysch and its Tellian substrate contradicts the conformable interpretation, thereby allowing for an allocthonous reinterpretation in agreement with the remainder of the basin (Magné and Raymond, 1972; Lahondére et al., 1979; Moretti et al., 1991). Géry (1983) also recognised a conformable cover to the Kabylies in northern Algeria which consisted of Oligocene to lower Miocene limestones and continental conglomerates. The presence of continental and shallow marine facies coeval with deep marine Numidian Flysch deposition

similarly suggests a backthrust configuration (Figure 2.4). As with Tunisia, Andrieux et al. (1989) describes an undifferentiated micaceous flysh deposit above the petit Kabylies in north eastern Algeria.

2.3.1.3. Morocco and Spain

The Betic and Rif portions of the Alpine chain form an arc through southern Spain, the Gibraltar straights and western Morocco (Crespo-Blanc and Frizon de Lamotte, 2006). In Spain, the allocthonous Alpine units are thrust upon European continental, marine, and deep marine sediments of the Subbetic zone (Alcala-Garcia et al., 2001; Lujan et al., 2006) (Figure 2.4). In Morocco, Alpine nappes stack upon similar Jurassic to mid-Miocene African margin sequences of the Mesorif and Intrarif zones (Morley, 1988; Chalouan et al., 2006). Structurally above the Numidian Flysch in Spain, Palaeozoic to Tertiary metamorphic rocks (including amphibolite and blueschist facies) make up the Nevado-Filabride, Alpujarride and Malaguide internal complexes which were originally part of the Alboran (AlKaPeCa) domain (Gomez-pugnaire and Fernandezsoler, 1987; Weijermars, 1991; Sanz de Galdeano et al., 1993) (Figure 2.4). Within the Moroccan Rif, the Nevado-Filabride complex has no equivalent, however the Alpujarride and Malaguide complexes are represented by the Sebtide and Ghomaride units respectively (Puglisi et al., 2001; Gigliuto et al., 2004). These internal Rif and Betic units consist of an extensive series of shallow and deep marine sediments rich in metamorphic and granitic clasts (Gigliuto et al., 2004; Serrano et al., 2006) (Figure 2.4). Beneath the AlKaPeCa nappes, the flysch domain is split into the Aljibe, Algeciras and Bolonia units of Spain, and the equivalent Numidian Flysch, Beni-ider and Tala Lakraa nappes of Morocco (Didon et al., 1973; Lujan et al., 2006). The Numidian Flysch crops out in the central part of the Rif chain, and the southern tip of Spanish Betics (Wezel, 1970a; Stromberg and Bluck, 1998), while in eastern Morocco the Numidian Flysch is known to lie conformably upon Palaeogene to Oligocene mudstones (Leblanc and Feinberg, 1982). Structurally above the Numidian/Aljibe nappes, the Algeciras (Spain) and Beni Ider nappes (Morocco) contain turbidite deposits with metamorphic grains and mica rich sands while the Bolonia (Spain) and Tala Lakraa units (Morocco) show a mixed succession composition of quartzose and metamorphic sands (Didon and Hoyez, 1978; Zaghloul et al., 2002; Lujan et al., 2006) (Figure 2.4).

2.3.2. Petrology of Numidian Flysch sandstones and mudstones

A key characteristic of Numidian Flysch sandstones is that they are generally considered compositionally ultramature and texturally immature (i.e. Wezel, 1970b; Loiacono et al., 1983; Fornelli, 1998). This fundamental character is widespread throughout the western Mediterranean, in southern Italy (Loiacono et al., 1983; Carbone et al., 1987; Fornelli, 1998), Sicily (Broquet et al., 1963; Wezel, 1969; Caire and Duée, 1971), Tunisia (Yaich, 1992a; Riahi et al., 2007), Algeria (Moretti et al., 1988; Moretti et al., 1991), Morocco (Leblanc and Feinberg, 1982) and southern Spain (Didon et al., 1984; Stromberg and Bluck, 1998). This homogeneous character has supported the hypothesis of a single regional source area with cratonic characteristics (Carbone et al., 1987; Moretti et al., 1991; Fornelli and Piccarreta, 1997; Fornelli, 1998).

Previous studies demonstrate the Numidian Flysch to be rich in quartz (e.g. Wezel, 1969; Loiacono et al., 1983), with minor minerals reported to include feldspars, lithic grains, mica, clays, and a heavy mineral suite including zircon, tourmaline, Fe-Oxide, garnet and monazite (Gaudette et al., 1979; Fornelli and Piccarreta, 1997; Fornelli, 1998). Three published Quartz – Feldspar – Lithic (QFL) data sets from southern Italy (Loiacono et al., 1983; Carbone et al., 1987; Fornelli, 1998) show 55% of samples plot within the quartzarenite domain, although individual populations remain

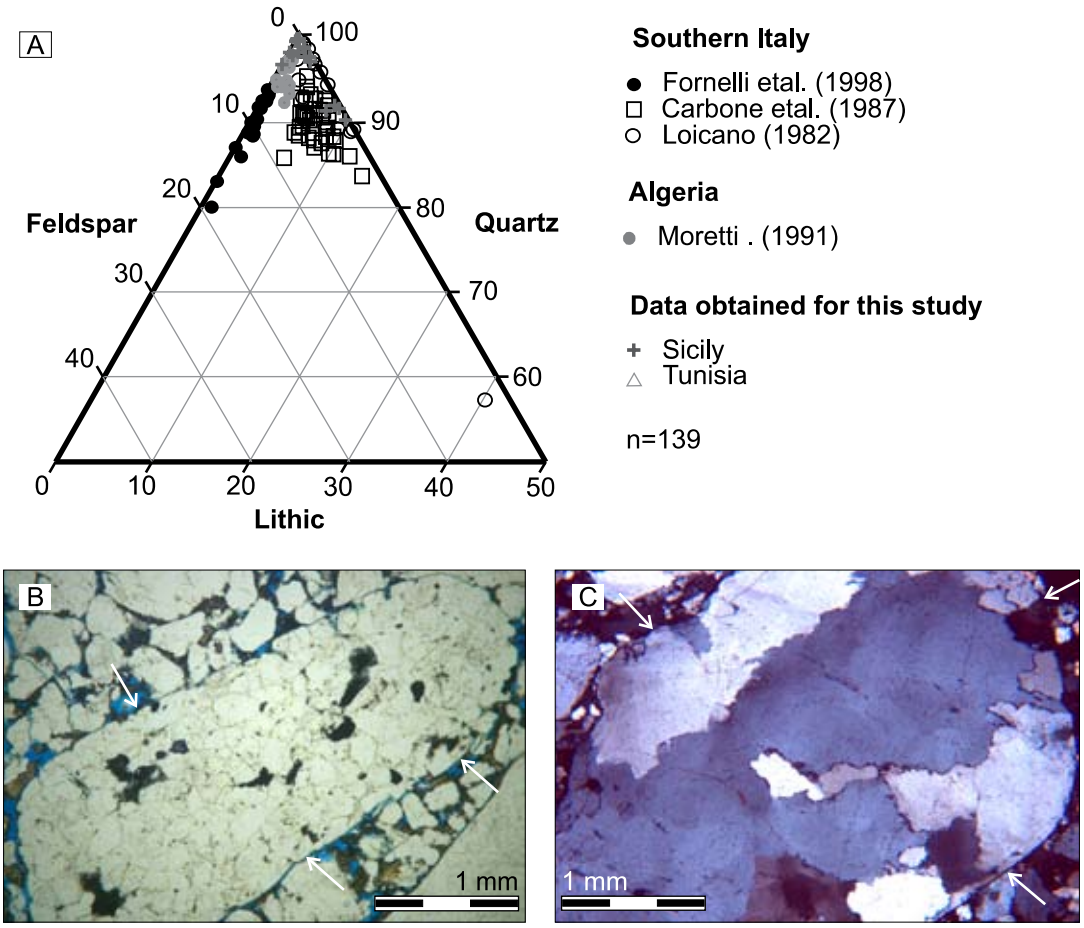

Figure 2.5.
A) Ternary diagram of literature samples from southern Italy and Algeria, and samples obtained for this study from Sicily and Tunisia. B) Plane polarised light photomicrograph of polycyclic Numidian Flysch quartz pebble, taken from the base of a channel complex, Finale, Sicily. C) Crossed polars photomicrograph of Quartz pebble showing internal pressure dissolution. From Cap Serat, Tunisia. Petrological abbreviations are: Q, quartz; Qp, Polycrystalline quartz; Qm, monocrystalline quartz; F, Feldspar total; Fk, Potassium Feldspar; L, Lithic grains.

well differentiated (Figure 2.5a) with samples of Fornelli (1998) mostly within the subarkose field, Loiacono et al. (1983) within the sublitharenite field, and Carbone et al. (1987) within the quartzarenite field. Chemical analysis by Fornelli and Piccarreta (1997) and Puglisi (1994) also plot samples in the sublitharenite and quartzrenite fields respectivley. Algerian (QFL) data from Moretti et al. (1991) plot completely within the quartzarenite region (Figure 2.5a). Similarly, observations from Sicily (Wezel, 1969), Tunisia (Yaich, 1992a), and Morocco (Leblanc and Feinberg, 1982) suggest a pure quartzarenite composition although no QFL data from either Morocco or southern Spain have been published. Italian deposits therefore show a distinction in terms of their composition currently not recognised in other localities. A strong grainsize bimodality within the quartz fraction is often recognised as a characteristic of the Numidian Flysch sandstones, typically with dominant populations of ~62μm (silt), and 250μm to 2 mm (medium sand to granule) (Wezel, 1969; Didon et al., 1984; Fornelli, 1998). Fornelli (1998) however differentiate a compositional bimodality of grainsize in Italy, between fine lithic grains of slate, chert and phyllite, and coarse lithic grains of granitoid material.

The few studies of Numidian Flysch shales have primarily focussed upon diagenetic overprinting in the context of the Sicilide basin (Dongarra and Ferla, 1982; Balenzano and Moresi, 1992; Aldega et al., 2007). Barbera et al. (2009) however add to the provenance debate with a statistical geochemi-

cal analysis of Numidian Flysch shales in comparison to internal shales of the Troina Tusa Flysch, the early Cretaceous Monte Soro Flysch, and the upper Cretaceous Scagliose Formations of Sicily. Discriminant analysis finds internal unit chemical ratios indicative of weathered paragneisses and phyllites, typical of the Hercynian metamorphic basement of the European Peloritan block (AlKaPe-Ca domain). Numidian Flysch shale chemical ratios show signatures indicative of heavily weathered cratonic sandstones in direct contrast to the internal units.

As part of this study, we performed x-ray diffraction and point counting (the Gazzi-Dickinson method) on 20 samples from northern and central Sicily and 4 from northern Tunisia, with 400 counts per slide. All samples plotted in the quartzarenite zone with an average bulk composition of Q92, F2, L6 (Figure 2.5) (See appendix 6 for raw data). The ranges of the three principle minerals from all samples are Q91-100, F0-3 and L0-10. Within the quartz fraction, polycrystalline grains show a range Qp1-68, and approximately equal percentages of orthoclase and plagioclase were counted throughout the samples. Our analysis reveals samples to contain minor quantities of rounded detrital glauconite, albite, anorthite, rare examples of bioclasts and a single example of rutile from Tunisia. Authigenic minerals include mica and chlorite, while abundant mud grains within the clastic matrix of many samples and not counted in our compositional analysis, represent mud rip-up clasts compatible with a turbidite origin as interpreted at outcrop.

Grainsize bimodality was also recognised, with a finer fraction of 100-300 μm and a coarser fraction of 500 μm to 2mm. The coarsest grains were found to generally consist of polycrystalline quartz (Qp) (Figures 2.5b and 2.5c) while the finer grains consist of monocrystalline quartz, and minor amounts of feldspar, glauconite, mica and lithic grains. Qp grains commonly show both internal pressure dissolution and quartz overgrowths, signifying a polycyclic origin and a previous burial compaction (Figure 2.5c). This polycyclicity has also been recognised in deposits of Tunisia (Fildes et al., 2010), Sicily (Wezel, 1969), Gibraltar (Lancelot et al., 1977) and Italy (Fornelli, 1998). Our outcrop studies in Sicily and Tunisia showed that facies rich in coarse grains are mainly found in poorly sorted conglomerates which are interpreted as frictional debris flow deposits and associated with large channel complexes (Figure 2.2b). Common turbidite deposits found away from chanellised bodies (Figure 2.2a) are generally finer grained such that grainsize bimodality in outcrop may therefore be attributed to the flow process involved and not directly to a distinct source or input to the basin.

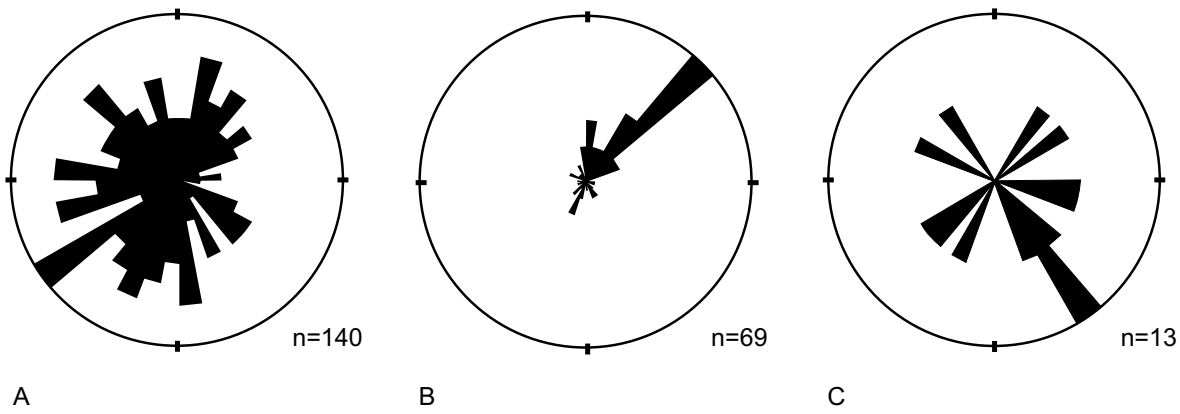

Figure 2.6.
Paleocurrent rose diagrams of the Numidian Flysch: A) Published data from Algeria, Tunisia, Sicily and southern Italy. See section 3.3 for references. B) Data measured for this study from the Madonie region of northern Sicily. C) Data measured for this study from northern Tunisia.

Both published data, and data sourced for this study were analysed using ternary plots (QFL, QmFL or QmQpF) (see figure 2.5 for abbreviation list) and normalised binary plot methods of Chiocchini and Cipriani (1996) (Fk/F : Q/Q+F, Qm/Q : Q/Q+F, Qm/Q : Fk/F). These methods failed to resolve Individual petrofacies populations based upon sample location or age. Comparison of the new data to the published QFL data from Italy and Algeria similarly failed to resolve definable differences, although in general, Tunisian, Sicilian and Algerian samples show slightly higher quartz percentages (average = 95%) than Italian samples which tend to contain more sedimentary lithic (Ls) or feldspar grains (average Q=90%).

2.3.3. Palaeoflow orientations of density flow deposits

A majority of publications concerning Numidian Flysch provenance have centred around palaeoflow orientations measured primarily from flute and sole marks on the base of density flow deposits. Palaeoflow orientations within the Numidian Flysch continue to be controversial, with published results from the same location differing by as much as 180° (Wezel, 1969; Parize et al., 1986; Parize and Beaudoin, 1987; Parize et al., 1999). Furthermore, an assumption is often made that average measured palaeoflow orientations directly represent the direction of the basin floor relative

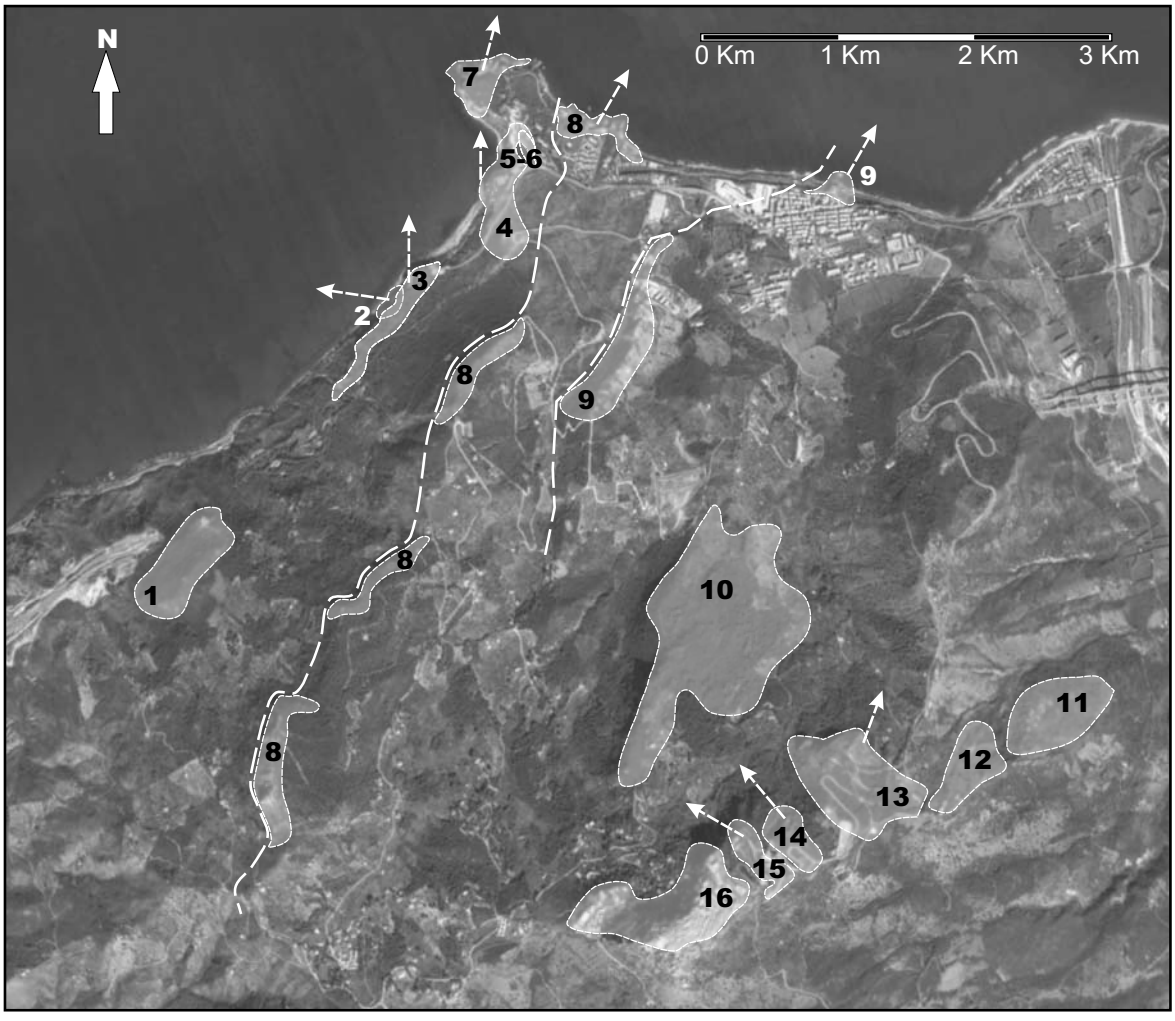

Figure 2.7.
Annotated satellite photograph of Capo Raisigerbi headland, northern Sicily. Sixteen incisional channel complexes, examined during fieldwork, are numbered sequentially with younging (i.e. 1 the oldest, 16 the youngest). The extent of each channel complex outcrop is marked in white, and the associated dominant paleocurrent orientation is shown such that a systematic paleocurrent swing is observed with younging. North is towards the bottom of the image. See section 2.3.3 for details.

to the location of flow initiation (e.g. Yaich, 1992a; Parize et al., 1999; Stow et al., 1999). On this basis several authors have proposed a northern or southern source based purely upon measured palaeoflow orientations.

A review of 140 published palaeoflow orientations from Algeria (Hoyez, 1975; Moretti et al., 1991; Laval, 1992; Vila et al., 1995), Tunisia (Hoyez, 1975; Parize et al., 1986; Parize and Beaudoin, 1987; Yaich, 1992a), Sicily (Wezel, 1969; Wezel, 1970b; Parize et al., 1986; Parize et al., 1999) and southern Italy (Carbone et al., 1987; Fornelli, 1998) suggests that no single orientation is dominant within the amalgamated dataset (Figure 2.6a). 102 palaeoflow orientations presented by Hoyez (1975) from Algeria and Tunisia (their figure 1) demonstrates the complexity of the problem with opposite sense flow orientations measured in very close proximity.

Sole marks, the preferred flow indicator, are surprisingly rare within Numidian Flysch exposures due perhaps to their lack of preservation in coarse grained sediment. For this study we recorded data mainly from basal flute marks with some data from dune scale cross beds, ripples and slump hinge orientations in locations in the Madonie national park of northern Sicily (Figure 2.6b), and at Tabarka, Cap Serat and Ras el Koran in northern Tunisia (Figure 2.6c). In northern Sicily a dominant northeast direction was recorded (mean vector of 17.6°) for density flow deposits (Figure 2.6c, n=69). This agrees well with data of Wezel (1969) and Wezel (1970b) but differs from Parize et al. (1986) and Parize and Beaudoin (1987) by approximately 150°. Data recorded for this study include flow orientations of nine large scale channel complexes in the area of Ponte Finale, Sicily (previously recognised by Johansson et al., 1998). Within the Sicilian channel complexes we measured a systematic palaeoflow swing of 90° from northwest to northeast, and back to northwest (with younging) through 450 m of stratigraphy (Figure 2.7). This is interpreted as sinuosity of the channel complex system. Mapping of the channel complexes using aerial photographs (Google earth) shows an outcrop trend towards the NW and NE in agreement with measured flow orientations. Northerly measurements from Numidian Flysch deposits of central Sicily (Contrada di Romana) are in agreement with Johansson et al. (1998) who recognised the section to be overturned. The orientations presented here disagree with data of Parize et al. (1986) and Parize and Beaudoin (1987) by approximately 160°.

Measurements we recorded in Tunisia (n=13) are wide ranging with a mean vector of 141° (Figure 2.6c). As suggested by Hoyez (1975) it cannot be said with confidence what the dominant pal-

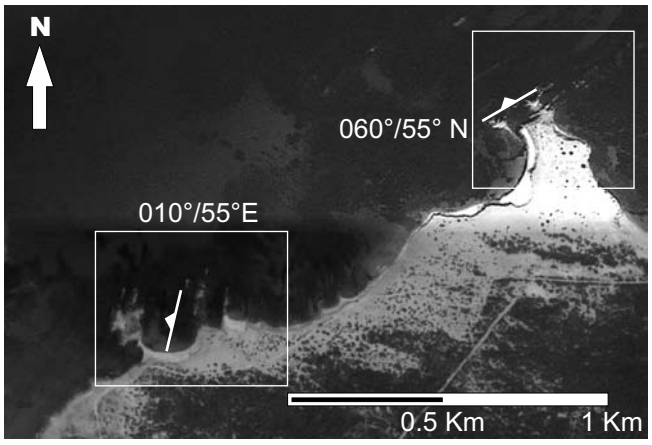

Figure 2.8.
An aerial photograph of the Ras el Koran section, northern Tunisia which demonstrates a 50°change in strike over 1.5 km of coastal section.

aeocurrent orientation is. We also observed during this field study that the Ras el Koran section, northern Tunisia undergoes a 50° variation in the strike of the beds over 1.5 km in an east to west coastal transect, subsequently confirmed using aerial photographs (Figure 2.8). It is noted that this is the section from which Yaich (1992a) measured southwards palaeocurrent orientations. This observation, and the general lack of a statistically significant palaeocurrent orientation, places doubt on the reliability of measurements from this locality and others.

2.3.4. Detrital zircon chronology

Detrital zircons from the Numidian Flysch of Spain, Gibraltar and Sicily have been dated by Lancelot et al. (1976) and Lancelot et al. (1977). Two populations are defined, with 90 to 95% of zircons representing ages of 1830±100 Ma and 5-10% of zircons representing ages of 1350±60 Ma. In

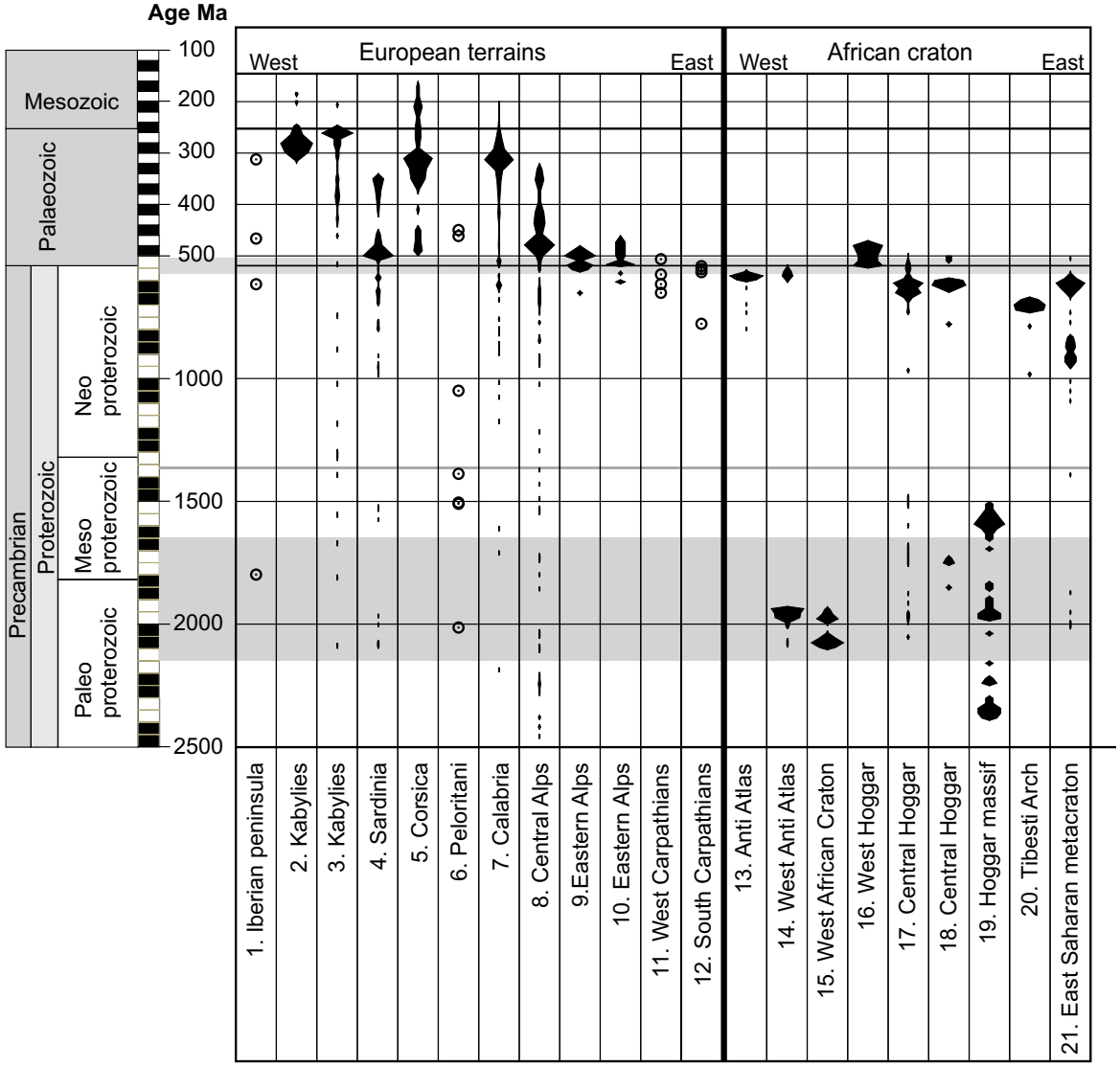

Figure 2.9.

Frequency histograms of zircon age ranges from possible Numidian Flysch basement source rocks. Numidian Flysch detrital zircon age ranges, highlighted in grey, are taken from Lancelot et al. (1976), Lancelot et al. (1977), Gaudette et al. (1975), Gaudette et al (1979), and unpublished data from Anadarko Exploration (see section 3.4 for details). Zircon ages of basement areas are taken from: 1) Lancelot et al. (1985); 2) Hammor et al. (2006); 3) Peucat et al (1996); 4) Giacomini et al. (2005); 5) Rossi et al. (2003); 6) Trombetta et al. (2004); 7) Micheletti et al. (2008); 8) Schaltegger (1993); 9) Neubauer (2002); 10) Neubauer (2002); 11) Neubauer (2002); 12) Neubauer (2002); 13) Ingliss et al. (2004); 14) Walsh et al. (2002); 15) Peucat et al. (2005); 16) Paquette et al. (1997); 17) Bertrand et al. (1986); 18) Abdallah et al. (2007); 19) Peucat et al. (2003); 20) Suayah et al. (2006); 21) Kuster et al. (2008). Where it was impossible to construct frequency histograms through a lack of points, circles are placed to denote age data.

both cases the populations are interpreted as having an extrusive volcanic morphology. Zircon dates from the Numidian Flysch of northern Tunisia obtained by Gaudette et al. (1975) and Gaudette et al. (1979) are found in the range of 1750±100 Ma. In comparison, Fildes et al., (2010) present much younger ages of 514 ± 19 Ma, and 550 ± 28 Ma from the Numidian Flysch of Tunisia and Sicily.

Figure 2.9 shows detrital zircon age ranges for the Numidian Flysch in comparison to a review of published U/Pb zircon ages taken from basement units around the western Mediterranean. European terrains presented include basement of the European craton from Iberia, the central Alps of Italy, the Carpathians and the Serbomacedonian massif (see figure 2.9 for references). Also presented are basement terrains of the AlKaPeCa domain, which represents the basement to the northern orogenic wedge (Calabria, Peloritan, Kabylies, Corsica, Sardinia). Included within the African terrains are the West African craton and basement to its west, the Hoggar and Tibesti massifs, and the east African craton.

Data are presented in the format of frequency histograms such that it is apparent that basement ages from African terrains do not contain U/Pb zircon dates younger than mid Ordovician, and a majority of dates lie within the Panafrican and Eburnian age ranges (550-650 Ma and 2Ga respectively (Bertrand et al., 1986; Guiraud et al., 2005; D'Lemos et al., 2006). In contrast, European terrains show peak zircon frequencies of Cambro-Ordovician age (ie 450 – 550 Ma), and Carboniferous to Permian age (ie 350-250 Ma, Hercynian ages). Exceptions to this trend are Hercynian age zircons found within intrusions of the southern Sinai (Kohn et al., 1992) and within the Morocco Hercynian chain (Tahiri et al., 2007) of North Africa. While the Moroccan Hercynian deformation chain is significant, intrusions within it are relatively small and are found predominantly on the Atlantic margin, while apatite fission track data from Saddiqi et al., 2009 suggests that they were uplifted and heavily eroded in the Jurassic and early Cretaceous. For these reasons they are considered of limited importance to this study.

The AlKaPeCa domain Kabylie blocks of northern Algeria are particularly well studied using U/Pb zircon dating, and a number of key events in their evolution are recorded. Data from the Kabylie blocks is summarised as a case study in figure 2.10. As with figure 2.9, zircon ages of up to 2.1 Ga are recorded (Peucat et al., 1996). However, most key dates lie within the age range of the Hercynian event (225-450 Ma (Bossière and Peucat, 1985; Peucat et al., 1996; Festa et al., 2006)) as Laurasia collided with Gondwana, which was recorded in the Kabylie blocks by a magmatic phase, regional metamorphism and subsequent crustal thinning (Schaltegger, 1993; Peucat et al., 1996; Hammor et al., 2006). The youngest dates observed relate to the Oligocene to Miocene Alpine continental collision and subsequent tectonic unroofing (Lonergan and White, 1997; Cheilletz et al., 1999; Hammor et al., 2006). The Cretaceous eo-Alpine orogeny and Alpine events are also recorded in zircons from the European Peloritani, Calabrian and Sardinian domains (Cheilletz et al., 1999; Hammor et al., 2006, and references therein).

2.4. Drawing conclusions about Numidian Flysch provenance

2.4.1. Is the Numidian Flysch sourced from a single region?

Given the vast regional extent and long duration of Numidian Flysch deposition, the question arises as to whether the Numidian Flysch represents a single source region. Given the many suggestions

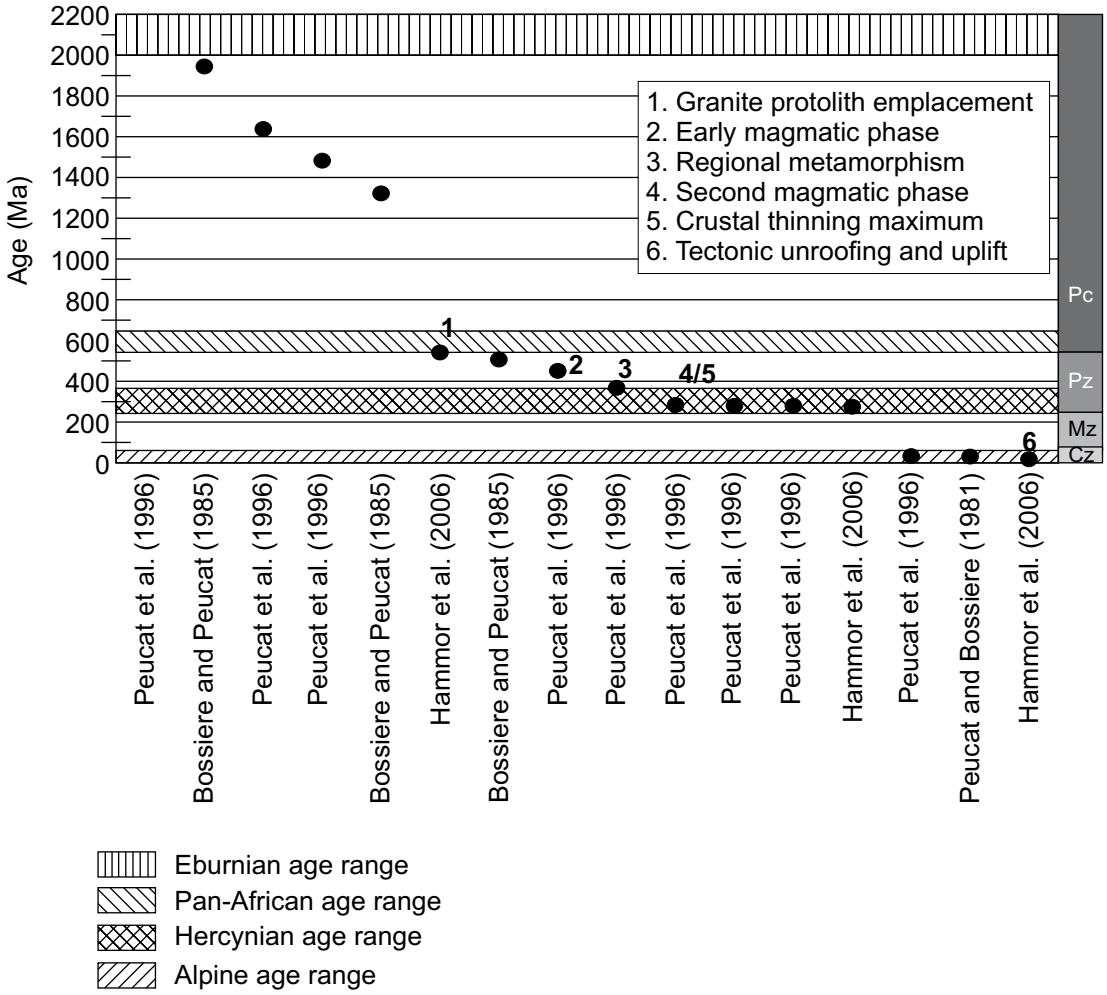

Figure 2.10.
Key published Ur/Pb zircon ages from the European Kabylie blocks of northern Algeria, with associated interpretations. The age ranges of key European and African tectonic events are included: Pc, Precambrian; Pz, Paleozoic; Mz, Mesozoic; Cz Cenozoic.

of both a European and African source, the possibility remains that sediment is sourced from both the north and south. Laval (1992) also suggested a new source area to the north of the Kabylie block (AlKaPeCa) in order to account for complications arising from the Numidian Flysch being interpreted to sit conformably above the internal Kabylie blocks (see section 2.3.1.2).

The similarity of the Numidian Flysch petrofacies throughout the western Mediterranean suggests that the Numidian Flysch is a formation sourced from either a single region, several regions with a very similar lithology, or distant source regions coupled with a transport history long enough to remove minerals less stable than quartz (e.g. Garzanti et al., 2007). Comparison of Numidian Flysch mineralogy with contemporaneous units of the Mauretanian flysch subdomain also reveal a stark difference, with northern deposits enriched in volcanic and metamorphic clasts (e.g the micaceous and immature sandstones of Algeria, Tunisia and Sicily (Laval, 1992; Belayouni et al., 2010) and the Tufiti di Tusa formation of Sicily and Italy (<30% quartz) (Pescatore et al., 1992; de Capoa et al., 2002). This implies a gross disparity of source region with the consistently ultramature Numidian Flysch sandstones. Minor percentages of volcanic and metamorphic clasts in Numidian Flysch sands from southern Italy (Figure 2.5a) have been interpreted in terms of foredeep mixing of the Numidian Flysch, and a metamorphic/volcaniclastic facies sourced from Sardinia and Corsica (Fornelli and Piccarreta, 1997), rather than representing source region lithology. The depositional location of southern Italian deposits is also rather distinct from that of North Africa, representing the

southern border of the Lucanian ocean, and thereby creating the potential for mixing of axial sediments from the Lucanian foredeep with those of the MFB (Fornelli and Piccarreta, 1997; Fornelli, 1998). Regardless of indicating a specific source area, the north-south compositional disparity provides compelling evidence that the Numidian Flysch facies throughout the chain is sourced from one region (whether northern or southern) with the immature arenaceous facies of Mauretanian subdomain sourced from a separate region. Coupled with this, the inability to differentiate sandstone samples from Algeria, Tunisia and Sicily using ternary and binary plots, suggests that the Numidian Flysch does not represent sediment sourced from both the northern and southern margins of the basin concurrently. It is interpreted therefore that the compositional homogeneity indicates a single source for the Numidian Flysch sandstones.

2.4.2. A northern or southern source?

As with the homogeneous petrological characteristics of the Numidian Flysch (Figure 2.5), the structural position of Numidian Flysch nappes is similar throughout the entire Alpine chain (Figure 2.4). A trend from south to north of African margin units, Numidian Flysch nappes, immature arenaceous and argillaceous flysch nappes, and European crystalline basement is recognised, and constrained most clearly in Sicily. African units consist of carbonate platforms in Italy and Sicily, continental to marine Tellian facies in Tunisia and Algeria, and similar rocks in Morocco. Immature arenacous and argillaceous units thrust above the Numidian Flysch are recognised as the Tufiti di Tusa and Troina Tusa Formations of Sicily and southern Italy, the Galite Flysch in Tunisia, undifferentiated micaceous flysch of northern Algeria, and metamorphic clast rich sandstones of the Algeciras, Beni Ider, Bolonia and Tala Lakraa units in Morocco and Spain. Therefore, a location of deposition between the Mauretanian subdomain and the African margin units is well resolved. Confirmation in Tunisia of an allocthonous contact between the Numidian Flysch and African Tellian units also places the Numidian Flysch in the same external position of the MFB. The nature of the contact between the Numidian Flysch and the internal Kabylie block in Algeria mirrors this debate, and biostratigraphic dating suggests a backthrust contact between the two units (Magné and Raymond, 1972; Lahondére et al., 1979). Given the similarity of the petrofacies and structural position of the Numidian Flysch throughout the rest of the chain, placing the Numidian Flysch basin to the north of the Kabylie block in Algeria as suggested by Laval (1992) is considered highly unlikely. A backthrust geometry which places the Numidian Flysch above the Kabylie block would again place Numidian Flysch nappes in a position similar to the remainder of the Alpine chain (Figure 2.4). The recognition of a continental and shallow marine environment, coeval with Numidian Flysch deposition in the Kabylie domain (Raymond, 1976; Géry, 1983) also affirms this interpretation. The recognition of micaceous flysch by Andrieux et al. (1989) above the petit Kabylie also suggests a very similar structural sequence as in the rest of the chain. Despite the Algerian debate, it is noticeable that studies concerned primarily with correlating stratigraphic and tectonostratigraphic units of the entire MFB consistently point to an external location for the Numidian Flysch and an internal position for Mauretanian flysch, and by default an African and AlkaPeCa source region respectively (Puglisi, 1987; Guerrera et al., 1993; Balogh et al., 2001; Puglisi et al., 2001; de Capoa et al., 2002; de Capoa et al., 2004; Guerrera et al., 2005; de Capoa et al., 2007).

The regional definition of Mauretanian and Massylian subdomains based upon contrasting petrofacies further suggests that the Numidian Flysch source region is different to that of the internal Mauretanian flysch. QFL analysis of the reviewed data plots Numidian Flysch sandstones within the cratonic source zone as suggested by Folk (1951) and Dickinson and Suczek (1979). Their large regional extent, homogeneity and polycyclic nature indicates reworking of a laterally exten-

sive quartzarenite sandstone, again indicative of a cratonic region. Statistical geochemical analysis of Numidian Flysch shales (Barbera et al., 2009) similarly finds a compositional contrast against the mudstones of Mauretanian units, with a composition indicative of a highly weathered cratonic sandstone source which is in good agreement with the sandstone modal analysis. In contrast, the mineralogy of Mauretanian flysch sandstones appears well constrained to the AlKaPeCa domain. Igneous grains including phyllites and granites, reported in Mauretanian flysch deposits from southern Spain, Morocco and southern Italy match lithologies of the AlKaPeCa domain, and are interpreted as sourced from them (Mazzoleni, 1991; Fornelli and Piccarreta, 1997; De Galdeano et al., 2006). Mauretanian sandstones rich in volcanic grains are similarly interpreted as being sourced from the AlKaPeCa magmatic arc to their immediate north (Ferla and Alaimo, 1976; Pescatore et al., 1992; Balogh et al., 2001; Puglisi et al., 2001; Puglisi, 2008). Analysis of Mauretanian unit shales in Sicily similarly assigns a Peloritan block (AlKaPeCa) provenance, interpreted as paragneiss and phyllite source rocks (Barbera et al., 2009). Despite these lithological connections strongly suggesting an African source for the Numidian Flysch quartz, various authors have recognised relatively minor amounts of quartz sands in the transgressive cover to the AlKaPeCa domain (Bossière and Peucat, 1986). Critelli et al. (2008) describes Triassic fluviatile redbeds from the internal zones of the Betic, Magrebian and Apennines which are quartzarenitic or quartzolithic. They transgress upon, and are derived from Hercynian AlKaPeCa basement blocks, and are subsequently enriched in quartz through weathering processes. Caire and Duée (1971) also compared thermoluminescence curves from Numidian Flysch quartz with sediments of the Kabylie and Peloritan blocks, concluding that Sardinia represents an alternative source region for quartz pebbles within the Numidian Flysch.

U/Pb zircon data is perhaps the most unequivocal indicator of provenance available in this study. Providing a representative volume of the source rock is weathered, and given that specific age populations cannot be preferentially removed during transport, it is expected that sediment sourced from any terrain will contain a representative frequency distribution of zircon ages as recorded by the host rock(s). Sampling of localised areas may however not reflect regional age populations, and bias associated with preferential sampling of certain areas, due to factors such as accessibility, may distort regional populations. The three main age populations within the Numidian Flysch (Palaeoproterozoic, upper Mesoproterozoic, and upper Neoproterozoic to Cambrian) define a source in which: (a) The Eburnian and Panafrican events are represented; (b) Neither the Hercynian or Alpine events are represented.

While African basement contains only Cambrian and Precambrian zircon ages, some European basements reviewed contain minor frequencies of Precambrian zircons, and relatively high frequencies of Panafrican age zircons (550-650 Ma) (Figure 2.9). Lancelot et al. (1985), Schaltegger (1993), Micheletti et al. (2008) and Fiannacca et al. (2008) all interpret panafrican zircons from European metasediment basement in Iberia and Calabria to be representative of detrital sediments sourced from the African craton and transported north during Gondwanan times, rather than a European record of the panafrican event. A case study review of the Kabylie blocks of northern Algeria demonstrates that despite the presence of Precambrian zircons, a majority of zircons are within the age ranges of the Hercynian and Alpine events (Figure 2.10). This profile has similarly been recognised in the Peloritan and Calabrian blocks (Figure 2.9), and effectively exempts these AlKaPeCa domain blocks as suitable source regions, despite the presence of some quartz rich material. Lancelot et al., (1985) did however record Hercynian age zircons from the immature Troina Tusa Flysch Formation of Sicily (termed the Gréso micacé in that study), deposited within the Mauretanian subdomain and contemporanoues with the Numidan Flysch (Section 2. 3.1.1 and Figure 2.4). In contrast, data from the African craton show a very good general correlation to Numidian Flysch

detrital data. In particular, dates from the Moroccan fringes of the west African craton and the Hoggar (Bertrand et al., 1986; Paquette et al., 1997; Walsh et al., 2002; Peucat et al., 2003; Peucat et al., 2005; Abdallah et al., 2007) correlate well with the 1830±100 Ma population of Lancelot et al. (1977) from Spain and Sicily, the 1750±100 Ma population of Gaudette et al. (1975) and Gaudette et al. (1979) (Tunisia), and the 514 ± 19 Ma, and 550 ± 28 Ma ages of Fildes et al. (2010). The minor population of extrusive volcanic zircons centred upon 1350±60 Ma is a common date found in central and southern Africa (Milner et al., 1995; Jerram et al., 1999; Becker et al., 2006 etc), but is however not well matched in the data we have reviewed in North Africa.

Given the Cambrian to Precambrian constraints of detrital zircon ages, the cratonic petrofacies of both Numidian Flysch sandstones and Numidian Flysch shales, and the external position within the nappe pile, a northern AlKaPeCa source is effectively negated. Overall, this provides a clear correlation of African sourced Numidan quarzarenites (the Massylian subdomain) and AlKaPeCa sourced deep marine clastics with a compositionally immature character (the Mauretanian subdomain). However, while our review gives no dominant conclusion to the palaeocurent debate, several works consisting of more localised data sets do give consistent orientations leading to interpretations, primarily, of southerly directed flow from a northern source (e.g. Parize et al., 1986; Parize and Beaudoin, 1987; Laval, 1992; Parize et al., 1999; Fildes et al., 2010). The apparent contradiction between these results and the bulk of evidence suggesting a southern source, is addressed below (section 2.2.4.3).

2.4.3. The viability of the palaeocurrent debate

There is an underlying assumption within the palaeoflow debate that the average flow orientation is indicative of the direction from flow source (eg shelf or slope environment) to the location of deposition (eg the lower slope or basin floor). In this manner, the direction of flow transport denotes the dip direction of the basinal slope. This interpretation has previously been challenged by Hoyez (1975), and a number of arguments exist that challenge this assumption which is inherent to the palaeoflow debate.

The large scale palaeocurrent study of Hoyez 1975 (n=102) and the data presented here (n=140) suggest that on a basin scale there is no statistically significant average palaeoflow orientation (Figure 2.6a). A majority of studies based upon palaeocurrent data focus upon specific localities however, and it remains possible that location specific studies record a local palaeodip-slope, which over the length of the 2000 km basin could be highly variable. A review of analogue basins suggests that flow orientation within foreland basins is indeed highly variable and does not represent the slope dip direction. Examples of the Quaternary Barbados accretionary prism, the Tertiary Alpine, Apennine and Pindos basins, the Cretaceous Magellanes basin in Chile, and the Permian Arkoma basin from the central United States, show that a majority of flow orientations measured at outcrop run parallel to the basin strike and not perpendicular to it (Ross and Houseknecht, 1987; Sutherland, 1988; Faugères et al., 1993; Sinclair, 1997; Avramidis and Zelilidis, 2001; Mutti et al., 2003; Cibin et al., 2004; Shultz et al., 2005). An arcuate geometry as found in the Tertiary Alpine basin would therefore produce palaeoflow variations that mirror variations in basin strike, with a systematic 120° change throughout the length of the basin (Sinclair, 1997). The Sicillide portion of the MFB is interpreted during the Oligocene to have a >50° arcuate geometry (Figure 2.12) and a similar variation in flow direction may therefore be expected. Studies of flow deposits which are proximal to the basin margins however, often document orientations which are at a high angle to the basin strike (Cainelli, 1994; Sinclair, 1997; Avramidis and Zelilidis, 2001; Eschard et al., 2003)

and these deposits represent flows deposited on the basin slope rather than the basin floor. The context of flow orientation measurements is therefore vital prior to interpretations of basin architecture. Furthermore, on a scale substantially less than that of the basin, density flow systems in slope settings demonstrate a high degree of variability. The systematic 90° variability of Numidian Flysch palaeoflow observed within a 5 km wide, 450 m thick channel system in northern Sicily illustrates this problem (Figure 2.7), and indeed observation of modern slope systems demonstrates that many channel systems can be highly sinuous in nature (Peakall et al., 2000; Deptuck et al., 2007; Wynn et al., 2007). Submarine slope systems are also often highly structured, as in the passive margin examples of Angola (Fraser et al., 2005; Gee et al., 2007), the Niger delta (Heinio and Davies, 2007), and the Nile delta (Samuel et al., 2003). In these examples, salt or mud diapirism, regional tectonics, en masse gravitational sliding of the entire slope system, and the local effects of mass wasting can have a considerable impact upon the transport direction of both channel systems and unconfined density flows (Haughton, 2000; Shultz and Hubbard, 2003; Ferry et al., 2005). Channel system orientations in active margin settings are similarly observed to be controlled primarily by thrust-fault segmentation, giving rise to ponded basins in the hanging wall synform, in which reflection of turbidity currents from topography is increasingly being recognised (Faugères et al., 1993; Huyghe et al., 2004; Estrada et al., 2005; Mutti et al., 2009).

A further level of complication arises during emplacement of Numidian Flysch nappes upon the African foreland. Numidian Flysch channel outcrops in central Sicily have been shown to be overturned (Johansson et al., 1998), and in Ras el Koran, northern Tunisia, the Numidian Flysch stratigraphy is observed to change strike by 50° (Figure 2.8) suggesting that structural emplacement has involved rotation. Indeed, several palaeomagnetic studies in Sicily and southern Italy (Channell et al., 1990; Oldow et al., 1990; Speranza et al., 2003; Monaco and De Guidi, 2006) have demonstrated a 70° clockwise rotation of the nappe pile from the Langhian (immediately post Numidian Flysch) until the end of continental collision in the late Tortonian (Monaco and De Guidi, 2006) while in central Italy an anticlockwise rotation has been described (Maffione et al., 2008). Nappe pile rotations of between 55° and 76° have also been reported for the Moroccan and Spanish sectors of the MFB (Lonergan and White, 1997 and references therein).

Despite sedimentary complications, the effect of both basin and outcrop scale tectonics renders palaeocurrent evidence highly unreliable. Given the considerable problems, the provision of a northern AlKaPeCa source in certain localities can be largely dismissed. Constraints by zircon chronology, sandstone and mudstone petrology, and location within the nappe pile, suggest that an African craton source remains the only viable option.

2.5. Implications of a constrained African source

2.5.1. Possible African source regions

The Continental Intercalaire (Ivaldi, 1977; Lancelot et al., 1977; Moretti et al., 1991) and Pharusian series (Moretti et al., 1991) of western and central Africa, the Nubian sandstone of the Sirt basin in Libya (Wezel, 1970a; Johansson et al., 1998) and Permo-Triassic and Cambro-Ordovician continental sandstones of southern Tunisia (Gaudette et al., 1975; Gaudette et al., 1979) have all been suggested as source terrains for the Numidian Flysch (Figure 2.3). A review of zircon age ranges (Figure 2.9) suggests that the western Anti Atlas of Morocco, the West African craton and the Hoggar massif all provide a good correlation with Eburnian age detrital zircons of the Numidian Flysch.

Zircon ages of the west and central Hoggar also provide a match to panafrican age detrital zircons from the Numidian Flysch. The minor population of volcanic Numidian Flysch zircons centred upon 1350±60 Ma is a common date found in central and southern Africa (Milner et al., 1995; Becker et al., 2006) but not in North Africa. The possibility remains that a Mesoproterozoic volcanic source exists in North Africa that has yet to be sufficiently dated, else long distant transport from central Africa must be invoked. While these cratonic basement terrains are likely candidates for the origin of Numidian Flysch zircons, the polycyclic nature of Numidian Flysch sediments require that they do not represent first cycle sediments but reworked sandstones which have previously undergone burial compaction (see section 2.3.2) (Figure 2.5c).

The oldest abundant quartz rich sandstones in North Africa are first cycle mature quartz sands (75-100% quartz) of Cambro-Ordovician age found in Morocco, Algeria, Libya and east to the Persian Gulf (Avigad et al., 2005; Ghienne et al., 2007). They contain zircons from the entire Proterozoic and upper Archean, with suites of mainly Neoproterozoic age (0.5-1.25 Ga), upper Palaeoproterozoic to mid Mesoproterozoic (1.6-2.0 Ga) and upper Neoarchean to lowermost Palaeoproterozoic (2.4-2.8 Ga), in very good agreement with Numidian Flysch zircon age ranges (Figure 2.9) (Avigad et al., 2003, their figure 3; Avigad et al., 2005). The sands were eroded during continental scale uplift of basement during the panafrican orogeny (Avigad et al., 2005) and sustained significant reworking towards the north during the Cambro-Ordovician glaciation (Ghienne and Deynoux, 1998; Moreau et al., 2005). The Pharusian is a similar series which infills topography generated during transpression and Neoproterozoic intrusion events in the western Hoggar and West African craton (Caby, 2003). Fluvial, alluvial and deltaic sediments were fed into molassic basins (Ahmed and Moussinepouchkine, 1987), while volcanic greywackes were fed into deeper basins (Caby et al., 1977).

The original definition of the term Continental Intercalaire describes continental sediments deposited throughout Algeria, Tunisia and Libya, deposited between the Namurian (lower Carboniferous) and upper Cenomanian marine series (Kilian, 1931). Continental Intercalaire sediments crop out between the Hoggar and the West African craton, between the Hoggar and the Algerian Atlas belt, and in the Ghadames basin of Libya and Tunisia (Lefranc and Guiraud, 1990). Significant quartz rich sandstones are also found in the lower Triassic and Early Cretaceous continental sediments of the Oued Mya basin, central and northern Algeria, and in Early Cretaceous sediments of west Algeria and Libya (Lefranc and Guiraud, 1990). Triassic sediments of the Berkine basin (Algeria) filled topography of the Hercynian unconformity, and contain thick fluvial sequences with an average composition of 88% quartz (Rossi et al., 2002). These Triassic sandstones are interpreted to be sourced from pre-Hercynian sequences, and basement rocks of the Hoggar (Rossi et al., 2002).

Numidian Flysch sediment shares both zircon and petrological characteristics with sediments of the Cambro-Ordovician and Continental Intercalaire sandstones. Both of these extensive series are interpreted as being sourced from the Hoggar massif and other cratonic basement. It seems likely therefore that the Numidian Flysch may be a reworking of these sandstone series which today crop out in southern Tunisia and central Algeria. While it is not possible to further constrain individual source areas, the Numidian Flysch may be considered a reworking of African continental series by Cenozoic northwards draining fluvial systems.

2.5.2. Location and timing of Numidian Flysch sediment input

2.5.2.1 Timing of deposition versus basin tectonics

Outcrop maps compiled by Wezel (1970a) suggest that Numidian Flysch sediments are concentrated in northern Morocco, and in a zone from eastern Algeria to southern Italy (Figure 2.1).

Oligocene to mid-Miocene Numidian Flysch deposition is observed throughout the western Mediterranean (Lahondére et al., 1979; Moretti et al., 1991; Torricelli and Biffi, 2001) although important diachreneity is observed. In the Algerian-Tunisian and Spanish-Moroccan sections of the basin, deposition occurs from the lower or mid Oligocene, while in the Sicilide basin deposition commences from the Oligocene–Miocene transition, some 5 Myrs later. In the Algerian-Tunisian portion of the basin, deposition ceases by the Burdigalian, while continuing until the mid Miocene throughout the remainder of the basin. The Sicilide basin thus only records early to mid Miocene age sediments (Carbone et al., 1987; Faugères et al., 1992).

Southwards migration of the AlKaPeCa domain and the related allocthony since the Oligocene (Cassola et al., 1991; Puglisi et al., 2008) have displaced Numidian Flysch deposits significantly from their depositional locations (Geel and Roep, 1998; Speranza et al., 2003). Moroccan deposits were thrust westwards infront of the Alboran plate while Sicilide deposits were thrust eastwards and then southwards by as much as 200 km, in front of the Peloritan and Calabrian blocks (Geel and Roep, 1998; Speranza et al., 2003; de Capoa et al., 2007) (Figure 2.12). The basin closed in Algeria and Tunisia as the continental Kabylie and Galite blocks docked with the African margin from the latest Oligocene until the Burdigalian (Caby, 1996; Cheilletz et al., 1999; Mauffret et al., 2004). Numidian Flysch deposition in Algeria and Tunisia therefore ended earliest, in the latest Aquitanian to earliest Burdigalian, correlating with the time of basin closure (Figures 2.11 and 2.12).

Continental collision and basin closure in the Moroccan and Sicilide sections of the basin occurred much later than Algeria and Tunisia, being roughly contemporaneous in the Serravelian (de Capoa et al., 2004; de Capoa et al., 2007) (Figure 2.11). While deposition in Morocco and Spain occurs throughout the Oligocene and Miocene, in the Sicilide basin the onset of deposition correlates with the timing of closure of the Tunisian and Algerian sector of the basin, suggesting that sediment was routed laterally away from the closing basin towards Sicily (Figure 2.12). Sicilide deposition ends in the latest Burdigalian to Langhian (Didon et al., 1984; Faugerès et al., 1992), roughly coincident with the end of Spanish and Moroccan deposition.

2.5.2.2 The location and style of sediment input

One of the key arguments against an African source region has been the lack of a suitable sediment pathway from the African craton to the southern margin of the MFB (Caire and Duée, 1971; Hoyez, 1975; Parize et al., 1999). Wezel (1970a), originally suggested a Nubian source from the Sirt basin in Libya, and invoked sediment bypass across the Libyan continental shelf through a channel system. Such a system has however not been observed. Structural juxtaposition of the deep marine Numidian Flysch with sandstones of the shallow marine Bejaoua Group in Tunisia (Figure 2.4), has led to the suggestion that feeder channels were present in northern Tunisia, perhaps also responsible for propagating sediments towards Algeria along the basin axis (Wezel, 1970a; Wildi, 1983). In eastern Tunisia, the Fortuna Delta, suggested as a candidate for sediment feeding (Benomran et al., 1987; Johansson et al., 1998), has subsequently been questioned due to its east and south palaeoflow towards the Pelagian basin (Vanhouten, 1980), its compositional immaturity (Yaich, 1992b) and dating, which suggests pebble rich horizons do not correlate with clastic periods within the Numidian Flysch basin (Yaich et al., 2000). Detrital zircon data from the

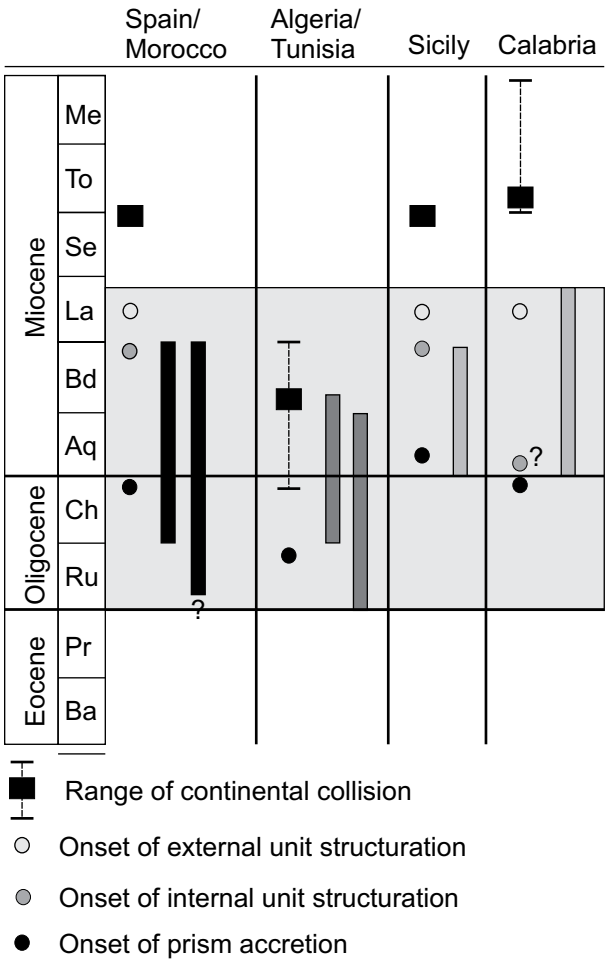

Figure 2.11.
Age ranges of Numidian Flysch deposition in comparison to regional tectonic events. Spain, Gibraltar, Morocco data from: Didon et al. (1984); Kaminski et al. (1996); Stromberg and Bluck (1998); deCapoa et al. (2007). Algeria, Tunisia data from: Magne and Raymond (1974); Lahondere et al. (1979); Moretti et al. (1991); Caby (1996); Cheilletz et al. (1999); Toricelli and Biffi (2001); Mauffret et al. (2004); Guerrera et al. (2005); Boukhalfa et al. (2009). Sicilide basin data from: Cello and Mazzoli (1999); Bonardi et al. (2003); Artoni (2007); deCapoa et al. (2007); Iannace et al. (2007); Maffione et al. (2008); Putignano and Schiattarella (2008), and biostratigraphic data obtained for this study (see section 2.2).

Fortuna Delta shows ages of 1698 ±67 Ma (Fildes et al., 2010) which, although significantly different from the Numidian Flysch detrital zircons of Fildes et al. (2010), are similar to Numidian Flysch data from Lancelot et al. (1977) and Gaudette et al. (1979). The interpretation of structureless massive sandstones filling submarine channels and produced by sustained, steady (or near-steady) state flows in northern Sicily (Johansson et al., 1998), also implicitly requires hyperpycnal input from a river to the deep basin. In Algeria, Vila et al. (1995) has suggested a major sediment input point from the interpretation of deep-marine channelised sandstones in Numidian Flysch deposits. In Morocco, Geel and Roep (1998) point out that westward migration of the Alboran plate may have detached Numidian Flysch deposits from an Algerian or Tunisian input point, such that a separate feeder system is not required. The feeder-system models proposed in these studies require that established and isolated fluvial drainage systems transported sediment into the basin, although with the exception of the Fortuna Delta, large-scale contemporaneous fluvial or deltaic deposits have yet to be reported. It remains possible that other such deposits are buried beneath allocthonous units of the Alpine chain or else removed by the forebulge unconformity, however this remains a problem for the African source model.

An increasing number of outcrop, morphological, and seismic studies are recognising submarine fan systems that were active during relative or eustatic highstand conditions (Mitchum and Van Wagoner, 1991; Clark, 1995; Weber et al., 1997; Weber et al., 2003; Pattison, 2005; Carvajal and Steel, 2006; Covault et al., 2007; Shanmugam, 2008; Uroza and Steel, 2008) such that low stand fan systems represent only a portion of the deep marine sequence stratigraphic model. In transgressive to relative highstand conditions, a range of mechanisms have been suggested to loft sediment from a shelf environment and transport it basinwards without the need of direct shelf feeder systems. Studies by Shanmugam (2008), Stow and Mayall (2000), El Kadiri et al. (2006a) suggest that flooding of the shelf during the initial transgression, and storm events, Tsunami and longshore currents during highstand conditions are capable of debouching large volumes of sediment from the shelf to the slope.

Figure 2.13 correlates Numidian Flysch depositional periods with the global Cenozoic Oxygen

isotope curve of Zachos et al. (2001) and the sealevel curves of Haq et al., (1987) and Van Sickel et al. (2004). Negative Oxygen isotope trends are indicative of global cooling from the Palaeocene-Eocene thermal maximum (Zachos et al., 2001; Abreu and Haddad, 1998; Ernst et al., 2006; Sluijs et al., 2008). The Eocene then records a low order cooling, which is reversed in the late Oligocene similarly recorded by negative Oxygen isotope trends (Zachos et al., 2001) (Figure 2.13). Numidian Flysch deposition therefore occurred during a low-order glacioeustatic transgression, recognised in outcrop studies throughout the entire western Mediterranean (Grasso et al., 1994; El Kadiri et al., 2006b) including Tunisia (Jeddi, 1994), Morocco (Maate et al., 1995; Hlila et al., 2004; Serrano et al., 2006), Sicily (Grasso et al., 1994; Pedley and Renda, 1998) and Corsica (Ferrandini et al., 1998). Further to this, the onset of prism accretion in the north of the basin, began in the Oligocene, correlating with the beginning of foreland basin flexural loading. As the accretionary prism migrated southwards, basin subsidence increased until Numidian Flysch deposits became structured. The Miocene therefore represents a time of maximum slope subsidence (through the proximity of the prism and the corresponding flexural loading), and thus the deepest water according to foreland basin flexural subsidence models (Sinclair 1997; DeCelles and Giles, 1996 etc).

The Numidian Flysch therefore broadly correlates with times of high sea level, such that prograding fluvio-deltaic systems, typically interpreted to transport sediment across the subaerially exposed shelf to the basin during lowstand conditions (Woolfe et al., 1998; Posamentier, 2001; Catuneanu, 2002), may not have existed during Numidian Flysch deposition. A linear source of many relatively minor fluvial drainage systems may therefore be the preferred option, depositing sediment directly upon the submerged shelf environment, prior to current and storm reworking on to the slope, as is the case in present day California (Covault et al., 2007; Paull et al., 2005). On a basin scale, the laterally continuous distribution of Miocene age Numidian Flysch outcrops between Algeria and Tunisia, and between Sicily and southern Italy (Figures 2.1 and 2.12), would appear to represent a relatively linear source, or else isolated local input points with axial migration of density flows along the basin floor. Further characterisation of either a slope or basin floor depositional location, may help to clarify this point, however a linear source would help explain the lack of contemporaneous, large scale fluvial and deltaic systems reported in North Africa.

2.5.3. Controls upon Numidian Flysch sedimentation

2.5.3.1 Eustatic controls

As discussed previously (section 2.5.2.2), sequence stratigraphic models typically suggest that lowstand conditions play a major role in acti edge where direct feeding into the basin is possible. In addition to having major implications upon the style of sediment input, this has major implications upon the timing of deposition. The correlation of Numidian Flysch deposition with a low-order glacioeustatic highstand and transgression in the Oligocene-Miocene (section 2.5.2), suggests however that contrary to these models, the onset of Numidian Flysch deposition is not controlled by sediment progradation across the shelf during a lowstand systems track.

At present, a majority (but not all) of highstand deepwater clastic system examples are recognised associated with the large continental margins of the western and eastern United States, the west coast of Africa and the Bengal fan. In studies of the California borderland highstand fan system, Covault et al. (2007) suggest that a narrow shelf and high sediment input that is reworked by longshore currents during highstand conditions, forces clastic sediments along the shelf to canyon heads at the shelf break. Thus, during highstand conditions, the sedimentation rate is calculated

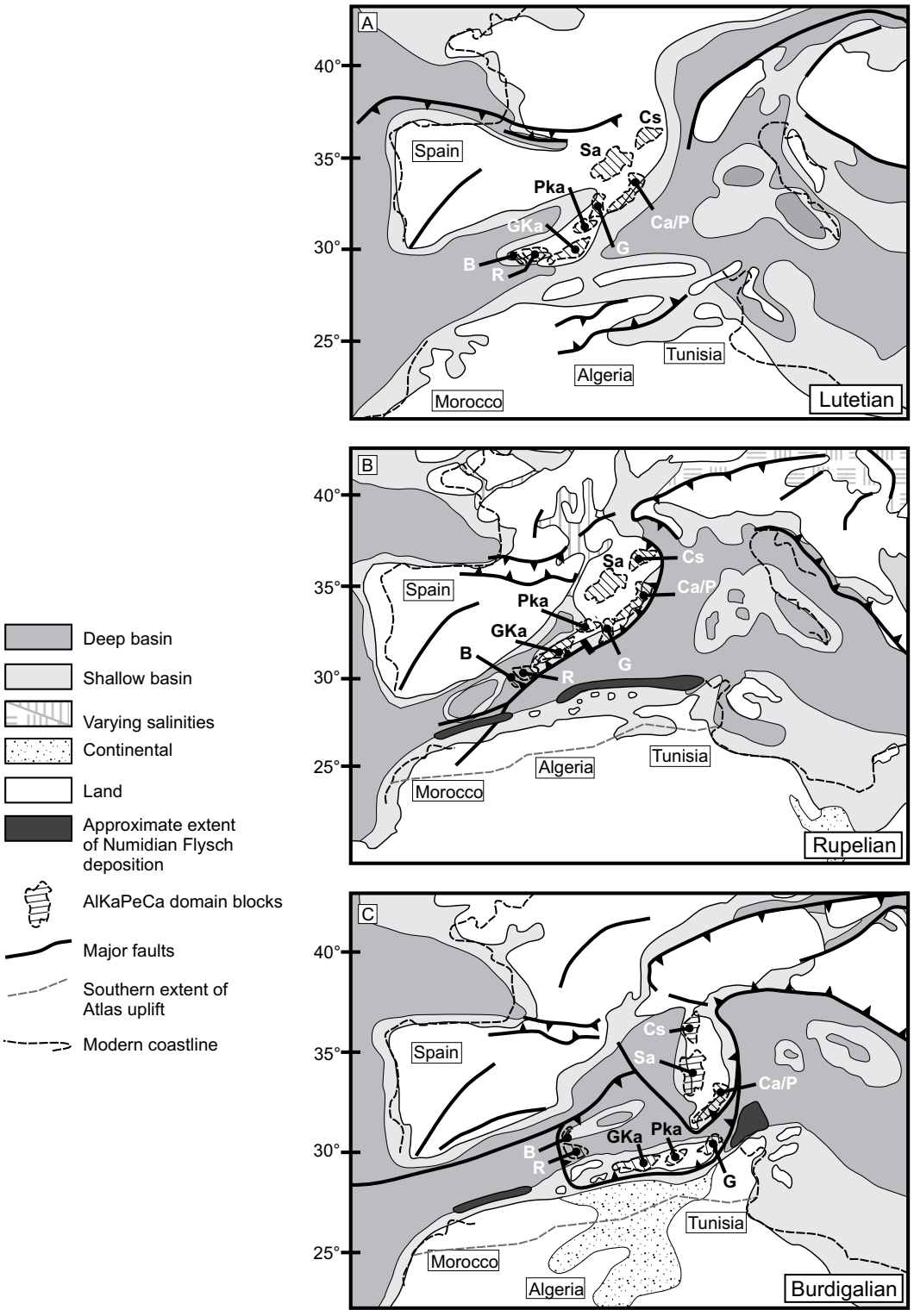

Figure 2.12.

Eocene, Oligocene and Miocene Paleogeopraphic maps redrawn from Meulenkamp and Sissingh, (2003) (Peri-Tethys project. See also Dercourt et al. (2000) and Gaetani et al. (2003)) and modified with the locations of individual blocks from the AlKaPeCa domain (data from Cohen (1980); Geel and Roep (1998); Speranza et al. (2003); Mauffret et al. (2004). Thrust tectonics related to subduction processes in the early Burdigalian north of Algeria are modified according to the model of Mauffret et al. (2004). The approximate extent of Numidian Flysch deposition is shown for each map (see section 5.2.2 for references). A: Paleocene to Eocene with a Lutetian age shown. Pre Numidian Flysch deposition, pre foreland basin stage. B: Oligocene to Burdigalian with a Rupelian age shown. C: Aquitanian to Burdigalian with a Burdigalian age shown. See section 5.2.1 for discussion. AlKaPeCa block abbreviations are: B, Betic; R, Riff; Cs, Corsica; Sa, Sardinia; Ca/P, Calabria and Peloritan; G, Galite block; Pka, Petit Kabylie; Gka, Grand Kabylie.

as being significantly greater than the equivalent lowstand rate. Carvajal and Steel (2006) however studied a moderately-wide Maastrichtian shelf system from Wyoming (United states) in which a high sediment supply was able to overcome the effects of eustacy and substantial shelf width. Given that Numidian Flysch deposition is directly out of phase with low order lowstand events, it is suggested that they do not exert a significant control upon Numidian Flysch sedimentation. The effects of higher order eustatic cycles upon sedimentation and depositional architectures remains unknown however, and requires higher resolution correlation between individual clastic packages and relative sea-level signals. The detailed and well dated stratigraphy required for such an analysis is currently not available throughout a majority of the MFB.

2.5.3.2 Tectonic controls

The Atlas event generated uplift in response to an early phase (pre Alpine) of Africa-Europe convergence from the late Cretaceous (Piqué et al., 2002), and has been attributed as accommodating between 17 and 45% of the total Cenozoic shortening (Gomez et al., 2000). Uplift occurred throughout the whole of North Africa coeval with deposition of the Numidian Flysch. Uplift in Morocco is recognised in several phases including the upper Cretaceous, a paroxysmal Lutetian phase, and a Lutetian to Bartonian phase (Benest and Bensalah, 1995). In Algeria, rapid uplift which produced molasse deposits, is interpreted to have occurred in the late Lutetian (Benest and Bensalah, 1995; Bracene and Frizon de Lamotte, 2002). In northern Tunisia, work on the Medjez-el-Bab anticline similarly constrains a Maghreb wide uplift event in the mid to late Eocene (Masrouhi et al., 2008), while in central Tunisia, uplift effected platform carbonate sediments are late Palaeocene to early Eocene in age (El Ghali et al., 2003). A later Oligocene phase, regarded as the peak uplift event in Morocco is also evidenced throughout the Maghreb in the high Atlas mountains of Morocco (El Harfi et al., 2001; Ait Brahim et al., 2002) and in Tunisia and Algeria (Frizon de Lamotte, 2005). Structures described include broad folds, oblique strike-slip faulting and a predominance of thrust faults (Burollet, 1991; Benest and Bensalah, 1995; Frizon de Lamotte, 2005; Khomsi et al., 2006), which terminate in the south at a physiographic boundary called the Saharan flexure (Piqué et al. 2002) (Figure 2.12). A correlation of Atlas uplift events to the onset of Numidian Flysch deposition (Figure 2.13) demonstrates that deposition occurs during an increase in uplift rates throughout North Africa, with peak uplift rates during deposition in the Moroccan, Algerian, and Tunisian sectors of the basin. Substantial and prolonged uplift across the whole of North Africa, would certainly generate the shedding of sediment with a cratonic sandstone petrofacies towards the North African margin, and must be considered a major factor in controlling the timing of onset of Numidian Flysch clastic deposition.

2.5.3.3 Climatic controls

The Eocene-Oligocene boundary at which Numidian Flysch deposition first occurs, marks the start of intermittent ice sheets in Antarctica and the trend towards an ice house world (Miller et al., 1991). A consequent increase in continental drainage is reported from many locations.

During the Oligocene and Miocene, a gradation from carbonate to clastic dominated deposition is recognised throughout North Africa. In a review of African margin basins, Benomran et al. (1987) cites several significant clastic Formations which commence at this time; sandstone filled channels and troughs are known to cut Oligocene carbonates in the eastern and north-western sectors of the Sirt basin of Libya (Selley, 1968). In Tunisia, mid Oligocene sandstones of the Fortuna Delta conformably cover Eocene shales and shallow water carbonates (Vanhouten, 1980), while in the Pelagian basin to the east, sandy carbonates of the Al Mayah Formation and sandstones of the Sousse

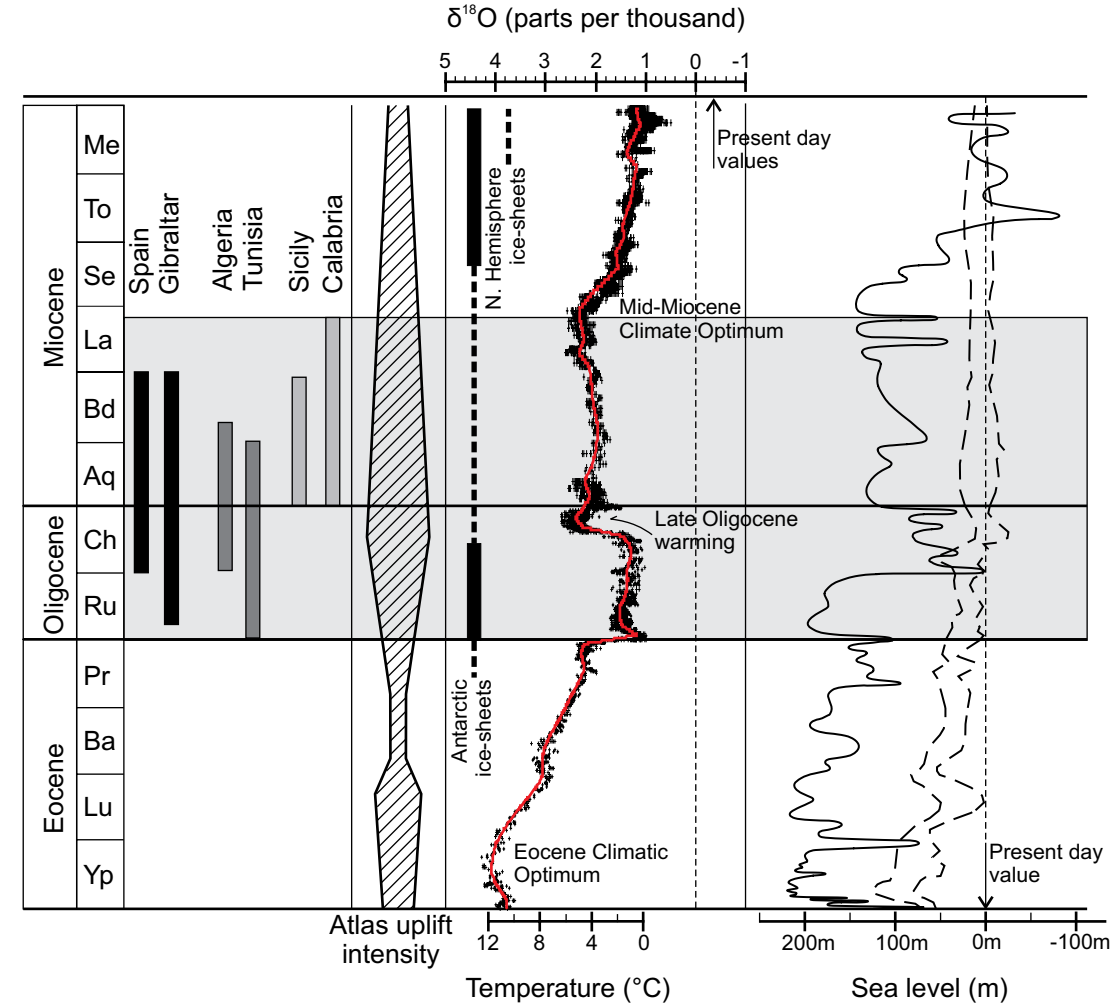

Averaged $\delta^{18}O$ curve. Redrawn from Zachos et al. (2001)

Short term eustatic curve of Haq et al. (1987)

R2 sealevel curve (Max-min envelope) of Van Sickel et al. (2004)

Figure 2.13.
Age ranges of Numidian Flysch deposition in comparison to contemporaneous global and regional events: Atlas uplift intensity (see text for references). Averaged global Oxygen isotope data of benthic taxa from more than 40 ODP sites, with major climate events highlighted (redrawn from Zachos et al. (2001). Estimates of sealevel, from the global eustatic chart of Haq et al. (1987) and Van Sickel et al. (2004).

Formation give way eastwards to the deep marine Djerba Formation. In southern Sicily, Montanari (1986) reports that the northwest Hyblean plateau varies from limestones and marls to calcarenites and sandy argillaceous sediments in the early Miocene. Reviewing Algerian continental sediments from the Atlas domain of northern Algeria, Kheidri et al. (2007) similarly shows a clastic input in the Oligocene with undifferentiated clastic sediments succeeding limestone, marl and evaporate units of mid-Cretaceous to Eocene age. In Malta, John et al. (2003) interprets increased African continental runoff in the early to mid Miocene based upon a switch from limestone to marls and an increase in Kaolinite clays at the expense of Smectite.

Studies of North African palaeogeography in the Oligocene and Miocene confirm that the climate was considerably wetter than at present times, resulting in increased drainage. Fossil records of Crocodilians in Libya and Tunisia constrain a tropical environment for the Miocene and perhaps as early as the Eocene-Oligocene boundary (Markwick, 1998, Llinás Agrasar, 2004). Similarly,

evolutionary diversification of the mammalian order Macroscelidea (the Elephant Shrew) suggests that North Africa (the current Rif-Tellian domain) retained a tropical environment until the mid-late Miocene boundary (Douady et al., 2003). It has also been suggested that North Africa may have contained Miocene tropical forest and savannah in some areas despite a very poorly preserved continental climate record (Fluteau et al., 1999 and references therein; Burgoyne et al., 2005).

Relativlely little is also known about Cenozoic drainage patterns of North Africa, although the palaeo river Nile is known to have prograded northwards across Egypt in the Oligocene, with major delta deposition occurring in the mid-Miocene (Burke and Wells, 1989 and references therein). In Algeria and Libya, a now extinct Miocene river system termed the Eoshabi also drained the Hoggar and Tibesti massifs northwards towards the Gulf of Sirt (Goudie, 2005). Fluteau et al. (1999) also demonstrate through a grid point mathematical model that the northern front of the African monsoon lay approximately at the palaeolatitude of the uplifted Hoggar region of southern Algeria (22°N), considerably to the north of the present day position. Rainfall of up to 2 mm/day is predicted for monsoon months over the North African margin. John et al. (2003) also suggests that short lived Miocene glacial events (Mi global events events of Miller et al., 1991) punctuating the generally cooling climate served to push the intertropical convergance zone nothwards towards the North African margin resulting in increased rainfall and continental drainage. Ruddiman et al. (1989) suggest furthermore that uplift of the Atlas belt (see section 2.5.3.2) would have the capacity to form barriers to oceanic moisture fluxes in North Africa from at least the early Miocene, which may presumably enhance drainage of the uplifting Atlas belt.

Few studies have been carried out in order to detect the effect of climate upon North African drainage at this time, however dramatic coeval increases in sedimentation from offshore Angola have similarly been attributed to global cooling and specific Mi glacial events (Lavier et al., 2001). Therefore, while uplift of the Atlas belt of North Africa coincides with the start of Numidian Flysch deposition, global climatic conditions may also play a substantial role in the drainage of the uplifting belt.

2.6. Conclusions

The 50 year controversy surrounding the provenance of the Numidian Flysch has had a detrimental effect upon the understanding of both the Maghrebian Flysch Basin architecture and controls upon Numidian Flysch deposition. A comprehensive review of published data, integrated with data obtained for this study, suggests that the African craton is the only suitable candidate source region of clastic material for the Numidian Flysch. The northern source hypothesis is not supported by these data, and is therefore not viable. Given the significant geographic extent and duration of the Numidian Flysch system, a solution to the provenance problem and the placing of the Numidian Flysch within a basinal context, has the potential to offer significant insights into the controls upon Cenozoic drainage of the North African margin. A North African source region also constrains the Numidian Flysch to be a passive margin sequence, rather than a flysch deposit (Sensu stricto).

Petrological and zircon analysis constrain the polycyclic, quartzarenite petrofacies of Numidian Flysch sandstones to a large cratonic source region that has zircons of Eburnian and Panafrican age, but none of Hercynian and Alpine age. Around the western Mediterranean realm, North Africa is the only regional domain that satisfies these requirements. A review of the location of Numidian Flysch nappes within the Alpine thrust belt confirms the Numidian Flysch to have been deposited in a southern, external location (i.e. proximal to the North African margin). Immature sandstones of the northern Mauretanian subdomain have characteristics including a volcanic, granite and

metamorphic clast rich petrofacies and a Hercynian age zircon suite. The location of Mauretanian subdomain nappes within the Alpine chain, constrains a depositional location to the north of the Numidian Flysch, while their lithofacies and zircon suite show a strong affinity with the basement blocks of the northern AlKaPeCa domain. A clear distinction of northerly and southerly sourced flysch deposits is therefore observed.

The suggestion of a northern source from uniform palaeocurrent evidence is considered highly unlikely given the observation of sinuous channel systems in Sicily, variable thrust belt strike in Tunisia, and published palaeomagnetic studies which demonstrate large horizontal rotations of the nappe pile during emplacement. An extensive review of available palaeocurrent data similarly indicates no statistically significant flow direction throughout the basin. Moreover, analogue foreland basin systems typically show a dominant palaeoflow that is parallel to basin strike, such that the inherent assumption in the palaeoflow argument, that flow orientation is indicative of the direction from source to basin, is also considered invalid.

Recognition of Numidian Flysch depositional diachroneity from biostratigraphic dating, both published and obtained for this study, constrains three main sedimentary input areas, in Morocco; Algeria and Tunisia; and south of Sicily. A review of regional basin tectonic events and their timings demonstrates a shifting of depocentre from Tunisia towards the Sicillide basin in the Aquitanian, controlled by diachronous closure of the basin. In general, the location and timing of sediment deposition shows a close agreement with published tectonic models and palaeogeographies of the MFB.

In contrast to conventional sequence stratigraphic models of submarine fans systems, timing of deposition of the Numidian Flysch sandstone is not in phase with sea-level falls or lowstand events. On a low order timescale, this rules out eustacy as a controlling factor upon the timing of Numidian Flysch deposition. Timing of deposition does however show a very good correlation with Atlas uplift events throughout North Africa. Furthermore, climatic studies evidence increased North African continental drainage and marine clastic deposition, occurring contemporaneously with Numidian Flysch deposition. The Numidian Flysch therefore represents a large scale Cenozoic drainage system on the North African passive margin, in which sediment was sourced from a tectonically uplifted hinterland, while the timing of deposition appears to be controlled by a combination of hinterland uplift intensity and global climatic variations.

References.

Abdallah, N., Liegeois, J.P., De Waele, B., Fezaa, N. and Ouabadi, A., 2007. The Temaguessine Fe-cordierite orbicular granite (Central Hoggar, Algeria): U-PbSHRIMP age, petrology, origin and geodynamical consequences for the late Pan-African magmatism of the Tuareg shield. Journal of African Earth Sciences, 49: 153-178.

Abreu, V.S. and Haddad, G.A., 1998. Glacioeustatic fluctuations; the mechanism linking stable isotope events and sequence stratigraphy from the early Oligocene to middle Miocene. Special Publication - Society for Sedimentary Geology, 60: 245-259.

Ahmed, A.A.K. and Moussinepouchkine, A., 1987. Lithostratigraphy, sedimentology and evolution of 2 intramontane molassic basins of the Pan-African range - Serie-Pourpree de Lahnet, northwest of Hoggar, Algeria. Journal of African Earth Sciences, 6(4): 525-535.

Ait Brahim, L., Chotin, P., Hinaj, S., Abdelouafi, A., El Adraoui, A., Nakcha, C., Dhont, D., Charroud, M., Sossey Alaoui, F., Amrhar, M., Bouaza, A., Tabyaoui, H. and Chaouni, A., 2002. Paleostress evolution in the Moroccan African margin from Triassic to present. Tectonophysics, 357(1-4): 187-205.

Alcala-Garcia, F.J., Martin-Martin, M. and Lopez-Galindo, A., 2001. Clay mineralogy of the Tertiary sediments in the internal subbetic of Malaga Province, S Spain; implications for geodynamic evolution. Clay Minerals, 36(4): 615-620.

Aldega, L., Corrado, S., Grasso, M. and Maniscalco, R., 2007. Correlation of diagenetic data from organic and inorganic studies in the Apenninic-Maghrebian fold-and-thrust belt: A case study from eastern Sicily. Journal of Geology, 115(3): 335-353.

Andrieux, J., Djellit, H. and Aubouin, J., 1989. Structure de la Petite Kabylie occidentale (Algerie); flyschs “ultra” et flyschs externes. Comptes Rendus de l’Academie des Sciences, Serie 2, Mecanique, Physique, Chimie, Sciences de l’Univers, Sciences de la Terre, 309(11): 1191-1196.

Avigad, D., Kolodner, K., McWilliams, M., Persing, H. and Weissbrod, T., 2003. Origin of northern Gondwana Cambrian sandstone revealed by detrital zircon SHRIMP dating. Geology, 31(3): 227-230.

Avigad, D., Sandler, A., Kolodner, K., Stern, R. J., McWilliams, M., Miller, N. and Beyth, M., 2005. Mass-production of Cambro-Ordovician quartz-rich sandstone as a consequence of chemical weathering of Pan-African terranes: Environmental implications. Earth and Planetary Science Letters, 240(3-4): 818-826.

Avramidis, P. and Zelilidis, A., 2001. The nature of deep-marine sedimentation and palaeocurrent trends as-evidence of Pindos foreland basin fill conditions. Episodes, 24(4): 252-256.

Balenzano, F. and Moresi, M., 1992. Le peliti del Flysch Numidico nell’Appennino Meridionale. Mineralogica et Petrographica Acta., 35: 139-156.

Balogh, K., Cassola, P., Pompilio, M. and Puglisi, D., 2001. Petrographic, geochemical and radiometric data on Tertiary volcano-arenitic beds from the Sicilian Maghrebian Chain: Volcanic sources and geodynamic implications. Geologica Carpathica, 52(1): 15-21.

Barbera, G., Lo Giudice, A., Mazzoleni, P. and Pappalardo, A., 2009. Combined statistical and petrological analysis of provenance and diagenetic history of mudrocks: Application to Alpine Tethydes shales (Sicily, Italy). Sedimentary Geology, 213(1-2): 27-40.

Becker, T., Schreiber, U., Kampunzu, A.B. and Armstrong, R.A., 2006. Mesoproterozoic rocks of Namibia and their plate tectonic setting. Journal of African Earth Sciences, 46(1-2): 112-140.

Belayouni, H., Brunelli, D., Clocchiatti, R., Di Staso, A., Hassani, I. E. E. A. E., Guerrera, F., Kassaa, S., Ouazaa, N. L., Martín, M. M., Serrano, F., Tramontana, M., 2010. La Galite Archipelago (Tunisia, North Africa): Stratigraphic and petrographic revision and insights for geody-

namic evolution of the Maghrebian Chain. Journal of African Earth Sciences, 56(1): 15-28.

Benest, M. and Bensalah, M., 1995. L'Eocene continental dans l'avant-pays alpin d'Algerie; environnement et importance de la tectogenese atlasique polyphasee. Bulletin du Service Geologique de l'Algerie, 6(1): 41-59.

Benomran, O., Nairn, A.E.M. and Schamel, S., 1987. Sources and dispersal of mid-Cenozoic clastic sediments in the central Mediterranean region. In: F. Lentini (Editor), Atti del convegno su; Sistemi avanfossa-avampaese lungo la Catena Appenninico-Maghrebide. Memorie della Societa Geologica Italiana. Societa Geologica Italiana, Rome, Italy, pp. 47-68.

Bertrand, J. M., Michard, A., Boulier, A.-M. and Dautel, D., 1986. Structure and U/Pb geochronology of central Hoggar (Algeria); a reappraisal of its Pan-African evolution. Tectonics, 5(7): 955-972.

Bonardi, G., Giunta, G., Ligouri, V., Perrone, V., Russo, M., Zuppetta, A., Ciampo, G., 1980. Osservazioni sull'evoluzione dell'Arco Calabro-Peloritano nel Miocene inferiore: la Formazione di Stilo-Capo d'Orlando. Bollettino Della Societa Geologica Italiana, 99: 365-393.

Bonardi, G., de Capoa, P., Di Staso, A., Estevez, A., Martin-Martin, M., Martin-Rojas, L., Perrone, V. and Tent-Manclus, J. E., 2003. Oligocene-to-Early Miocene depositional and structural evolution of the Calabria-Peloritani Arc southern terrane (Italy) and geodynamic correlations with the Spain Betics and Morocco Rif. Geodinamica Acta, 16(2-6): 149-169.

Bossière, G. and Peucat, J.J., 1985. New Geochronological Information by Rb-Sr and U-Pb Investigations from the Pre-Alpine Basement of Grande Kabylie (Algeria). Canadian Journal of Earth Sciences, 22(5): 675-685.

Bossière, G. and Peucat, J.J., 1986. Structural Evidence and Rb-Sr, Ar-39-40 Mica Ages Relationships for the Existence of an Hercynian Deep Crustal Shear Zone in Grande Kabylie (Algeria) and Its Alpine Reworking. Tectonophysics, 121(2-4): 277-294.

Bouillin, J.P. and Glacon, G., 1973. De-couverte de Cretace et d'Eocene de type Tellien charries sur le socle de la Petite Kabilye aux environes d'El Milia (Constantinois, Algerie). Compte Rendus de l'Académie des Sciences, 267: 1517-1519.

Bouillin, J.P., Durand-Delga, M. and Olivier, P., 1986. Betic-Rifian and Tyrrhenian arcs; distinctive features, genesis and development stages. Elsevier, Amsterdam, Netherlands, pp. 281-304.

Boukhalfa, K., Ismail-Lattrache, K.B., Riahi, S., Soussi, M. and Khomsi, S., 2009. Analyse biostratigraphique et sédimentologique des séries éo-oligocènes et miocènes de la Tunisie septentrionale : implications stratigraphiques et géodynamiques. Comptes Rendus Geosciences, 341(1): 49-62.

Boyer, S.E. and Elliott, D., 1982. Thrust systems. American Association of Petroleum Geologists Bulletin, 66(9): 1196-1230.

Bracene, R. and de Lamotte, D.F., 2002. The origin of intraplate deformation in the Atlas system of western and central Algeria: from Jurassic rifting to Cenozoic-Quaternary inversion. Tectonophysics, 357(1-4): 207-226.

Broquet, P., Duée, G., Caire, A. and Truillet, R., 1963. Distinction de deux series a facies flysch dans le Nord-Est silicien. Compte Rendus de l'Académie des Sciences de Paris, 257(19): 2856-2858.

Burgoyne, P.M., van Wyk, A.E., Anderson, J.M. and Schrire, B.D., 2005. Phanerozoic evolution of plants on the African plate. Journal of African Earth Sciences, 43: 13-52.

Burke, K. and Wells, G.L., 1989. Trans-African Drainage System of the Sahara - Was It the Nile. Geology, 17(8): 743-747.

Burollet, P.F., 1991. Structures and tectonics of Tunisia. Tectonophysics, 195(2-4): 359-369.

Caby, R., Dostal, J. and Dupuy, C., 1977. Upper Proterozoic volcanic graywackes from northwestern Hoggar (Algeria) - Geology and Geochemistry. Precambrian Research, 5(3): 283-297.

Caby, R., 1996. A review of the in Ouzzal granulitic terrane (Tuareg shield, Algeria): Its significance within the Pan-African Trans-Saharan belt. Journal of Metamorphic Geology, 14(6): 659-666.

Caby, R., 2003. Terrane assembly and geodynamic evolution of central-western Hoggar: a synthesis. Journal of African Earth Sciences, 37(3-4): 133-159.

Cainelli, C., 1994. Shelf processes and canyon/channel evolution controlling turbidite systems: Examples from the Sergipe-Alagoas basin, Brazil. GCSSEPM Foundation 15th Annual Research Conference, Submarine Fans and Turbidite systems, December 4-7, 1994.

Caire, A. and Duée, G., 1971. The Quartz pisolites from the Numidian originate in Sardinia, not in the Sahara. Compte Rendus Hebdomadaires des Seances de l'Academie des Sciences, Paris, 270(26): 1381-3183.

Carbone, S., Lentini, F., Sonnino, M. and De Rosa, R., 1987. Il flysch numidico di Valsinni (Appennino lucano). Bollettino Della Societa Geologica Italiana, 106(2): 331-345.

Carminati, E., Wortel, M.J.R., Spakman, W. and Sabadini, R., 1998. The role of slab detachment processes in the opening of the western-central Mediterranean basins: some geological and geophysical evidence. Earth and Planetary Science Letters, 160(3-4): 651-665.

Carmisciano, R., Coccioni, R., Corradini, D., D'alessandro, A., Guerrera, F., Loiacono, F., Moretti, E., Puglisi, D. & Sabato, L. 1987. Nuovi datti sulle "successioni miste" inframioceniche dell'Algeria (Grande kabilia) e della Sicilia (Monti Nebrodi); Confronti con analoghe successioni torbiditiche nell'Arco di Gibilterra e nell'Appennino Lucano. Memorie della Societa Geologica Italiana, 38: 551-576.

Carr, M.D. and Miller, E.L., 1979. Overthrust Emplacement of the Numidian Flysch Complex in the Westernmost Mogod Mountains, Tunisia - Summary. Geological Society of America Bulletin, 90(6): 513-515.

Carvajal, C.R. and Steel, R.J., 2006. Thick turbidite successions from supply-dominated shelves during sea-level highstand. Geology, 34(8): 665-668.

Cassola, P., Giammarino, S., Puglisi, D. and Villa, G., 1991. Nuovi dati sedimentologico-petrografici e biostratigrafici sulla formazione di Piedimonte (Sicilia nord-orientale). Memorie della Societa Geologica Italiana, 47: 213-223.

Cassola, P., Loiacono, F., Moretti, E., Nigro, F., Puglisi, D. and Sbarra, R., 1995. The Reitano Flysch in the northern sector of Nebrodi Mountains (NE Sicily): sedimentological, petrographical and structural characters. Giornale di Geologia serie 3, 57: 195-217.

Catalano, R., Distefano, P. and Vitale, F.P., 1995. Structural Trends and Paleogeography of the Central and Western Sicily Belt - New Insights. Terra Nova, 7(2): 189-199.

Catalano, R., Di Stefano, P., Sulli, A. and Vitale, F.P., 1996. Paleogeography and structure of the Central Mediterranean: Sicily and its offshore area. Tectonophysics, 260(4): 291-323.

Catuneanu, O., 2002. Sequence stratigraphy of clastic systems: concepts, merits, and pitfalls. Journal of African Earth Sciences, 35(1): 1-43.

Cello, G. and Mazzoli, S., 1998. Apennine tectonics in southern Italy: a review. Journal of Geodynamics, 27(2): 191-211.

Chalouan, A., El Mrihi, A., El Kadiri, K., Bahmad, A., Salhi, F. and Hlila, R., 2006. Mauretanian flysch nappe in the northwestern Rif Cordillera (Morocco): deformation chronology and evidence for a complex nappe emplacement. Tectonics of the Western Mediterranean and North Africa, 262: 161-175.

Channell, J.E.T., Oldow, J.S., Catalano, R. and D, A.B., 1990. Paleomagnetically determined rotations in the western Sicillian fold and thrust belt. Tectonics, 9(4): 641-660.

Cheilletz, A., Ruffet, G., Marignac, C., Kolli, O., Gasquet, D., Feraud, G. and Bouillin, J. P., 1999. Ar-40/Ar-39 dating of shear zones in the Variscan basement of Greater Kabylia (Algeria). Evidence of an Eo-Alpine event at 128 Ma (Hauterivian-Barremian boundary): geodynamic

consequences. Tectonophysics, 306(1): 97-116.
Chiocchini, U. and Cipriani, N., 1996. Petrologic binary diagrams for characterizing and comparing arenites. Sedimentary Geology, 103(3-4): 281-289.
Cibin, U., Di Giulio, A., Martelli, L., Catanzariti, R., Poccianti, S., Rosselli, C. and Sani, F., 2004. Factors controlling foredeep turbidite deposition: the case of Northern Apennines (Oligocene-Miocene, Italy). In: S.A. Lomas and P. Joseph (Editors), Confined Turbidite Systems. Geological Society Special Publication, pp. 115-134.
Clark, M.S., 1995. The Cozy Dell Formation; delta progradation and turbidite deposition during sea-level highstand. American Association of Petroleum Geologists Bulletin, 79(4): 581.
Cohen, C.R., 1980. Plate Tectonic Model for the Oligo-Miocene Evolution of the Western Mediterranean. Tectonophysics, 68(3-4): 283-311.
Coutelle, A., 1979. Structure des unites externes du Tell algerien de la region d'Akbou; succession des phases tectoniques. Compte Rendu Sommaire des Seances de la Societe Geologique de France, 21(1, Supplement): 20-22.
Covault, J.A., Normark, W.R., Romans, B.W. and Graham, S.A., 2007. Highstand fans in the California borderland: The overlooked deep-water depositional systems. Geology, 35(9): 783-786.
Crespo-Blanc, A. and de Lamotte, D.F., 2006. Structural evolution of the external zones derived from the Flysch trough and the South Iberian and Maghrebian paleomargins around the Gibraltar arc: a comparative study. Bulletin De La Societe Geologique De France, 177(5): 267-282.
Critelli, S., Mongelli, G., Perri, F., Martin-Algarra, A., Martin-Martin, M., Perrone, V., Dominici, R., Sonnino, M., Zaghloul, M. N., 2008. Compositional and geochemical signatures for the sedimentary evolution of the Middle Triassic-Lower Jurassic continental redbeds from western-central Mediterranean alpine chains. Journal of Geology, 116(4): 375-386.
D'Lemos, R.S., Inglis, J.D. and Samson, S.D., 2006. A newly discovered orogenic event in Morocco: Neoproterozic ages for supposed Eburnean basement of the Bou Azzer inlier, Anti-Atlas Mountains. Precambrian Research, 147(1-2): 65-78.
de Capoa, P., Guerrera, F., Perrone, V., Serrano, F. and Tramontana, M., 2000. The onset of the syn-orogenic sedimentation in the Flysch Basin of the Sicilian Maghrebids: state of the art and new biostratigraphic constraints. Eclogae Geologicae Helvetiae, 93(1): 65-79.
de Capoa, P., Di Staso, A., Guerrera, F., Perrone, V., Tramontana, M. and Zaghloul, M. N., 2002. The Lower Miocene volcaniclastic sedimentation in the Sicilian sector of the Maghrebian Flysch Basin: geodynamic implications. Geodinamica Acta, 15(2): 141-157.
de Capoa, P., Di Staso, A., Guerrera, F., Perrone, V. and Tramontana, M., 2004. The age of the oceanic accretionary wedge and onset of continental collision in the Sicilian Maghrebian Chain. Geodinamica Acta, 17(5): 331-348.
de Capoa, P., Di Staso, A., Perrone, V. and Zaghloul, M.N., 2007. The age of the foredeep sedimentation in the Betic-Rifian Mauretanian Units: A major constraint for the reconstruction of the tectonic evolution of the Gibraltar Arc. Comptes Rendus Geoscience, 339(2): 161-170.
DeCelles, P.G. and Giles, K.A., 1996. Foreland basin systems. Basin Research, 8(2): 105-123.
De Galdeano, C. S., El Kadiri, K., Simancas, J. F., Hlila, R., Lopez-Garrido, A. C., El Mrihi, A. and Chalouan, A., 2006. Paleogeographical reconstruction of the Malaguide-Ghomaride Complex (Internal Betic-Rifian Zone) based on Carboniferous granitoid pebble provenance. Geologica Carpathica, 57(5): 327-336.
Dejong, K.A., 1975. Gravity Tectonics or Plate Tectonics - Example of Numidian Flysch, Tunisia. Geological Magazine, 112(4): 373-381.
Deptuck, M.E., Sylvester, Z., Pirmez, C. and O'Byrne, C., 2007. Migration-aggradation history and

3-D seismic geomorphology of submarine channels in the Pleistocene Benin-major Canyon, western Niger Delta slope. Marine and Petroleum Geology, 24: 406-433.

Dercourt, J., Gaetani, M., Vrielynck, B., Barrier, E., Biju-Duval, B., Brunet, M.F., Cadet, J.P., Crasquin, S. and Sandulescu, M., 2000. Atlas Peri-Tethys, Palaeogeographical Maps. CCGM/CGMW, Paris: 24 maps and explanatory notes, 269 pp.

Dickinson, W.R. and Suczek, C.A., 1979. Plate-Tectonics and Sandstone Compositions. AAPG Bulletin, 63(12): 2164-2182.

Didon, J., Durand-Delga, M. and Komprobst, J., 1973. Homologies geologiques entre les deux rives du de´troit de Gibraltar. Bulletin - Societe Geologique de France, 15: 78-105.

Didon, J. and Hoyez, B., 1978. Le Numidien dans l'arc be´tico-rifian; hypothe`ses sur sa mise en place se´dimentaire et tectonique. Ann. Soc. Geol. Nord, 98: 9-24.

Didon, J. Duranddelga, M., Esteras, M., Feinberg, H., Magnè, J., Suter, G., 1984. The Numidian Sandstones Formation in the Gibraltar Arch Stratigraphically Lies between Oligocene Clays and Burdigalian (Lower Miocene) Marls. Comptes Rendus De L Academie Des Sciences Serie 2, 299(3): 121-128.

Dongarra, G. and Ferla, P., 1982. Le argille di Portella Colla e del Flysch Numidico auct. (M. Madonie; Sicilia); Aspetti deposizionali e diagenetici. Rendiconti della Societa Italiana di Mineralogia e Petrologia., 38(3): 1119-1133.

Douady, C.J., Catzeflis, F., Raman, J., Springer, M.S. and Stanhope, M.J., 2003. The Sahara as a vicariant agent, and the role of Miocene climatic events, in the diversification of the mammalian order Macroscelidea (elephant shrews). Proceedings of the National Academy of Sciences of the United States of America, 100(14): 8325-8330.

El Euchi, H., Fourati, L., F, H. and Saidi, M., 1998. Structural style and hydrocarbon habitat in northern Tunisia. The sixth Tunisian petroleum exploration and production conference (Tunis). Field trip guide book(13).

El Euchi, H., Saidi, M., Fourati, L. and El Maherssi, C., 2004. Northern Tunisia Thrust Belt: Deformation Models and Hydrocarbon Systems. AAPG Hedberg series, Deformation, fluid flow, and reservoir appraisal in foreland fold and thrust belts(1): 371-390.

El Ghali, A., Ben Ayed, N., Bobier, C., Zargouni, F. and Krima, A., 2003. Les manifestations tectoniques synsedimentaires associees a la compression eocene en Tunisie; implications paleogeographiques et structurales sur la marge Nord-Africaine. Comptes Rendus - Academie des sciences. Geoscience, 335(9): 763-771.

El Harfi, A., Lang, J., Salomon, J. and Chellai, E.H., 2001. Cenozoic sedimentary dynamics of the Ouarzazate foreland basin (Central High Atlas Mountains, Morocco). International Journal of Earth Sciences, 90(2): 393-411.

El Kadiri, K., Chalouan, A., Bahmad, A., Salhi, F. and Liemlahi, H., 2006a. "Transgressive washing" concept: a sequence stratigraphic approach for calci- and siliciclastic turbidites. In: G. Moratti and A. Chalouan (Editors), Tectonics of the Western Mediterranean and North Africa. Geological Society, London, Special Publications, pp. 45-53.

El Kadiri, K., Hlila, R., De Galdeano, C. S., Lopez-Garrido, A. C., Chalouan, A., Serrano, F., Bahmad, A., Guerra-Merchan, A. and Liemlahi, H., 2006b. Regional correlations across the Internides-Externides front (northwestern Rif Belt, Morocco) during the Late Cretaceous-Early Burdigalian times: palaeogeographical and palaeotectonic implications. Tectonics of the Western Mediterranean and North Africa, 262: 193-215.

Elter, P., Grasso, M., Parotto, M. and Vezzani, L., 2003. Structural setting of the Apennine-Maghrebian thrust belt. Episodes, 26(3): 205-211.

Ernst, S.R., Guasti, E., Dupuis, C. and Speijer, R.P., 2006. Environmental perturbation in the southern Tethys across the Paleocene/Eocene boundary (Dababiya, Egypt): Foraminiferal and

clay mineral records. Marine Micropaleontology, 60(1): 89-111.

Eschard, R., Albouy, E., Deschamps, R., Euzen, T. and Ayub, A., 2003. Downstream evolution of turbiditic channel complexes in the Pab Range outcrops (Maastrichtian, Pakistan). Marine and Petroleum Geology, 20(6-8): 691-710.

Estrada, F., Ercilla, G. and Alonso, B., 2005. Quantitative study of a Magdalena submarine channel (Caribbean Sea): implications for sedimentary dynamics. Marine and Petroleum Geology, 22(5): 623-635.

Faugères, J.C., Broquet, P., Duée, G. and Imbert, P., 1992. Sedimentary Record of Volcanic and Paleocurrent Events in the Numidian Sandstones of Sicily - the Tuffites and Contourites of Karsa. Comptes Rendus De L Academie Des Sciences Serie 2, 315(4): 479-486.

Faugères, J.C., Gonthier, E., Griboulard, R. and Masse, L., 1993. Quaternary sandy deposits and canyons on the Venezuelan margin and south Barbados accretionary prism. Marine Geology, 110(1-2): 115-142.

Ferla, P. and Alaimo, R., 1976. I graniti e le rocce porfiriche calc-alcaline e k-andesitiche nel conglomerato trasgressivo del Miocene inferiore dei monti Peloritani (Sicilia). Memorie della Societa Geologica Italiana, 17: 123-133.

Ferrandini, M., Ferrandini, J., Loye-Pilot, M. D., Butterlin, J., Cravatte, J. and Janin, M. C., 1998. Le Miocene du bassin de Saint-Florent (Corse); modalites de la transgression du Burdigalien superieur et mise en evidence du Serravallien. Geobios, 31(1): 125-137.

Ferry, J.N., Mulder, T., Parize, O. and Raillard, S., 2005. Concept of equilibrium profile in deep-water turbidite system: effects of local physiographic changes on the nature of sedimentary process and the geometries of deposits. Geological Society, London, Special Publications, 244(1): 181-193.

Festa, V., Caggianelli, A., Kruhl, J. H., Liotta, D., Prosser, G., Gueguen, E. and Paglionico, A., 2006. Late-Hercynian shearing during crystallization of granitoid magmas (Sila massif, southern Italy): regional implications. Geodinamica Acta, 19(3-4): 185-195.

Fiannacca, P., Williams, I.S., Cirrincione, R. and Pezzino, A., 2008. Crustal contributions to Late Hercynian peraluminous magmatism in the southern Calabria-Peloritani Orogen, southern Italy: Petrogenetic inferences and the gondwana connection. Journal of Petrology, 49(8): 1497-1514.

Fildes, C., Stow, D., Riahi, S., Soussi, M., Patel, U., Milton, A. J., Marsh, S., 2010. European provenance of the Numidian Flysch in northern Tunisia. Terra Nova, 22(2): 94-102.

Fluteau, F., Ramstein, G. and Besse, J., 1999. Simulating the evolution of the Asian and African monsoons during the past 30 Myr using an atmospheric general circulation model. J. Geophys. Res., 104(D10): 11995-12018.

Folk, R.L., 1951. Stages of textural maturity in sedimentary rocks. Journal of Sedimentary Research, 21: 127-130.

Fornelli, A. and Piccarreta, G., 1997. Mineral and chemical provenance indicators in some early Miocene sandstones of the Southern Apennines (Italy). European Journal of Mineralogy, 9(2): 433-447.

Fornelli, A., 1998. Petrological features of a Numidian section in the Lucanian Apennine (southern Italy). Geological Journal, 33(3): 177-191.

Fraser, A. J., Hilkewich, D., Syms, R., Penge, J., Raposo, A. and Simon, G., 2005. Angola Block 18; a deep-water exploration success story. In: A.G. Dore, B.A. Vining (Editors), Petroleum Geology: North-West Europe and Global Perspectives - Proceedings of the 6th Petroleum Geology Conference. Geological Society, London, pp 1199-1216.

Frizon de Lamotte, D., 2005. About the Cenozoic inversion of the Atlas domain in North Africa. Comptes Rendus Geosciences, 337(5): 475-476.

Gaetani, M., Dercourt, J. and Vrielynck, B., 2003. The Peri-Tethys Programme: achievements and results. Episodes, 26(2): 79-93.

Garzanti, E., Doglioni, C., Vezzoli, G. and Ando, S., 2007. Orogenic belts and orogenic sediment provenance. Journal of Geology, 115(3): 315-334.

Gaudette, H.E., Hurley, P.M. and Lajmi, T., 1975. Source area of the Numidian flych of Tunisia as suggested by detrital zircon ages. The geological society of America annual meetings, 7, September 1975, Boulder Colorado, pp. 1083-1084.

Gaudette, H.E., Hurle, P.M. and Lajmi, T., 1979. Provenance Studies in Tunisia by U-Pb Ages of Detrital Zircons. American Association of Petroleum Geologists Bulletin, 63: 456.

Gee, M.J.R., Gawthorpe, R.L., Bakke, K. and Friedmann, S.J., 2007. Seismic geomorphology and evolution of submarine channels from the Angolan continental margin. Journal of Sedimentary Research, 77(5-6): 433-446.

Geel, T. and Roep, T.B., 1998. Oligocene to middle Miocene basin development in the Eastern Betic Cordilleras, SE Spain (Velez Rubio Corridor-Espuna): reflections of West Mediterranean plate-tectonic reorganizations. Basin Research, 10(3): 325-343.

Gelard, J.P., 1969. Le flysch a base schisto-greseuse de la bordure meridionale et orientale du massif de Chellata (Grande-Kabylie, Algerie). Compte Rendu Sommaire des Seances de la Societe Geologique de France, 8: 292-293.

Géry, B., 1983. Age and Tectonic Situation of the Allochthonous Sedimentary Formations in Northern Grande Kabylie - an Example in the Djebel Aissa-Mimoun. Comptes Rendus De L Academie Des Sciences Serie 2, 297(9): 729-734.

Ghienne, J. and Deynoux, M., 1998. Large-scale channel fill structures in Late Ordovician glacial deposits in Mauritania, Western Sahara. Sedimentary Geology, 119(1-2): 149-151.

Ghienne, J. F., Boumendjel, K., Paris, F., Videt, B., Racheboeuf, P. and Salem, H. A., 2007. The Cambrian-Ordovician succession in the Ougarta Range (western Algeria, North Africa) and interference of the Late Ordovician glaciation on the development of the Lower Palaeozoic transgression on northern Gondwana. Bulletin of Geosciences, 82(3): 183-214.

Giacomini, F., Bomparola, R.M., Ghezzo, C. and Guldbransen, H., 2006. The geodynamic evolution of the Southern European Variscides: constraints from the U/Pb geochronology and geochemistry of the lower Palaeozoic magmatic-sedimentary sequences of Sardinia (Italy). Contributions to Mineralogy and Petrology, 152(1): 19-42.

Gigliuto, L.G., Ouazani-Touhami, A., Puglisi, D., Puglisi, G. and Zaghloul, M.N., 2004. Petrography and geochemistry of granitoid pebbles from the Oligocene-Miocene deposits of the internal Rifian chain (Morocco): A possible new hypothesis of provenance and paleogeographical implications. Geologica Carpathica, 55(3): 261-272.

Giunta, G., 1985. Problematiche ed ipotesi sul bacino numidico nelle Maghrebidi siciliane. Bollettino della Societa Geologica Italiana, 104(2): 239-256.

Golonka, J., 2004. Plate tectonic evolution of the southern margin of Eurasia in the Mesozoic and Cenozoic. Tectonophysics, 381(1-4): 235-273.

Gomez, F., Beauchamp, W. and Barazangi, M., 2000. Role of the Atlas Mountains (northwest Africa) within the African-Eurasian plate-boundary zone. Geology, 28(9): 775-778.

Gomez-pugnaire, M.T. and Fernandezsoler, J.M., 1987. High-Pressure metamorphism in metabasites from the Betic Cordilleras (SE Spain) and its evolution during the Alpine orogeny. Contributions to Mineralogy and Petrology, 95(2): 231-244.

Gottis, C., 1953. Stratigraphie et tectonique du « flysch » numidien en Tunisie septentrionale. Compte Rendus Hebdomadaires des Seances de l'Academie des Sciences, Paris, 236: 1059-1061.

Goudie, A.S., 2005. The drainage of Africa since the cretaceous. Geomorphology, 67(3-4): 437-

456.

Grasso, M., Pedley, H.M. and Maniscalco, R., 1994. The application of a late Burdigalian-early Langhian highstand event in correlating complex Tertiary orogenic carbonate successions within the central Mediterranean. Géologie Méditerranéenne, 21(1-2): 69-83.

Guerrera, F., Martinalgarra, A. and Perrone, V., 1993. Late Oligocene-Miocene Syn-/-Late-Orogenic Successions in Western and Central Mediterranean Chains from the Betic Cordillera to the Southern Apennines. Terra Nova, 5(6): 525-544.

Guerrera, F., Martin-Martin, M., Perrone, V. and Tramontana, M., 2005. Tectono-sedimentary evolution of the southern branch of the Western Tethys (Maghrebian Flysch Basin and Lucanian Ocean): consequences for Western Mediterranean geodynamics. Terra Nova, 17(4): 358-367.

Guiraud, R., Bosworth, W., Thierry, J. and Delplanque, A., 2005. Phanerozoic geological evolution of Northern and Central Africa: An overview. Journal of African Earth Sciences, 43(1-3): 83-143.

Hammor, D., Bosch, D., Caby, R. and Bruguier, O., 2006. A two-stage exhumation of the Variscan crust: U-Pb LA-ICP-MS and Rb-Sr ages from Greater Kabylia, Maghrebides. Terra Nova, 18(5): 299-307.

Haq, B.U., Hardenbol, J. and Vail, P.R., 1987. Chronology of Fluctuating Sea Levels since the Triassic. Science, 235(4793): 1156-1167.

Haughton, P.D.W., 2000. Evolving turbidite systems on a deforming basin floor, Tabernas, SE Spain. Sedimentology, 47(3): 497-518.

Heinio, P. and Davies, R.J., 2007. Knickpoint migration in submarine channels in response to fold growth, western Niger Delta. Marine and Petroleum Geology, 24: 434-449.

Hlila, R., El Kadiri, K., Chalouan, A. and El Mrihi, A., 2004. Late Eocene-Burdigalian transgressive cover of the Betico-Rifan internal zones; paleogeographic and paleotectonic significance. Congres Geologique International, Resumes, 32(1): 769-770.

Hoyez, B., 1975. Dispersion du materiel quartzeux dans les formations aquitaniennes de Tunisie septentrionale et d' Algerie nord-orientale. Bulletin - Societe Geologique de France, 25(6): 1147-1156.

Huyghe, P., Foata, M., Deville, E., Mascle, G. and Caramba Working, G., 2004. Channel profiles through the active thrust front of the southern Barbados prism. Geology, 32(5): 429-432.

Iannace, A., Vitale, S., D'Errico, M., Mazzoli, S., Di Staso, A., Macaione, E., Messina, A., Reddy, S. M., Somma, R., Zamparelli, V., Zattin, M. and Bonardi, G. 2007. The carbonate tectonic units of northern Calabria (Italy): a record of Apulian palaeomargin evolution and Miocene convergence, continental crust subduction, and exhumation of HP-LT rocks. Journal of the Geological Society, 164: 1165-1186.

Inglis, J. D., MacLean, J. S., Samson, S. D., D'Lemos, R.S., Admou, H. and Hefferan, K., 2004. A precise U--Pb zircon age for the Bleid granodiorite, Anti-Atlas, Morocco: implications for the timing of deformation and terrane assembly in the eastern Anti-Atlas. Journal of African Earth Sciences, 39: 277-283.

Ivaldi, J.P., 1977. Natural and Artificial Thermoluminescence of Kabyle Permo-Trias and Saharian Continental Inter-Calaire Detrital Series (Algeria) - Data for a Paleogeography of Numidian Sandstones. Comptes Rendus Hebdomadaires Des Seances De L Academie Des Sciences Serie D, 284(8): 611-614.

Jeddi, R.S., 1994. Les depots silico-clastiques oligo-miocenes en Tunisie atlasique centrale; modele d'environnement et evolution paleogeographique. ETAP Memoir Series, 7: 419-440.

Jerram, D.A., Mountney, N., Holzforster, F. and Stollhofen, H., 1999. Internal stratigraphic relationships in the Etendeka group in the Huab Basin, NW Namibia: understanding the onset of

flood volcanism. Journal of Geodynamics, 28(4-5): 393-418.

Johansson, M., Braakenburg, N.E., Stow, D.A.V. and Faugères, J.C., 1998. Deep-water massive sands: facies, processes and channel geometry in the Numidian Flysch, Sicily. Sedimentary Geology, 115(1-4): 233-265.

John, C.M., Mutti, M. and Adatte, T., 2003. Mixed carbonate-siliciclastic record on the North African margin (Malta) - Coupling of weathering processes and mid Miocene climate. GSA Bulletin, 115(2): 217-229.

Kheidri, H.L., Zazoun, R.S. and Sabaou, N., 2007. Neogene tectonic history of the Sub-Bibanic and M'sila Basins, northern Algeria: Implications for hydrocarbon potential. Journal of Petroleum Geology, 30(2): 159-173.

Khomsi, S., Bedir, M., Soussi, M., Ben Jemia, M.G. and Ben Ismail-Lattrache, K., 2006. Highlight of Middle-Late eocene compressional events in the subsurface of eastern Tunisia (Sahel): Generality of the Atlasic phase in North Africa. Comptes Rendus Geoscience, 338(1-2): 41-49.

Kilian, C.M., 1931. Des principaux complexes continentaux du Sahara. Compte Rendu Sommaire des Seances de la Societe Geologique de France, 9: 109-111.

Knott, S.D., 1987. The Liguride Complex of Southern Italy - a Cretaceous to Paleogene Accretionary Wedge. Tectonophysics, 142(2-4): 217-226.

Kohn, B.P., Eyal, M. and Feinstein, S., 1992. A major late Devonian-early Carboniferous (Hercynian) thermotectonic event at the NW margin of the Arabian-Nubian sheild: Evidence from Zircon fission track dating. Tectonics, 11(5): 1018-1027.

Kuster, D., Liegeois, J.P., Matukov, D., Sergeev, S. and Lucassen, F., 2008. Zircon geochronology and Sr, Nd, Pb isotope geochemistry of granitoids from Bayuda Desert and Sabaloka (Sudan): Evidence for a Bayudian event (920-900 Ma) preceding the Pan-African orogenic cycle (860-590 Ma) at the eastern boundary of the Saharan Metacraton. Precambrian Research, 164(1-2): 16-39.

Lahondére, J.C., Feinberg, H. and Haq, B.U., 1979. Dating of Numidian Sandstone of Eastern Algeria - Structural Consequences. Comptes Rendus Hebdomadaires Des Seances De L Academie Des Sciences Serie D, 289(4): 383-386.

Lancelot, J., Reille, J.L., Broquet, P. and Mattauer, M., 1976. Datation U - Pb des zircons detritiques du flysch numidien d'Espagne et de Sicile; consequences paleogeographiques (U-Pb dating of detrital zircons in the Numidian flysch of Spain and Sicily; paleogeographic consequences.).

Lancelot, J., Reille, J.L. and Wezel, F.C., 1977. Etude morphologique et radiochronologique de zircons détritiques des flyschs "numidien" et "gréso-micacé". Bulletin De La Societe Geologique De France, 7(19): 773-780.

Lancelot, J.R., Allegret, A. and Iglesias Ponce de Leon, M., 1985. Outline of Upper Precambrian and Lower Paleozoic evolution of the Iberian Peninsula according to U-Pb dating of zircons. Earth and Planetary Science Letters, 74(4): 325-37.

Laval, F., 1974. Precisions sur la tectonique des flyschs dans l'Est de la Grande Kabylie (Algerie). Comptes Rendus Hebdomadaires des Seances de l'Academie des Sciences, Serie D: Sciences Naturelles, 279(20): 1609-1612.

Laval, F., 1992. Gravity Depositional Systems and Sedimentary Megasequence of the Numidian Flysch Formation, North and East of the Grande Kabylie Massif (Algeria). Geodinamica Acta, 5(4): 217-233.

Lavier, L.L., Steckler, M.S. and Brigaud, F., 2001. Climatic and tectonic control on the Cenozoic evolution of the West African margin. Marine Geology, 178(1-4): 63-80.

Leblanc, D. and Feinberg, H., 1982. Tectonic and Stratigraphic Improvements About the Numidian of Eastern Rif (Morocco) - Geodynamic Implications. Bulletin De La Societe Geologique De

France, 24(4): 861-865.
Lefranc, J.P. and Guiraud, R., 1990. The continental intercalaire of northwestern Sahara and its equivalents in the neighbouring regions. Journal of African Earth Sciences, 10(1-2): 27-77.
Lentini, F., Carbone, S., Di Stefano, A. and Guarnieri, P., 2002. Stratigraphical and structural constraints in the Lucanian Apennines (southern Italy): tools for reconstructing the geological evolution. Journal of Geodynamics, 34(1): 141-158.
Loiacono, F., Paglionica, A. and Pellegrino, M.C., 1983. Le quarzoareniti del Flysch Numidico di Campomaggiore (PZ); indagini per l'utilizzazione in campo industriale. Geologia Applicata e Idrogeologia, 18(1): 63-80.
Llinás Agrasar, E., 2004. Crocodile remains from the Burdigalian (lower Miocene) of Gebel Zelten (Libya). Geodiversitas, 26(2): 309-321.
Lonergan, L. and White, N., 1997. Origin of the Betic-Rif mountain belt. Tectonics, 16(3): 504-22.
Lujan, M., Crespo-Blanc, A. and Balanya, J.C., 2006. The Flysch Trough thrust imbricate (Betic Cordillera): A key element of the Gibraltar Arc orogenic wedge. Tectonics, 25(6): 1-17.
Maate, A., Martin-Perez, J. A., Martin-Algarra, A., Serrano, F., Aguado, R., Martin-Martin, M. and El Hajjaji, K., 1995. Le Burdigalien inferieur de Boujarrah (Rif septentrional, Maroc) et la signification paleotectonique des series miocenes transgressives sur les zones internes betico-rifaines. Comptes Rendus de l'Academie des Sciences, Serie II. Sciences de la Terre et des Planetes, 320(1): 15-22.
Maffione, M., Speranza, F., Faccenna, C., Cascella, A., Vignaroli, G. and Sagnotti, L., 2008. A synchronous Alpine and Corsica-Sardinia rotation. Journal of Geophysical Research-Solid Earth, 113(B3): 25.
Magné, J. and Raymond, D., 1972. North of Great Kabylia (Algeria), Numidian with Age between Middle Oligocene and Lower Burdigalian. Comptes Rendus Hebdomadaires Des Seances De L Academie Des Sciences Serie D, 274(23): 3052-3055.
Markwick, P.J., 1998. Fossil crocodilians as indicators of Late Cretaceous and Cenozoic climates; implications for using palaeontological data in reconstructing palaeoclimate. Palaeogeography, Palaeoclimatology, Palaeoecology, 137(3-4): 205-271.
Masrouhi, A., Ghanmi, M., Slama, M. M. B., Youssef, M. B., Vila, J. M. and Zargouni, F., 2008. New tectono-sedimentary evidence constraining the timing of the positive tectonic inversion and the Eocene Atlasic phase in northern Tunisia: Implication for the North African paleo-margin evolution. Comptes Rendus Geoscience, 340(11): 771-778.
Mauffret, A., de Lamotte, D.F., Lallemant, S., Gorini, C. and Maillard, A., 2004. E-W opening of the Algerian Basin (Western Mediterranean). Terra Nova, 16(5): 257-264.
Mazzoleni, P., 1991. Le rocce profiriche nel conglomerato basale della formazione di Stilo-Capo d'Orlando. Memorie della Societa Geologica Italiana, 47: 557-565.
Meulenkamp, J.E. and Sissingh, W., 2003. Tertiary palaeogeography and tectonostratigraphic evolution of the Northern and Southern Peri-Tethys platforms and the intermediate domains of the African-Eurasian convergent plate boundary zone. Palaeogeography Palaeoclimatology Palaeoecology, 196(1-2): 209-228.
Michard, A., Chalouan, A., Feinberg, H., Goffe, B. and Montigny, R., 2002. How does the Alpine belt end between Spain and Morocco? Bulletin De La Societe Geologique De France, 173(1): 3-15.
Micheletti, F., Fornelli, A., Piccarreta, G., Barbey, P. and Tlepolo, M., 2008. The basement of Calabria (Southern Italy) within the context of the Southern European Variscides: LA-ICPMS and SIMS U-Pb zircon study. Lithos, 104(1-4): 1-11.
Miller, K.G., Wright, J.D. and Fairbanks, R.G., 1991. Unlocking the Ice House - Oligocene-Miocene Oxygen Isotopes, Eustasy, and Margin Erosion. Journal of Geophysical Research-Solid

Earth and Planets, 96(B4): 6829-6848.

Milner, S.C., Le Roex, A.P. and O'Connor, J.M., 1995. Age of Mesozoic igneous rocks in northwestern Namibia, and their relationship to continental breakup. Journal of Geological Society of London, 152: 97-104.

Mitchum, J.R.M. and Van Wagoner, J.C., 1991. High-frequency sequences and their stacking patterns: sequence-stratigraphic evidence of high-frequency eustatic cycles. Sedimentary Geology, 70(2-4): 131-147.

Monaco, C. and De Guidi. G., 2006. Structural evidence for Neogene rotations in the eastern Sicilian fold and thrust belt. Journal of Structural Geology, 28(4): 561-574.

Montanari, L., 1986. Aspetti tettono-sedimentari dell' Oligocene e Miocene in Sicilia e aree contigue. Giornale di Geologia, serie 3, 48: 99-112.

Moreau, J., Ghienne, J.F., Le Heron, D.P., Rubino, J.L. and Deynoux, M., 2005. 440 Ma ice stream in North Africa. Geology, 33(9): 753-756.

Moretti, E., Coccioni, R., Guerrera, F., Lahondére, J. C., Loiacono, F. and Puglisi, D., 1988. Numidian Flysch of the Constantine Mountains (Tell-Orientale, Algeria). American Association of Petroleum Geologists Bulletin, 72(8): 1015-1015.

Moretti, E., Coccioni, R., Guerrera, F., Lahondére, J. C., Loiacono, F. and Puglisi, D., 1991. The Numidian Sequence between Guelma and Constantine (Eastern Tell, Algeria). Terra Nova, 3(2): 153-165.

Morley, C.K., 1988. The tectonic evolution of the Zoumi Sandstone, western Moroccan Rif. Journal of Geological Society, 145: 55-63.

Mutti, E., Tinterri, R., Benevelli, G., di Biase, D. and Cavanna, G., 2003. Deltaic, mixed and turbidite sedimentation of ancient foreland basins. Marine and Petroleum Geology, 20(6-8): 733-755.

Mutti, E., Bernoulli, D., Lucchi, F.R. and Tinterri, R., 2009. Turbidites and turbidity currents from Alpine 'flysch' to the exploration of continental margins. Sedimentology, 56(1): 267-318.

Neubauer, F., 2002. Evolution of late Neoproterozoic to early Paleozoic tectonic elements in Central and Southeast European Alpine mountain belts: review and synthesis. Tectonophysics, 352(1-2): 87-103.

Oldow, J.S., Channell, J.E.T., Catalano, R. and B. D, Argenio., 1990. Contemporaneous thrusting and large-scale rotations in the western Sicilian fold and thrust belt. Tectonics, 9(4): 661-681.

Paquette, J.L., Caby, R., Djouadi, M.T. and Bouchez, J.L., 1997. U-Pb dating of the end of the Pan-African orogeny in the Tuareg shield: the post-collisional syn-shear Tioueine pluton (Western Hoggar, Algeria), Symposium 55 on Post-Collisional Magmatism, Strasbourg, France, pp. 245-253.

Parize, O., Beaudoin, B., Burollet, P. F., Cojan, I., Fries, G. and Pinault, M., 1986. A Northern Origin for the Sandy Material of Numidian Flysch (Sicily and Tunisia). Comptes Rendus De L Academie Des Sciences Serie 2, 303(18): 1671-1674.

Parize, O. and Beaudoin, B., 1987. Clastic Dikes in the Numidian Flysch (Tunisia, Sicily) - Their Relations with the Paleomorphology. Comptes Rendus De L Academie Des Sciences Serie 2, 304(3): 129-134.

Parize, O., Beaudoin, B. and Fries, G., 1999. Deep-water massive sands: facies, processes and channel geometry in the Numidian Flysch, Sicily - comment. Sedimentary Geology, 127(1-2): 111-118.

Patterson, R.T., Blenkinsop, J. and Cavazza, W., 1995. Planktic Foraminiferal Biostratigraphy and 87Sr/86Sr Isotopic Stratigraphy of the Oligocene-to-Pleistocene Sedimentary Sequence in the Southeastern Calabrian Microplate, Southern Italy. Journal of paleontology, 69(1): 7-20.

Pattison, S.A.J., 2005. Isolated highstand shelf sandstone body of turbiditic origin, lower Kenilworth Member, Cretaceous Western Interior, Book Cliffs, Utah, USA. Sedimentary Geology,

177(1-2): 131-144.

Paull, C.K., Mitts, P., Ussler, W., Keaten, R. and Greene, H.G., 2005. Trail of sand in upper Monterey Canyon: Offshore California. Geological Society of America Bulletin, 117(9-10): 1134-1145.

Peakall, J., McCaffrey, B. and Kneller, B., 2000. A process model for the evolution, morphology, and architecture of sinuous submarine channels. Journal of Sedimentary Research, 70(3): 434-448.

Pedley, H.M. and Renda, P., 1998. A regionally correlatable high to lowstand signal from late Burdigalian-early Langhian outliers in western Sicily, Italy. Bollettino Della Societa Geologica Italiana, 117(1): 39-53.

Pescatore, T., Renda, P. and Tramutoli, M., 1992. “Tufiti di Tusa” e flysch Numidico nella Lucania centrale (Appennino meridionale). Reudiconto della Academia delle Scieza F, 59(131): 57-72.

Peucat, J.J., Mahdjoub, Y. and Drareni, A., 1996. U-Pb and Rb-Sr geochronological evidence for late Hercynian tectonic and Alpine overthrusting in Kabylian metamorphic basement massifs (northeastern Algeria). Tectonophysics, 258(1-4): 195-213.

Peucat, J.J., Drareni, A., Latouche, L., Deloule, E. and Vidal, P., 2003. U-Pb zircon (TIMS and SIMS) and Sm-Nd whole-rock geochronology of the Gour Oumelalen granulitic basement, Hoggar massif, Tuareg shield, Algeria. Journal of African Earth Sciences, 37(3-4): 229-239.

Peucat, J.J., Capdevila, R., Drareni, A., Mahdjoub, Y. and Kahoui, M., 2005. The Eglab massif in the West African Craton (Algeria), an original segment of the Eburnean orogenic belt: petrology, geochemistry and geochronology. Precambrian Research, 136(3-4): 309-352.

Piqué, A., Tricart, P., Guiraud, R., Laville, E., Bouaziz, S., Amrhar, M. and Ouali, R. A., 2002. The Mesozoic-Cenozoic Atlas belt (North Africa): an overview. Geodinamica Acta, 15: 185-208.

Posamentier, H.W., 2001. Lowstand alluvial bypass systems: Incised vs. unincised. American Association of Petroleum Geologists Bulletin, 85(10): 1771-1793.

Puglisi, D., 1987. Le successioni torbiditiche cretacico-terziarie della Sicilia nord-orientale nel quadro dell’evoluzione del settore meridionale dell’Arco Calabro-Peloritano e della Catena Maghrebide siciliana. Giornale di Geologia (serie 3°), 49(1): 167-185.

Puglisi, D., 1994. Caratteri petrochimici delle arenarie delle unita torbiditiche oligo-mioceniche della Sicilia nord-orientale. Mineralogica et Petrographica Acta, 37: 393-415.

Puglisi, D., Zaghloul, M.N. and Maate, A., 2001. Evidence of sedimentary supply from plutonic sources in the Oligocene-Miocene flyschs of the Rifian Chain (Morocco); provenance and paleogeographic implications. Bollettino Della Societa Geologica Italiana, 120(1): 55-68.

Puglisi, D., 2008. Oligocene-Miocene sandstone suites from the Gibraltar and Calabria-Peloritani Arcs: provenance changes and paleogeographic implications. Geologica Carpathica, 59(6): 525-535.

Putignano, M.L. and Schiattarella, M., 2008. Geology, geomorphology, and exhumation modalities of the Monte Motola structure, Cilento region, southern Italy. Bollettino Della Societa Geologica Italiana, 127(3): 477-493.

Raymond, D., 1976. Sedimentary and Tectonic Evolution of Northwest Great Kabylia Algeria During the Course of the Alpine Cycle. Annales Scientifiques de l’Universite de Besancon Geologie(26): 47-76.

Riahi, S., Khalfa, K.B., Soussi, M. and Ismail-Lattrache, K.B., 2007. The Numidian Flysch Complex of Onshore Tunisia (Southern Kroumirie Range) - Facies Analysis and Stratigraphic Review. EAGE conference letters, 3rd North African/Mediterranean Petroleum& Geosciences Conference and Exhibition. Tripoli, Libya, 26 - 28 February 2007.

Ross, L.M. and Houseknecht, D.W., 1987. Petrographic Constraints on Provenance and Sediment

Dispersal Patterns, Atokan Sandstones of Arkoma Basin, Oklahoma and Arkansas. Association of Petroleum Geologists Bulletin, 71(8): 996-996.

Rossi, C., Kalin, O., Arribas, J. and Tortosa, A., 2002. Diagenesis, provenance and reservoir quality of Triassic TAGI sandstones from Ourhoud field, Berkine (Ghadames) Basin, Algeria. Marine and Petroleum Geology, 19(2): 117-142.

Rossi, P., Cocherie, A., Fanning, C.M. and Deloule, T., 2003. Variscan to eo-Alpine events recorded in European lower-crust zircons sampled from the French Massif Central and Corsica, France, Joint Assembly of the EGS/AGU/EUG, Nice, FRANCE, pp. 235-260.

Ruddiman, W.F. et al., Sarnthein, M., Backman, J., Baldauf, J. G., Curry, W. B., Dupont, L. M., Janecek, T. R., Pokras, E. M., Raymo, M. E., Stabell, B., Stein, R., Tiedemann, R., 1989. Late Miocene to Pleistocene evolution of climate in Africa and the low-latitude Atlantic; overview of Leg 108 results. Proceedings of the Ocean Drilling Program, Scientific Results, 108: 463-484.

Saddiqi, O., El Haimer, F. Z., Michard, A., Barbarand, J., Ruiz, G. M. H., Mansour, E. M., Leturmy, P., Frizon de Lamotte, D., 2009. Apatite fission-track analyses on basement granites from south-western Meseta, Morocco: Paleogeographic implications and interpretation of AFT age discrepancies. Tectonophysics, 475(1): 29-37.

Samuel, A., Kneller, B., Raslan, S., Sharp, A. and Parsons, C., 2003. Prolific deep-marine slope channels of the Nile Delta, Egypt. Association of Petroleum Geologists Bulletin, 87(4): 541-560.

Sanz de Galdeano, C., Serrano, F., Lopez Garrido, A.C. and Martin Perez, J.A., 1993. Palaeogeography of the late Aquitanian-early Burdigalian basin in the western Betic internal zone. Geobios, 26(1): 43-55.

Schaltegger, U., 1993. The Evolution of the Polymetamorphic Basement in the Central Alps Unraveled by Precise U-Pb Zircon Dating. Contributions to Mineralogy and Petrology, 113(4): 466-478.

Selley, R.C., 1968. Near-shore marine and continental sediments of the Sirte basin, Libya. Quaterly Journal of the Geological Society of London, 124: 419-460.

Serrano, F., Sanz de Galdeano, C., El Kadiri, K., Guerra-Merchan, A., Lopez-Garrido, A. C., Martin-Martin, M. and Hlila, R., 2006. Oligocene-early Miocene transgressive cover of the Betic-Rif internal zone; revision of its geologic significance. Eclogae Geologicae Helvetiae, 99(2): 237-253.

Shanmugam, G., 2008. The constructive functions of tropical cyclones and tsunamis on deep-water sand deposition during sea level highstand: Implications for petroleum exploration. Association of Petroleum Geologists Bulletin, 92(4): 443-471.

Shultz, M.R. and Hubbard, S., 2003. Slump-generated topographic control of deepwater sediment dispersal and preservation patterns and resultant stratigraphic architecture, Tres Pasos Formation, southern Chile. In: C. Chidsey Thomas, Jr. (Editor), 2003 AAPG annual convention with SEPM. American Association of Petroleum Geologists and Society of Economic Paleontologists and Mineralogists. Tulsa, OK, United States. 2003.

Shultz, M.R., Fildani, A., Cope, T.D. and Graham, S.A., 2005. Deposition and stratigraphic architecture of an outcropping ancient slope system; Tres Pasos Formation, Magallanes Basin, southern Chile. In: M. Hodgson David and S. Flint Stephen (Editors), Submarine slope systems; processes and products. Geological Society of London. London, United Kingdom. 2005.

Sinclair, H.D., 1997. Tectonostratigraphic model for underfilled peripheral foreland basins: An Alpine perspective. Geological Society of America Bulletin, 109(3): 324-346.

Sluijs, A., Brinkhuis, H., Crouch, E. M., John, C. M., Handley, L., Munsterman, D., Bohaty, S. M.,

Zachos, J. C., Reichart, G. J., Schouten, S., Pancost, R. D., Damste, J. S. S., Welters, N. L. D., Lotter, A. F. and Dickens, G. R., 2008. Eustatic variations during the Paleocene-Eocene greenhouse world. Paleoceanography, 23(4): 1-18.

Speranza, F., Maniscalco, R. and Grasso, M., 2003. Pattern of orogenic rotations in central-eastern Sicily: implications for the timing of spreading in the Tyrrhenian Sea. Journal of the Geological Society, 160: 183-195.

Stow, D.A.V., Johansson, M., Braakenburg, N. and Faugères, J.C., 1999. Deep-water massive sands: facies, processes and channel geometry in the Numidian Flysch, Sicily - reply. Sedimentary Geology, 127(1-2): 119-123.

Stow, D.A.V. and Mayall, M., 2000. Deep-water sedimentary systems: New models for the 21st century. Marine and Petroleum Geology, 17(2): 125-135.

Stromberg, S.G. and Bluck, B., 1998. Turbidite facies, fluid-escape structures and mechanisms of emplacement of the Oligo-Miocene Aljibe Flysch, Gibraltar Arc, Betics, southern Spain. Sedimentary Geology, 115(1-4): 267-288.

Suayah, I.B., Miller, J.S., Miller, B.V., Bayer, T.M. and Rogers, J.J.W., 2006. Tectonic significance of Late Neoproterozoic granites from the Tibesti massif in southern Libya inferred from Sr and Nd isotopes and U-Pb zircon data. Journal of African Earth Sciences, 44(4-5): 561-570.

Sutherland, P.K., 1988. Late Mississippian and Pennsylvanian Depositional History in the Arkoma Basin Area, Oklahoma and Arkansas. Geological Society of America Bulletin, 100(11): 1787-1802.

Tahiri, A., Simancas, J. F., Azor, A., Galindo-Zaldivar, J., Gonzalez Lodeiro, F., El Hadi, H., Martinez Poyatos, D., Ruiz-Constan, A., 2007. Emplacement of ellipsoid-shaped (diapiric?) granite; structural and gravimetric analysis of the Oulmes Granite (Variscan Meseta, Morocco). Journal of African Earth Sciences, 48(5): 301-313.

Talbi, F., Melki, F., Ben Ismail-Lattrache, K., Alouani, R. and Tlig, S., 2008. Le Numidien de la Tunisie septentrionale: donnees stratigraphiques et interpretation geodynamique. Estudios Geologicos, 64(1): 31-44.

Torricelli, S. and Biffi, U., 2001. Palynostratigraphy of the Numidian Flysch of northern Tunisia (Oligocene-early Miocene). Palynology, 25: 29-55.

Tricart, P., Torelli, L., Argnani, A., Rekhiss, F. and Zitellini, N., 1994. Extensional Collapse Related to Compressional Uplift in the Alpine Chain off Northern Tunisia (Central Mediterranean). Tectonophysics, 238(1-4): 317-329.

Trombetta, A., Cirrincione, R., Corfu, F., Mazzoleni, P. and Pezzino, A., 2004. Mid-Ordovician U-Pb ages of porphyroids in the Peloritan Mountains (NE Sicily): palaeogeographical implications for the evolution of the Alboran microplate. Journal of the Geological Society, 161: 265-276.

Uroza, C.A. and Steel, R.J., 2008. A highstand shelf-margin delta system from the Eocene of West Spitsbergen, Norway. Sedimentary Geology, 203(3-4): 229-245.

Vanhouten, F.B., 1980. Mid-Cenozoic Fortuna Formation, Northeastern Tunisia - Record of Late Alpine Activity on North African Cratonic Margin. American Journal of Science, 280(10): 1051-1062.

Van Sickel, W.A., Kominz, M.A., Miller, K.G. and Browning, J.V., 2004. Late Cretaceous and Cenozoic sea-level estimates: backstripping analysis of borehole data, onshore New Jersey. Basin Research, 16(4): 451-465.

Vila, J.M., 1978. Definition de la nappe neritique constantinoise, element structural majeur de la chaine alpine d'Algerie orientale. Bulletin de la Societe Geologique de France, 20(5): 791-794.

Vila, J. M., Feinberg, H., Lahondère, J. C., Gourinard, Y., Chouabbi, A., Magné, J. and Durand-Delga, M., 1995. The Sandy Uppermost Oligocene Channel and the Miocene of Sidi-Affif

Area in Their East Algerian Structural Setting - the Saharan Origin of the Numidian and the Calendar of the Miocene Overthrusts. Comptes Rendus De L Academie Des Sciences Serie 2, 320(10): 1001-1009.

Walsh, G.J., Aleinikoff, J.N., Benziane, F., Yazidi, A. and Armstrong, T.R., 2002. U-Pb zircon geochronology of the Paleoproterozoic Tagragra de Tata inlier and its Neoproterozoic cover, western Anti-Atlas, Morocco. Precambrian Research, 117(1-2): 1-20.

Weber, M.E., Wiedicke, M.H., Kudrass, H.R., Huebscher, C. and Erlenkeuser, H., 1997. Active growth of the Bengal Fan during sea-level rise and highstand. Geology (Boulder), 25(4): 315-318.

Weber, M.E., Wiedicke-Hombach, M., Kudrass, H.R. and Erlenkeuser, H., 2003. Bengal Fan sediment transport activity and response to climate forcing inferred from sediment physical properties. Sedimentary Geology, 155(3-4): 361-381.

Weijermars, R., 1991. Geology and Tectonics of the Betic Zone, Se Spain. Earth-Science Reviews, 31(3-4): 153-236.

Wezel, F.C., 1969. Lineamenti Sedimentologico Del Flysch Numidico Della Sicilia Nord-Orientale. Memorie Degli Instituti Di Geologia e Mineralogia Del L'Universita Di Padova, 26: 1-32.

Wezel, F.C., 1970a. Numidian Flysch - an Oligocene - Early Miocene Continental Rise Deposit Off African Platform. Nature, 228(5268): 275-276.

Wezel, F.C., 1970b. Geologica Del Flysch Numidico Della Sicilia Nord-Orientale. Memorie-Societa Geological Italiana, 9(2): 225-280.

Wildi, W., 1983. The orogenic belt of the Rif (Morocco) and the Tell (Algeria, Tunisia) - structure, stratigraphy, paleogeographic and tectonic evolution from the Triassic to the Miocene. Revue De Geologie Dynamique Et De Geographie Physique, 24(3): 201-297.

Woolfe, K.J., Larcombe, P., Naish, T. and Purdon, R.G., 1998. Lowstand rivers need not incise the shelf: An example from the Great Barrier Reef, Australia, with implications for sequence stratigraphic models. Geology, 26(1): 75-78.

Wynn, R.B., Cronin, B.T. and Peakall, J., 2007. Sinuous deep-water channels: Genesis, geometry and architecture. Marine and Petroleum Geology, 24: 341-387.

Yaich, C., 1992a. Dynamics of the Oligomiocene Detritic Facies of Tunisia. Journal of African Earth Sciences, 15(1): 35-47.

Yaich, C., 1992b. Sedimentologie, tectonique (et variations relatives du niveau marin) dans les formations du Miocene inferieur a moyen, Tunisie centrale et orientale. Géologie Méditerranéenne, 19(4): 249-264.

Yaich, C., Hooyberghs, H.J.F., Durlet, C. and Renard, M., 2000. Stratigraphic correlation between the Numidian formation (North Tunisia) and Oligo-Miocene deposits of central Tunisia. Comptes Rendus De L Academie Des Sciences Serie 2 Fascicule a-Sciences De La Terre Et Des Planetes, 331(7): 499-506.

Zachos, J.C., Shackleton, N.J., Revenaugh, J.S., Palike, H. and Flower, B.P., 2001. Climate response to orbital forcing across the Oligocene-Miocene boundary. Science, 292(5515): 274-278.

Zaghloul, M.N., Guerrera, F., Loiacono, F., Maiorano, P. and Puglisi, D., 2002. Stratigraphy and petrography of the Beni Ider Flysch in the Tetouan area (Rif chain, Morocco). Bollettino Della Societa Geologica Italiana, 121(1): 69-85.

Zaghloul, M.N., Di Staso, A., De Capoa, P. and Perrone, V., 2007. Occurrence of upper Burdigalian silexite beds within the Beni Ider Flysch Fm. in the Ksar-es-Seghir area (Maghrebian Flysch Basin, Northern Rif, Morocco): stratigraphic correlations and geodynamic implications. Bollettino Della Societa Geologica Italiana, 126(2): 223-239.

Chapter 3.

Downslope variations in density flow lithofacies and depositional architectures. The Numidian Flysch Formation of Sicily.

Chapter 3. Downslope variations in density flow lithofacies and depositional architectures. The Numidian Flysch Formation of Sicily.

Abstract.

Assessing the downslope variations in submarine fan architecture and depositional facies is of paramount importance in reconstructing density flow processes and the controls upon them. Seismic studies are increasingly recognising topographically complex slopes and their impact upon transiting turbidity currents, detailed analysis of depositional facies however are restricted to outcrop studies where sufficient exposure exists. This study describes downslope variations within the Numidian Flysch Formation of Sicily, focussing upon three key sections within a northwest to southeast downslope trend. Depositional architectures and the proportion of lithofacies are presented in order to constrain downslope changes and the controls upon density flows, with particular emphasis upon the role of an interpreted Channel Lobe Transition Zone.

A northernmost section contains 16 large entrenched channel-complexes stacked within a 5 km wide system. They are interpreted as an upper slope, slope-confined channel system. To the south, km wide channel-complexes aggradationally stack within a lower slope environment. In central Sicily a 570 m thick stacked lobe complex is interpreted, consisting of stacked progradational cycles. A marked change is recorded within the upper part of the section, with highly variable palaeocurrents, less coarse grained deposits and an increase in the thickness of turbidite mudcaps (T_e). Above this, a highly amalgamated granular sandstone section is interpreted as a Channel Lobe Transition Zone. This latter progression bears strong similarities to ponded-to-bypass successions from intraslope ponded basins in the Alpine Tertiary Basin, and this possibility is discussed.

Upslope of the CLTZ, deposition occurs dominantly through aggradation of coarse-grained massive sandstones, while downslope of the CLTZ, deposition results from waning turbulent flows. The CLTZ therefore marks a point of change in depositional style within the downslope trend. The architecture of the CLTZ itself consists of deep scours filled with rapidly deposited bedload deposits in the form of granular sandstones, and coarse grained suspension deposits from turbidity currents. Flows are interpreted to experience an increase in turbulence coupled with a drop in basal shear stress across the CLTZ, resulting in scouring of the substrate and deposition of coarse grained sediment through loss of flow capacity. The remaining low density flow bypasses to the lobe producing graded deposits. The CLTZ thus modulates flow behaviour and strongly impacts downslope depositional facies trends. This downslope trend is described and placed within a basin context.

3.1. Introduction

Understanding the downslope architecture and facies variations of submarine slope systems is of paramount importance in reconstructing their evolution and understanding the controls upon them. In particular, the ability to create models of depositional architectures and facies variability within slope systems is of major interest to the hydrocarbon industry. Studies of modern systems using sidescan sonar, and recent or ancient systems using 3D seismic data, have enabled depositional elements in submarine fans to be mapped in high resolution (e.g Posamentier and Kolla, 2003). They also allow submarine fans to be placed in context of a much larger slope system, and the

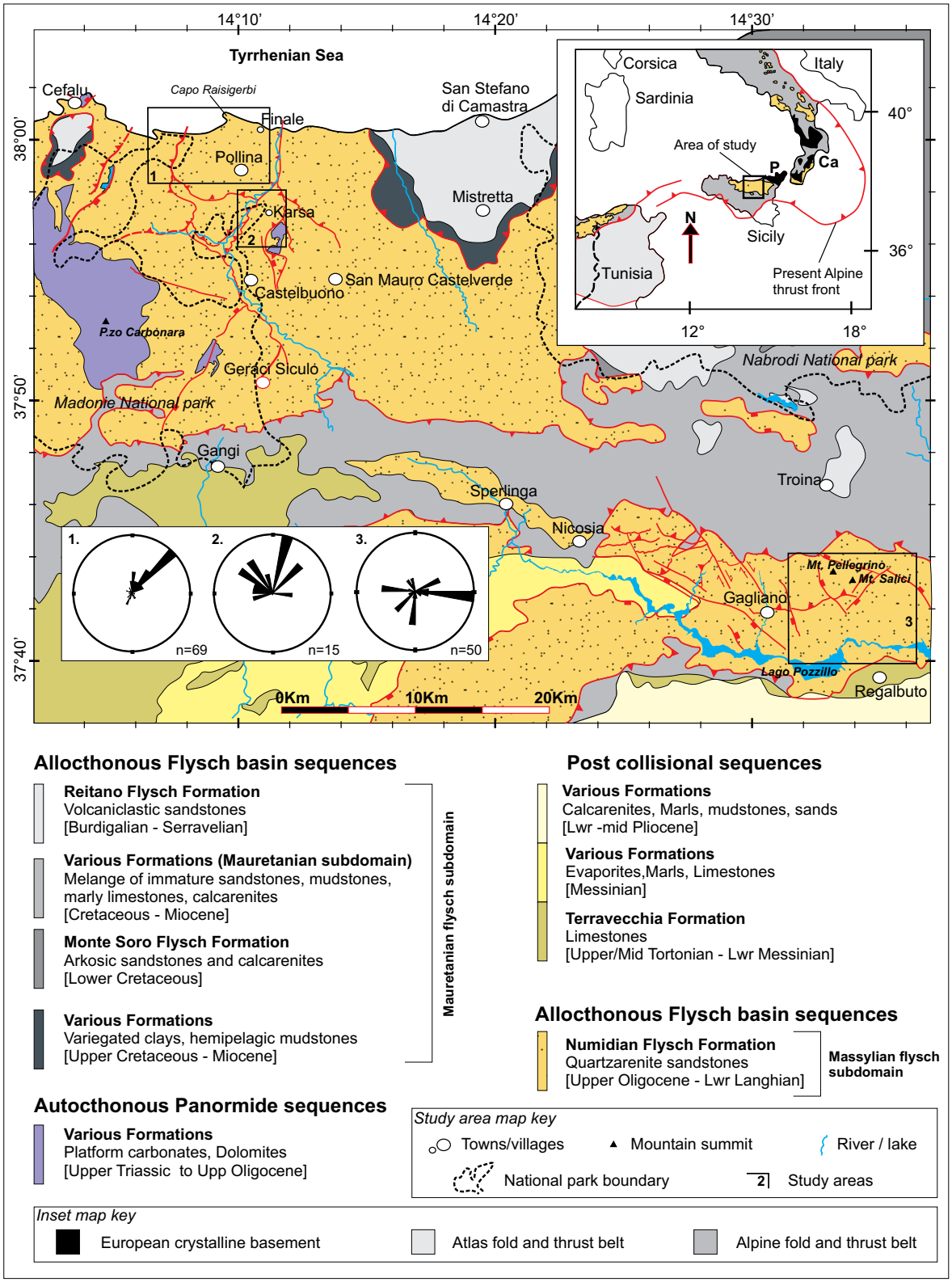

Figure 3.1.

Regional map and location of study area (see text for details). Map of Sicily redrawn from Bigi et al. (1991), Lentini et al. (1974), Carbone et al. (1990), and mapping undertaken for this study. Three study areas are presented from northwest to southeast, corresponding to: 1. Finale; 2. Karsa; 3. Mt. Salici. Rose diagram displays palaeocurrent data for all three study areas.

structural or topographic controls upon the systems evolution to be assessed (e.g Gee and Gawthorpe, 2006). Such studies have shown the complexity inherent resulting from mobile substrate, slope deformation and autocyclic effects. The interpretation of a topographically complex slope

system in the Gulf of Mexico with an interpreted ponded-to-bypass evolution is one such example (e.g Prather et al., 1998). Work on modern systems such as the Agadir fan have also highlighted the importance of features such as Channel Lobe Transition Zones (CLTZ) which separate channel mouths from basin floor lobe deposits across a significant break of slope (See Wynn et al., 2002 and references therein).

Outcrop studies generally suffer from constraints including outcrop dimensions, weathering, and local tectonics. Spectacular and unique examples however such as the Pab Formation of Pakistan (Eschard et al., 2003) or the Karoo Basin in South Africa (Prélat et al., 2009) offer seismic scale architectures coupled with a high-resolution facies analysis which is typically lacking in seismic studies. Such large scale and relatively unstructured outcrops are rare however given that oceanic basins ultimately undergo compression and closure. Nevertheless, topographically complex slopes and their impact upon density flows are being increasingly well documented, as with the Tertiary Alpine Basin of France (e.g Amy et al., 2007). Studies such as Ito (2008) also recognise the importance of features such as Channel Lobe Transition Zones in changing flow behaviour through the incorporation of substrate mud. They remain sparsely documented however with few well-documented examples.

The Numidian Flysch Formation of Sicily outcrops within nappes of the Alpine aged fold and thrust belt. As such it suffers familiar complexities in relation to placing sections within the context of a slope system. Previous studies however recognise a proximal to distal trend over ~35 km. Here we document the facies and depositional architectures of three sections from northern and central Sicily which span this palaeogeographic trend. Three key questions are discussed, namely; What density flow lithofacies and depositional elements can be observed within nappes of the Numidian Flysch Formation? Furthermore, can such depositional elements be recognised across the outcrop belt and be located within the context of a downslope palaeogeographic trend? Lastly, what controls are exerted upon density flows which transit the system and how are they manifest? Emphasis is placed upon describing an interpreted Channel Lobe Transition Zone and its impact upon modulating transiting flow behaviour. The characteristics of a ponded-to-bypass succession, related to an intraslope ponded basin, are also described and discussed within the context of the Maghrebian Flysch Foreland Basin.

3.2. Regional setting

The Oligo-Miocene Numidian Flysch Formation crops out in Spain, widely throughout North Africa, and in Sicily and southern mainland Italy as part of the Alpine aged fold and thrust belt (Figure 3.1). This discontinuous outcrop belt is over 2000 km in length and 10’s of Kilometres in width. The Numidian Flysch Formation represents a broadly linear series of submarine fans deposited into the Mahgrebian Flysch Basin (MFB), a precursor basin to the western Mediterranean basin.

3.2.1 The Maghrebian Flysch Basin

The Maghrebian Flysch Basin (MFB) was a foreland basin remnant of the neo-Tethys ocean in the western portion of the present day Mediterranean Basin (Figures 3.1 and 3.2). The basin was bordered to the north by an active margin which consisted of a southward verging accretionary prism, underlain by European crustal blocks which rode above northwards subducting oceanic crust (Golonka, 2004; Guerrera et al., 1993) (Figure 3.2.). To the south, the African margin formed a passive-margin to the basin.

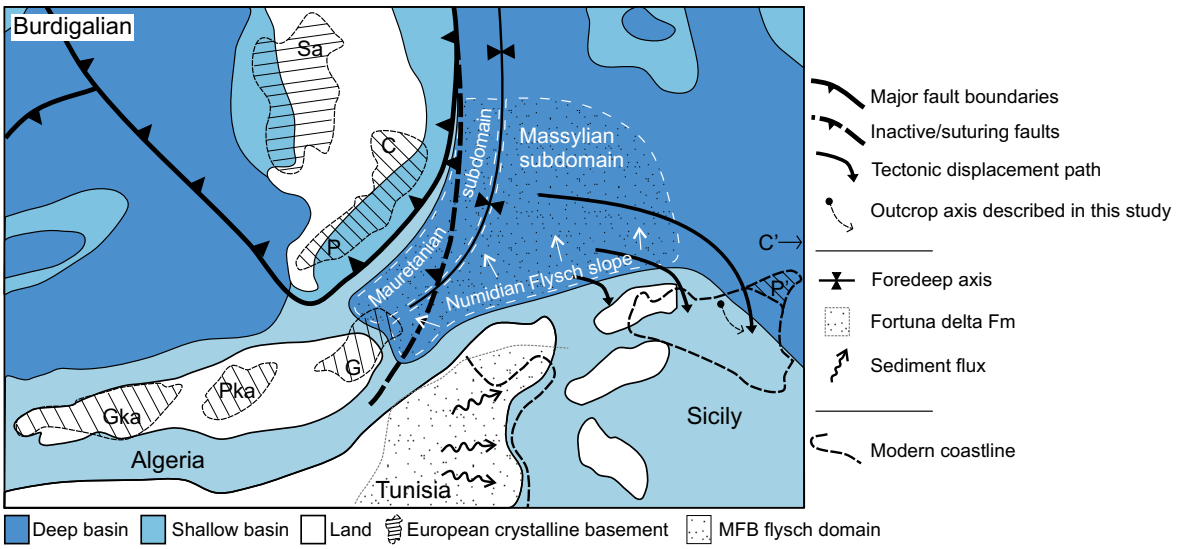

Figure 3.2.
Palaeogeographic reconstruction of the Sicilide basin during the Burdigalian. Major elements redrawn from Meulenkamp & Sissingh (2003) (Peri-Tethys project. See also Dercourt et al. (2000)). The location of the Fortuna delta is shown. Approximate sediment flux orientation of Numidian Flysch Formation (Massylian subdomain) is also shown. Tectonic displacement paths of Numidian Flysch Fm nappes, based upon palaeomagnetic data, are taken from Speranza et al. (2003). AlKaPeCa block abbreviations, basement to the northern, European margin of the basin are: Gka, Grand Kabylie; Pka, Petit Kabylie; G, Galite block; Sa, Sardinia; C, Calabria; P, Peloritan. P' and C' denote the final allocthonous position of the Peloritani and Calabrian blocks respectively. The approximate location of the outcrop axis (post nappe transport) described in this study is shown. Figure 2. Palaeogeographic reconstruction of the Sicilide basin during the Burdigalian. Major elements redrawn from Meulenkamp & Sissingh (2003) (Peri-Tethys project. See also Dercourt et al. (2000)). The location of the Fortuna delta is shown. Approximate sediment flux orientation of Numidian Flysch Formation (Massylian subdomain) is also shown. Tectonic displacement paths of Numidian Flysch Fm nappes, based upon palaeomagnetic data, are taken from Speranza et al. (2003). AlKaPeCa block abbreviations, basement to the northern, European margin of the basin are: Gka, Grand Kabylie; Pka, Petit Kabylie; G, Galite block; Sa, Sardinia; C, Calabria; P, Peloritan. P' and C' denote the final allocthonous position of the Peloritani and Calabrian blocks respectively. The approximate location of the outcrop axis (post nappe transport) described in this study is shown.

African margin foreland sequences consist of thick Mesozoic to Cenozoic age platform carbonates and shallow marine clastic deposits (Thomas et al., 2010, their figure 4). Units derived from the northern margin consist of European derived crustal blocks (i.e the Kabylie, Galite, Peloritani and Calabrian blocks) transgressed by continental conglomerates, shallow marine limestones and very coarse grained turbidite sequences including canyon confined deposits (Bonardi et al., 1980; Gery, 1983; Mazzoleni, 1991; Patterson et al., 1995).

Prolific deep marine clastic deposits also crop out, transgressing thick sections of basin mudstones but detached from crustal basement. Two distinct petrofacies are recognised, comprising an immature heterolithic series (Mauretanian deposits) and a quartzarenite Numidian series (Massylian deposits) (de Capoa et al., 2002; Guerrera et al., 1993; Thomas et al., 2010). The palaeogeographic relationship between these two series has been much debated but a recent regional review of available evidence (Thomas et al., 2010) constrains a European basement derived Mauretanian petrofacies and an African derived Numidian petrofacies (e.g Thomas et al. (2010) and references therein). The Numidian Flysch Formation therefore represents the offshore portion of a regional drainage system on the Oligo-Miocene North African passive margin. The term flysch, applied to the Numidian Flysch Formation by Gottis (1953), remains as a result of the intense debate surrounding either a northern or southern provenance for Numidian Flysch Formation clastic material.

3.2.2 The Sicilide sub-basin

Deposits of the MFB from Sicily and southern mainland Italy share a similar tectonostratigraphic history and are grouped together into the Sicilide sub-basin, representing the eastern of three such sub-basins (de Capoa et al., 2000).

In northern Sicily, Numidian Flysch Formation deposits transgress thick Triassic to Oligocene platform carbonates, dolomites, and marls of the Panormide complex (Figure 3.1). Numidian Flysch Formation sediments locally onlap this complex towards the north (Lentini et al., 1974) (Figure 3.1). In central Sicily and southern Italy however the Numidian Flysch Formation transgresses thick basin mudstones of Eocene to Miocene age (Carbone et al., 1990; Carbone et al., 1987).

A majority of studies on the Numidian Flysch Formation have focussed in northern Sicily and the Madonie National Park where thick sandstone packages are exposed. Wezel (1969) recognised channelized graded sandstones, ‘rhythmic silts’ and mudstones, and laminated sandstones and marls. They were interpreted to represent turbidity currents, pseudolaminar sand flows (e.g non cohesive debris flows), and grain flows. These associations were interpreted as representing outer shelf, continental rise and basin floor environments within an overall regressive trend (Wezel, 1969; Wezel, 1970). Subsequent recognition that the Numidian Flysch Formation was allocthonous and highly structured (e.g.Broquet et al., 1973) led to a reinterpretation including three depositional sequences representing basin-axial channel and lobe deposits in western Sicily (Pescatore et al., 1987). A regressive upwards trend was interpreted to be controlled by southwards migration of the accretionary prism. In southern Italy, depositional lobes have also been interpreted, accompanied by large scale (<200 m thick) debris flow deposits (Carbone et al., 1987). In northern Sicily, large sandstone channels have been described by Johansson et al. (1998) representing erosive conduits incising through muddy slope sediments.

Placing sedimentological studies of the Numidian Flysch Formation within the framework of a slope architecture has proved problematic. Several authors have suggested that deposits in southern Sicily are distal in comparison to deposits of northern Sicily (Broquet et al., 1973; Caire and Mascle, 1969; Faugeres et al., 1992; Hoyez, 1974) and this has resulted in central Sicilian deposits being named internal (e.g internal to the basin) and northern Sicilian deposits being termed external (e.g external to the basin) (e.g Broquet et al., 1973; Caire and Mascle, 1969; Faugeres et al., 1992). Faugeres et al. (1992) also interpreted a regressive sequence in both northern and central Sicily and placed it within a southwards proximal to distal trend, correlated using biostratigraphy and a tuffite marker bed.

3.3. Study areas

The work presented here focuses upon prominent sandstone outcrops which form a roughly northwest to south-east axis in central Sicily from the Madonie National Park in the North, to Regalbuto in central Sicily (Figure 3.1). Previous work on the Numidian Flysch Formation of Sicily has concentrated upon this axis (see section 3.2.2) and the inferred proximal to distal trend within it. We therefore characterise three sections within this axis in order to test architectural and facies variations and trends from northwest to southeast;

The Finale section is located on the northern coastline of Sicily within the Madonie national park (Figure 3.1). Approximately 10 km east of Cefalu, coastal cliff sections within an 8 km wide nappe expose excellent laterally continuous outcrops which can be traced for 6 km around the Capo Raisigerbi headland. The Karsa section is located 6.5 km south of the coastline (Figure 3.1) where

Kilometre scale nappes with hanging wall anticline geometries expose moderately to steeply dipping sandstone packages. Steep topography make accessibility a problem, but sections are characterised on both the west and east sides of the Pollina river valley.

The Mt. Salici section is 10 km north of Regalbuto and 6 km north of lago Pozillo (Lake Pozillo). It is 44 km southeast of the Karsa section (Figure 3.1). Here, large deci-kilometer scale nappes contain shallowly dipping sections exposed across a topographically isolated ridge of peaks (Mt Salici – 1142 m, Mt Pellegrino – 1138 m, Pzo Cardace – 1043 m). The section is exposed over 2.6 km via access roads to a series of wind turbines.

3.4. Results

3.4.1 Lithofacies

A range of lithofacies are recognised throughout the three study areas. They are described here using the density flow nomenclature of Dasgupta (2003) such that flows are grouped into; turbidity currents, hyperconcentrated flow, debris flow, and subaqueous grain flow, with increasing sediment to water ratio. They correspond to turbulent, transitional (between turbulent and plastic), laminar, and collisional flow characteristics respectively. Laminar debris flow deposits are subdivided into cohesive and noncohesive types based upon lithology, with noncohesive being equivalent to sandy debris flows of Shanmugam (1997). Table 3.1 summarises the following lithofacies and their associations.

3.4.1.1 Matrix-supported conglomerates (FA-1)

This association groups conglomerates which contain a high proportion of pebbles and varying amounts of mud in the matrix (Figure 3.3).

FA-1a corresponds to poorly sorted pebble conglomerates with relatively low amounts of mud in the matrix (Figure 3.3a). Beds reach 0.8 m thick with scoured bases such that stacked beds are highly amalgamated and laterally continuous for less than 40 m (Figure 3.3a). Clasts of rounded to well rounded pebbles are held within a poorly sorted matrix of mud to coarse sand. No normal grading is observed. Clasts may reach 70 mm in length although typically are 10 to 30 mm. Clasts may be imbricated throughout the thickness of the bed and small flutes may be present at the bed base. Small mud clasts form part of the matrix. These deposits indicate turbulence preceding and traction during deposition. They are interpreted to represent bedload deposition from the lower, hyperconcentrated portion of a well stratified turbidity current.

Mud and mud clast supported conglomerates (FA-1b) differ from the former facies due to a high percentage of mud (~30-70%) and abundance of mud-clasts within the matrix (figure 3.3b). Beds are similarly ungraded and very poorly sorted with randomly orientated pebbles up to 30 mm in width. In specific patches throughout the bed thickness, the conglomerate becomes clast supported (Figure 3.3c). Beds reach 1.5 m thick with scoured bases (<0.3 m). FA-1b is similar to FA-1a with respect to these characteristics although the matrix is dominated by mud and contains rounded to elongate mud clasts which reach 1.2 m in length and contribute up to 50% of the bed volume. A cohesive debris flow origin is interpreted with the clasts floating within a matrix of substantial yield strength. The similarity with FA-1a suggests that this represents a flow transformation from FA-1a through incision and incorporation of substrate mud. Break up of mud clasts and direct entrainment of unconsolidated mud would serve to bulk out the matrix thereby altering the flow character from

Facies association	Facies	Sedimentary structures	Turbidite divisions*	Bounding surface	Thickness	Secondary features	Interpretation	Figure
FA-1: Matrix supported conglomerates	FA-1a: Poorly sorted pebble conglomerate	Flutes, Pebble imbrication	S3	Sharp high relief base. Sharp top	0.05-0.8 m	Some clast imbrication. Occasional reverse grading	Deposition from lower hyperconcentrated part of bi-partite turbidite	3a
	FA-1b: Mud and mud-clast supported conglomerate	-	-	Sharp, planar to moderate relief base. Sharp top	0.5-1.5 m	Abundant mud clasts <1.5 m long	Cohesive debris flow (transformation facies from Fa-1a)	3b, 3c
FA-2: Massive deposits	FA-2a: Mudstones rich in silt to granule clasts	-	-	Sharp planar base and sharp low relief top	0.05-5 m	Ungraded, very poorly sorted. Rare examples of floating sandstone blocks <0.75 m long	Cohesive debris flow	3d, 3e
	FA-2b: Poorly sorted granular sandstones	-	-	Sharp high relief base, Sharp top	0.1-1 m	Ungraded, very poorly sorted. Rare pebbles, common mud clasts (maybe imbricated). Associated with scours	Deposition from lower hyperconcentrated part of bi-partite turbidite	3f
	FA-2c: Massive moderately to well sorted sandstones	Rare flutes. mm scale mud clasts	- T_e	Sharp planar base. Sharp to graded transitional top	0.05-8 m	Ungraded, structureless deposits. Fine to coarse sand. Mud cap (Te) common in thin examples. Mud clast horizons in thicker examples	Aggradation from bypassing quasi steady flow OR non-cohesive debris flow	3g, 3h
	FA-2d: Thinly banded sandstones and mudstones	-	M2a-M2b H2	Sharp planar base.	<0.3 m	Ungraded sandstones with dewatering. Sharp boundary with mudstones. Banding on mm to cm scale	Flows intermediate between laminar and fully turbulent. Banded slurry flow (subdivision M2a and M2b)	3i, 15f
FA-3: Graded sandstones with interbedded mudstones	FA-3a: Normally graded silt to coarse sandstone beds commonly interbedded	Flutes, Parallel lamination, Ripples	T_a, T_b, T_c, T_d, T_e	Sharp, planar to moderate relief base. Sharp to graded transitional top	0.01-1.5 m	Loaded bases, flame structures	Waning turbidity current surge	3j, 3k, 3l
	FA-3b: Normally graded silt to medium sandstone with co-genetic mudstone cap	Rare upper-stage plane beds at sandstone top	H3	Sharp planar base. Graded deformed top	0.1-0.2 m	Poorly sorted Mudstone cap, typically loaded into lower sandstone	Waning turbidity current surge and co-genetic cohesive debrite (Linked Debrite)	3m, 3n

* T subdivisions from Bouma (1962);S subdivisions from Lowe (1982); H subdivisions from Haughton et al (2009); M subdivisions from Lowe and Guy (2000).
- Lithofacies colours correspond with facies percentages in figure 17.

Table 3.1. (Previous page)
A table of lithofacies associations from the Numidian Flysch Formation of Sicily.

transitional to laminar (Dasgupta, 2003).

3.4.1.2 Massive deposits (FA-2)

Massive deposits are here defined as beds which are ungraded, with the exception of some top only coarse tail grading, and are predominantly structureless (e.g primary sedimentary structures). These deposits are therefore not wholly suitable for classification within the Bouma scheme (Bouma, 1962). Four lithofacies are represented based upon gross physical character.

Facies FA-2a are mudstones rich in silt to granule clasts. They are very poorly sorted but are predominantly mud rich (Figure 3.3d). Beds are typically 0.3 m thick but may reach 5 m with conformable to slightly (<0.1 m) erosive bases. Beds are structureless and ungraded and bioturbation is common throughout, including sub vertical to vertical and V shaped burrows (*Ophiomorpha rudis* and *Diplocraterion habichi* respectively) (Figure 3.4g and 3.4i). In some examples, large rounded sand blocks, coherent but deformed at times, float randomly throughout the matrix and reach 75 cm in length (Figure 3.3e) implying significant matrix yield strength. This facies is interpreted therefore to represent the product of cohesive debris flows.

FA-2b deposits are poorly-sorted granular sandstones. Beds of this facies reach 1 m in thickness but are highly variable with well scoured bases. Deposits are very poorly sorted with silt to granule grain sizes (Figure 3.3f). Angular clasts of medium to very coarse sand are however the dominant grainsize. Rare isolated pebbles reach 30 mm in diameter. Grading and sedimentary structures are not observed within this facies. Mud rip up clasts can be numerous, particularly where this facies infills scours, either distributed throughout the bed or concentrated at bed top. Deposits from Mt. Salici show common imbrication of mud clasts, however examples from Finale and Karsa do not. The association of this facies with scours and a typically erosive base suggests turbulence, while poor sorting and lack of grading suggest rapid deposition. Where imbricated mud clasts are present, bedload deposition from the lower hyperconcentrated portion of a turbidity current is interpreted, with imbrication of mud clasts occurring through shear from the overriding turbulent flow. Where there is no evidence for traction, rapid deposition through collapse of turbulence and loss of capacity may be responsible.

Facies FA-2c represents massive, moderately to well sorted sandstones with a fine to coarse grainsize. Beds are dominantly ungraded and contain no sedimentary structures with the exception of some basal flutes (Figures 3.3g and 3.3h). Thinner beds (<1 m thick) are typically interbedded with mudstones, while thicker beds (1- 8 m) typically occur within successions of stacked massive sandstones (Figure 3.3g). Beds are typically sharply bound with planar bases and can show coarse tail grading up to the upper surface. Thick examples may show small flame structures at the bed base with rarer examples of pipes and dish and pillow structures. Horizons of small mud clasts (<10 mm) are also common within thick examples and are sometimes observed to disappear laterally or cross cut one another (Figure 3.7c). Within thin examples, *Thalassinoides* bioturbation is common on bed bases while *Helminthoida* (Nereites ichnofacies) and *Gyrochorte* type traces have been observed on bed tops (Figure 3.4a and 3.4b). Also present on thin bed tops are rare curvilinear traces which resemble Polychaete worm etchings (Figure 3.4d).

There has been much discussion surrounding the origin of deep-water-massive-sandstones (see

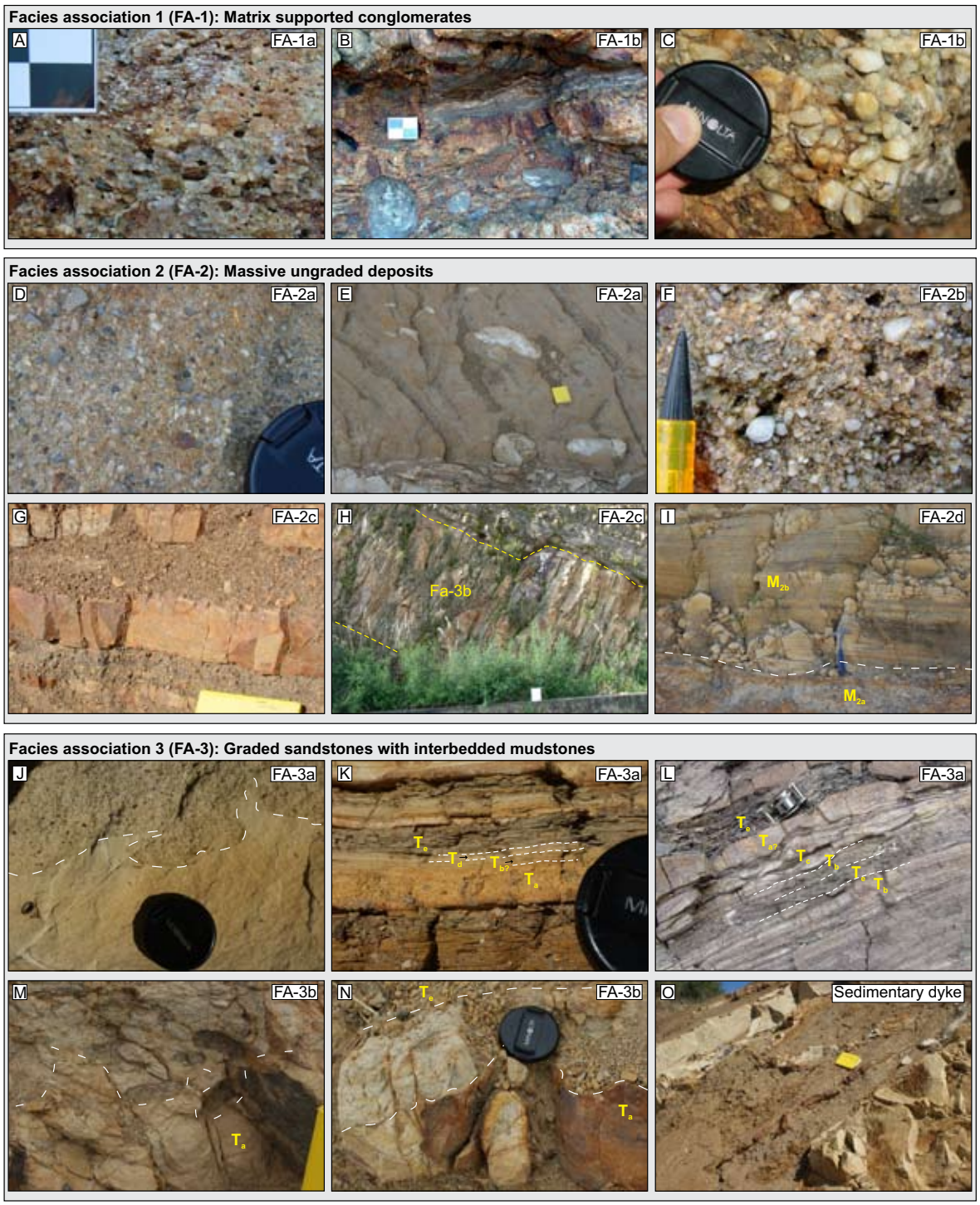

Figure 3.3.

Density flow facies: A; FA-1a; Poorly sorted pebble conglomerate, channel complex CR7, Finale. B; FA-1b; Mud and mud clast supported conglomerate, and C; detail of clast supported section. Channel complex CR7, Finale. D; FA-2a; Mudstones rich in silt to granule clasts and E; example of sandstone boulders floating within matrix. Mt. Salici. F; FA-2b; Poorly sorted granular sandstones. Channel complex CR4, Finale. G; FA-2c; Massive moderately to well sorted sandstones, thin bedded (<1 m and interbedded with mudstones) and H; thick bedded (4 m thick example). Ambroggio, near Finale, and Karsa village respectively. I; FA-2d; Thinly banded sandstones and mudstones, M2a and M2b subdivision (see text for details). Mt. Pelegrino, near Mt. Salici. J,K,L; FA-3a; Normally graded silt to coarse sandstone commonly interbedded. Examples of Bouma subdivisions from Mt. Salici and Karsa. M,N; FA-3b; Normally graded silt to medium sandstones with co-genetic mudstone cap. Mt. Salici. O; Sand intrusion, ptymatically folded. Mt. Salici.

critiques by Mulder and Alexander (2001), Shanmugam (2002), and Kneller and Branney (1995)). A fluted substrate, normally graded tops, and mud caps in thinner examples indicate turbulence as an

important depositional process, while the lack of sedimentary structures suggests rapid deposition preventing traction at the flow/deposit interface. This facies is therefore interpreted as aggradational deposition from a quasi-steady turbidity current as discussed by Kneller and Branney (1995). In stacked examples however where flutes and mud caps (Te) are absent, a non-cohesive debris flow mechanism cannot be ruled-out (sensu Shanmugam, 2000).

Facies FA-2d consists of medium grained sandstones banded with alternating mudstones (Figure 3.3i) on a 5 to 20 mm scale. Stacked bands form 'beds' up to 0.3 m thick with bases which are planar or locally scoured up to 30 mm. Individual sandstone bands are structureless and ungraded and maintain similar thicknesses across the outcrop extent. Their bases are sharp and planar to diffuse, but may show loading into interbanded mudstones. Banded mudstones range from 2 to 30 mm thick, contain some silt to fine sand but are also ungraded and structureless. Mudstone bands are generally much thinner than the sandstone bands. 'Banded beds' range from 0.3 to 1.5 m thick and are interbedded with mudstone beds <0.4 m thick containing some silt to medium sand (<20%).

Both the banded and interbedded mudstones are similar, and have the character of Fa-2a (Mudstones rich in silt to granule clasts) albeit better sorted with a finer grainsize fraction. A laminar, cohesive debris flow origin is considered likely. Within banded beds, diffuse boundaries and loading between sandstones and mudstones suggests a genetic link between bands. The banded sandstones lack structures and grading inherent in discrete waning turbulent flows, and are therefore interpreted to result from laminar or transitional flow processes (sensu Dasgupta, 2003).

Lowe and Guy (2000) describe similar genetic banded beds from the Britannia Formation of the North sea. Termed banded slurry beds, they have subsequently been recognised from the Forties event beds (Everest field, North Sea) and the lower Ross Formation and termed H2 hybrid event beds (sensu Haughton et al., 2009). They are interpreted to represent hybrid flows intermediate between fully turbulent and laminar flow regimes (Haughton et al., 2009) which form through stratification of a mud rich turbulent surge in which coarse clastic grains settle to form lighter bands. Subsequent enrichment of the flow base in cohesive mud generates a basal layer which freezes to form a darker band (Lowe and Guy, 2000). The examples described here conform to this description and are therefore interpreted as the M2b (macrobanded slurry flow) subdivision of Lowe and Guy (2000). Interbedded mudstone beds containing silt to medium sand may represent the M2a (mixed slurried) subdivision (sensu Lowe and Guy (2000)).

3.4.1.3 Graded sandstones with interbedded mudstones (FA-3)

Facies FA-3a consists of normally graded beds, reaching 1.5 m thick but averaging 0.25 m (Figures 3.3j, 3.3k, 3.3l). This facies includes those typically categorized by the Bouma sequence (Bouma, 1962) and correspond to the arenaceous-pelitic facies of Mutti and Ricci Lucchi (1978). A subdivision according to the Bouma sequence is used: T_a; Normally graded fine to coarse sandstone, with scattered pebbles up to 2 cm in width, concentrated near the bed base which may show a thin coarsening upwards trend. The base is commonly erosional and mud rip up clasts are often present. T_b; Laminated silts to medium sandstones with upper-stage plane beds throughout. T_c; Fining upwards medium sandstone to silt with isolated ripples. T_d; laminated silt. T_e; Mudstone cap, which can be bioturbated. Subdivisions are commonly organised as T_a, T_{abe}, T_{ace}, T_{ae}. Facies FA-3a represents progressive deposition from a waning (unsteady), or non-uniform, turbulent surge.

Facies FA-3b contains a lower sandstone unit with characteristics of a Bouma T_a subdivision, and an upper moderately sorted mudstone to siltstone unit. The total thickness varies from 0.1 to 0.2 m (Figures 3.3m and 3.3n). Lower sandstone beds are typically massive and unstructured but coarse tail graded. Bed bases are relatively planar with little or no erosion. Upper stage plane-bed lamination is rare within the top of the sandstone. The upper muddy subdivision is typically as thick as the sandstone, ungraded and may contain mud rip up clasts. Mud clasts reach 150 mm long, are distributed throughout the bed thickness with random orientations, and may be foundered into the lower sandstone unit (Figure 3.3m). In upper beds where silt is a dominant grainsize, a contorted ductile texture is apparent. Where the contact between the units is abrupt, foundering or loading is common. Contacts can also show rapid grading however from fine sand to mud over a few millimetres. Facies FA-3b shows the characteristics of a turbidite with a co-genetic linked debrite (Haughton et al., 2009; Haughton et al., 2003). They are inferred to represent sandstone deposition from a waning turbulent surge, followed by deposition of a cohesive debris flow which was part of the same event but was partitioned further upslope (Haughton et al., 2009).

3.4.1.4 Discordant and terminating beds

A variety of bed geometries include abrupt terminations, cross cutting, and rapid dip changes.

Folded and truncated beds (FA-4a) occur in sections <40 m thick. Sections consist of mudstones interbedded with thin and non amalgamated sandstones. The sandstone beds are folded, and may be truncated by other beds which cross cut at a high angle of dip (e.g figure 3.9b). Where exposure allows, the folded section can be observed to unconformable overlie a relatively planar base of mudstones and thin sandstones. Conformable beds of similar facies can also be observed to truncate the folded beds at the section top such that folded sequences are bound below and above by undeformed stratigraphy.

This facies geometry indicates a discrete deformation event in which mudstones and interbedded sandstones are remobilised. Bed truncations suggests some that examples contain several episodes of remobilisation. A slump origin is therefore interpreted, with the latter examples representing a complex of slump bodies.

Discordant and irregular bedding (FA-4b) includes sandstones surrounded by structureless mudstones which have highly irregular thickness changes and often terminate over a few centimetres to metres. The beds are typically structureless and ungraded but may contain mud clasts. Beds can also dip at any angle ranging from the stratigraphic horizontal (e.g bed normal) to perpendicular (Figure 3.3o). Folding of such beds is common, as are branching geometries whereby a bed splits into two or more separate ends.

These geometries are observed on two primary scales. Minor ‘finger like’ protrusions are common, reaching 0.1 m thick and projecting from the edges of large sandstone bodies including bedding and channel forms. Larger beds reach 0.5 m thick and can be traced for several metres (Figure 3.3o). They can show ramp-flat geometries and cross cut other conformable sandstone beds.

These beds are interpreted as clastic injectites which penetrate thick mudstone dominated successions. Vertically orientated geometries represent dyke style intrusions subsequently deformed through compaction and ptygmatic folding. Large horizontal beds represent sill intrusion.

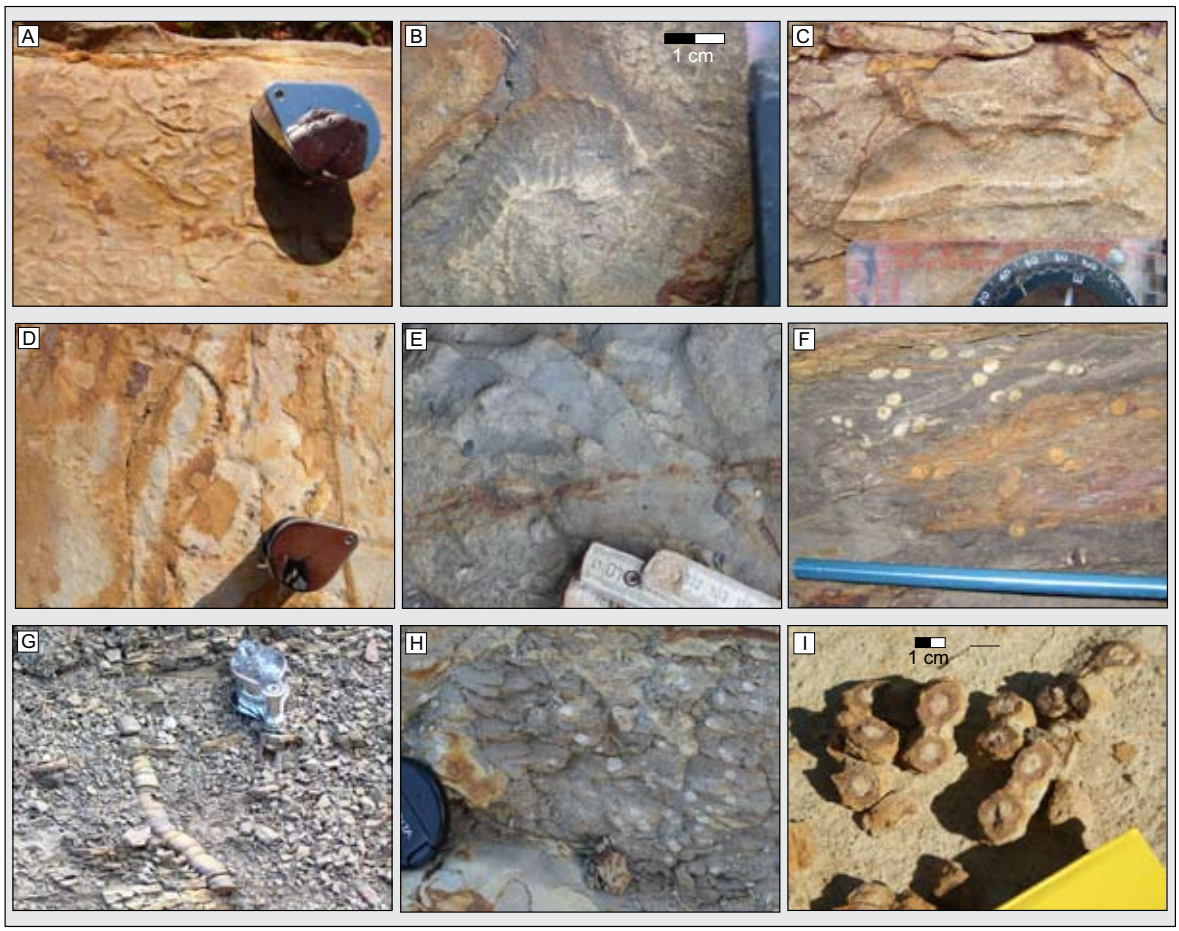

Figure 3.4.
Examples of trace fossils within the Numidian Flysch Fm of Sicily. A; *Helminthoida Mollasica*, Nereites icnofacies. Traces on bed top (Fa-3a). Karsa village. B; *Gyrochorte* ichnogenus on bed top (FA-3a, Ta division), Finale village. C; Bilobate winding and unbranched form (*Gyrochorte* or *Taphrheminthopsis*?). Karsa village. D; Rare trace reminiscent of Serpulid Polychaetes etchings. Bed top (FA-2c), Karsa village. E; Small scale *Thallasinoides* traces. Finale village. F; *Arenicolites* tubes. Capo Raisigerbi headland. G; Subvertical burrow with geopetal fill (*Ophiomorpha rudis*). Capo Raisigerbi headland. H; *Planolites* type burrows. Mt. Salici. I; V or U shaped *Diplocraterion habichi* burrows within FA-2a. Mt. Salici.

3.4.2 Section descriptions

The three areas of study (Figure 3.1) are here described from north-west to south-east.

3.4.2.1 The Finale section

A 650 m thickness of stratigraphy is exposed from the coast near Finale to the village of Pollina at 735 m elevation (Figure 3.1). The stratigraphy dips 30° towards the coast (north), and due to the topography, outcrops locally young southwards towards Pollina. Superb coastal outcrops allow characterisation of large bodies of stacked sandstones encased within mudstones (Figure 3.5). Bodies range from 80 to 400 m in width and up to 90 m thick. Strongly concave-up basal geometries are common where observed, coupled with approximately flat surfaces defining the body top. A clear channel-form geometry is therefore recognised.

In total, 16 large channel forms are mapped (Figures 3.5 and 3.6). They consist of stacked sandstones and conglomerates and contain channel-wide erosional surfaces which truncate bedding (Figure 3.5). Such surfaces bound a generally repeatable progression of facies with very coarse grained sandstones and conglomerates (FA-1a, 2b, 2c) overlain by thickly stacked massive sandstones (FA-2c) and interbedded normally graded sandstones (FA-3a).

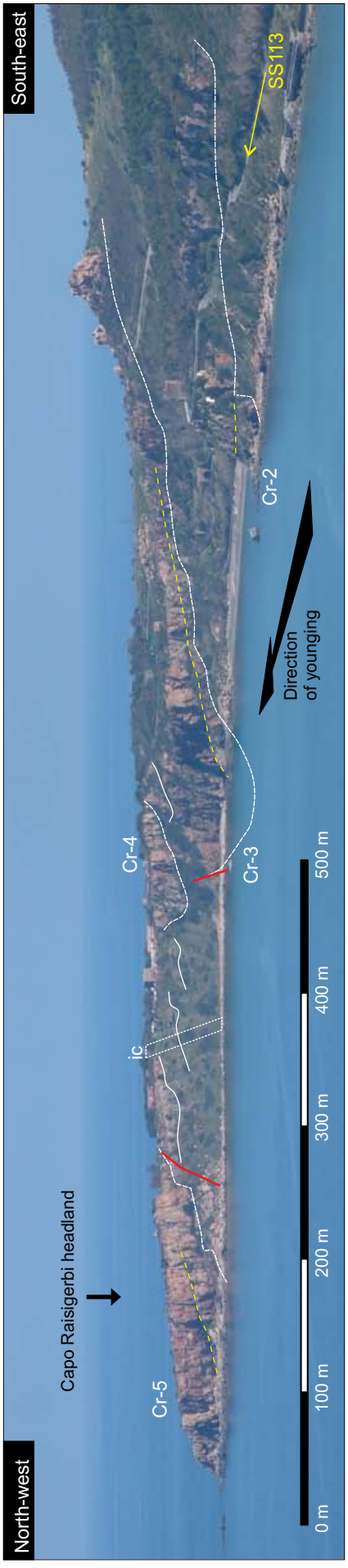

Figure 3.5.
Photo-panorama of Capo Raisigerbi headland, Finale section of northern Sicily. Incisional channel-complexes are labelled Cr-2 to Cr-5 with younging. Incisional channel-complex bases are marked in white. Dashed yellow lines highlight erosional surfaces marking the base of stacked channel-elements within a channel-complex (see text). The box 'IC' marks a 75 m thick inter-channel sequence described within the text. White solid lines mark significant scour surfaces within the interchannel section. Faults marked in red. Channel-complexes are observed to stack laterally towards the east (shown by the black arrow), separated by 10's of metres of fine-grained sediment.

A hierarchy similar to Sprague et al. (2002) and Campion et al. (2000) is used here to define the bodies as channel-complexes. They contain 2 or more individual channel-elements which are stacked to form a complex. Channel elements contain relatively conformable sand rich sequences, bound above and below by either mudstones or a laterally extensive erosional surface. Where several channel-complexes occur in proximity, a channel-complex-set is defined. Two or more channel-complex-sets are grouped to form a channel system.

In total, 16 channel-complexes are mapped in the Finale area, numbered as Cr-1 through Cr-16 with younging (Cr denoting the Capo Raisigerbi headland at Finale) (Figures 3.5 and 3.6). Channel-complexes Cr-1 to Cr-8 are observed to systematically offset stack eastwards along the coastline (Figure 3.5 and 3.6). They are separated vertically by <10's of metres of mudstones with thin turbidite deposits (FA-3a). Channel-complexes Cr-9 to Cr-16 outcrop along the Pollina ridgeline where they show a non-systematic stacking pattern. Two separate groups of channel-complexes are therefore recognised, forming two channel-complex-sets within the Finale channel system.

The margins of channel complexes Cr-2, 6 and 7 can be traced from the coastline towards Pollina village for <4.5 km with a north eastwards orientation (Figure 3.6). This matches palaeoflow data recorded from flutes, cross beds and ripples within the channel complexes and in interchannel areas (Figure 3.1). Viewed in planform however, channel complexes show some sinuosity (e.g complexes Cr-3, 5, 6 and 7. Figure 3.6) and complex Cr-4 is observed to plunge beneath complex Cr-5.

On the Capo Raisigerbi headland the margins of 3 channel-complexes (Cr-3, Cr-4, and Cr-5) are observed to cut down into a 75 m thick section (Figure 3.5. Box ic) comprising mudstones interbedded with laminated and rippled medium to coarse turbidites (FA-3_a, $T_{a,b,c}$), massive granular sandstones (FA-2b), mud rich cohesive debrites (FA-2a), and lenticular

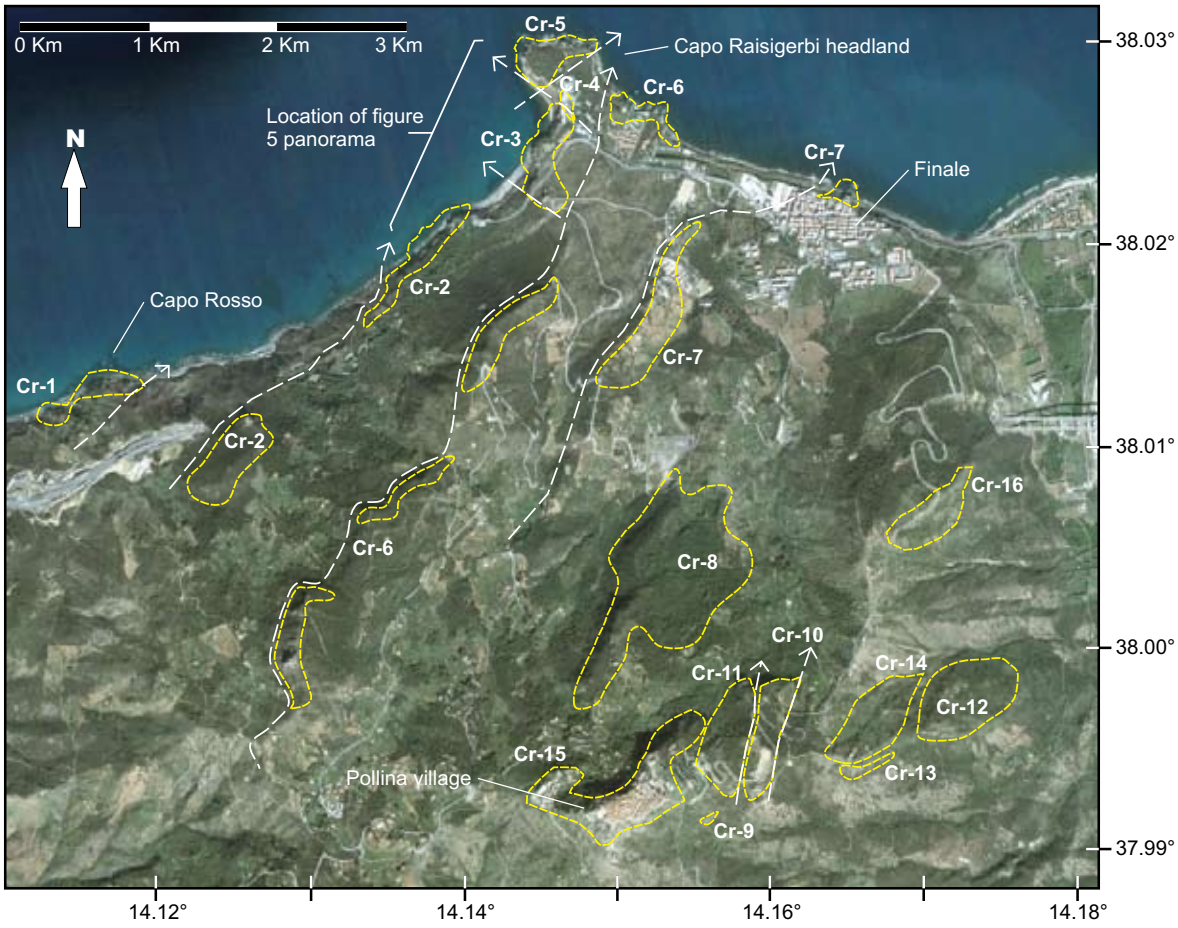

Figure 3.6.
Annotated Google Earth aerial photograph of Capo Raisigerbi headland, northern Sicily. Sixteen incisional Channel complexes, mapped during fieldwork, are numbered sequentially with younging (i.e. 1 the oldest, 16 the youngest). The extent of each channel complex outcrop is marked in white. Arrows denote the orientation of the channel complex margin.

bodies of stacked sandstone which reach 5 m thick (Figure 3.5). At the base of complexes Cr-3 and Cr-5, and at the top of complex Cr-5, beds of these facies are erosionally truncated against stacked sandstones of the channel-complex fill. Both channel-complex margins show horizontal terraces separated by steeply incising surfaces, dipping locally up to 90° (Figure 3.5).

A majority of the channel-complex fill consists of thick beds (<8 m thick) of coarse to very coarse massive sandstones (FA-2c) which onlap the basal surface (Figure 3.7b). The steepest dipping margin sections are closely associated with very coarse grained facies however, including stacked sequences of conglomerates (FA-1a) which are extremely amalgamated both vertically and laterally where they onlap the margin (Figure 3.7b). This facies also drapes incisional surfaces which define the base of channel-elements, stacked within channel-complexes. Relief of the incisional surface varies between a few metres over the channel-complex width, and local high relief incision of up to 10 m (Figure 3.5). A progression of coarse facies (Fa-1a, Fa-1b, Fa-2b) to massive sandstones (Fa-2c) and interbedded mud rich conglomerates (Fa-1b) (Figure 3.7a and 3.7d) is common throughout the sections studied. Such coarse facies tend to be localised and pinch out laterally onto the channel-complex or channel element basal erosion surface. Towards the channel-complex margins, ungraded sandstones (Fa-2c) therefore lie directly upon the basal surface and either amalgamate with beds of the same facies from a previous channel-element, or directly overlie mudstones below the channel-complex base. Slump bodies (FA-4a) up to 4 m thick are relatively common in channel-elements, typically consisting of rare thin turbidites (FA-3a) interbedded with

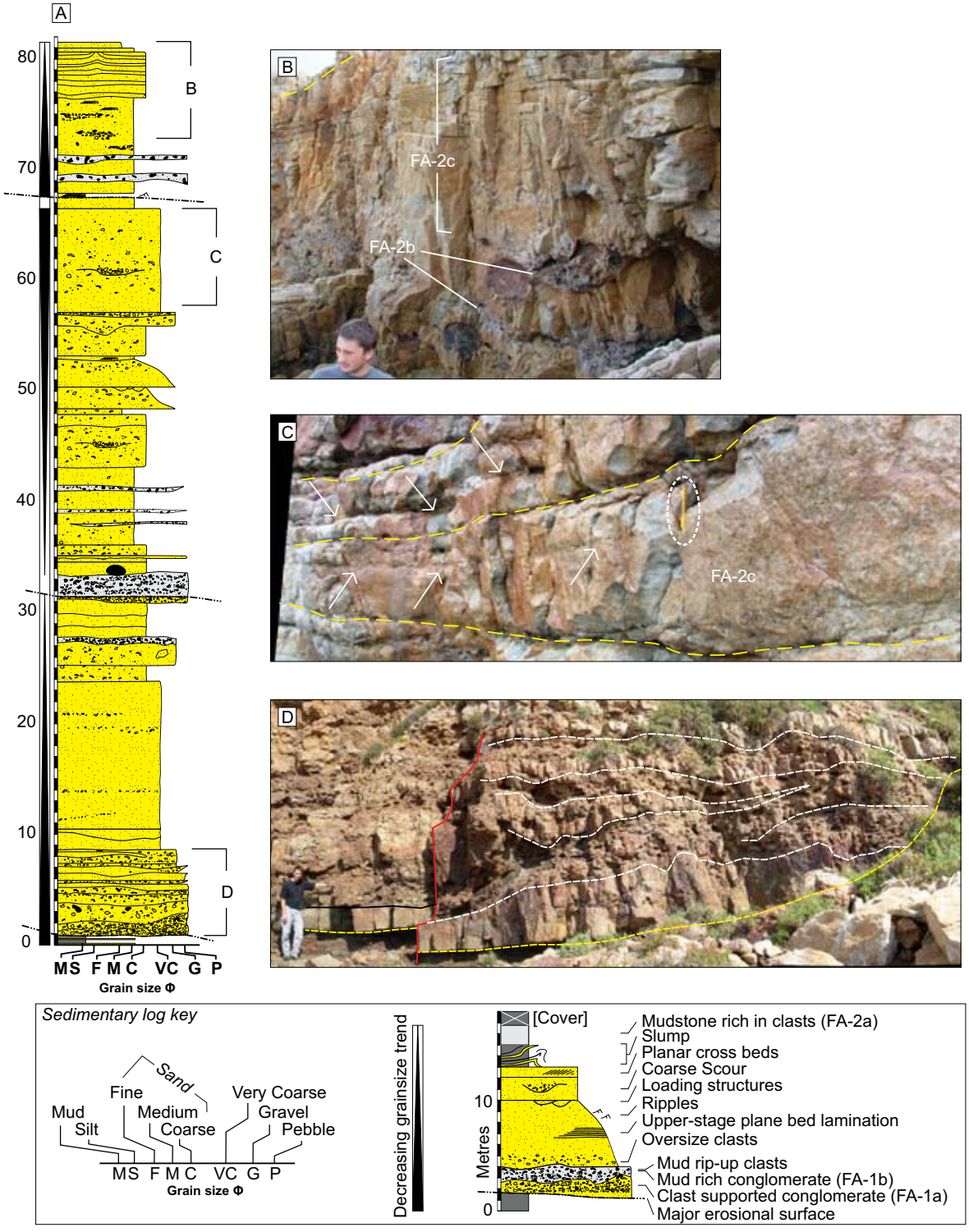

Figure 3.7.

Plate detailing the sedimentology of channel complex Cr-5, Capo Raisigerbi headland, Finale. A; Sedimentological log through channel complex Cr-5. See log key for details. B; The complex top with laterally restricted beds of poorly sorted granular sandstones with large mud clasts (FA-2b), and metre scale dewatering chimneys folding the uppermost beds. C; Beds of massive sandstone facies (FA-2c) containing pinching lenses of mud clasts (picked out with white arrows) mid way through the bed. Note Yellow pencil for scale. D; Photograph of basal conglomerates (FA-1a) and massive sandstones (FA-2c) onlapping the complex base (yellow dashed line to the right.).

mudstones, and thinner bedded massive sandstones (FA-2c). Slump fold vergance is typically at a high angle to, or parallel to the northeastwards palaeo-dip slope. Channel-complex fill broadly fines upwards from conglomeratic to thin bedded (<0.2 m) coarse sand deposits in the majority of channel-element examples studied (e.g channel-complex Cr-5. See figure 3.7a).

The overall section records a >5 km width channel system, consisting of 16 mappable channel complexes which are slightly sinuous. Interchannel lithofacies (predominantly massive ungraded beds) and the presence of channelised deposits are atypical of levee environments (e.g Kane et al., 2007), and are observed to be truncated by channel complex margins. Channel complexes are therefore interpreted as entrenched into a northeast dipping palaeoslope rather than aggradationaly confined by levee construction. The presence of coarse grained interbedded facies, scours, and isolated channel bodies in interchannel areas suggests that flows are laterally confined to this slope location. Given that incision is observed up to the complex top, out of channel sediments are interpreted to generally precede individual channel-complex fills, although multiple phases of re-incision within the same channel-complex could make them of similar age. Conglomeratic facies (FA-1a and FA-1b) are similar to the bypass facies of Lowe (1982), representing proximal deposition of very coarse grained bedload from hyperconcentrated bipartite turbidity currents, and bypass of the remainder flow. The repetition of a fining upwards facies trend, separated by incisional surfaces (e.g stacked channel-elements), signifies the repeated switch from bypass to fill within each channel-complex. Observations of slumping with a vergance which is at a high angle to palaeoflow suggests localised collapse of the channel-complex margin. Overall, the high degree of entrenchment with slope incision of <90 m indicates an above grade slope (Kneller, 2003), typical of proximal upper slope locations or a tectonically uplifting slope environment (e.g Mayall et al., 2010).

3.4.2.2 The Karsa section

South of Pollina village, stratigraphy is exposed on either side of the Pollina river valley (Figure 3.1). The base of Numidian Flysch Formation sandstones are exposed over 1.9 km in a north-south orientation, on the western hillside with a broadly synclinal geometry (Figures 3.8 and 3.9a). Basal turbidites deposits (FA-3a) and massive sandstones (FA-2c) are observed to cut the top of a large slump complex (FA-4a), at least 25 m thick, which can be traced for 700 m southwards along the river bank and consists of mudstones with folded and truncated thin sand beds (FA-3a) (Figure 3.9b).

At the northern end of the section a vertical cliff, 215 m high, exposes stacked, amalgamated sandstone beds (Figure 3.9d). The 25 m thick slump which outcrops beneath the sandstones base is centred upon this amalgamated section. While it is difficult to assess the architecture in detail, several concave upwards surfaces in excess of 50 m wide and 5 m deep are observed to truncate underlying bedding. A 60 m thick slump (FA-4a) within the lower section also contains a folded lenticular sand body encased within mudstones (Figure 3.9e). Unfortunately a lack of access and the high degree of amalgamation make further interpretation difficult, but indicate channelization and erosion at this locality.

Towards the south the amalgamated section separates into discrete sandstone packages separated by fine grained sediments. 6 major packages are observed, totalling 600 m thick (named Package A through F), that are correlated across a network of low displacement normal faults for 1.5 km along the valley side (Figure 3.8). Sandstone packages consist of massive sandstone beds up to 2.5 m thick (FA-2c), some examples of coarse grained turbidite deposits (FA-3a) and some cohesive debrites (FA-2a). Beds are arranged into thinning upwards sequences between 0.5 and 4 m thick. The sandstone packages are vertically separated by mudstones and thin beds of fine grained turbidites (FA-3a, $T_{a,b,c}$), with minor slumped units less than 1 m thick. Vertical amalgamation therefore decreases substantially to the south from a minimum net:gross of 0.9 in the north, to 0.65

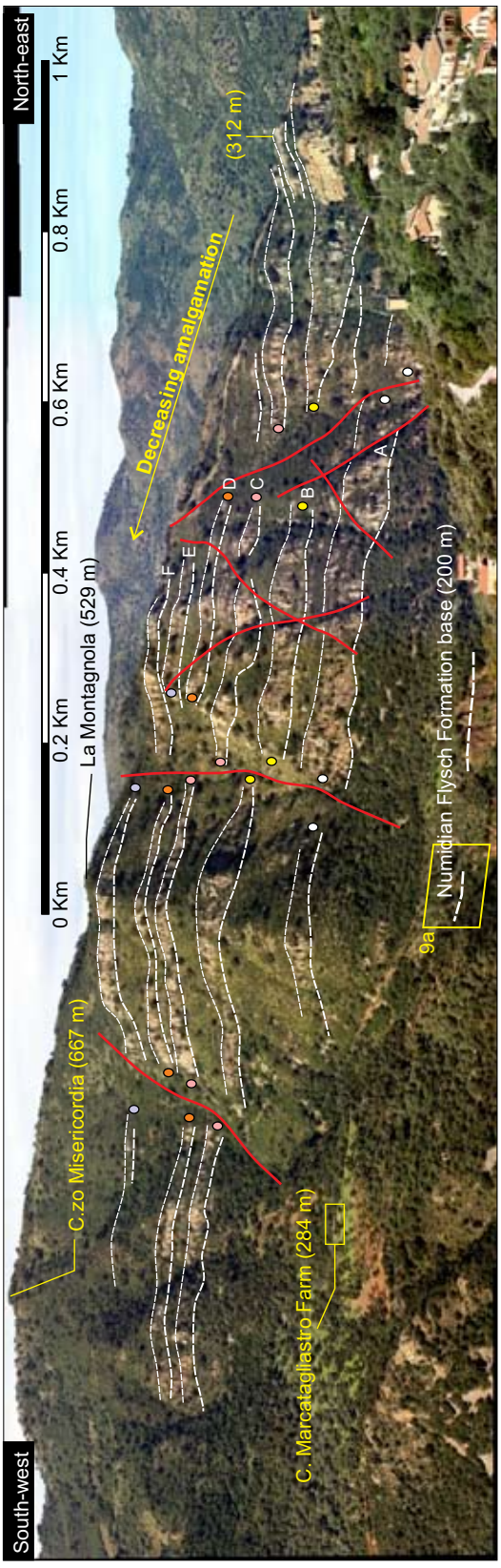

Figure 3.8.
Photo-panorama of the Pollina river cliff (Karsa section, northern Sicily). The northern, highly amalgamated end is hidden (see figure 9d), however the subdivision into 6 sandstone packages towards the south can be traced. Coloured circles show correlation of packages across low offset normal faults.

1 km to the south, and 0.51 in a measured section (Figure 3.10) 3.5 km to the south. While correlatable, the 6 sand packages are not laterally continuous, and show variations in thickness including concave-up basal geometries (Figure 3.8). Package B thickens towards the amalgamated northern end while package C reaches a maximum thickness 400 m to the south of the amalgamated end.

The uppermost part of the adjacent less confined belt crops out on the eastern side of the valley near the village of Karsa (Figure 3.1). Here, steeply dipping bedding surfaces are exposed with a 750 by 300 m lateral continuity. 175 m of section are exposed, also consisting of thinning upwards (TU) sequences, and an overall fining upwards from coarse sand to silt at the very top of the section (Figure 3.10). The thickest TU sequences near the section base reach 30 m thick and consist of massive sandstone beds (FA-2c) up to 2.5 m thick, with heavily loaded tops. Basal flutes indicate a dominant northeast to north flow orientation at this locality. Typical deep-marine ichnofossils including *Helminthoida molassica* (Nereites ichnogenus) and a winding, unbranched form of bioturbation (perhaps *Gyrochorte* or *Taphrheminthopsis*) are observed on some bed tops (Figures 3.4a, 3.4b and 3.4c). Towards the top of the member, TU sequences decrease to 10 to 40 cm thick, consisting of thin bedded, fine grained turbidites (FA-3a) and thin massive sandstones (FA-2c), interbedded with mm thick mudstone drapes (Figures 3.9c and 3.10). The top of these thin Ta deposits can also be rippled with thin mudstone partings infilling the relief. Minor slumping is also evident with an 18 m thick slump of mudstones and thin sandstones containing an amalgamated sand body 1.5 m thick (Figure 3.10, 102–125 m). The slump body top is truncated by a 3 m thick channel body with a fill of coarse massive sandstones.

The architecture of the northern Karsa section including concave channelform geometries suggests a highly amalgamated axis of channelised flow deposits with a width in excess of 300 m. Separa-

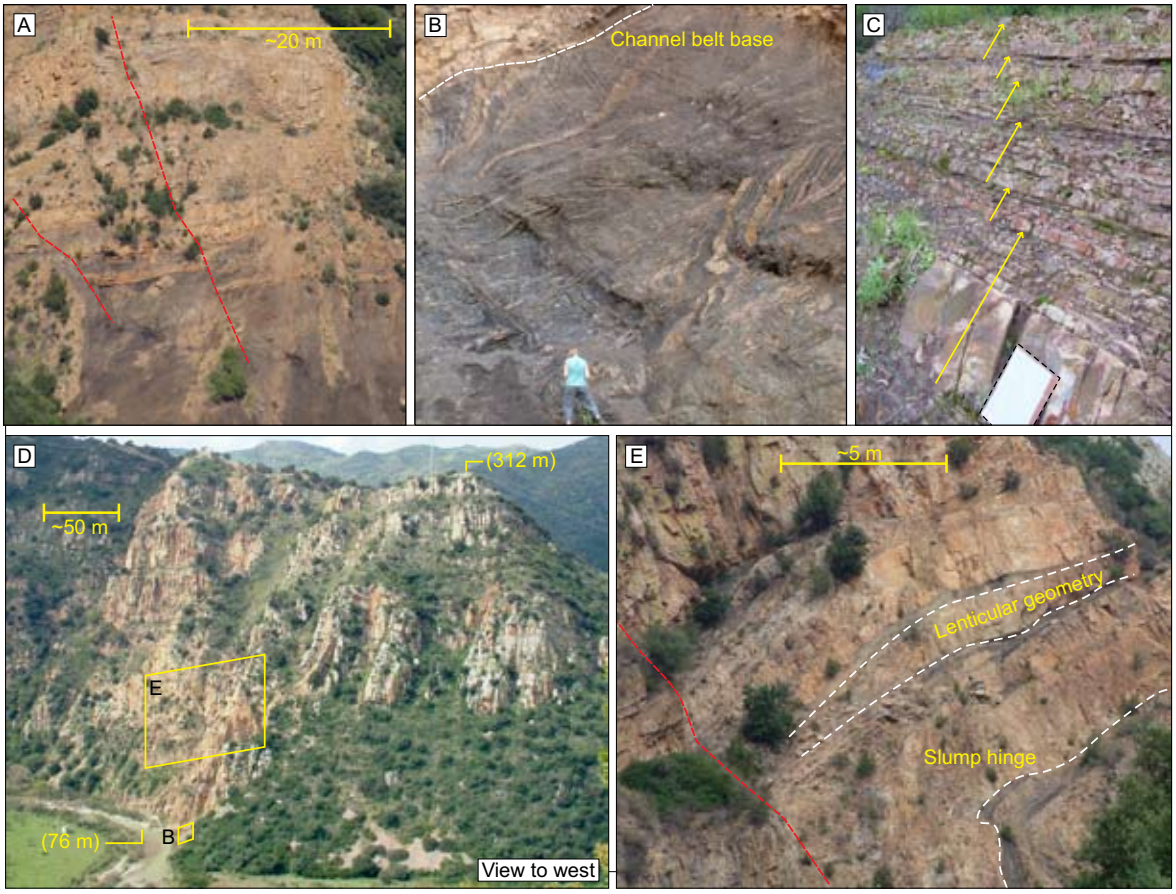

Figure 3.9.
Images from the Karsa section, northern Sicily. A; Base of Numidian Flysch Formation incising into mudstones (see figure 8 for location). B; ~25 m thick slump beneath the Karsa section, the base of which is marked. Geologist for scale. C; Fining and thinning upwards (FUTU) sequences composed of turbidites (T_a) and thin bedded massive sandstones (FA-2c). They represent overbanking within a channelised environment, off-axis from the fan valley. Note A4 clipboard (bottom of picture) for scale. D; Large scale view of the northern amalgamated end. The location of figures 9b and 9e are shown. E; Detail of the amalgamated northern end of the Karsa section showing the top of a 40 m thick slump body containing lenticular channel geometries.

tion of the section into 6 discrete packages towards the south gives a total width for the system in excess of 2.5 km however. Packages to the south represent less amalgamated flow deposits separated by periods of fine grained sedimentation, while packages A and B clearly thin towards the south. Vertical stacking of channel forms would produce this architecture, with stacked and amalgamated channel axes in the north and thinner channel margin environments to the south.

In terms of channel hierarchy it is interpreted that packages of stacked sandstones in the off-axis portion (e.g packages A to F; figure 3.8) represent individual channel complexes which amalgamate towards the north. Concave surfaces within this northern axis (e.g Figure 3.9e) therefore represent stacked channel elements. Outcrop quality does not allow for the interpretation of channel complex sets however.

Within channel complex margins, the dominance of interbedded fine grained T_a deposits and some massive ungraded sandstones (FA-2c) in beds up to several metres thickness is atypical of levee environments however but is similar to channel margin facies recognised from the Finale section (see chapter 5.2 for full description of this), with common slumping (e.g Figure 3.10, 105 – 120 m) representing bank collapse. These features are typical of large scale channel systems as recognised within submarine channel process models including Sprague et al. (2005) and McHargue et

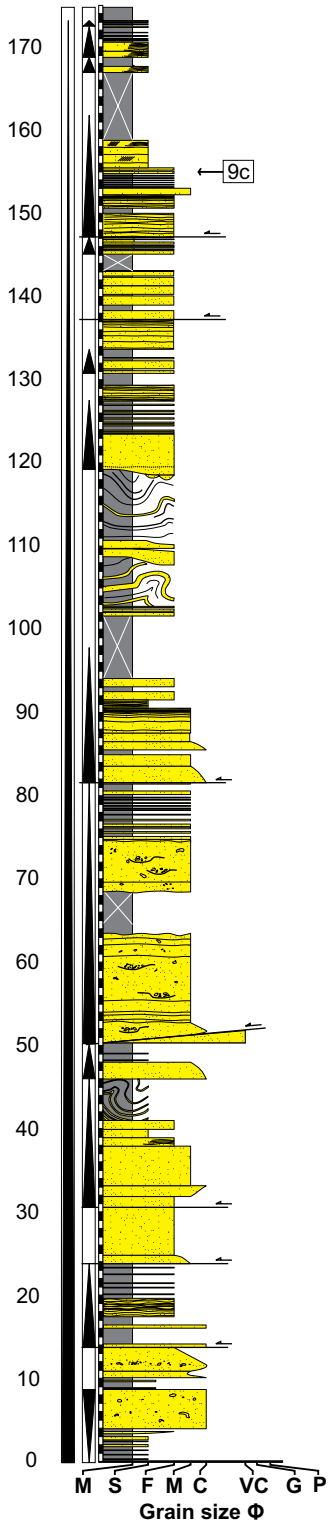

Figure 3.10.
A sedimentary log from Karsa, representing the uppermost part of the off-axis portion sequence. See figure 7 for key to log features. The location of figure 9c is shown.

al. (2010). A similar channel complex margin architecture is likely to have existed to the north of the sections described but has subsequently been removed during emplacement. Both the amalgamated axis and less confined off-axis areas are aggradational (>600 m) and show little sign of entrenchment, indicating a below-grade slope and resulting slope accommodation space.

An extensive slump complex cut by the section base indicates large scale slope mass wasting, and may have been responsible for producing a topographic low which subsequently 'captured' flows at the location of the channel axis. This evolution is reported from slope channel systems including the ancient Tres Pasos Formation in Chile (Armitage et al., 2009) and pleistocene channel systems from the Gulf of Mexico imaged with seismic data (Hackbarth and Shew, 1993).

3.4.2.3 The Mt. Salici section

A single large nappe forms the ridgeline of Mt. Salici to the south-east of Nicosia (Figure 3.1). Beds dip to the north producing 1800 m of stratigraphy from Lago Pozzillo (Lake Pozzillo) to the summit of Mt. Salici. Three major subdivisions are recognised based upon gross depositional architectures.

3.4.2.3.1 Lower subdivision

Northwards from Lago Pozzilo (Figure 3.1), a 1150 m thick succession consists of isolated lenticular sandstone bodies (Appendix). Their width varies from 50 to 1000 m and from 3 to tens of metres thick. Over 15 bodies occur in a belt over 2.4 km in width with an evenly distribund. Flows are thus laterally confined within channel bodies that display a strong lenticular geometry. Channel bodies do not show lateral stacking patterns or systematic variations in size through the section. Vegetation cover prevents characterisation of more muddy lithologies between the channels.

3.4.2.3.2 Middle subdivision

The middle subdivision is 570 m thick and consists of prominent and laterally extensive packages of sandstones which may be traced east-west for 6.5 km, but correlated for up to 3.5 km, on the steep flank of Mt. Salici (Figures 3.11 and 3.12). Packages are labelled A to L and reach a maximum of 60 m thick, as with the basal sandstone package (Package A) in the west. They are composed primarily of stacked, coarse grained turbidites (FA-3a; T_a) (Figure 3.12). Bed bases are locally erosive and also display loading and flame structures. Thin, fine-grained turbidites and massive sandstones (FA-2c) interbedded with mudstones are observed in the lower or upper parts of sandstone packages. From 500 – 570 m within the section (Figure 3.12), sandstone packages become significantly thinner, containing

Figure 3.11.
Photo-panorama and interpretation of the southern flank of Mt. Salici (middle and upper subdivisions) showing the geometry of major sand packages (in yellow) and the location of the sedimentological log (Figure 15). Sandstone packages are labelled A to L (See sedimentological log, figure 15).

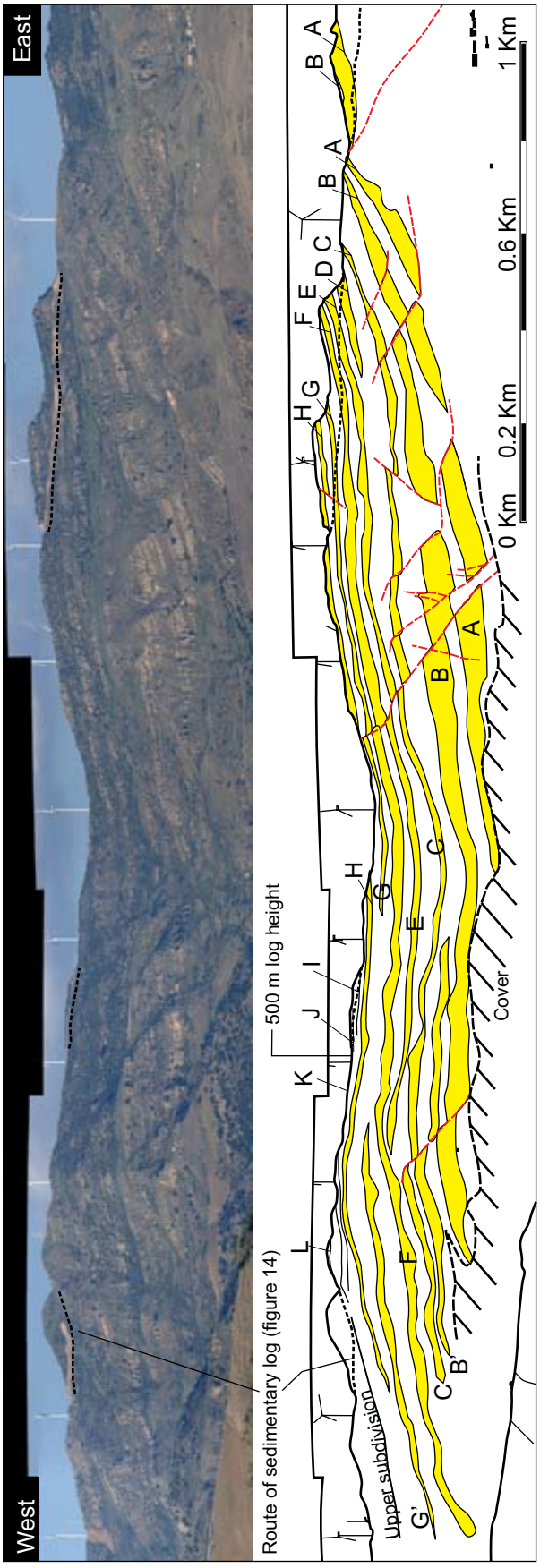

medium to coarse grained turbidites which can be heavily dewatered and contain *Thalassinoides* bioturbation on the bed base and *Skolithos* type burrows near the bed top (Figure 3.13c). Package tops throughout the section are often connected to beds above by clastic dykes (FA-4b), up to 0.4 m thick and which often show ptygmatic folding (Figure 3.3o). A majority of sandstone packages are massive and contain no overall grainsize trend throughout their thickness. Package A however fines upwards while packages D and J coarsen upwards (Figure 3.12). Lateral continuity is variable, with packages D, E, G and H gradually pinching out (Figure 3.11). Package D in particular thins from 25 m and disappears over approximately 300 m into vegetation covered fine-grained sediments. Package E however can be traced for approximately 3.2 km, thinning towards the west from a maximum of 28 m thick, and appears to be truncated by the stratigraphically higher package F (Figure 3.11).

Between the sandstone packages, fine-grained heterogeneous sequences are recessively weathered. Fine grained sediments consist mainly of mudstones with thin bedded siltstones and sandstones of turbidity current origin (FA-3a; T_{abcde}). Thin turbidites display some ripples and intense horizontal lamination (FA-3a; T_{bc}). Massive ungraded sandstone beds (FA-2c) also tend to be interbedded with mudstones and reach 1 m thick. Fine grained sequences are arranged into repeated coarsening and thickening upwards cycles (CUTU) ranging from 1 to 32 m thick. Cycles typically consist of silt or fine sandstones with mudstone caps up to 30 mm thick (T_e), reaching coarse or granular turbidites (FA-3a; T_a) with similar mudstone caps (T_e) towards the top (Figure 3.3k). Thin beds at the base may be remobilised amid slump bodies (FA-4a), and a cohesive debris flow

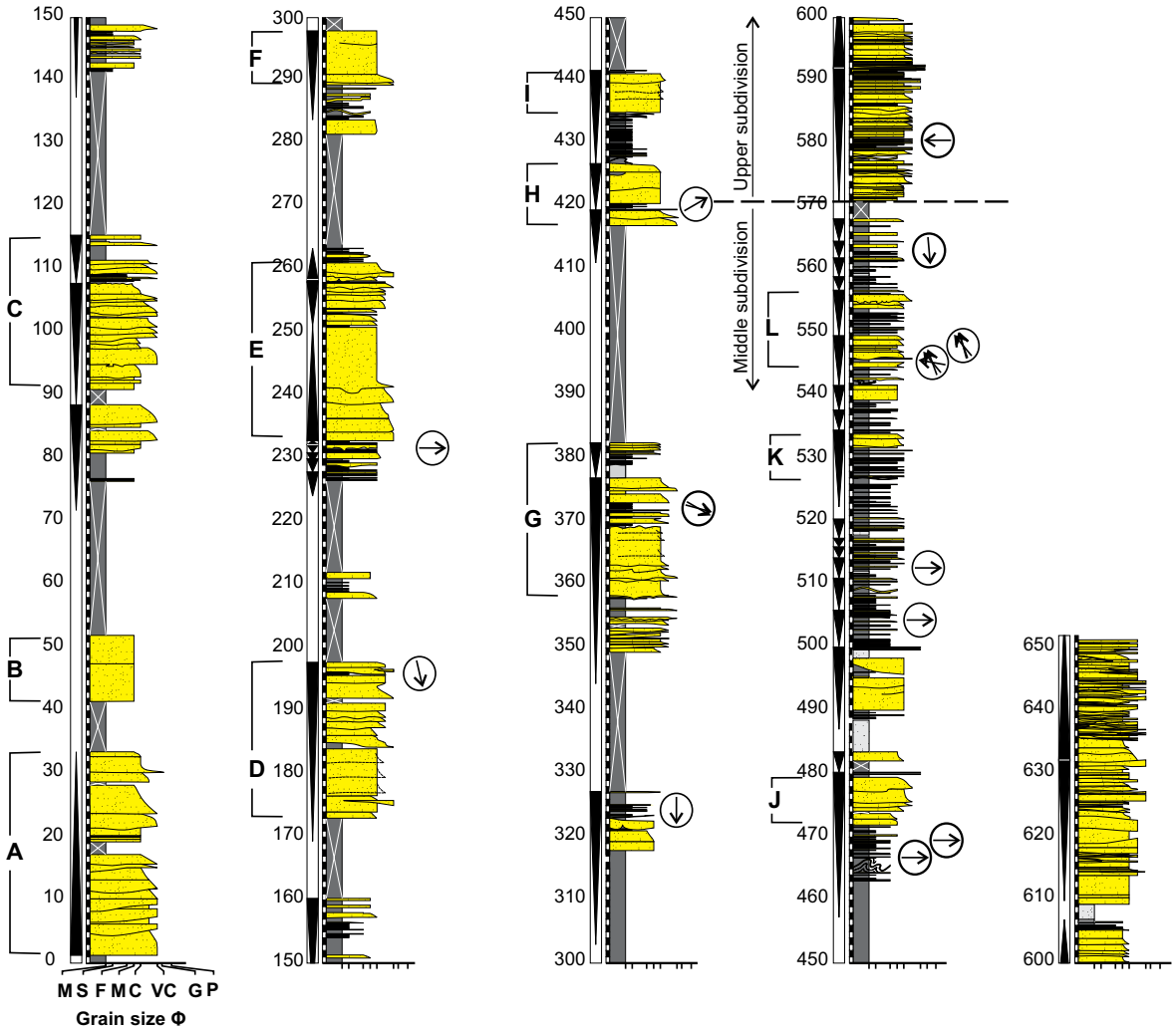

Figure 3.12.
650 m sedimentological log through the mid and upper subdivisions of the Mt. Salici section. Labelled major sand packages (A through L) correspond to those highlighted in the photo-panorama of figure 14. See figure 3.7 for key to log features.

containing coarse clasts and floating sandstone blocks may cap the cycle (Figures 3.3e and 3.12). Palaeocurrents, measured primarily from fine-grained beds, record extreme variability throughout the section (Figures 3.1 and 3.12, 465 – 490 m).

Through the lower 500 m of section, CUTU sequences are capped by sandstone packages which complete the coarsening and thickening upwards trend (e.g packages E, F, G, I and J). Within the upper 70 m (500 – 570 m), CUTU sequences are directly stacked upon one another or are capped by sandstone packages less than 3 m thick (Figure 3.12 and 3.13a). Above 500 m, turbidite mudstone caps (FA-3a; T_e) reach 0.4 m thick, significantly thicker than within the lower section, and are often heavily bioturbated (Figure 3.13a and 3.13b). Linked Debrite deposits (FA-3b) are also observed within this upper section. The transition to these facies changes is relatively abrupt at around 500 m although vegetation cover of finer grained sediments below may hide a more gradual transition.

Isolated channel forms are also observed within the upper 70 m varying from 6 to 15 m in width and between 2 and 4 m thick (Figure 3.14). They are clearly erosional into, and truncate fine-grained beds of the CUTU cycle. Erosionally based flow deposits, including coarse-grained turbidites (FA-3a; Ta) and massive granular sandstones (FA-2b) comprise their fill (Figure 3.14b and

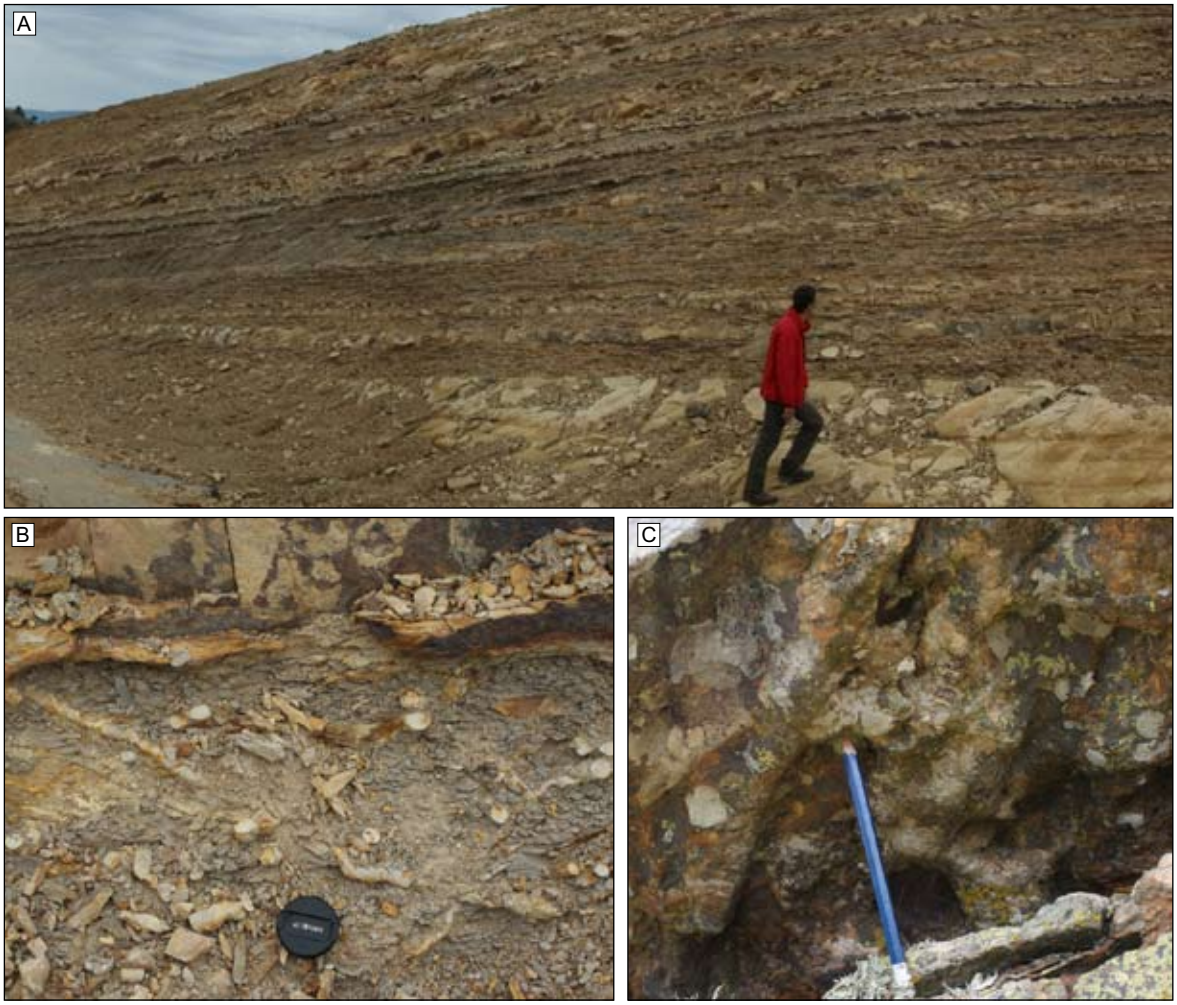

Figure 3.13.
Uppermost part of the Middle subdivision of the Mt. Salici section (560 m on log, figure 12). A; pan of section. B; >0.3 m thick Bouma Te,subdivision, heavily bioturbated (*Ophiomorpha rudis*, *Arenicolltes* (isp?), capping Bouma Ta turbidite sands. C; *Thalassinoides* burrows on the base of turbidite Ta sandstones.

3.14c). Above sequence H, two such channels occur, incising midway through the CUTU cycle (one example shown in figure 3.14a).

The laterally extensive packages of amalgamated turbidite deposits with pinching margins indicate a very low aspect ratio channelised architecture. Palaeoflow is however highly variable (Figure 3.1 and 3.12) with orientations measured primarily from flutes and ripples in all directions. As such the true width of packages A to L are unknown. Fine-grained turbidite deposits arranged into coarsening-upwards and thickening-upwards cycles (CUTU), and displaying a wide variation in palaeocurrent orientations, are commonly attributed to progradation cycles within terminal lobe environments but have also been described from submarine channel levees (e.g Kane et al., 2007). An interpretation of channel-levee environments is attractive given the presence of low aspect ratio channel architectures, interspersed with fine-grained sequences which may represent constructional levees. Kane et al. (2007) suggests that thickening upward cycles within levees of the Rosario Formation of Baja, California, are the result of flows which become sequentially thicker in comparison to levee height such that deeper and sandier portions of the flow are able to overbank. This results in thicker and sandier deposits through time. Thickening upwards cycles within levees are however relatively rare, and are often recorded isolated amidst fining and thinning upwards cycles as with the Wheeler Gorge conglomerates and Juniper ridge conglomerates of California (Walker, 1985 and Hickson and Lowe, 2002, respectively) and the Cerro Toro Fm of southern Chile (Beaubouef,

2004). While studying the Wheeler Gorge conglomerates, Walker (1985) proposed that levees contained a diagnostic facies (ccc-turbidites) that show “a reasonable proportion of beds containing convolute lamination, climbing ripples and ripped up mud clasts”. ccc-turbidites have subsequently also been observed in channel-levees of the Rosario Fm (Kane et al., 2007), Kirkgecit Fm (Cronin et al., 2000) and the Pleistocene of the Peri-Adriatic basin, central Italy (Di Celma et al., 2010). The Mt. Salici section does contain abundant convolute lamination, however climbing ripples are not observed and mud rip-up clasts are extremely rare within finer grained sequences. In contrast, Bouma T_a beds with planar non-erosive bases are the dominant facies (74%) with subordinate upper-stage plane beds (29%), isolated ripples and rare ripple trains (12%). Cohesive debrites are also observed, (2.5%), found interbedded throughout CUTU sequences, and linked debrites are interpreted within the upper 70m of the middle subdivision (2%) (See appendix 9 for raw data). Debris flow facies are unlikely to represent repeated overbanking, given the very coarse grainsize of cohesive debris flow deposits (including rafted blocks), and laminar flow process interpreted. Linked debrites are however being increasingly recognised from distal lobe environments (e.g Haughton et al., 2009). Based upon the measured apparent widths and thicknesses of sandstone packages, aspect ratios of <0.01 are calculated, which are similar to confined lobe dimensions from the Golo fan offshore Corsica (Deptuck et al., 2008). Given the presence and proportion of flow facies observed and the aspect ratios of sandstone packages, a complex of stacked lobes is therefore interpreted.

Coarsening and thickening upwards interbedded turbidite deposits record fine grained lobe fringe deposits succeeded by coarser grained more proximal deposits. Similar evolutions are recognised from the Crocker Formation (Lambiase et al., 2008), the Golo fan offshore Corsica (Gervais et

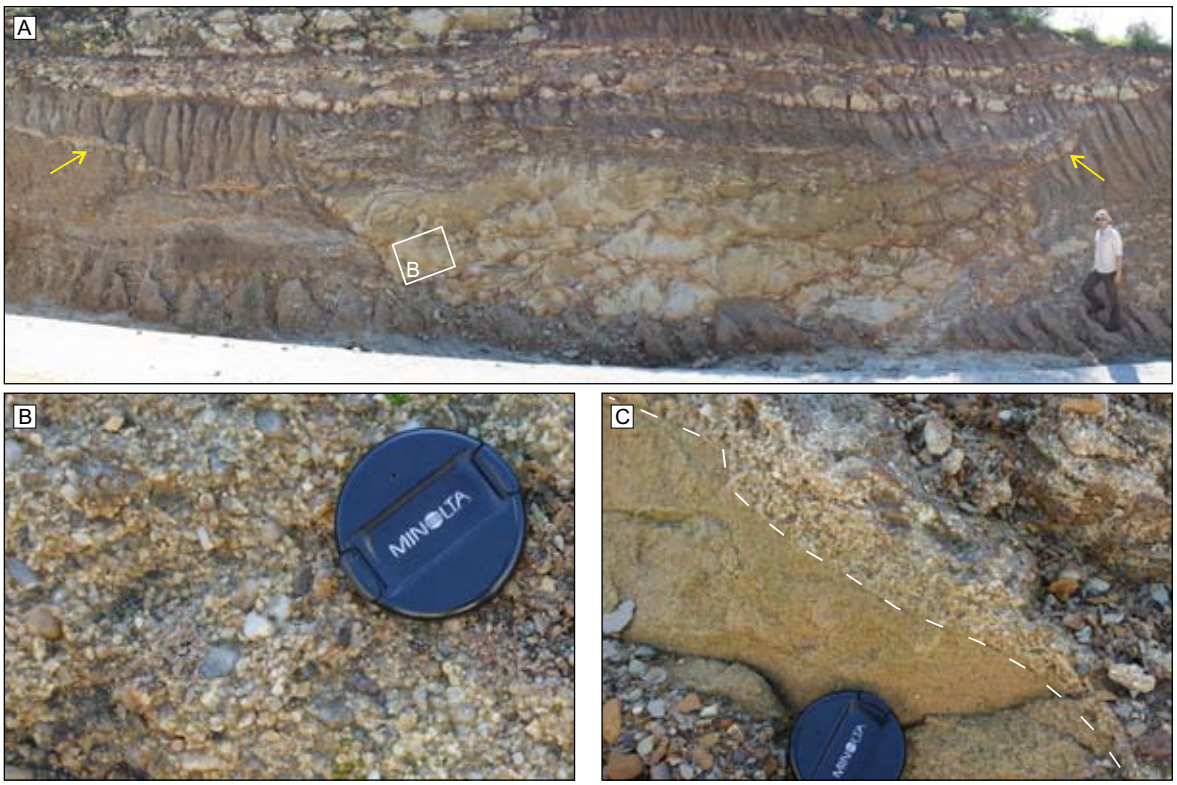

Figure 3.14.
A distributary channel from the Mt. Salici section, 2 m above sand package H (Figures 3.14 and 3.15). Fill is massive, very coarse sandstone or granule beds (Figure 3.14b and 3.14c). Channel incises mudstones and coarsening and thickening upwards beds. Note injectite ‘wings’ from each channel margin (yellow arrows) as recognised in seismic channel examples from the North Sea (e.g. Alba field).

al., 2006) and the Ross Formation in Ireland (Macdonald et al., 2011). This progradational trend produces coarsening and thickening upwards cycles culminating in sharp based low aspect ratio channelised sandstones of the lobe axis. Prominent lobe axis sandstones therefore highlight offset stacking within the 3.5 km extent of the outcrop (Figure 3.11), likely as a result of lobe switching and compensation cycles.

Stacking of CUTU lobe sequences without the presence of coarse-grained packages (e.g. 500 m upwards), record relatively distal lobe off-axis or lobe fringe environments (e.g Prélat et al., 2009) in which minor distributary channels are observed (Figure 3.14). The presence of unstable substrate, common at the base of CUTU sequences, show that lobe fringes in particular suffer from instability and minor mass movement. Minor distributary channels which are observed to incise midway through a continuous CUTU lobe sequence demonstrate bypass of substantial very-coarse grained flows through the active lobe off-axis environment. As such, more than one depocentre appears to be active at any one time as oversize or particularly coarse and erosive flows traverse the fan. This has also been observed in the mapping of lobes using 3D seismic data from the Pleistocene East Kalimantan fan of Indonesia (Saller et al., 2008) where up to 6 depocentres (frontal splays in their terminology) were mapped per lobe.

3.4.2.3.3 Upper subdivision

Immediately above the middle subdivision a change in architectural style, facies and stacking patterns is observed (Figure 3.12). The uppermost 80 m of the section are well exposed in sections forming the summits of Mt. Salici and Mt. Pellegrino. The 80 m thick sequence can be traced for 1.3 km along strike, limited by the topography of the peaks. Overall, the vertical sequence is broadly composed of two ~30 m thick sequences separated by a 3 to 5 m thick muddy package of slump and cohesive debris flow deposits recognised in both sections. It consists almost entirely of vertically and horizontally amalgamated coarse grained sandstones and gravels such that depositional architectures are extremely complicated and laterally restricted (Figure 3.15). Turbulent surge deposits (FA-3a; T_a) show erosive bases consisting of coarse to very coarse sandstones with granular clasts. Massive sandstone beds similarly consist of medium to granular sandstones with scattered pebbles up to 10 mm across (FA-2c, 2d). Mudclasts may account for 70% of bed lithology, either randomly orientated or less commonly with an imbrication which has no uniform orientation throughout the section (Figure 3.15d). Beds reach 3 m thick and may be laterally extensive beyond outcrop limits (>40 m). Horizontal bed amalgamation is very common and most beds show highly variable (e.g figure 3.15e). A 17m thick section of banded sandstones and mudstone deposits (FA-2d) mark the base of the Mt. Pellegrino section corresponding to the macro banded slurry flow division (M2b) of Lowe and Guy (2000) (Figure 3.3 and 3.15f). Some thicker mud rich bands up to 50 cm thick may represent the megabanded subdivision (M2a). They have not been recognised anywhere else in this study.

Shallowly dipping erosional and undulatory surfaces (<40° dip) may be commonly traced for up to 40 m, while rare steeply incised margins (<70° dip) reach 2 m in depth (Figures 3.15b and 3.15c). Such scours may reach greater than 7-8 m in depth (measurements are constrained by the outcrop dimensions) and truncate massive sand and granule beds (FA-2b, 2c). Within these scours, very coarse grained gravel deposits (FA-2b), commonly dominated by randomly orientated mud rip up clasts, fill the entire structure as either; a single event bed (Figure 3.15c); or are interbedded with massive medium to coarse grained sandstones (FA-2c) (Figure 3.15b). Within stacked scour fill, very coarse grained gravel beds (<10 cm) are commonly observed to thin and pinch-out horizontally within coarse massive sandstones (FA-2c), forming a lobate geometry over several metres

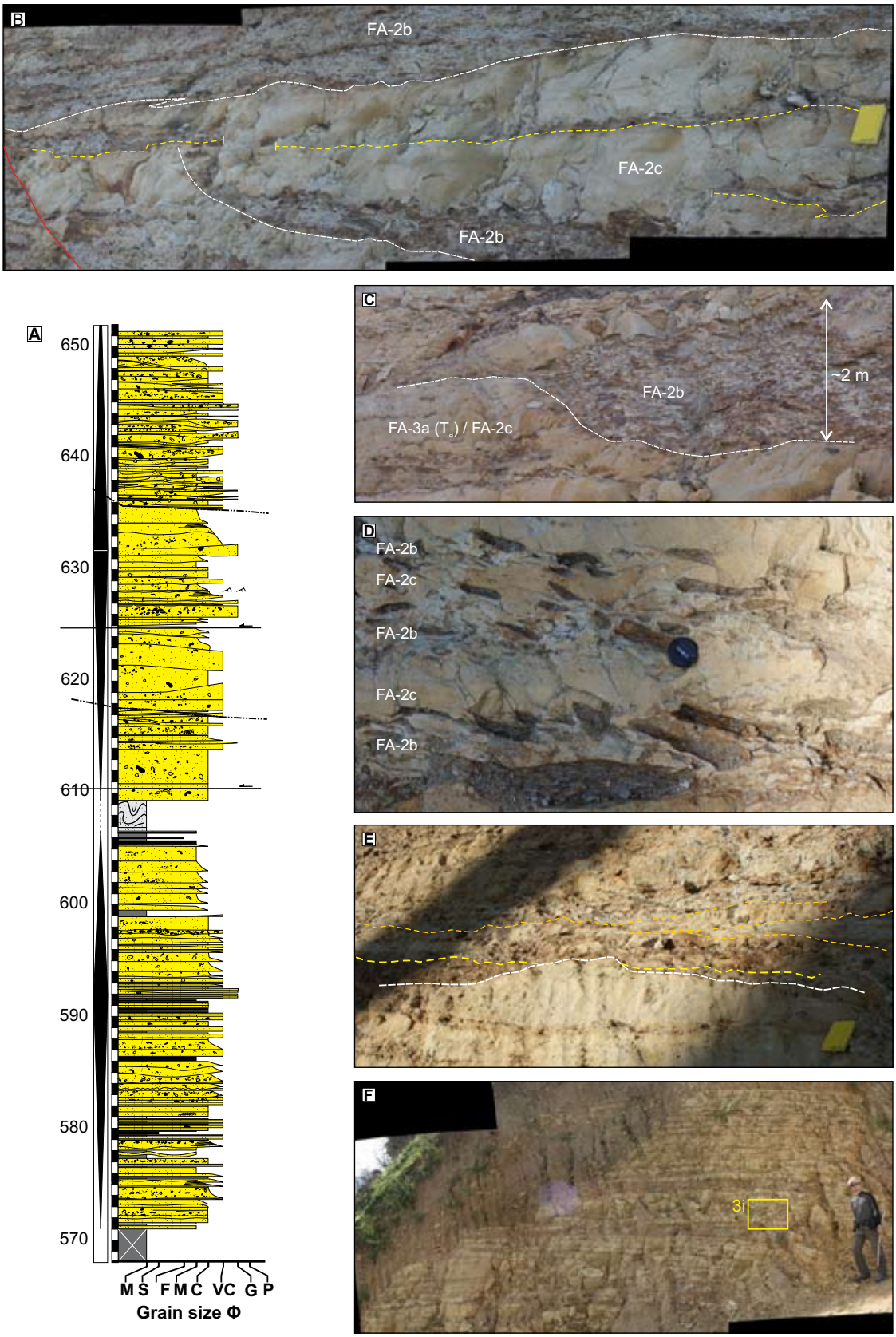

Figure 3.15.

Plate detailing the Channel-Lobe-Transition-Zone, the upper subdivision of the Mt. Salici section. A; Sedimentary log of the CLTZ at Mt. Salici. Major incisional surfaces are marked; normal faults in black dashed lines. Crude thickening/coarsening and thinning/fining trends are observed. White crosses denote cover. B; Photo-panorama showing a typical section of the CLTZ. A scour feature draped by facies FA-2b rich in mud clasts and filled with massive coarse sandstones (FA-2c). Pinching lenses of mud-clast rich FA-2b are highlighted in yellow. C; A steep sided scour 2 m deep filled with a single bed of mud-clast rich granular sandstones (FA-2b). Scour incises stacked beds of massive sandstones (FA-2c). D; Thin layers

Figure 3.15 continued....
of massive granular sandstones (FA-2b) with strongly imbricated mud clasts, interbedded with massive coarse sandstones (FA-2c). E; A minor erosional remnant approximately 0.6 m high, bounded by scours to either side which are filled with massive granular sandstones (FA-2c). F; Section of banded slurry flows (sensu Lowe & Guy., 2000) from base of Mt. Pelegrino section (see appendix 13). The location of figure 3i is shown.

(Figure 3.15b). Scour features may also be observed separated by a non-eroded 'high' of coarse sandstone (Figure 3.15e). These minor erosional remnants are less than 0.6 m high, representing erosion of less than a single bed thickness. Adjacent scours are filled with the same granular facies rich in randomly orientated mud clasts (FA-2b). Scours and non-eroded high sequences are generally truncated above by beds of coarse sandstone.

This subdivision is remarkable in its heterogeneity and lack of fine-grained sediments. The coarse grain size, scouring and high degree of amalgamation would tend to indicate a high-energy environment, however as it conformably overlies a stacked lobe complex a relatively distal environment must be countered. The proportion of facies and the architectures observed are also substantially different to those of channel-complexes in more proximal settings (see Figure 3.17). Scours which incise into coarse deposits throughout the section, the presence of erosional remnants, and the non uniformity of bed thickness indicate that flows underwent a sustained period of enhanced turbulence with rapid lateral switching of erosion. The mix of coarse grained bedload deposits and less common coarse grained waning turbulent flow deposits suggests rapid deposition was followed by subsequent stripping of a turbulent upper part, and bypass of finer grainsize fractions.

There are two environments described within modern fans which conform to this style of morphology and associated facies. Wynn et al. (2002) describes concentrated erosive features including minor channels, lineations and scours, and also erosional remnants, from Channel Lobe Transition Zones (CLTZ). The CLTZ is a zone linking a channel mouth with a depositional lobe, typically at a break of slope, in which rapid deceleration, thickening, and lateral spreading of flows scours the sea floor, often inferred as a hydraulic jump. Coarse grained sediments are typically recognised in long-wavelength sediment waves and transverse bedforms (Kenyon et al., 1995), while shallow cores from the Rhone CLTZ contained well sorted medium to coarse sands (Wynn et al., 2002). High backscatter acoustic facies, recorded from side-scan sonar data of the Rhone and Agadir CLTZ's, are also interpreted to represent coarse grained (sandy) sediments (Wynn et al., 2002). There are relatively few outcrop studies which describe and interpret a CLTZ in ancient systems. Cornamusini (2004) identified a CLTZ from the Macigno Costiero turbidite system in the Northern Apennines of Italy. Facies consist of thin-bedded pebble beds, massive pebbly sandstones and cross-stratified sandstones (their facies association 2; Coarse grained sandstones) characterised by amalgamation surfaces and scours. Boiano (1997) finds similar irregular and scoured coarse-grained sandstones and granule conglomerates in a CLTZ interpreted from the Gorgoglione Flysch Formation of the Italian Apennines. Ito (2008) finds erosion of the substrate in a CLTZ from the Otadai Formation, Japan, in which turbidity currents incorporate mud clasts and transform to debris flows. The coarse grained facies described from these studies are similar to Facies FA-2c and 2b from this study, which are the dominant facies recorded. Similar facies and irregular morphologies have however also been recognised in the Labrador Basin Sandy Submarine Braid Plane (SSBP) (Hesse et al., 2001). Contrary to a CLTZ, the Labrador SSBP is not confined to a location separating a channel and lobe, but extends for 700 km across the basin plane. Such features are rarely recognised however and seem to be more commonly recognised in high latitude systems (see Hesse et al. (2001) and references therein). We therefore interpret this sequence as a CLTZ, succeeding a stacked lobe complex, resulting in a progradational sequence.

3.4.3 Biostratigraphic dating

Biostratigraphic dating of hemipelagic mudstones from the three described sections produced a poorly preserved early Miocene assemblage (Benthic and planktonic foraminifera and radiolaria) for the northern sections (Finale and Karsa) and barren samples for the Mt. Salici section. The presence of radiolarian species *Didymocyrtis cf. prismatica* within channel complex Cr-3 from Finale (Figure 3.6) constrains an upper limit of latest Burdigalian (Nigrini and Sanfilippo, 2001) for the Finale sequence. This is in agreement with biostratigraphy used during regional mapping (Lentini et al., 1974), and a later study by Faugeres et al. (1992) who reported a mid to upper Burdigalian age for the Karsa section. To the west, Pescatore et al. (1987) described lobe deposits from western Sicily with an upper Oligocene (Chattian) to Langhian age. These summarised results therefore do not allow for correlation or differentiation between the sections described, and an early Miocene age is established.

3.5. Discussion

3.5.1 The stratigraphic relationship between study areas

The Finale, Karsa and Mt. Salici sections described here correspond to an entrenched slope channel system, an aggradational vertically stacked channel system, and a stacked lobe complex succeeded by a channel lobe transition zone respectively. Given the low biostratigraphic resolution and lack of key marker beds, correlation between the sections has not been possible. The base of the Numidian Flysch Formation does crop out in all three study areas however, with Numidian Flysch sandstones transgressing platform carbonate sequences around Finale and Karsa (Figure 3.1) and Numidian Flysch sandstones transgressing basin mudstones of the Argille Varicolori Formation in central Sicily (Figure 3.1). The age of the formation base is poorly constrained and the possibility of diachroneity must be raised.

Recorded palaeocurrent orientations from each section show a large variability (Figure 3.1). The Finale section shows a northeastwards trend which matches the orientation of channel complex margins (Figure 3.1 and 3.6). The Karsa section shows a wide range directed towards the northwest and northeast (Figure 3.1). The Mt. Salici section however does not show a statistically significant orientation (Figure 3.1). Overall therefore no single downslope orientation is preferred based upon the palaeocurrent data. Given that clockwise rotations of 70° to 120° are recorded for nappes in Sicily (e.g Oldow et al., 1990; Speranza et al., 2003) the reliability of palaeocurrents as regional indicators of slope orientation is also questioned.

Several authors have suggested that sections in northern Sicily are proximal equivalents to those of central Sicily and Faugeres et al. (1992) correlates the Karsa section with a one at Sperlinga, 20 km North West of the Mt. Salici section (Figure 3.1), using biostratigraphy and a unique tuffite marker bed. Away from this northwest to southeast outcrop axis, the Numidian Flysch Formation landscape consists of broad low hills formed by mudstones and thin bedded sandstones and silts. The focus of sedimentological studies on this outcrop axis therefore allows a degree of confidence that a genuine trend is being recognised within nappes of the Sicillide basin. Therefore, while correlation across nappes has not been possible in this study, we place the three sections in a general downslope trend from a slope entrenched channel system (the Finale section) to an aggradational channel system (the Karsa section) and a stacked lobe complex (the Mt. Salici section). Their time

equivalence is unconstrained and they are interpreted to represent case studies only within an Aquitanian to Burdigalian Numidian Flysch fan.

3.5.2 Depositional architectures within the fan

The Finale, Karsa, and Mt. Salici sections are respectively interpreted as a proximal above-grade channel-complex-set; a relatively distal below-grade channel system; and a stacked lobe complex stratigraphically succeeded by a Channel-Lobe-Transition-Zone. According to Mutti and Ricci Lucchi (1978) these environments may be ascribed to upper, mid and outer fan locations respectively based upon their facies, stacking patterns and depositional architectures.

The entrenched channel system interpreted within the Finale section evidences an above grade slope environment in which flows incise and experience a high degree of confinement within slightly sinuous channels. An uplifting slope can generate entrenched channels (Gee et al., 2009; Mayall et al., 2010), however upper slope environments similarly experience entrenchment where the slope gradient is higher than an idealised equilibrium profile governed by properties of the flow including sediment calibre and velocity (Kneller, 2003). This is typically in proximal upper slope locations die to the sigmoidal geometry of continental scale clinoforms (Carvajal et al., 2009; Kneller, 2003). The hierarchy of depositional elements evidences three superimposed waxing-waning cycles (of increasing magnitude and/or duration) which stack to produce a system 650 m thick and 5.7 km in width. Despite entrenchment at the channel complex scale, the system therefore aggrades through 650 m. Entrenchment through slope uplift is therefore unlikely and an upper slope environment is interpreted. The system is therefore seismic in scale and similar in size to entrenched upper slope channel systems imaged in seismic data from offshore west Africa (e.g Abreu et al., 2003; Mayall et al., 2010). Although dating resolution is poor, Carvajal et al. (2009) calculates a global average of 500 m/Myr for slope aggradation rates. Applied to the Finale section this would represent a ~3rd order duration of 1.3 Myr which is also similar to seismically imaged systems from west Africa (Mayall et al., 2006). Channel complexes (mappable units in outcrop) reach 90 m thick and 500 m in width and would therefore also be capable of seismic characterisation. The Finale section is therefore an appropriate analogue for seismically imaged slope confined channel systems.

In contrast to the Finale section, the Karsa section is interpreted as vertically stacked channel complexes which are highly amalgamated within a northern axis. While the section is 2.3 km in width, the assumption of an approximately symmetrical channel system would produce a total width of ~5 km. Channel complexes are therefore significantly wider (>2.3 km) yet thinner (<50 m) than channel complexes of the Finale section. Complexes are also less entrenched, with vertical stacking resulting from a below grade slope environment whereby complexes have sufficient accommodation space to aggrade. In order to maintain flow confinement with aggradation, levee construction is expected, as recognised from constructive channel systems in both outcrop and seismic studies (Pirmez and Imran., 2003; Kane et al., 2007). While not observed during this study, a levee system may be therefore exist in the south of the study area. Aggradational channel system architectures are recognised throughout medial and lower slope environments where slope gradient begins to decrease, flows will begin to decelerate and flow size will diminish (Pirmez and Imran, 2003). The Karsa section is therefore interpreted as representing a medial to lower slope location.

At Mt. Salici, a stacked lobe complex indicates a relatively low gradient environment. The middle subdivision fines upwards with the loss of amalgamated sandstone packages and a dominance of thin sandstones interbedded with thick mudstones. The Channel Lobe Transition Zone (CLTZ)

which stratigraphically succeeds it results from flows which rapidly slow, resulting from a rapid decrease in slope gradient and/or lateral confinement (Wynn et al., 2002). The Mt. Salici section is therefore interpreted as a low gradient setting such as a basin floor environment. The transition to the CLTZ represents a progradation of the system, possibly with a sequence boundary at the transition between the two environments. The mudstone rich upper portion of the middle subdivision (Figure 3.12; 500-570 m) can therefore be interpreted as deposition during a gradual switch off of the fan during transgressive systems tract (TST). The unpredictable palaeocurrents recorded from this section suggest however that a simple terminal lobe model is inappropriate to explain the architectures observed, and that flows experienced deflection or reflection from topography. The fining upwards transition within the middle subdivision also occurs primarily through thickening of T_e mudstone caps associated with thin bedded turbidites. Decreasing flow energy during a transgression and fan shutdown could be expected to result in finer grained deposits but also waning flows and high sediment fall out rates. In contrast, sandstones towards the top of the section are still coarse grained and can be massive indicating they were not all depositing through unsteadiness, and that bypass was still occurring. While T_e deposits may result from strong bypass of flows and deposition from the finer grained flow tail, the proportion of T_e to the rest of the deposit (T_a,T_b) reaches 75%. The increasing thickness of the T_e mudstone cap therefore suggests high volumes of very fine grained sediment are not bypassed in contrast to the coarser portion of the flow.

The transition from channel complexes (Mt. Salici lower subdivision) to stacked lobes (middle subdivision) signifies a decrease in slope gradients whereby flows switch from incision and bypass to waning conditions and deposition. The upper transition from stacked lobe complex to CLTZ (upper subdivision) results in a switch back to incision and bypass, and is similar in terms of facies and depositional architectures to examples from slopes with evolving topography. Such progressions from depositional lobes to bypassing channels are commonly recognised in ponded basins including the Gulf of Mexico (Prather et al., 1998) , and in the Grès d'Annot Formation with an upwards transition to the Coyer canyon (Sinclair and Tomasso, 2002). In this interpretation (see figure 3.16), flow ponding leads to highly variable palaeocurrent orientations due to deflection and reflection of flows (Sinclair and Tomasso, 2002) (Figure 3.16c). An increase in the thickness of Te deposits relative to Ta to Tc deposits may similarly result from intraslope topography which traps the dlilute suspension cloud above a turbulent flow (Figure 3.16d). This occurs towards the top of the middle subdivision and requires intraslope deformation to occur during deposition of the middle member. The transition from incisional channels to stacked lobes at the base of the middle subdivision can also be explained by intraslope deformation which would decrease slope gradients, serving to gradually pond flows upslope at the Mt. Salici section (Figure 3.16a and 3.16b).

Finally, incision through the intrabasin high restores bypass, with scouring and a return to coarse deposition at the section top (upper subdivision) (Figure 3.16e). Diagnostic evidence in the form of onlap and intraformation unconformities have not been documented, however this interpretation accounts for field evidence which a simple progradation model does not.

3.5.3 Flow-process variability

Significant changes in the proportion of lithofacies observed within the three sections. Proximal sections within northern outcrops are dominated by massive sandstones (FA-2c), conversely, graded turbidity current deposits (FA-3a) are the dominant facies in the distal Mt. Salici section. Figure 3.17 shows the proportions of lithofacies for each section (See Appendix 9 for raw data). This is not intended as a comparison of the same stratigraphic interval but a discussion on the differences

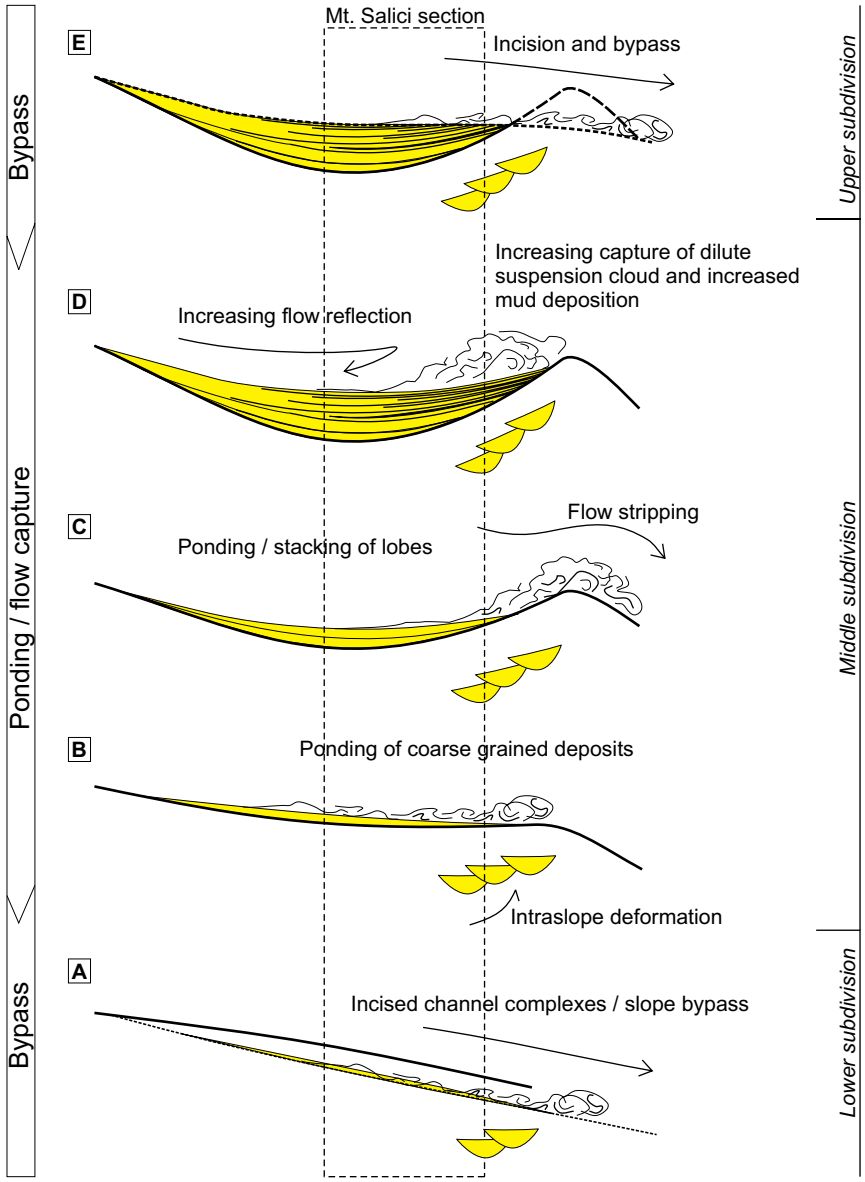

Figure 3.16.
A schematic model for the formation of the Mt. Salici section. The box denotes the location of the Mt. Salici section. A; Initial bypass of flows, with slope incision (and levee's?), observed in the lower subdivision. B; Intraslope deformation generates lowering of the slope gradient and ponding of flows, observed at the base of the middle subdivision. C; Continued intraslope deformation and flow ponding. Flow stripping is likely during this phase (Sinclair and Tomasso, 2001). D; At a threshold barrier height, flows are deflected and reflected back into the basin. Lack of bypass results in thick turbidite T_e mudstone caps. E; Flow incision through the intraslope high occurs, with re-establishment of bypass across the ponded basin.

in flow processes for each described environment. For example, while the CLTZ stratigraphicaly succeeds stacked lobe deposits at the Mt. Salici section, treating them as isolated depositional element examples and recognising significant facies differences, allows a measure of flow process differentiation between these two environments.

In the proximal sections of Finale and Karsa, flows were confined within channel-complexes where massive sandstone deposits aggraded from quasi-steady flows (Kneller and Branney, 1995). In channel-complexes of Finale, the degree of confinement and a steep above-grade slope would have promoted flow bypass and inhibited unsteadiness, such that waning turbulent surge deposits are relatively uncommon (<26%) except within overbank areas where low density flows became unconfined. Kneller and McCaffrey (2003) suggest that proximal flows will experience a complicat-

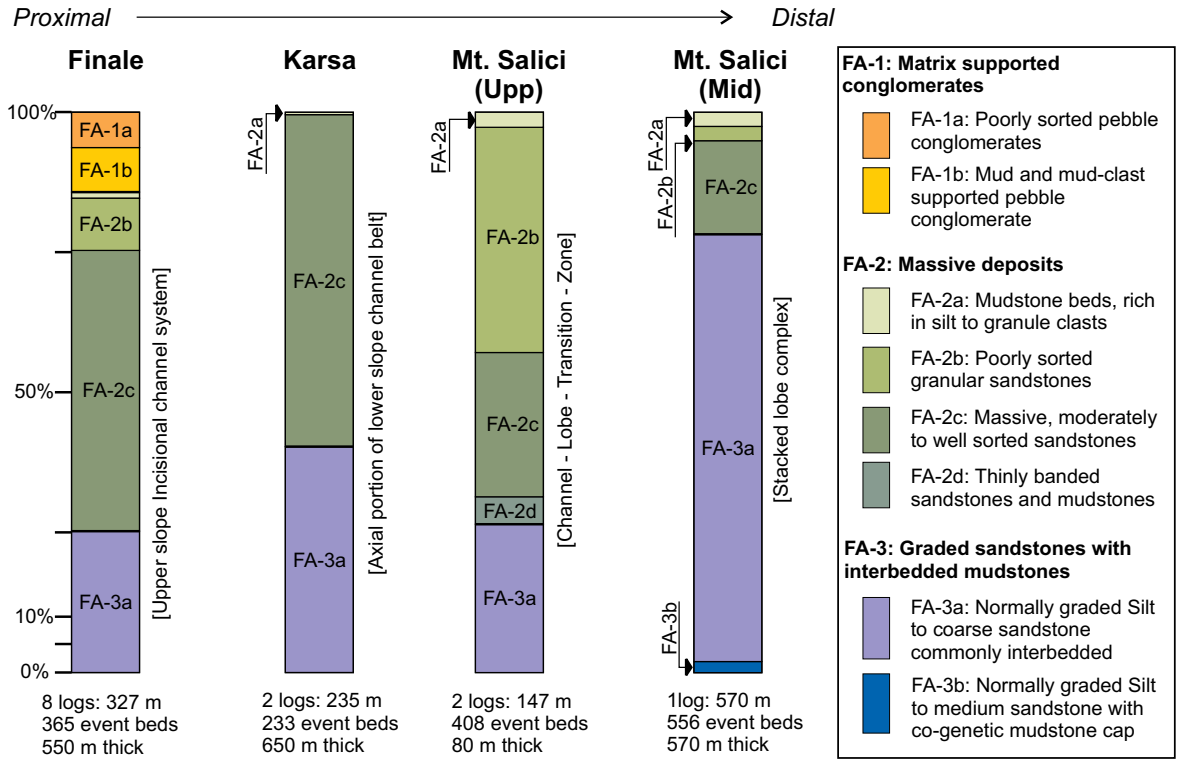

Figure 3.17.
A quantative comparison of the facies proportions between the main environments interpreted in this study. Environments are taken out of a stratigraphic context such that they represent an environmental case study only. Percentages are calculated from the number of event beds logged (and not their thickness) in order to account for the number of flow types and not the volume of those flows. The number and total thickness of sedimentary logs used, the number of event beds counted, and the stratigraphic thickness of the section are included below each case study.

ed longitudinal velocity profile composed of velocity spikes which may account for minor incisional surfaces and mud clast trains which occur mid-way through aggradational beds (FA-2c. e.g figure 3.7c). If massive sandstone facies represent non-cohesive debris flow deposits, deposition would have occured when the flow shear stress fell below the flow yield strength and grain-to-grain friction prompted collapse and deposition (Dasgupta, 2003; Enos, 1977). Major and Iverson (1999) speculate that high friction at the flow margins is also important and in the confined channel-complex settings of Finale such friction with channel-complex walls would have played a key role in prompting deposition. A lowering of the channel floor gradient would similarly have promoted deposition, which would have occurred during backfilling of the channel. This similarly applies to facies FA-1a and 1b (hyperconcentrated bipartite turbidity current and cohesive debris flow respectively) which only occur in this proximal section. Facies indicative of surge-type turbidity currents (FA-3a) are however recognised within unconfined slope deposits throughout all sections, including adjacent to upper slope channel bodies.

At Mt. Salici, channel-complexes of the lower subdivision are composed of the same combination of thick turbidite deposits, and massive facies deposited through steady aggradation within a confined environment (FA-2c). Within lobe environments however the dominant flow facies are graded sandstones (<76%) displaying the characteristics of Bouma subdivisions ($T_{a, b, c}$) (Figure 3.17). They are interpreted as the product of waning surge turbidity currents as expected within low gradient, unconfined basin floor environs. In contrast, over 57% of beds within the CLTZ section are massive sandstones (FA-2b and 2c). In particular, a high proportion of poorly sorted granular sandstones (FA-2b; >31%), indicate bedload deposition (e.g traction carpet deposits) despite stratigraphically succeeding fine-grained suspension sedimentation deposits of the lobe. Taken as an

isolated environmental case study, the CLTZ thus marked a point of downslope change in the gross character of flow deposits from massive ungraded, to structured and graded.

The CLTZ itself dominantly contains large scours filled with coarse grained sediment. Hydraulic jumps are often inferred to occur across Channel Lobe Transition Zones due to flows exiting a confined channel at a break of slope (Morris et al., 1998; Wynn et al., 2002). Hydraulic jumps occur when confined supercritical flows pass through a decrease in slope gradient, across which they slow and become subcritical (Garcia and Parker, 1989). As flows slow, ambient water is entrained which substantially thickens the flow and generates turbulence that scours the substrate. A hydraulic jump is however not perquisite at a CLTZ (see Ito, 2008; Lee et al., 2004; Macías et al., 1998; Morris et al., 1998) in order to scour the substrate and deposit coarse sediment. Within the Mt. Salici CLTZ, the large percentage of poorly sorted granular sandstones (FA-2b) suggests that coarse grained bedload was being deposited from bypassing turbidity currents as predicted by flume experiments including Garcia and Parker (1989) and Garcia (1993) who calculated a drop in bed shear stress, and deposition of coarse grained bedload immediately downslope of a gradient change. Flows therefore underwent a loss of competence and sediment was dumped. The remainder, finer grained sediment fraction then bypassed to the lobe environment where deposition occurred through waning flow, recorded as Bouma type facies. It has not possible to prove a genetic link between the scours and their coarse grained fill in the Mt. Salici section, although large scour surfaces which contain several stacked event beds signify erosion from several flows which bypassed the outcropping CLTZ completely.

Banded slurry flows within the CLTZ (<5% of event beds) record flow behaviour which was transitional between laminar and fully turbulent and which primarily required a high degree of mud within flows (Lowe and Guy 2000). Mud rich flows are perhaps unexpected given the relatively poorly sorted but clean sandstones of proximal sections. Mud clasts are also numerous within both massive beds and graded sandstones of the CLTZ (e.g Figures 3.15a, 3.15b, 3.15c) while in proximal sections they are smaller and confined to massive well sorted sandstones (Fa-2c) and isolated beds of granular sandstones (Fa-2b) (Figure 3.7b and 3.7c). While unquantified, this observation may be explained by erosion and incorporation of muddy substrate by turbulent flows within the proximal CLTZ, a similar process to that interpreted by Ito (2008) from the Otadai Formation of Japan.

3.5.4 Within context of the Sicilide basin

The northwest to southeast palaeogeographic trend described here matches similar interpretations from previous studies. Palaeomagnetic data and palinspastic reconstructions of the closure of the Sicilide basin evidence large horizontal rotations of the nappes prior to and during emplacement. Magnitudes of rotation vary between 70° (Monaco and De Guidi, 2006) and 120° (Oldow et al., 1990) in a clockwise direction. This suggests an approximately north east proximal to distal trend when restored.

Lobe deposits are also described by Pescatore et al. (1987) from western Madonie signifying a laterally equivalent depocentre. Lobe deposits in southern Italy (Carbone et al., 1987), along the same palaeogrographic trend (~north east), represent a distal equivalent to this section. Their Aquitanian to Langhian age, assigned by Carbone et al. (1987), compared with the (younger) Aquitanian to Burdigalian aged sections described in this study, suggests a later basin closure in the east however, in agreement with basin structural models (see Thomas et al. (2010), and references

therein). Diachronous basin closure from west to east would therefore serve to tilt the foredeep basin floor towards the east in the same orientation as the basin axis. This may explain the long runout distances required to deposit distal turbidites far to the east in southern Italy. When viewed within the context of intraslope ponded basins, it seems probable that these lobe environments represent lateral or downslope depocentres separated by intraslope basinal highs.

3.6 Conclusions

Three key sections of the Numidian Flysch Formation are described from northern and central Sicily. Their incorporation into the Alpine aged fold and thrust belt coupled with low resolution biostratigraphy prevents direct correlation of the sections. By describing them in terms of facies and architecture variations however the sections show a proximal upper slope to distal basin floor trend towards the southeast in agreement with previous studies of the Numidian Flysch Formation in Sicily.

At Finale, incisional channel-complexes with coarse-grained facies indicate an above grade, upper slope environment. To the south, aggradationally stacked channel complexes of the Karsa section are characteristic of a below-grade lower slope environment. In central Sicily, a stacked lobe complex is recognised, succeeded by deposits of a Channel-Lobe-Transition-Zone. The slope was aggradational throughout all these sections, promoting incision and flow confinement within upper slope channel complexes, aggradation of channel and overbank deposits in lower slope channel complexes, and stacking of lobe complexes on a low gradient basin floor. The characteristics and proportions of facies within each section indicate that the Channel-Lobe-Transition-Zone plays a substantial role in modulating flows, thereby; a) enhancing turbulence, and b) promoting deposition of massive coarse grained sediment, and leading to bypass of finer grained waning turbulent flows to depositional lobes.

The possibility of a ponded intraslope evolution for the Mt. Salici section is discussed to explain flow reflection and changes in the proportion of Bouma Te deposits relative to turbidity current bedload deposits (T_a to T_c). Contemporaneous lobe deposits described from western Sicily and southern Italy may therefore represent similar intraslope depocentres. Furthermore, complex palaeocurrent measurements (a reason for the enduring Numidian Flysch Formation provenance debate), routinely recorded throughout the basin may be explained by such ponding and deflection of flows.

Once clockwise horizontal nappe rotations are taken into account, the proximal to distal trend becomes approximately north or northeast. It is interpreted that African sourced sediment was fed north and eastwards into the developing Mahgrebian Flysch Basin from northern Tunisia. Diachronous basin closure and consequent eastwards tilting of the basin floor is proposed as a mechanism to generate the long run-out turbidity current lobe deposits in southern Italy.

References.

Abreu, V., Sullivan, M., Pirmez, C. and Mohrig, D., 2003. Lateral accretion packages (LAPs): an important reservoir element in deep water sinuous channels. Marine and Petroleum Geology, 20(6-8): 631-648.

Amy, L.A., Kneller, B.C. and McCaffrey, W.D., 2007. Facies architecture of the Gris de Peira Cava, SE France: landward stacking patterns in ponded turbiditic basins. Journal of the Geological Society, 164: 143-162.

Armitage, D.A., Romans, B.W., Covault, J.A. and Graham, S.A., 2009. The Influence of Mass-Transport-Deposit Surface Topography on the Evolution of Turbidite Architecture: The Sierra Contreras, Tres Pasos Formation (Cretaceous), Southern Chile. Journal of Sedimentary Research, 79(5): 287-301.

Beaubouef, R.T., 2004. Deep-water leveed-channel complexes of the Cerro Toro Formation, Upper Cretaceous, southern Chile. Aapg Bulletin, 88(11): 1471-1500.

Boiano, U., 1997. Anatomy of a siliciclastic turbidite basin: The Gorgoglione Flysch, Upper Miocene, southern Italy: Physical stratigraphy, sedimentology and sequence-stratigraphic framework Sedimentary Geology, 107(3-4): 231-262.

Bonardi, G. et al., 1980. Osservazioni sull'evoluzione dell'Arco Calabro-Peloritano nel Miocene inferiore: la Formazione di Stilo-Capo d'Orlando. Bollettino Della Societa Geologica Italiana, 99: 365-393.

Bouma, A.H., 1962. Sedimentology of some Flysch deposits: A graphic approach to facies interpretation. 168 pp: Elsevier.

Broquet, P., Duee, G. and Mascle, G., 1973. Existence of Deformations Prior to Middle Miocene Carriage in Internal Numidian between Gangi and Nicosia (Nebrodi Mountains, Sicily). Comptes Rendus Hebdomadaires Des Seances De L Academie Des Sciences Serie D, 277(5): 477-478.

Caire, A. and Mascle, G., 1969. Relations between Internal Flysch External Numidian and Upper Miocene around Rocca Busambra (Western Sicily). Comptes Rendus Hebdomadaires Des Seances De L Academie Des Sciences Serie D, 268(5): 756.

Campion, K.M. et al., 2000. Outcrop expression of confined channel complexes. Deep-water reservoirs of the world: SEPM, Gulf coast section, 20th annual Research Conference, 20th annual Research Conference 127-50.

Carbone, S., Catalano, S., Grasso, M., Lentini, F. and Monaco, C., 1990. Carta Geologica Della Sicilia Centro-Orientale (1: 50,000) Instituto di Scienze della Terra.

Carbone, S., Lentini, F., Sonnino, M. and De Rosa, R., 1987. Il flysch numidico di Valsinni (Appennino lucano). Translated Title: The numidic flysch of Valsinni, Lucanian Apennines. Bollettino Della Societa Geologica Italiana, 106(2): 331-345.

Carvajal, C., Steel, R. and Petter, A., 2009. Sediment supply: The main driver of shelf-margin growth. Earth-Science Reviews, 96(4): 221-248.

Cornamusini, G., 2004. Sand-rich turbidite system of the Late Oligocene Northern Apennines foredeep: physical stratigraphy and architecture of the 'Macigno costiero' (coastal Tuscany, Italy). Geological Society, London, Special Publications, 222(1): 261-283.

Cronin, B.T., Hurst, A., Celik, H. and Türkmen, I., 2000. Superb exposure of a channel, levee and overbank complex in an ancient deep-water slope environment. Sedimentary Geology, 132(3-4): 205-216.

Dasgupta, P., 2003. Sediment gravity flow - the conceptual problems. Earth-Science Reviews, 62(3-4): 265-281.

de Capoa, P. et al., 2002. The Lower Miocene volcaniclastic sedimentation in the Sicilian sector of

the Maghrebian Flysch Basin: geodynamic implications. Geodinamica Acta, 15(2): 141-157.

de Capoa, P., Guerrera, F., Perrone, V., Serrano, F. and Tramontana, M., 2000. The onset of the syn-orogenic sedimentation in the Flysch Basin of the Sicilian Maghrebids: state of the art and new biostratigraphic constraints. Eclogae Geologicae Helvetiae, 93(1): 65-79.

Deptuck, M.E., Piper, D.J.W., Savoye, B. and Gervais, A., 2008. Dimensions and architecture of late Pleistocene submarine lobes off the northern margin of East Corsica. Sedimentology, 55(4): 869-898.

Di Celma, C., Cantalamessa, G., Didaskalou, P. and Lori, P., 2010. Sedimentology, architecture, and sequence stratigraphy of coarse-grained, submarine canyon fills from the Pleistocene (Gelasian-Calabrian) of the Peri-Adriatic basin, central Italy. Marine and Petroleum Geology, 27(7): 1340-1365.

Enos, P., 1977. Flow regimes in Debris flows. Sedimentology, 24(1): 133-142.

Eschard, R., Albouy, E., Deschamps, R., Euzen, T. and Ayub, A., 2003. Downstream evolution of turbiditic channel complexes in the Pab Range outcrops (Maastrichtian, Pakistan). Marine and Petroleum Geology, 20(6-8): 691-710.

Faugeres, J.C., Broquet, P., Duee, G. and Imbert, P., 1992. Sedimentary Record of Volcanic and Paleocurrent Events in the Numidian Sandstones of Sicily - the Tuffites and Contourites of Karsa. Comptes Rendus De L Academie Des Sciences Serie Ii, 315(4): 479-486.

Garcia, M. and Parker, G., 1989. Experiments on hydraulic jumps in turbidity currents near a canyon-fan transition. Science, 245(4916): 393-396.

Garcia, M.H., 1993. Hydraulic jumps in sediment-driven bottom currents. Journal of Hydraulic Engineering-Asce, 119(10): 1094-1117.

Gee, M.J.R. and Gawthorpe, R.L., 2006. Submarine channels controlled by salt tectonics: Examples from 3D seismic data offshore Angola. Marine and Petroleum Geology, 23(4): 443-458.

Gervais, A., Savoye, B., Mulder, T. and Gonthier, E., 2006. Sandy modern turbidite lobes: A new insight from high resolution seismic data. Marine and Petroleum Geology, 23(4): 485-502.

Gery, B., 1983. Age and Tectonic Situation of the Allochthonous Sedimentary Formations in Northern Grande Kabylie - an Example in the Djebel Aissa-Mimoun. Comptes Rendus De L Academie Des Sciences Serie Ii, 297(9): 729-&.

Golonka, J., 2004. Plate tectonic evolution of the southern margin of Eurasia in the Mesozoic and Cenozoic. Tectonophysics, 381(1-4): 235-273.

Gottis, C., 1953. Stratigraphie et tectonique du « flysch » numidien en Tunisie septentrionale. Compte Rendus Hebdomadaires des Seances de l'Academie des Sciences, Paris, 236: 1059-1061.

Guerrera, F., Martinalgarra, A. and Perrone, V., 1993. Late Oligocene-Miocene Syn-/-Late-Orogenic Successions in Western and Central Mediterranean Chains from the Betic Cordillera to the Southern Apennines. Terra Nova, 5(6): 525-544.

Hackbarth, C.J. and Shew, R.D., 1993. Interpretation of a mid-Pleistocene leveed channel system using high-resolution seismic data, cores, and logs, Viosca Knoll, Northeast Gulf of Mexico. In: Anonymous (Editor), American Association of Petroleum Geologists 1993 annual convention. Annual Meeting Abstracts - American Association of Petroleum Geologists and Society of Economic Paleontologists and Mineralogists. American Association of Petroleum Geologists and Society of Economic Paleontologists and Mineralogists, Tulsa, OK, United States, pp. 112.

Haughton, P., Davis, C., McCaffrey, W. and Barker, S., 2009. Hybrid sediment gravity flow deposits - Classification, origin and significance. Marine and Petroleum Geology, 26(10): 1900-1918.

Haughton, P.D.W., Barker, S.P. and McCaffrey, W.D., 2003. 'Linked' debrites in sand-rich turbidite systems - origin and significance. Sedimentology, 50(3): 459-482.

Hesse, R., Klaucke, I., Khodabakhsh, S., Piper, D.J.W. and Ryan, W.B.F., 2001. Sandy submarine braid plains: Potential deep-water reservoirs. Aapg Bulletin, 85(8): 1499-1521.

Hickson, T.A. and Lowe, D.R., 2002. Facies architecture of a submarine fan channel–levee complex: the Juniper Ridge Conglomerate, Coalinga, California. Sedimentology, 49(2): 335-362.

Hoyez, B., 1974. Sedimentologie. - Cadre et evolution du bassin numidien sicilien. Structure and Evolution of Numidian Basin of Sicily. Comptes Rendus Hebdomadaires Des Seances De L Academie Des Sciences Serie D, 278(8): 1007-1010.

Ito, M., 2008. Downfan transformation from turbidity currents to debris flows at a channel-to-lobe transitional zone: The lower Pleistocene Otadai Formation, Boso Peninsula, Japan. Journal of Sedimentary Research, 78(9-10): 668-682.

Johansson, M., Braakenburg, N.E., Stow, D.A.V. and Faugeres, J.C., 1998. Deep-water massive sands: facies, processes and channel geometry in the Numidian Flysch, Sicily. Sedimentary Geology, 115(1-4): 233-265.

Kane, I.A., Kneller, B.C., Dykstra, M., Kassem, A. and McCaffrey, W.D., 2007. Anatomy of a submarine channel-levee: An example from Upper Cretaceous slope sediments, Rosario Formation, Baja California, Mexico. Marine and Petroleum Geology, 24: 540-563.

Kenyon, N.H., Millington, J., Droz, L. and Ivanov, M.K., 1995. Scour holes in a channel-lobe transition zone on the Rhone Cone. Atlas of deep water environments: architectural style in turbidite systems: 212-215.

Kneller, B., 2003. The influence of flow parameters on turbidite slope channel architecture. Marine and Petroleum Geology, 20(6-8): 901-910.

Kneller, B.C. and Branney, M.J., 1995. Sustained High-Density Turbidity Currents and the Deposition of Thick Massive Sands. Sedimentology, 42(4): 607-616.

Kneller, B.C. and McCaffrey, W.D., 2003. The interpretation of vertical sequences in turbidite beds: The influence of longitudinal flow structure. Journal of Sedimentary Research, 73(5): 706-713.

Lambiase, J.J. et al., 2008. The West Crocker formation of northwest Borneo: A Paleogene accretionary prism. Geological Society of America Special Papers, 436: 171-184.

Lee, S.E., Amy, L.A. and Talling, P.J., 2004. The character and origin of thick base-of-slope sandstone units of the Peira Cava outlier, SE France. Deep-Water Sedimentation in the Alpine Basin of Se France: New Perspectives on the Gres D'annot and Related Systems, 221: 331-347.

Lentini, F., Vezzani, L., Carveni, P., Copat, B. and Grasso, M., 1974. Carta Geologica della Madonie (Sicilia Centro - Settentrionale) (1:50,000). Instituto di Geologia dell'Universitá di Catania.

Lowe, D.R., 1982. Sediment gravity flows; II, Depositional models with special reference to the deposits of high-density turbidity currents. Journal of Sedimentary Petrology, 52(1): 279-297.

Lowe, D.R. and Guy, M., 2000. Slurry-flow deposits in the Britannia Formation (Lower Cretaceous), North Sea: a new perspective on the turbidity current and debris flow problem. Sedimentology, 47(1): 31-70.

Macdonald, H.A., Peakall, J., Wignall, P.B. and Best, J., 2011. Sedimentation in deep-sea lobe-elements: implications for the origin of thickening-upward sequences. Journal of the Geological Society, 168(2): 319-332.

Macías, J.L., Espíndola, J.M., Bursik, M. and Sheridan, M.F., 1998. Development of lithic-breccias in the 1982 pyroclastic flow deposits of El Chichón Volcano, Mexico. Journal of Volcanology and Geothermal Research, 83(3-4): 173-196.

Major, J.J. and Iverson, R.M., 1999. Debris-flow deposition: Effects of pore-fluid pressure and friction concentrated at flow margins. Geological Society of America Bulletin, 111(10): 1424-1434.

Mayall, M., Jones, E. and Casey, M., 2006. Turbidite channel reservoirs - Key elements in facies prediction and effective development. Marine and Petroleum Geology, 23(8): 821-841.

Mayall, M. et al., 2010. The response of turbidite slope channels to growth-induced seabed topography. Aapg Bulletin, 94(7): 1011-1030.

Mazzoleni, P., 1991. Porphyric rocks in the basal conglomerate from the Stilo-Capo d'Orlando Formation

Le rocce profiriche nel conglomerato basale della formazione di Stilo-Capo d'Orlando. Memorie della Societa Geologica Italiana, 47: 557-565.

McHargue, T. et al., 2010. Architecture of turbidite channel systems on the continental slope: Patterns and predictions. Marine and Petroleum Geology, 28(3): 728-743.

Monaco, C. and De Guidi, G., 2006. Structural evidence for Neogene rotations in the eastern Sicilian fold and thrust belt. Journal of Structural Geology, 28(4): 561-574.

Morris, Kenyon, Limonov and Alexander, 1998. Downstream changes of large-scale bedforms in turbidites around the Valencia channel mouth, north-west Mediterranean: implications for palaeoflow reconstruction. Sedimentology, 45(2): 365-377.

Mulder, T. and Alexander, J., 2001. The physical character of subaqueous sedimentary density flows and their deposits. Sedimentology, 48(2): 269-299.

Mutti, E. and Ricci Lucchi, F., 1978. Turbidites of the northern Apennines: introduction to facies analysis. International Geology Review, 20(2): 125 - 166.

Nigrini, C. and Sanfilippo, A., 2001. Cenozoic Radiolarian stratigraphy for low and middle latitudes with descriptions of biomarkers and stratigraphically useful species. Ocean Drilling Program, Technical Note (online), 27.

Oldow, J.S., Channell, J.E.T., Catalano, R. and D, A.B., 1990. Contemporaneous thrusting and large-scale rotations in the western Sicilian fold and thrust belt. Tectonics, 9(4): 661-681.

Patterson, R.T., Blenkinsop, J. and Cavazza, W., 1995. Planktic Foraminiferal Biostratigraphy and ⁸⁷Sr/⁸⁶Sr Isotopic Stratigraphy of the Oligocene-to-Pleistocene Sedimentary Sequence in the Southeastern Calabrian Microplate, Southern Italy. Journal of paleontology, 69(1): 7-20.

Pescatore, T., Renda, P. and Tramutoli, M., 1987. Facies ed evoluzione sedimentaria del bacino Numidico nelle Madonie occidentale (Sicilia). Memorie-Societa Geological Italiana, 38: 297-316.

Pirmez, C. and Imran, J., 2003. Reconstruction of turbidity currents in Amazon Channel. Marine and Petroleum Geology, 20(6-8): 823-849.

Posamentier, H.W. and Kolla, V., 2003. Seismic geomorphology and stratigraphy of depositional elements in deep-water settings. Journal of Sedimentary Research, 73(3): 367-388.

Prather, B.E., Booth, J.R., Steffens, G.S. and Craig, P.A., 1998. Classification, lithologic calibration, and stratigraphic succession of seismic facies of intraslope basins, deep-water Gulf of Mexico. Aapg Bulletin-American Association of Petroleum Geologists, 82(5): 701-728.

Prélat, A., Hodgson, D.M. and Flint, S.S., 2009. Evolution, architecture and hierarchy of distributary deep-water deposits: a high-resolution outcrop investigation from the Permian Karoo Basin, South Africa. Sedimentology, 56(7): 2132-2154.

Saller, A. et al., 2008. Characteristics of Pleistocene deep-water fan lobes and their application to an upper Miocene reservoir model, offshore East Kalimantan Indonesia. AAPG Bulletin, 92(7): 919-949.

Shanmugam, G., 1997. The Bouma Sequence and the turbidite mind set. Earth-Science Reviews, 42(4): 201-229.

Shanmugam, G., 2000. 50 years of the turbidite paradigm (1950s-1990s): deep-water processes and facies models - a critical perspective. Marine and Petroleum Geology, 17(2): 285-342.

Shanmugam, G., 2002. Ten turbidite myths. Earth-Science Reviews, 58(3-4): 311-341.

Sinclair, H.D. and Tomasso, M., 2002. Depositional evolution of confined turbidite basins. Journal of Sedimentary Research, 72(4): 451-456.

Speranza, F., Maniscalco, R. and Grasso, M., 2003. Pattern of orogenic rotations in central-eastern Sicily: implications for the timing of spreading in the Tyrrhenian Sea. Journal of the Geological Society, 160: 183-195.

Sprague, A.R. et al., 2005. Integrated slope channel depositional models: the key to successful prediction of reservoir presence and quality in offshore West Africa. CIPM, cuarto E-Exitep 2005, February 20-23 2005. Veracruz, Mexico.: 1-13.

Sprague, A.R. et al., 2002. The physical stratigraphy of deep-water strata; a hierarchical approach to the analysis of genetically related stratigraphic elements for improved reservoir prediction. In: Anonymous (Editor), AAPG annual convention with SEPM. American Association of Petroleum Geologists and Society of Economic Paleontologists and Mineralogists (AAPG). Tulsa, OK, United States. 2002.

Thomas, M.F.H., Bodin, S., Redfern, J. and Irving, D.H.B., 2010. A constrained African craton source for the Cenozoic Numidian Flysch: Implications for the palaeogeography of the western Mediterranean basin. Earth-Science Reviews, 101(1-2): 1-23.

Walker, R.G., 1985. Mudstones and thin-bedded turbidites associated with the upper cretaceous Wheeler Gorge conglomerates, California - a possible channel-levee complex. Journal of Sedimentary Petrology, 55(2): 279-290.

Wezel, F.C., 1970. Numidian Flysch - an Oligocene - Early Miocene Continental Rise Deposit Off African Platform. Nature, 228(5268): 275-&.

Wynn, R.B., Kenyon, N.H., Masson, D.G., Stow, D.A.V. and Weaver, P.P.E., 2002. Characterization and recognition of deep-water channel-lobe transition zones. Aapg Bulletin, 86(8): 1441-1462.

Chapter 4.

Architecture and evolution of the Finale channel system, the Numidian Flysch Formation of Sicily; Insights from a hierarchical approach.

Chapter 4. Architecture and evolution of the Finale channel system, the Numidian Flysch Formation of Sicily; Insights from a hierarchical approach.

Abstract

Large scale ancient channel systems are commonly imaged using seismic data and classified hierarchically. Where exposed at outcrop, similar scale ancient channel systems provide an opportunity to investigate subseismic scale architectures, produced for example through short duration autocyclic processes, and assess how they contribute to larger seismically imaged architectures. In this study, a seismic scale slope-confined channel system from the Numidian Flysch Formation of northern Sicily is described using a hierarchical classification scheme. The channel system 5.7 km wide and is organised within 3 hierarchical levels, comprising; 2 channel complex sets, 16 channel complexes, and 36 channel elements. Mappable channel complexes reach 500 m in width and 90 m thick.

Channel elements are bound by a basal erosion surface and generally stack to form channel complexes. They show a progression of incision and bypass from coarse grained stratified flows, to fill with aggrading massive sandstones interspersed with waning turbidite deposits. Waning flow deposits are relatively uncommon and flows are interpreted to predominantly deposit during quasi-steady flow conditions. Velocity fluctuations (non-uniformity) produce beds with complex grading patterns and indicate a proximal environment. Lateral expansion of channel element widths produces terracing within the complex margin, and has the capacity to alter flow rheology through incorporation of large mud volumes. Element thalwegs are sinuous and therefore offset from the thickest part of the complex. Complexes are also sinuous with some asymmetric cross sections.

Both channel-complexes and elements thicken with younging, indicating increased entrenchment through allocyclic forcing. The frequency distribution of channel-element thicknesses (n=35) also shows a positive skew centred around 12m, in agreement with data from examples of McHague et al. (2010) (n=834). Many factors effect depth of erosion including slope gradient, location and sediment calibre. We question whether this distribution similarity may result from a fundamental process at the channel-element scale however. We speculate that autocyclic processes may preferentially exert a lower erosional thickness at the element scale producing such a frequency distribution.

The use of a hierarchical classification scheme therefore highlights the importance of channel element sinuosity and stacking patterns and their impact upon seismic scale architectures. The quantification of specific hierarchical elements also allows the role of allocyclic forcing to be investigated.

4.1. Introduction

Submarine channels represent sustained conduits on submarine slopes formed through a combination of erosion and deposition from transiting density flows. In recent years, submarine channel architectures and the facies that fill them have been intensively studied using both outcrop and high quality industry 3D seismic data. With notable exceptions including the Kirkgeçit Formation of Turkey (e.g Cronin et al., 2005b), the Pab Formation of Pakistan (Eschard et al., 2003), and the

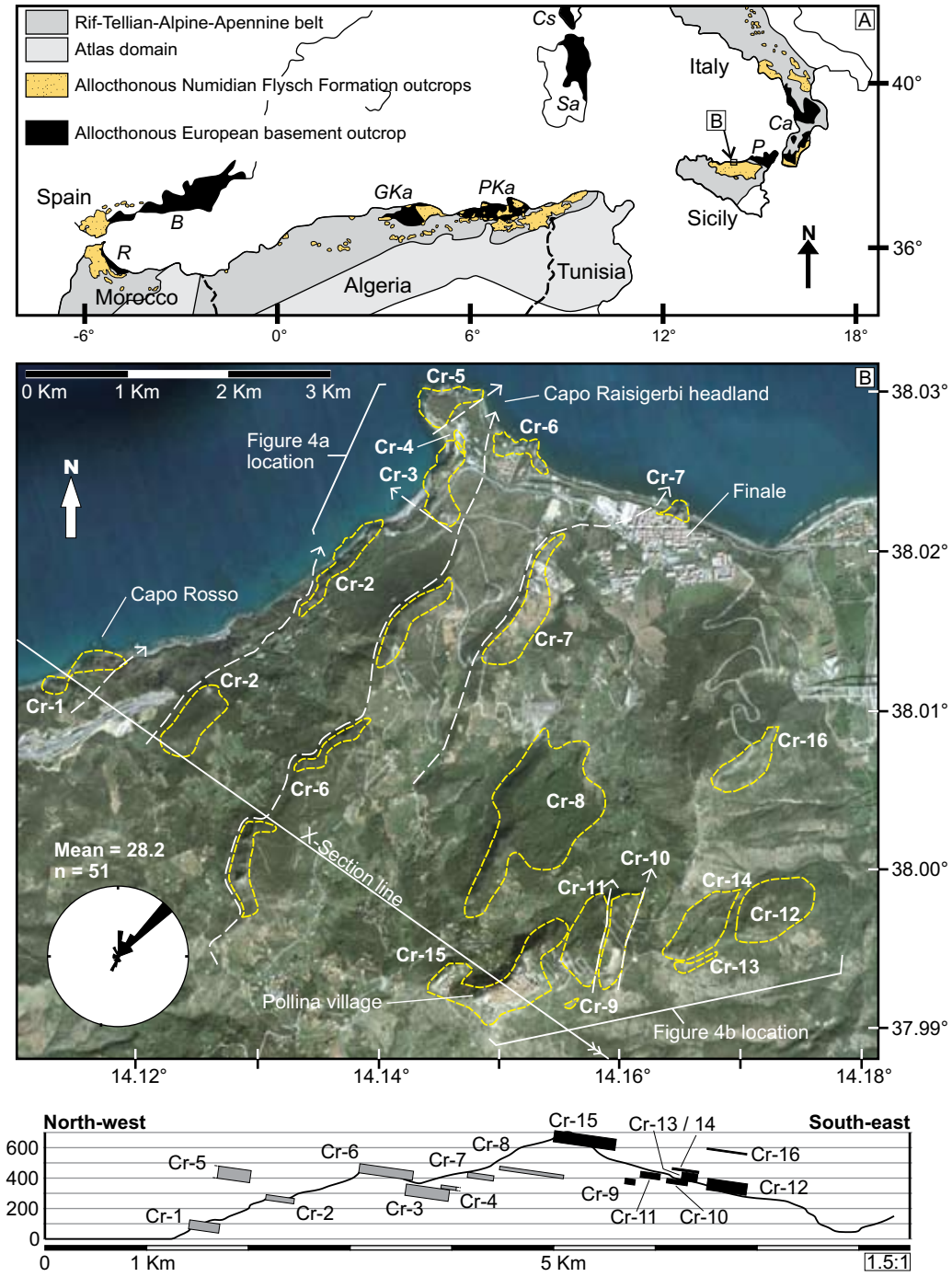

Figure 4.1.

Location map of the Numidian Flysch Formation outcrops (1a) and the area of study. 4.1b; Aerial photograph from Google Earth highlighting major channel complex outcrops in yellow and their names (see table 1 for nomenclature system). White dashed lines indicate lines of cliffs which demark outcrop trends. Arrows highlight the outcrop trend of channel complexes. A rose diagram (n= 51) displays the palaeoflow orientations of density flow deposits both within and outside of channel complexes such that a local northeastern palaeoslope is present. 4.1c; A schematic cross section (depositional strike orientation) with the location of channel complexes. Vertical exaggeration is 1.5. Grey and black infilled complexes correspond to the Capo Raisigerbi and Pollina channel complex sets respectively. Cross section is highlighted in figure 4.1b.

Gres du Champsaur of France (e.g Brunt and McCaffrey, 2007), studies of large-scale submarine channel systems are predominantly described using seismic data given the difficulties of sufficient outcrop exposure.

The manifestation of a channel systems evolution, in terms of architectures and the style of deposits which fill them, are of major importance to hydrocarbon exploration whereby models can provide

a degree of prediction in frontier provinces. Through outcrop and seismic studies, common evolutions associated with submarine channels have been recognised. At its most simple this may be described by a ‘waxing’ phase in which excavation of slope sediment occurs, followed by a ‘waning’ phase in which sediments fill the open channel form (McHargue et al., 2010). Through ancient outcrop and recent seismically imaged examples, this simple evolution has been recognised to repeatedly occur over a variety of time scales and magnitudes producing a complicated hierarchy of depositional elements (Abreu et al., 2003; Deptuck et al., 2007; Posamentier and Kolla, 2003). Erosional slope confined channel complexes (sensu Sprague et al., 2002) are a depositional element originally recognised within seismic data from the Gulf of Guinea (Cronin et al., 2005b) in which a well defined basal erosion surface confines smaller sandy channelised forms which commonly display a sinuous planform (Campion et al., 2000). Attempts to capture complexity such as this have resulted in several models based upon a variety of methods. Models by Campion et al. (2000), Mayall et al. (2010), McHargue et al. (2010), Navarre et al. (2002) and Sprague et al. (2002) are hierarchical and based upon recognition of major surfaces and architectural stacking patterns. These classifications are scale independent and, with the exception of Mayall et al. (2006) (their figure 6), are also time independent. In contrast, process based models such as Peakall et al. (2000) and Kneller (2003) link flow processes with changes in architectural style. Such models provide a way to characterise channel system architectures and infer channel processes based upon interpreted depositional elements. In particular, hierarchical models also allow for a methodical comparison between channel systems, although this approach is not yet commonplace within published studies.

This study presents a channel system from the Numidian Flysch Formation of Sicily. The system is similar in scale to large, seismically imaged examples from the Pleistocene Benin-major Canyon (Deptuck et al., 2007) and the Niger Delta (Catterall et al., 2010). This study aims to document the system using a hierarchical approach with the objective of answering the following questions. Are similar processes documented from different examples of the same hierarchy within the Finale channel system? How do processes within smaller scale nested architectural elements (e.g channel elements) contribute to the geometry of larger architectural elements (e.g channel complexes)? Both of these questions are important when considering heterogeneity and reservoir connectivity within channel bodies on a scale commonly mapped within seismic data. We also discuss the effect of allocyclic controls upon depositional elements of different hierarchies.

4.2. Geological background

The Numidian Flysch Formation is an Oligocene to mid-Miocene deep-marine deposit found throughout the entire western Mediterranean, cropping out in Spain, Morocco, Algeria, Tunisia, Sicily and southern mainland Italy (Wezel, 1970) (Figure 4.1a). It represents a linear series of roughly contemporaneous submarine fans on the North African passive margin, consisting of quartz rich sediment sourced from the African craton (Thomas et al., 2010). The Mahgrebian Flysch Basin (MFB) into which sediment was deposited (Figure 4.2), was a foreland basin remnant of the Neo-Tethys ocean in which oceanic crust was subducted northwards beneath European crustal blocks termed the AlKaPeCa terrains (de Capoa et al., 2000; Guerrera et al., 2005; Thomas et al., 2010).

European AlKaPeCa terrains and their sedimentary cover formed an accretionary prism at the northern margin of the basin as they migrated southwards during the Oligocene and Miocene (de Capoa et al., 2004). Continental collision with the African margin occurred from the early to upper Miocene such that basin deposits were thrust upon the North African margin, resulting in the

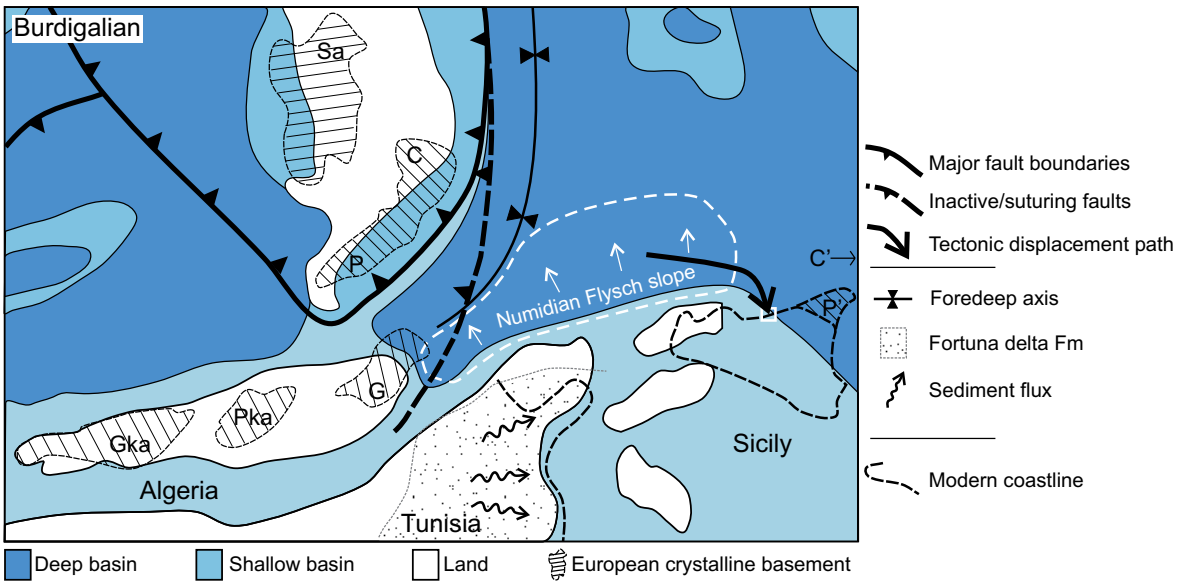

Figure 4.2.
Palaeogeographic map of the Sicilide basin during the Burdigalian (early Miocene), representing the eastern portion of the Maghrebian Flysch Basin (MFB). The outline of Sicily is shown along with the location of the study area in white. Allocthonous European basement blocks of the AlKaPeCa domain are shown; Gka = Grand Kabylie. Pka = Petit Kabylie. G = Galite block. P = Peloritani block. Ca = Calabrian block. Sa = Sardinia. The present day positions of the Peloritani block (in northeastern Sicily) and the Calabrian block (in southern Italy) are shown by the terms P' and Ca'. The approximate location of the Finale channel system prior to allocthonous transport if shown by the black arrow (allocthonous displacement path taken from (Speranza et al., 2003).

regional Alpine fold-and-thrust belt (Thomas et al., 2010 and references therein). Diachronous closure effectively split the basin into three sub-basins however, with the middle Tunisian/Algerian sector closing in the early Miocene and the western (Moroccan/Spanish sector) and eastern (Sicilide sector) sub-basins remaining open until the mid to late Miocene (Thomas et al., 2010). Numidian Flysch Formation deposits of the Sicilide basin, the subject of this study, were therefore deposited into a foreland basin embayment which opened north-eastwards towards the Italian Apennine Foreland Basin (Figure 4.2) (Guerrera et al., 2005).

4.2.1 The Sicilide basin

Numidian Flysch Formation deposits of the Sicilide basin crop out throughout northern and central Sicily, southern Italy, and transgressing the basement of the Galite block in northern Tunisia (Belayouni et al., 2010; Wezel, 1970) (Figure 4.1a). The North African passive margin was orientated approximately northeast – southwest and bordered by the Tunisian mainland and the Pelagian shelf to the south (Figure 4.2). In northern Tunisia, the Fortuna Formation, a major fluvio-deltaic complex, fed sediment eastwards towards the Pelagian shelf (Vanhouten, 1980). Its role in providing sediment to the North African margin and henceforth to Numidian Flysch Formation submarine fans has been long debated with no obvious conclusion (see Thomas et al. (2010) and references therein). Medium to Coarse grained shallow marine clastic deposits of the contemporaneous Bejaoua Group also crop out in northern Tunisia beneath nappes of the Numidian Flysch Formation (Riahi et al., 2010). A shallow marine shelf environment therefore separated the Numidian Flysch slope from the Tunisian shoreline while there was a distally steepened ramp environment to the east around Malta and southern Sicily (e.g Pedley et al., 1992) (Figure 4.2).

Little detail is known regarding the slope architecture of this passive margin due to the thrusted nature. (Wezel, 1970) however interpreted a slope and continental rise environment for deposits

in northern Sicily. Lobes have also been interpreted from western Sicily (Pescatore et al., 1987). In northern and central Sicily, a series of sandy channels have been described within a submarine slope environment (Johansson et al., 1998). They range from 150 m to 3 km in width, and include some examples described within this study (see section 4.2). Channels contain stacked beds of massive ungraded sandstones, and incise muddy slope deposits with no evidence for levee construction. (Johansson et al., 1998) interprets this massive sandstone facies as the deposits of high-density turbidity currents and debris flows. Three types of erosive channel are documented, based upon grainsize and channel dimensions (Johansson et al., 1998) although all are interpreted as erosive and to contain nested channels bodies. (Stow et al., 1999) elaborate on this interpretation and infer a correlation of some channels, providing a sinuous planform which is mapped for up to 10 km downslope. This study attempts to build upon this work.

4.3. Study area

In northern Sicily, several channel examples crop out along a 19 km stretch of coastline. They form prominent headlands of thick sandstones which protrude tens of metres into the Tyrrhenian sea. Two prominent groupings occur; 2 kilometres west of Cefalu, and 11 km east of Cefalu. Here we focus on the eastern grouping centred upon the town of Finale and the Capo Raisigerbi headland (Figures 4.1a, and 4.1b). This includes the Ponte Finale and Pollina channels previously documented by (Johansson et al., 1998). Here, stratigraphy is exposed in an 8 km wide thrust sheet dipping 20° towards the northeast. 650 m of discontinuous section is accessible in a north to south transect from coastal cliff sections to the town of Pollina at 970 m elevation (Figures 4.1b and 4.1c). Channel bodies were mapped using traditional field mapping techniques and Google Earth (Spot satellite imagery incorporating the Shuttle Radar Topography Mission (SRTM) digital elevation model, with 90 m resolution).

4.4. Results

16 major channel forms and several minor sandstone bodies were identified outcropping with a north-eastward outcrop trend which is readily identifiable within the topography of the north sloping hillslope (Figure 4.1b). Individual channel forms range from tens of metres to 400 m in width, and from >13 to 81 m thick (Tables 4.1 and 4.2). They are characterised by stacked sandstones and conglomerates which are bound by a discrete surface, adjacent to mudstone rich sediments. They are named as Cr-1 to Cr-16 with younging (Cr resulting from the Capo Raisigerbi headland; see Figure 4.1b) with the Ponte Finale and Pollina channels of (Johansson et al., 1998) here renamed as Cr-5 and Cr-15 respectively (see section 4.2). They crop out in a belt which has a width of 5.7 km. 8 Major channel outcrops were mapped along the coast (Cr-1 to Cr-8; Figure 4.1b) and 8 major channel outcrops were mapped along the ridgeline which culminates in the village of Pollina (Cr-9 to Cr-16; Figure 4.1b). The northwards hill slope in this area is slightly greater than stratigraphic dip such that several coastal channel complexes can be traced continuously, via outcropping cliff sections and breaks of topography, for up to 3.6 km with a north eastern orientation (Figure 4.1b).

Palaeoflow orientations were recorded from flutes, cross bedding and ripples both within channel forms and from deposits adjacent to them (Figure 4.1b). A dominant northeast orientation is recorded which matches the northeast trend of channel form outcrops (Figure 4.1b). A local northeast downslope trend is therefore recognised in accordance with Johansson et al. (1998) and Stow et al. (1999).

4.4.1 Lithofacies of the Finale section (5th order)

A variety of facies were observed both within the sandstone channel forms and in mudstone dominated sections adjacent to them. They are described here using the nomenclature of Dasgupta (2003) such that flows are grouped into; turbidity currents, hyperconcentrated flow, debris flow, and subaqueous grain flow, with increasing sediment to water ratio. They correspond to turbulent, transitional (between turbulent and plastic), laminar, and collisional flow characteristics respectively. Laminar debris flow deposits are subdivided into cohesive and noncohesive types based upon lithology, with noncohesive debris flows being equivalent to sandy debris flows of (Shanmugam, 2000), and hyperconcentrated density flows of Mulder and Alexander (2001). Figure 4.3 illustrates the major facies types.

Matrix supported conglomerates (FA-1) contain a high proportion of pebbles with varying amounts of mud in the matrix. Poorly sorted pebble conglomerates (FA-1a) correspond to conglomerates with relatively low amounts of mud in the matrix and clasts up to 70 mm in width (Figure 4.3a). Beds reach 0.8 m thick with highly scoured bases such that stacked beds are vertically amalgamated (see also figure 4.7a). Pebble clasts are held within a poorly sorted matrix of mud to coarse sand. They are ungraded to rarely reverse graded, can be imbricated throughout the bed thickness and may have basal flutes. This indicates turbulence prior to deposition, and traction during deposition. This facies is interpreted to represent bedload (traction carpet) deposition from the lower portion of a stratified turbidity current. This facies is equivalent to the S3 subdivision of (Lowe, 1982).

Mud and mud clast supported conglomerates (FA-1b) differ from the FA-1a due to a high percentage of mud (~30-70%) and an abundance of mud-clasts within the matrix (Figure 4.3b). Beds are similarly ungraded and very poorly sorted with randomly orientated pebbles up to 30 mm in diameter. In specific patches, the conglomerate becomes clast supported. Beds reach 1.5 m thick with moderately scoured bases. FA-1b is similar to FA-1a with respect to these characteristics although the matrix is dominated by mud and contains rounded to elongate mud clasts which reach 1.2 m in length and contribute up to 70% of the bed volume. A cohesive debris flow origin is interpreted with the clasts floating within a matrix of substantial yield strength. The high mud content of this facies may be present in the source sediment prior to flow initiation. This is likely to produce a laminar flow process however, and a consequent mechanism for the erosion and entrainment of mud clasts is problematic. Given the similarity in matrix and pebble content with FA-1a, a possible formative mechanism is that this facies represents deposits of a turbulent flow similar in character to FA-1a. Mud particles and mud clasts are subsequently entrained through turbulent erosion, resulting in a transformation to laminar flow and a cohesive debrite deposit. This mechanism is interpreted to explain the origin of cohesive debris flows occur across a channel lobe transition zone from the lower Pleistocene Otadai Formation of Japan (Ito 1998).

Massive ungraded deposits (FA-2) make up a majority of channel form fill. Their structureless and ungraded nature makes interpretation of deposition through waning turbulent flow problematic. **Massive muddy siltstones (FA-2a)** are found in interchannel areas and very rarely within channel forms. Beds are pale blue to dark grey, reach 0.4 m thick and are interbedded with mudstones (Figure 4.3c). They are structureless with the exception of bioturbation including Arenicolites. Ungraded silt to coarse sand grains are found within the matrix (<30%). They are interpreted as cohesive debris flow deposits, representing remobilisation of muddy sediments from upslope environments.

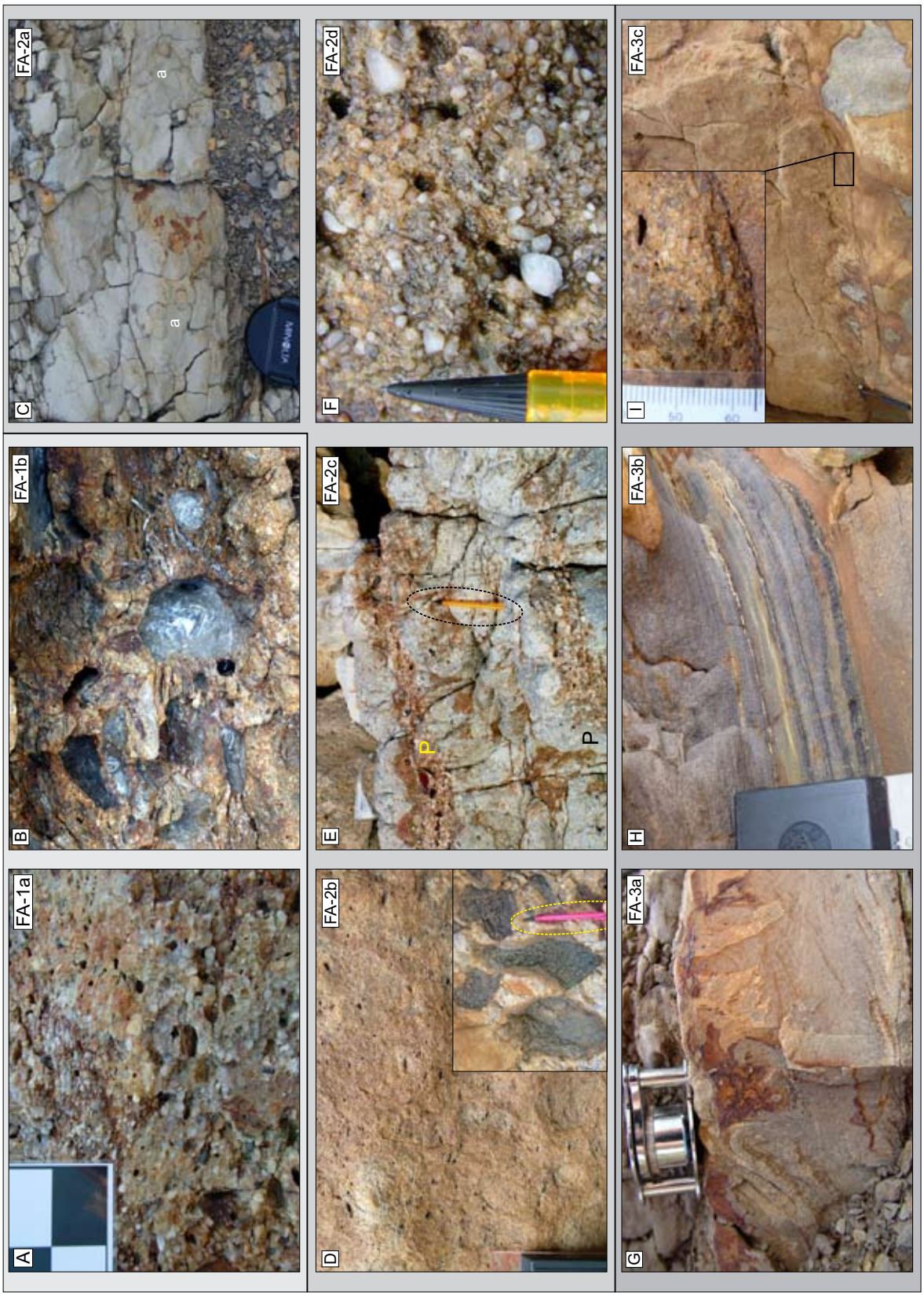

Figure 4.3.

Density flow facies of the Finale channel system. 4.3a; Matrix supported conglomerates of FA-1a. 4.3b; Mud and mud clast rich conglomerates (FA-1b) containing mud clasts <1 m in width. Note lens cap for scale. 4.3c; Massive muddy siltstones (FA-2a) in the Capo Raisigerbi interchannel area (see figure 4.7). 'a' denotes Arenocolites ichnogenera. 4.3d; Moderately to well sorted massive sandstones (FA-2b) in complex Cr-5. Note small mud clasts throughout. Inset shows same facies with numerous imbricated mud clasts. Example from Channel element Cr-3b. Note pencil for scale. 4.3e; Pebbly sandstone beds (FA-2c) denoted by P, interbedded with FA-2b in complex Cr-5. 4.3f; Poorly sorted granular sandstones (FA-2d) from the thalweg of element Cr-3a. Pencil for scale. 4.3g; Example of medium grained sandstone and interbedded mudstones

Figure 4.3 continued..
(FA-3a), Rippled and dewatered turbidite (Tc division) from complex Cr-7. 4.3h; Stacked laminated sandstones (FA-3b) from the base of element Cr-5d. 4.3i; Thick bedded graded sandstones (FA-3c). Note erosive base and rapid base-only fining upwards from granular sandstones (see inset) to coarse – medium sandstones.

Moderately to well sorted massive sandstones (FA-2b) are the most common facies recorded in channel forms and are also observed in lesser amounts in interchannel areas. Previous work on the Numidian Flysch Formation of Sicily has focussed upon this facies as an example of deep water massive sandstones (DWMS sensu (ohansson et al. (1998) and Stow and Johansson (2000)). Beds of fine to coarse grained sandstones range from a few centimetres to over 8 m in thickness, typically with planar bounding surfaces and tabular geometries. No sedimentary structures are evident apart from rare flutes and grading is absent apart from top-only normal grading in some examples (Figure 4.3d). Trains of mm scale mudclasts are distributed, concentrated at either bed base or top, or cross cutting one-another throughout the bed thickness. Some examples contain a coarser grainsize fraction (<10%) ranging from coarse to granular sand grains distributed throughout the bed thickness. These examples contain mudclasts up to 0.3 m long which form <50% of the deposit and can often be imbricated (Figure 4.3d). Mud clasts are however observed up to 1.5 m in diameter. The flow orientation from clast imbrication is variable and if often towards the channel form margin. A single example contains a set of planar cross bedding with a 0.4 m thickness. Dewatering structures are common including large scale loading, flame structures and rare pipe structures.

Flutes and top only normal grading indicate turbulent erosion prior to, and waning conditions only during the latter stages of deposition. The dominant massive ungraded character suggests suppression of sedimentary structures and aggradation beneath a quasi-steady turbulent flow is interpreted (sensu Kneller and Branney., 1995). The single observed example of cross bedding suggests that traction can occasionally occur across the flow-deposit interface, presumably due to a temporary decrease in the downward sediment flux which normally inhibits such processes (Kneller and Branney, 1995). Similar processes may also account for imbrication of mudclasts. Mud clasts are large enough however that they may protrude through a basal hyperconcentrated shearing layer (Hiscott, 1994; Kneller and Branney, 1995) and experience simple shear from the bypassing flow above. Where entirely ungraded, deposition through non-cohesive debris flow origin (sensu Shanmugam (2000) cannot be excluded however.

Some examples of moderately to well sorted massive sandstones contain large amounts (<40%) of well rounded pebbles up to 25 mm in diameter which display no grading (Figure 4.3e). These **pebbly sandstone beds (FA-2c)** occur interbedded with facies FA-2b within channel forms. Beds have well scoured bases and reach 1.5 m thick, often with the proportion of pebble clasts varying laterally from <10% to 40%. Commonly however, beds reach 0.3 m thick. Bed geometry is often lenticular and the bed top may downlap onto the channel element basal surface. This facies is similarly interpreted as representing aggradation beneath a quasi-steady turbulent flow with pebbles representing coarse grained bedload.

Poorly sorted granular sandstones (FA-2d) are found throughout channel forms. They differ from FA-2b with poorly sorted angular grainsizes of fine sand to granule and scattered mudclasts which are typically >2 mm but reach 0.5 m in width (Figure 4.3f and 4.6d). Silt and mud are virtually absent from the matrix of this facies. Beds reach 0.5 m thick with moderately scoured bases. This facies is found vertically stacked close to the base of a channel form, or else interbedded with facies FA-2b within the upper portions of channel forms (Figure 4.7d). Scoured bases and mud-

clasts suggest turbulence prior to deposition of this facies while poor sorting and the lack of grading negates waning flow conditions. This facies is interpreted to represent deposition from the hyper-concentrated lower portion of non-waning stratified turbidity current.

Graded deposits (FA-3) refer to deposits which are normally graded and commonly contain tractional sedimentary structures. **Thin to medium bedded siltstones and sandstones (FA-3a)** consist of deposits described by the Bouma classification scheme (sensu (Bouma, 1962). Beds consist of laminated and rippled fine to coarse sandstones (Bouma T_b and T_c subdivisions respectively) interbedded with mudstones (hemipelagic mudstones and T_e) (Figure 4.3g). Packages reach 0.3 m in thickness and can be interbedded with massive graded sandstones (T_a). Bioturbation including cruziana and planolites occur both on the top of sandstone beds and throughout mudstone caps (T_e). Normal grading throughout, coupled with traction structures, indicates waning turbulent flow as described from the Bouma classification scheme (Bouma, 1962). This facies is found close to some channel form margins and rarely near the top. This facies is however most common in interchannel locations. Where intensely laminated sandstones are stacked they are defined separately as **Stacked laminated sandstones (Fa-3b)**. Medium to coarse sandstones are planar laminated on a 1 – 25 mm scale and are vertically stacked to form tabular bed sets from 0.1 to 2 m thick (Figures 4.3h and 4.8a and 4.8c). Rare ripples and climbing ripple trains have been observed at the top of the laminated succession. In some examples, laminas are fining upwards bands within an overall fining upwards trend with some ripples at the bed top. In these circumstances, a waning flow with upper stage plane bed and ripple deposition may be interpreted as characterised with the Bouma T_b and T_c subdivisions (Bouma, 1962). Other examples reach 2 m thick without normal grading and no ripples, silt, or mud caps (e.g $T_{c,d,e}$) (Figure 4.8c). Laminas in these examples have slightly erosive bases, reach <0.25 m thick, and are ungraded but display alternating coarse and medium grainsizes. Such banding suggests fluctuations in flow competence and the facies is interpreted to represent flow non-uniformity within a waning surge (Kneller and McCaffrey, 2003; Lowe, 1982) whereby waxing velocity pulses control grain size deposition through fluctuations in shear velocity. This facies occurs within interchannel locations immediately adjacent to channel margins (Figure 4.8), and also within channel forms where they mark a significant switch of depositional style (Figure 4.7e).

Thick bedded graded sandstones (FA-3c) reach 1.5 m thick and do not contain sedimentary structures typical of the Bouma sequence. Beds have locally scoured bases and show base-only normal grading from granule or coarse sandstone to coarse or fine sandstone often with a grainsize break near the bed base (e.g granule to medium sand) (Figure 4.3i). mm scale mud clasts are commonly distributed throughout the bed. Unlike FA-3a, this facies is found interbedded with massive sandstones of FA-2b and has no preserved mud cap (e.g no T_e subdivision). Scouring and normal grading indicates turbulent bypass and deposition while the lack of structures suggests no traction at the flow/deposit interface. Direct suspension sedimentation may account for this, whereby a high downwards sediment flux prevents traction occurring (Lowe, 1982). Grainsize breaks in some examples may be indicative of absent grainsize populations within the source sediment, however this is not observed within all examples. Non-uniformity of the flow also provides an alternative interpretation, with longitudinal velocity pulses passing downstream through the flow. Shear stress would be temporarily increased, preventing deposition of ‘intermediate’ grainsize populations and resulting in an absent grainsize fraction (Kneller and McCaffrey, 2003).

4.4.2 Organisation of channel forms

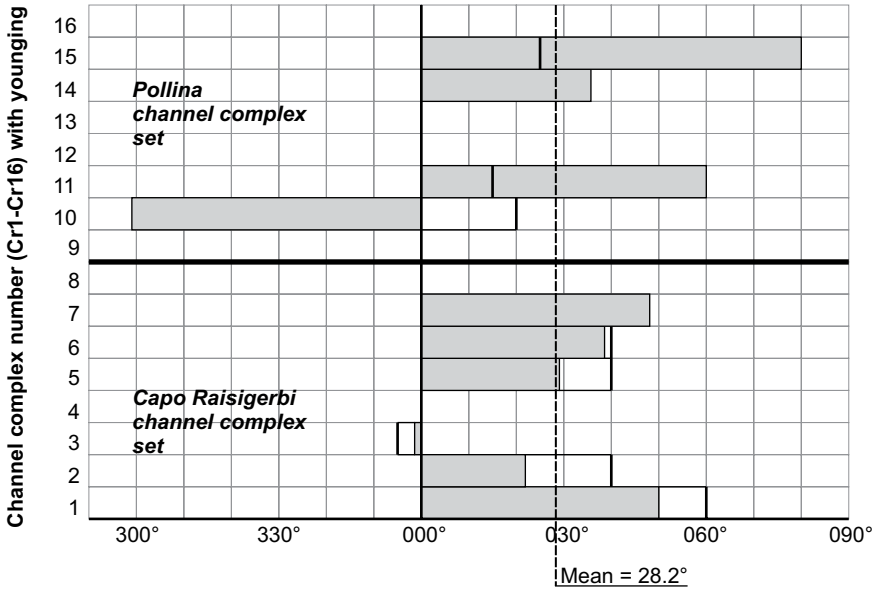

Figure 4.4.
Graph of palaeoflow orientations from the Finale channel system. Channel complex numbers make up the Y axis (Cr-1 to Cr-16) Solid grey bars denote measured orientations from density flow facies. Thick black lines mark the orientation of channel complex margins as measured from outcrop and aerial photographs.

The location of channel forms (Figure 4.1b) occurs within 2 groups as described within section 4. Channels Cr-1 to Cr-8 crop out along coastal sections where they are clearly observed to offset stack towards the southeast (Figure 4.1b). Projected on to a cross section constructed along depositional strike, they are observed to form a belt 3.6 km wide and a stratigraphic thickness of 420 m (Figure 4.1b, table 4.1). The palaeocurrents recorded from Cr-1 to Cr-8 also record a systematic change with younging, from the northeast to the north, and back towards the northeast (Figure 4.4). This is compared to a mean downslope orientation of 028° and is observed at outcrop on the Capo Raisigerbi headland, where channel Cr-3 plunges beneath channels Cr-4 and Cr-5 with an intersection angle of 35° (Figures 4.1b, 4.4 and 4.5a). In contrast, channel forms Cr-9 to Cr-16 crop out close together with no observed systematic stacking pattern across a narrow belt of 2.3 km width and a stratigraphic thickness of 320 m (Figures 4.1b and 4.1c). Palaeocurrent and outcrop orientations are also not observed to show a systematic variation (Figure 4.4). The Finale section therefore consists of 2 groups of channel forms with varying characteristics.

Hierarchy	Width (m)	Thickness (m)	Bounding surfaces	Stratigraphic order	Terminology	Nomenclature
4.	40 - 400	7 - 45	High relief erosional upper and lower	5th: 10 Kyr - 100 Kyr	**Channel element**	e.g Cr-1a, Cr-1b
3.	40 - 400	30 - 82	High relief erosional base Sharp planar top	4th: 100 Kyr - 1Myr	**Channel complex**	Cr-1 to Cr-16
2.	3600 2300	420 320	Bounding erosional surface?	≤3rd: 1 to 3 Myr	**Channel complex set (*ccs*)**	Capo Raisigerbi *ccs* Pollina *ccs*
1.	5700	650	Amalgamated bounding erosional surface?	3rd: 1 to 3 Myr	**Channel system**	Finale channel system

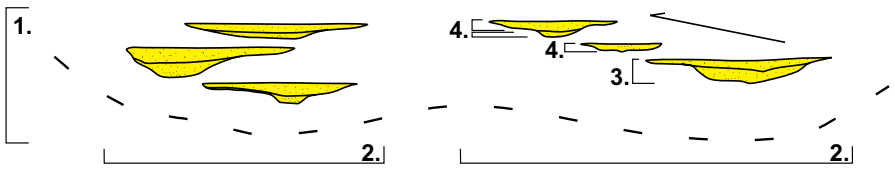

Table 4.1.
The hierarchy and nomenclature used for the Finale channel system.

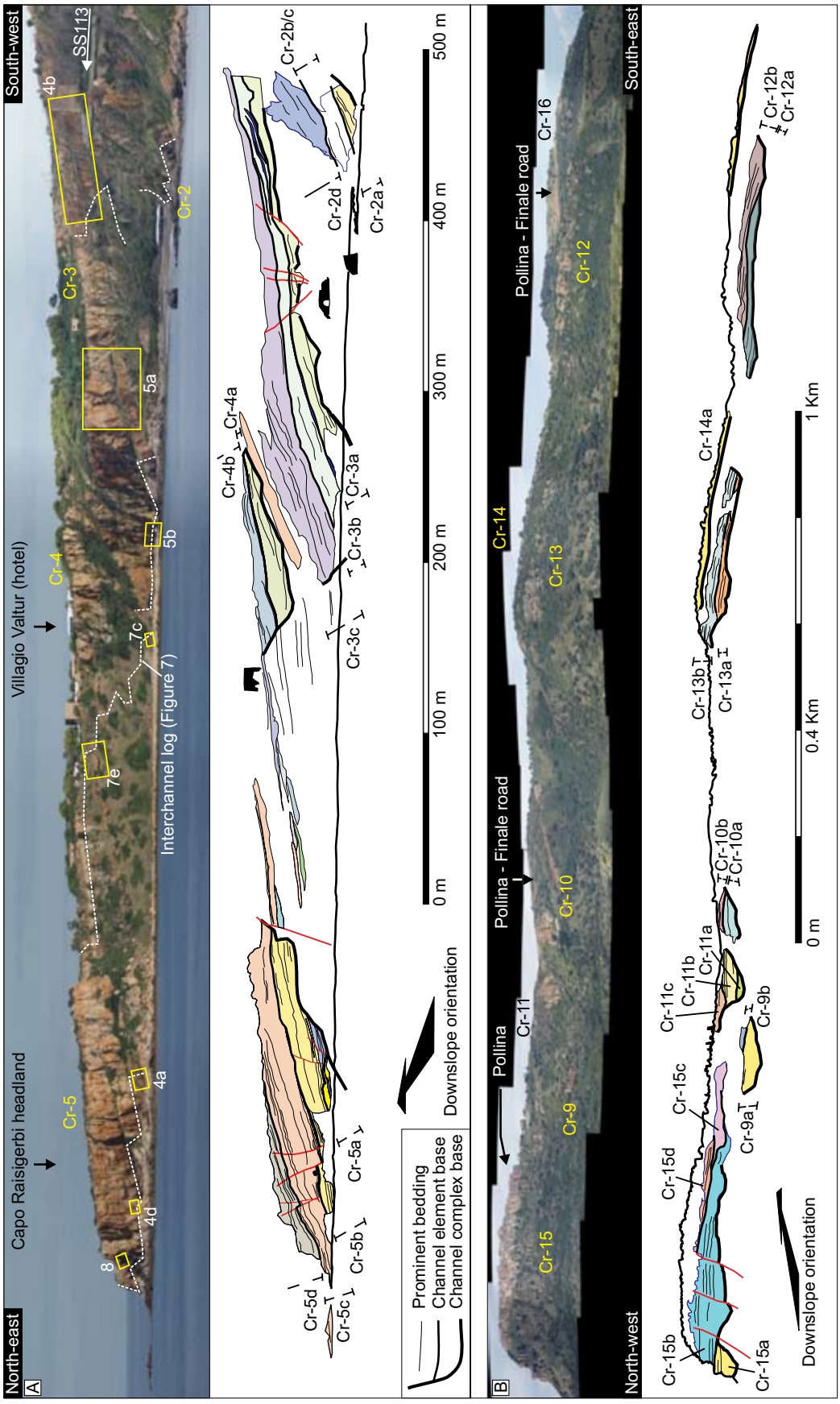

Figure 4.5.
Panoramic views and annotations of the channel complexes Cr-2 to Cr- 5 within the Capo Raisigerbi channel complex set (4.5a) and channel complexes Cr-9 to Cr-15 within the Pollina channel complex set (4.5b).

Channel Complex Set	Channel complex		Channel elements		Palaeoflow orientation		
	Number	Width / Thickness	Number	Thickness	Mean	Range	Outcrop
Capo Raisigerbi 3.4 Km width 380 m thick	**Cr1**	240 m / 59 m	2	18 41	050°	-	060°
	Cr2	210 m / ~35 m	4	7 8 8 >10	022.5°	0-25°	040°
	Cr3	300 m / 75 m	3	12 34 29	357.6°	330-040°	355°
	Cr4	>60 m / >23 m	2	12 >11	-	-	-
	Cr5	>220 m / >81 m	4	>9.6 31 37 13	28.6°	010-050°	-
	Cr6	480 m / ~60 m	>2	-	38.3°	020-060°	040°
	Cr7	>28 m / >35 m	2	>16 >12	47.5°	030-050°	038°
	Cr8	600 m / >20 m	-	-	-	-	-
Pollina 2.4 Km width 400 m thick	**Cr9**	c. 130 m / c. 37 m	2	26 11	-	-	-
	Cr10	c. 200 m / > 29 m	3	12 7 >10	298°	260-320°	020°
	Cr11	c. 90 m / -	>3	9 17 14	60°	-	015°
	Cr12	330 m / 75 m	>2	-	-	-	-
	Cr13	210 m / 57 m	>2	28 29	-	-	-
	Cr14	>200 m / >13 m	-	-	36°	010-080°	-
	Cr15	>500 m / 75 m	>3	25 16 34	80°	060-100°	025°
	Cr16	c.300 m / -	-	-	-	-	-

Table 4.2.
Depositional elements from the Finale channel system, including dimensions and palaeocurrent orientations.

Within channel forms, laterally extensive surfaces commonly occur and display an erosional topography (Figures 4.5, 4.6 and 4.7). Such surfaces divide channel fill into several distinct storeys of stacked sandstones and conglomerates (Figure 4.5). Packages of sediment bound by such surfaces vary from 7 to 41 m thick and are laterally bound by the channel-form margin. Channel forms thus display a sub-hierarchy of packages within the channel form scale. Given these observations, five orders of hierarchy are recognised within the Finale section; 1) 1 channel system. 2) 2 groups of channel forms. 3) 16 Channel forms. 4) 35 intra-channel packages. 5) Individual event beds.

Similar hierarchies are noted from many channel systems (Cronin et al., 2005b; Mayall et al., 2010; Navarre et al., 2002; Prélat et al., 2009) and here we apply a terminology similar to (Campion et al., 2000) such that mappable channel forms are termed channel complexes (e.g Cr-1 to Cr-16). Channel complexes consist of 2 or more stacked channel elements (e.g Cr-1a, Cr-1b etc) bound by erosional surfaces. In turn, channel complexes are grouped to form 2 channel complex sets (ccs) with the western group called the Capo Raisigerbi ccs and the eastern group called the Pollina ccs.. Channel complex sets are grouped together as the Finale channel system. The hierarchy and

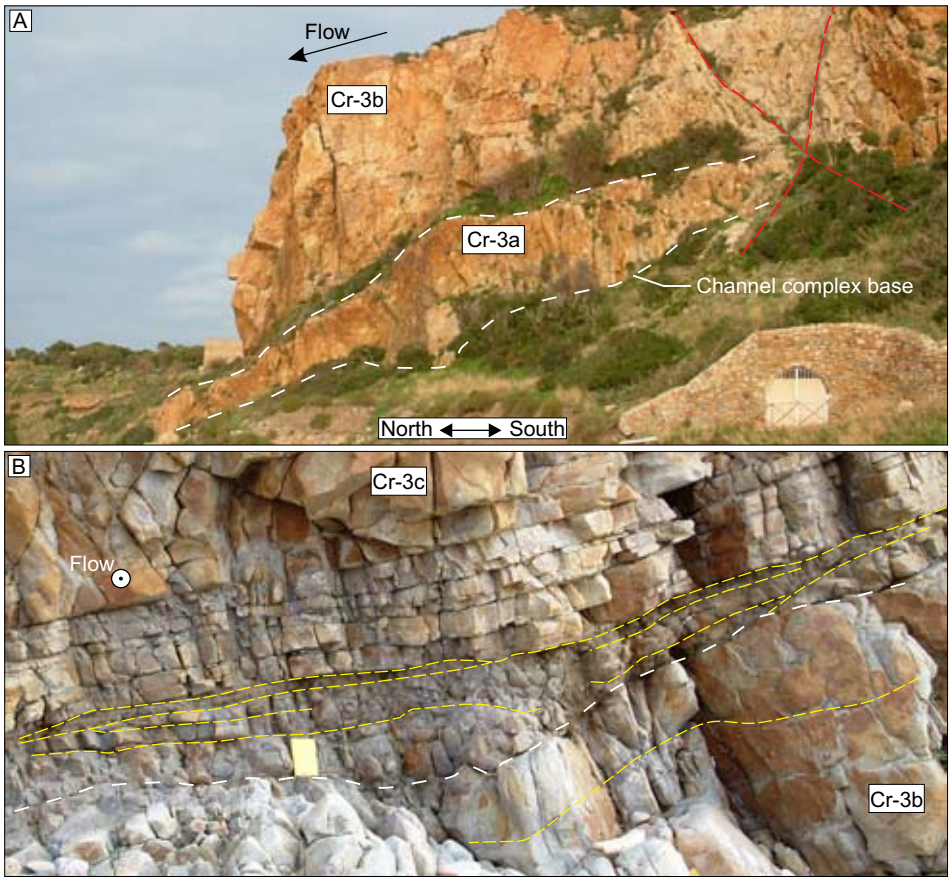

Figure 4.6.
Local incisions within channel element bases. 4.6a. Examples of downslope gradient changes in the basal surface of channel elements Cr-3a and 3b. Note flow is to the left of image. 4.6b; Subtle erosional topography on the base of channel element Cr-3c close to the northern margin. Note flow is out of the plane of the page.

the nomenclature used are shown in table 4.1 while table 4.2 shows this hierarchy as applied to the Finale section.

Where isolated singular channel forms are observed outside the confines of a channel complex they are termed channel elements but not included within table 4.2. While the classification scheme of (Mayall et al., 2006) is based upon sequence stratigraphic orders, the hierarchy used here, as with the versions of (Sprague et al., 2002) and (Campion et al., 2000), are scale and time independent, representing geometry only. Hierarchical numbers referred to within the text are thus geometrical (e.g Table 4.1) and not related to duration (e.g not stratigraphic orders in the sense of (Mayall et al., 2006).

4.4.2.1 Channel element architectures (4th order)

Channel elements range from 7 to 41 m thick and fill the entire complex width. The erosional surfaces which bound channel element fill are commonly moderately erosional with relief reaching a maximum observed value of c.10 m in element Cr-5b (Figure 4.5a). More commonly, as with elements in complexes Cr-3, Cr-5 and Cr-15, surfaces are relatively planar over the scale of the channel complex (Figure 4.5) with subtle erosional topography such that channel elements generally have a tabular geometry. Elements do not thin significantly towards the complex margin and obtuse angles are formed with the complex margin (4. 5).

In elements Cr-3a, Cr-3b, Cr-5b and Cr-11a, the basal surface is interrupted with a localised v-

Figure 4.7.

Panel depicting facies architectures and stacking within complexes. 4.7a; Beds of matrix supported conglomerates (FA-1a) and pebbly sandstones (FA-2c) amalgamated within the thalweg of element Cr-5b. Note channel complex margin picked out by white dashed line. The location of this photograph is shown in figure 5a. 4.7b; The distribution of coarse grained facies (FA-1a, 1b, 2b and 2c in complex Cr-3. The complex thalweg is offset 200 m to the east. 4.7c; Stacked laminated sandstones (FA-3b) and structureless Ta sandstones showing foundering and truncation from channel complex Cr-7. 4.7d;

Figure 4.7 continued..
Facies progression towards the top of complex Cr-5 (e.g element Cr-5d). Stacked massive sandstones with isolated large and rounded mudclasts are interbedded with granular sandstones rich in mudclasts. Note thinning of bedding and convex dewatering chimneys at complex top. 4.7e; Example of stacked laminated sandstones (FA-3b) bound below and above by massive sandstones (FA-2b) from channel element Cr-1a.

shaped erosional thalweg with steep margins (Figures 4.5, 4.6 and 4.7). In channel complex Cr-3, all three elements contain such localised erosion. Element Cr-3a shows a local V-shaped incision on the basal surface which cuts into muddy slope deposits beneath the complex base (Figure 4.6a). Towards the northern edge of the complex (Figure 4.5), the base of the subsequent element Cr-3b shows erosional topography localised in two areas separated by a 'high' (Figure 4.6a). Both these examples occur close to the channel complex centre but laterally offset from its thalweg. The base of element Cr-3c similarly shows a subtle (<0.5 m) incision close to the northern margin (Figure 4.6b). The orientation of the Cr-3 outcrop and measured palaeoflow indications confirm the outcrop to cut obliquely through the channel orientation (Figure 4.1a, table 4.2) such that v- shaped incisions of Cr-3a and Cr-3b appear to represent rapid downslope gradient changes in the basal surface.

On the Capo Raisigerbi headland, stratigraphically between complexes Cr-4 and Cr-5 are several isolated channel elements (i.e not stacked within a channel complex) with bases which incise inter-channel turbdite deposits interbedded with mudstones (Figures 4.1b and 4.5). Figure 4.8e details one such body, with an erosional base and a fill of stacked massive sandstones (FA-2b) and thin beds of coarse grained sandstones (FA-3a, T_a) (Figure 4.8d). As with channel complex examples, they have planar bases and tabular geometries with localised thickness variations due to incision. Unlike some channel complex confined examples, no very-coarse grained deposits are observed at the channel base. They are observed to systematically migrate laterally with younging, approximately along strike of the slope (Figures 4.b and 4.5). Subsequent channel bodies cut the margins of previous ones, such that they are laterally amalgamated.

4.4.2.2 Channel element fill (4th order)

Channel elements comprise an amalgamated succession of event beds bound by above and below by complex-wide erosional surfaces or the channel complex margin. Coarse grained conglomeratic or granular facies (FA-1a, FA-1b, FA-2c and FA-2d) are generally succeeded by stacked medium to coarse grained massive sandstones (FA-2b) interbedded with thick bedded graded sandstones (FA-3c) and poorly sorted granular sandstones rich in mud clasts (FA-2d). This progression is observed in elements from channel complexes including Cr-1, Cr-3 and Cr-5 (Figure 4.9). Elements stratigraphically higher within complexes are less likely to contain very coarse grained deposits, consisting predominantly of massive sandstones (FA-2b) (e.g Cr-2d and 5d. See Figure 4.9).

Facies FA-1a and 1b (Matrix supported conglomerates) are observed only within element Cr-5b where beds are vertically and horizontally amalgamated (Figures 4.7a and 4.9), accounting for ~60% of the channel element thickness. Beds fill a U shaped depression, representing the thalweg of the element, and are bound laterally and below by the channel complex margin. This is the thickest recorded part of element Cr-5b, and is offset from the complex thalweg towards the southern margin. The steepness of the complex margin reaches its maximum (≤vertical) where associated with this facies (Figures 4.5 and 4.7a).

In elements Cr-1b, Cr-3a, Cr-3b and Cr-8b (Figure 4.5), the basal surface is draped by poorly sorted granular sandstones (FA-2d) and pebbly sandstones (FA-2c) (e.g Figures 4.7b and 4.9). These

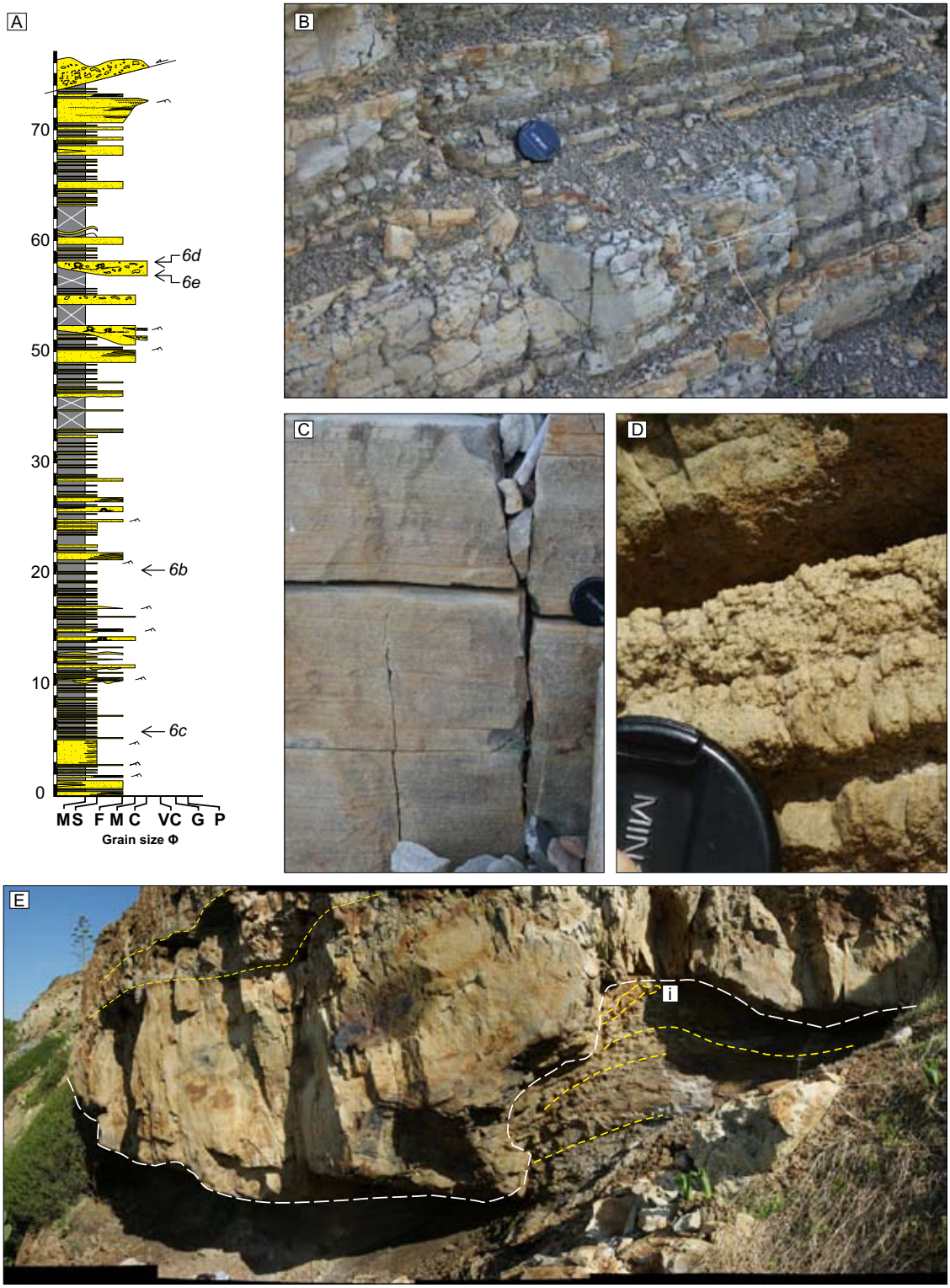

Figure 4.8.

Details of the Capo Raisigerbi headland interchannel area. See Figures 1b and 5a for location. 4.8a; Sedimentary log through the interchannel area. The location is shown in figure 4a. See figure 9 for sedimentary log key. 4.8b; Facies typical of interchannel areas; Beds of siltstone turbidites (Ta, Td?) and interbedded thin beds of mudstones (Te) and massive muddy siltstones (FA-2a). 4.8c; Beds of stacked laminated sandstones (FA-3b) <2 m thick at the base of the interchannel log. 4.8d; Thin coarse grained sandstone beds. From the top of the channel element shown in figure 8e. 4.8e; View of an isolated channel element (i.e not confined within a channel complex) within the interchannel area. The element is laterally amalgamated with other elements to the north (see figure 5a). Note incisional base (white dashed line) truncating mudstones and thin siltstones. A minor injection feature is highlighted (i).

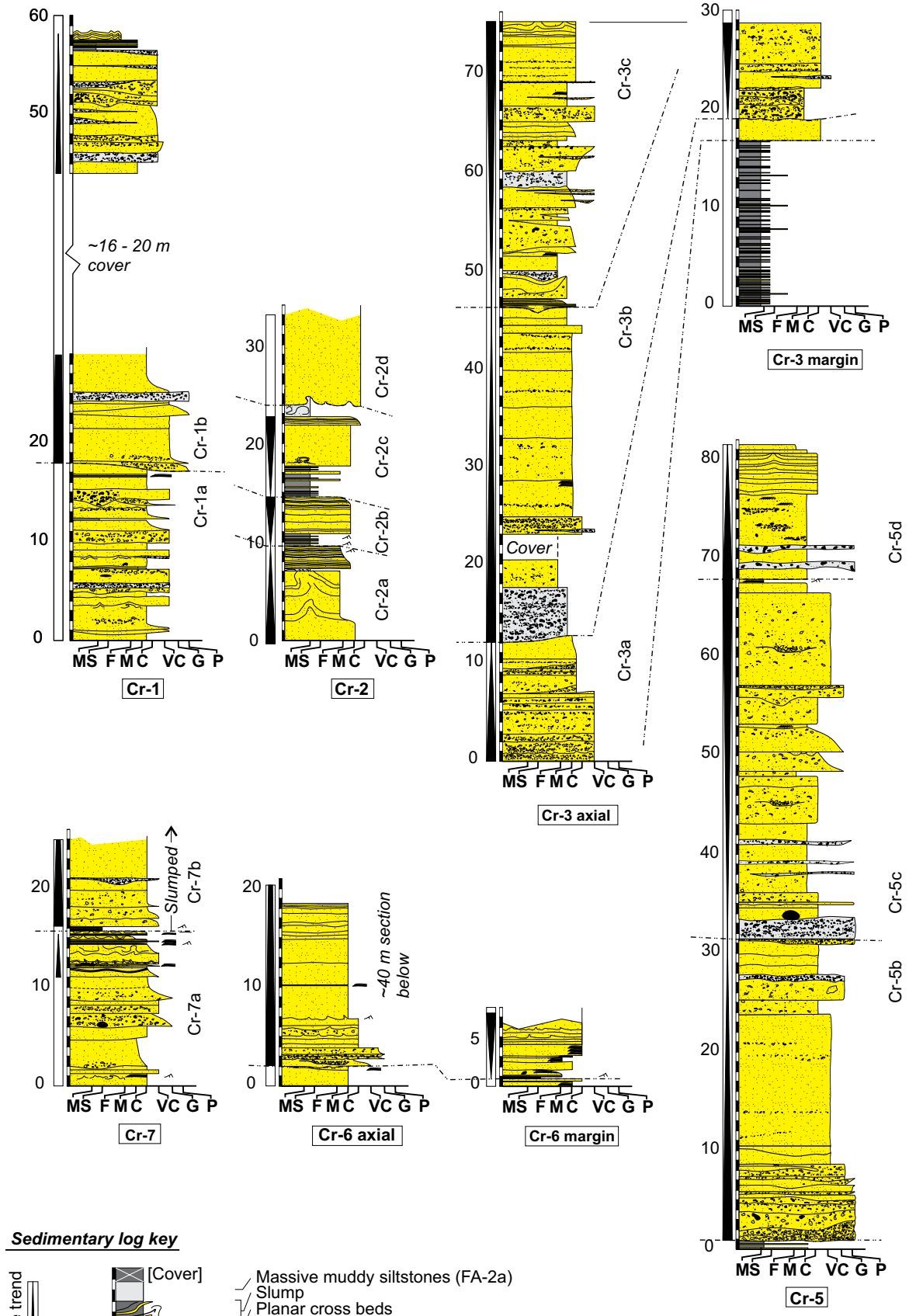

Sedimentary log key

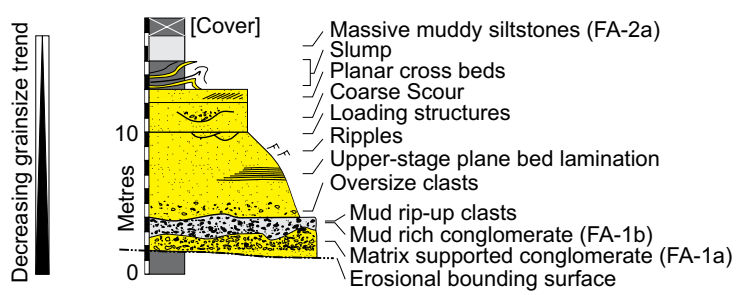

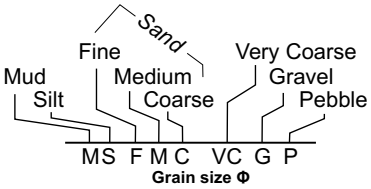

Figure 4.9. (Previous page)
Sedimentary logs from channel complexes Cr-1, Cr-2, Cr-3, Cr-5, Cr-6 and Cr-7. The locations of these logs are shown in figure 4.5a. Corellations between axial and marginal sections are shown for Cr-3 and Cr-6. The sedimentary log key is shown at the bottom.

coarse grained facies are laterally localised upon the element base, commonly but not always at the thickest part of the element, in contrast to massive sandstones (FA-2b) which fill the element width. In element Cr-3b, beds of coarse grained massive sandstones rich in imbricated mud clasts (FA-2b, figure 4.3d) and beds of poorly sorted granular sandstones (FA-2d) stack vertically and occur in two distinct locations towards the margin of the channel element, where the channel complex is thinnest (Figure 4.7b). The groups of stacked beds infill scoured zones of the element base and onlap to the scour margins. These amalgamated facies are laterally equivalent to a 5 m thick conglomeratic cohesive debris flow (FA-1b) which similarly infills an incised 'low' towards the opposite margin (Figures 4.5a, 4.7b and 4.9). Coarse grained facies are therefore also laterally offset from the channel complex and element thalweg.

The upper part of the majority of elements within the Finale channel system are dominated by moderately to well sorted massive sandstones (FA-2b) interbedded with thick normally graded sandstones (FA-3c) (Figures 4.5 and 4.9). Beds of poorly sorted granular sandstones (FA-2d) are also present containing mudclasts up to 0.5 m in diameter (Figure 4.7d), and pinch out over <12 m. Also within some examples of this upper subdivision (i.e elements; Cr-1a, Cr-2c, Cr-3c, Cr-5d, Cr-6 (unknown element number), and Cr-7a) are channel element wide beds of stacked laminated sandstones (FA-3b) which are often preserved across the entire complex (Figures 4.7e and 4.9). The transition to this upper subdivision is often sharp with planar based massive sandstones succeeding coarse grained deposits. Lateral to the localised coarse grained facies (e.g Fa-1), massive sandstones (Fa-2b) directly overlie the basal surface of the channel element and are thus amalgamated with massive sandstones of the preceding element (e.g Cr-5c and 5d). Where an element overlies horizontal terraces in the channel complex margin (e.g the southern margin of Complec Cr-3. See figure 4.5), massive sandstones directly overlie muddy interchannel facies.

In elements Cr-2c, 3b (margin), 5b and 8 (margin), fine grained turbidite deposits interbedded with mudstones (Fa-3a) coarsen and thicken upwards until succeeded by stacked beds of thick massive sandstones (FA-2b) (Figure 4.9). This is contrary to the general trend outlined above. These turbidite deposits are commonly massive (FA-3a, T_a) or consist of stacked laminated sandstones (FA-3b) and are often heavily dewatered (Figure 4.7c). Ichnogenera including *arenicolites* and *cruziana* are common on bed tops. This succession is observed close to the margins of channel element Cr-6 and also close to the top of channel element Cr-2b.

4.4.2.3 Channel element internal architectures (4th order)

In elements Cr-3c and Cr-5c, inclined sets of stacked beds are observed. Bedsets are 8 m and 4 m thick respectively and reach 40 m in width such that they do not represent the full thickness or width of the channel element (Figure 4.10). Beds are inclined between 25° and 45° at a high azimuth to the complex flow orientation (90°–100° difference for Cr-3c; 130° difference for Cr-5c) such that they dip obliquely upslope (Figure 4.1b). In element Cr-5c, beds downlap onto ungraded massive sandstones which represent the top of the previous channel element Cr-5b (Figure 4.10). Maximum bed dip is observed approximately within the middle of each inclined bed, with dips decreasing towards the base (Figure 4.10). The lower surface is approximately planar with small amounts of localised incision (<0.3 m). Stacked beds of massive sandstones (FA-2b) truncate the top of the inclined bed set producing a surface which has a hummocky geometry and amplitudes

of <0.5 m. Facies of inclined beds consist mainly of massive ungraded sandstones (FA-2b), with interbedded muddy cohesive debrite deposits (FA-2a). Beds also vary from 0.5 to 6 m thickness, perpendicular to the dipping bed surface. Bed contacts are generally smooth with local loading.

4.4.2.4 Channel complex architectures (3rd order)

The primary mappable unit within the Finale section is the channel complex. Channel complexes range from 60 to 500 m in width and 23 to 90 m thick (Tables 4.1 and 4.2). The width:depth ratio, difficult to calculate for most complexes due to insufficient exposure, ranges from approximately 3:1 to 7:1. The margins of complexes Cr-3, Cr-4, Cr-5, Cr-9, Cr-10 and Cr-11 (Figure 4.5) are observed to directly incise mudstone dominated slope deposits, with stacked amalgamated sandstone beds truncating fine to coarse grained turbidite deposits and interbedded mudstones (FA-3a) of the interchannel area. With the exception of Cr-11 which is V-shaped (Figure 4.5b), complex bases are relatively flat to U-shaped and have steep (≤vertical) sidewalls. Flat terraced sections of complex margins are however observed in several examples (e.g Cr-3, Cr-5, Cr-11; Figure 4.5). In a majority of channel complexes the entirety of the margin cannot be observed. Channel complexes Cr-3, Cr-11 and Cr-15 however show significant asymmetry with one steep margin and a terraced or shallowly dipping alternate margin (Figure 4.5). The thalweg of complex Cr-3 is not exposed although it is laterally offset ~300 m from the southern margin, and ~120 m from the northern margin (Figure 4.1b, 4.5, table 4.2) which has a steep dip of 70-80°. The thalweg is estimated as having a thickness >90 m. The southern margin has a similar dip but here the complex is measured at 12 m thick due to an extensive horizontal terrace giving a significant complex asymmetry. Complex Cr-11 has a similar geometry with the western margin containing a horizontal terrace. Complex Cr-15 however shows a gradual westward thickening from >15 m to a maximum of 75 m (Figure 4.5b).

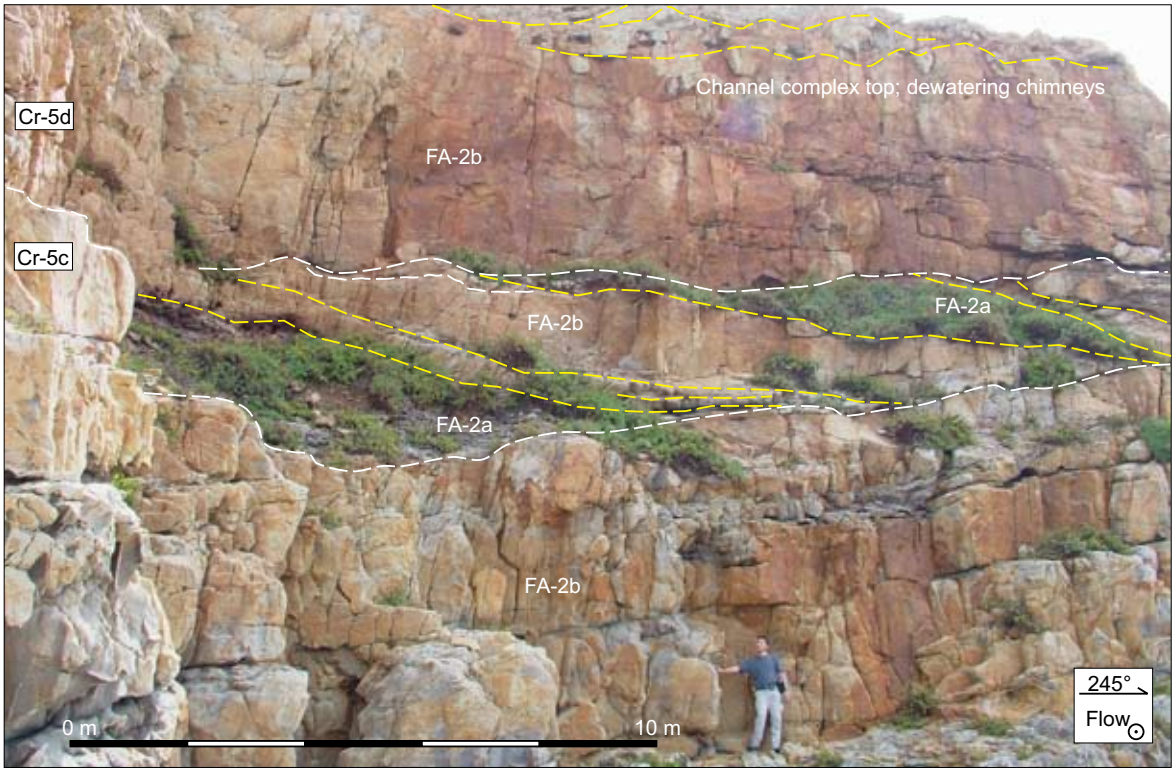

Figure 4.10.
View of the transition from channel element Cr-5c to 5d and an stacked inclined bedset (see section 4.4.2.3 for description). Inclined amalgamation surfaces are highlighted in yellow, white lines mark the lower and upper boundaries of the package. Dewatering chimneys also occur at the complex top. Note that flow is out of the plane of page.

The height of horizontal terraces above the complex thalweg often coincides with that of channel element bounding surfaces (4th order surfaces; Table 1). In the case of channel complex Cr-5, a horizontal terrace in the southern margin is coincidental with the planar base of channel element Cr-5b (Figure 4.5a). The thalweg of element Cr-5b however locally incises completely through the preceding element such that it rests upon a lower terrace in the complex margin. Similar juxtapositions are observed in the geometries of channel complexes Cr-11, 14 and 15 (Figure 4.5b).

Channel elements are generally observed to stack vertically within the confines of the complex bounding surface (Figure 4.5). In Cr-11 and Cr-15 however, elements are stacked with a degree of lateral offset (Figure 4.5b). In Cr-15, element Cr-15c (Figure 4.5b) forms the eastern boundary of the complex. It is truncated to the west by the subsequent element Cr-15d such that it is only preserved adjacent to the eastern margin of the complex. This architecture is similarly observed in complexes Cr-5 and Cr-11 (Figure 4.5) although in both instances, incomplete exposure does not allow for full characterisation.

Channel complexes contain between 2 (the minimum number to constrain the channel complex hierarchy level) and 4 channel elements although there is no systematic trend in the number of elements per complex throughout the system (Figure 4.11a and table 4.2). There is however a significant difference in the size of channel elements within any single complex (Table 4.2), although no common trend is observed for all complexes (e.g elements do not consistently thin upwards within a complex). Figure 4.11b plots the thickness of each channel element (those with confidence in measurement) against the thickness of the channel complexes they are nested within. A broad trend of thicker channel complexes containing thicker channel elements is observed (Figures 4.12c, 4.12d, table 4.2) and the 5 thickest channel complexes (Cr-5, 15, 3, 1, and 13) contain the 8 thickest channel elements.

The top of a majority of channel complexes consists of an element top containing fine to coarse massive sandstone (FA-2b) in stacked beds <1 m thick but typically <0.3 m thick (Figures 4.7d and 4.10). Beds thin upwards but grain size is mostly maintained and beds remain amalgamated (e.g not interbedded with fine grained facies). Beds are folded due to dewatering with amplitudes varying from 0.5 to 1.5 m, and wavelengths of <15 m. The uppermost beds are commonly truncated against a discrete surface at the channel complex top (Figures 4.7d and 4.10). Thin bedded fine grained facies (FA-3a, $T_{a,b,c,e}$) interbedded with mudstones overlay this surface.

4.4.2.5 Channel complex set architecture (2nd order)

Through mapping and characterisation of channel complexes, 2 channel complex sets (ccs) are defined (see section 4.4.2), named the Capo Raisigerbi ccs and the Pollina ccs (Figures 4.1b and 4.1c). As described in section 4.4.2, the 2 channel complex sets have different characteristics which define them. The Capo Raisigerbi ccs shows a consistent lateral offset stacking towards the southeast while the Pollina ccs shows a disorganised stacking pattern. Palaeocurrents similarly show an orientation trend in the Capo Raisigerbi ccs and not in the Pollina ccs.

The vertical thickness of channel complexes within the Capo Raisigerbi ccs varies from >20 m to 81 m with an mean thickness of 45 m (Table 4.2). There is no discernable trend of thickness variation within the channel complex set. The Pollina ccs contains complexes varying from >13 to 75 m thick and a mean value of 40 m (Table 4.2). There is however an increase in the thickness of complexes with younging. Complexes Cr-9 to Cr-11 are below average thickness (the mean value

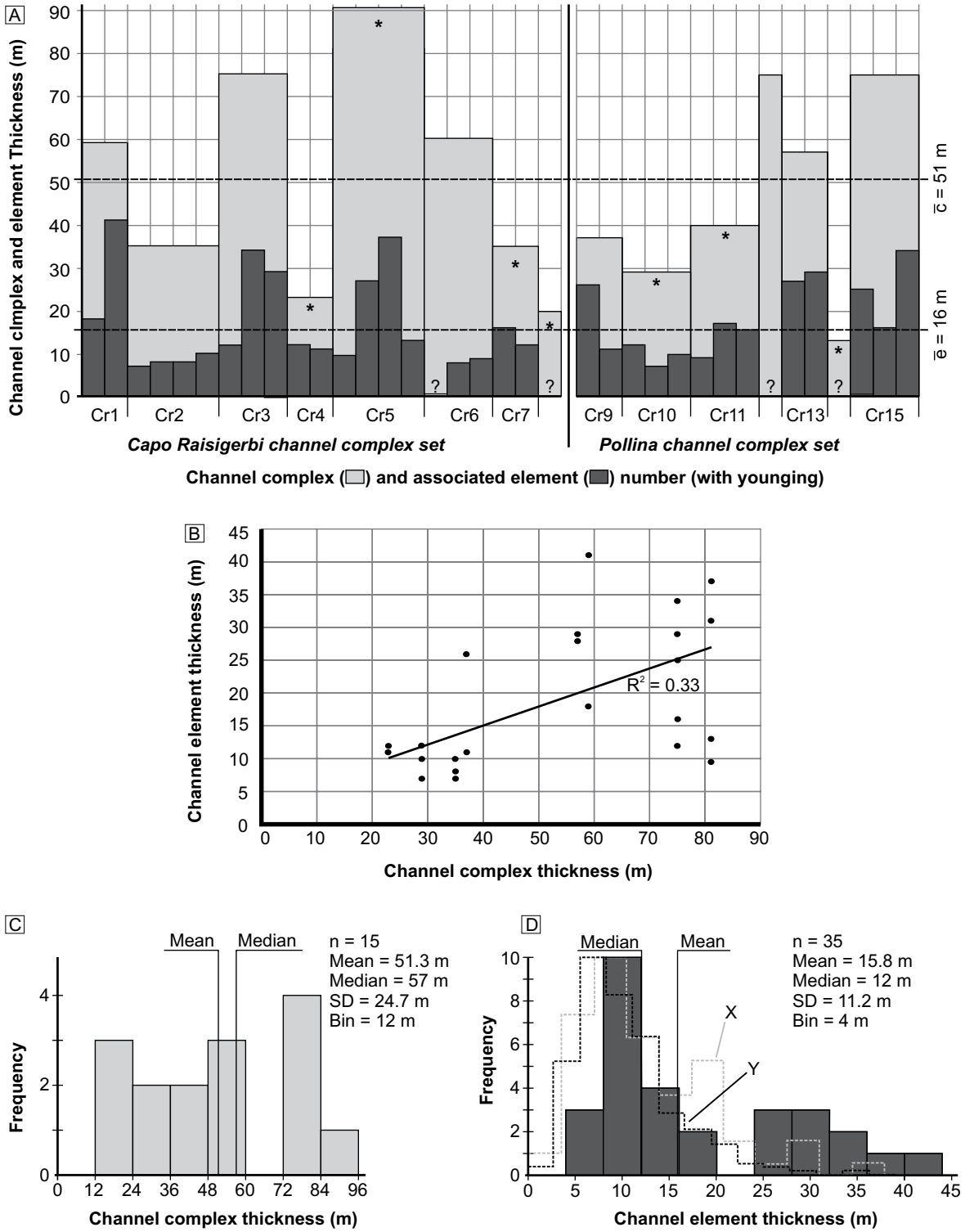

Figure 4.11.

Graphs of the dimensions of various channel hierarchies within the Finale channel system. 4.11a; Thickness data from channel complexes (light grey bars) and channel elements (dark grey bars) shown with younging. Asterisks denote thicknesses which are considered as underestimations due to poor outcrop quality. The width of the light grey channel complex bar denotes the number of channel elements within it. See also table 2 for data. 4.11b; A plot of the thickness of all channel elements (where confidence exists in the measurements) and their associated channel complex thickness. In general, thicker channel complexes contain thicker channel elements, and the 5 thickest complexes contain the 8 thickest elements between them. 4.11c; Frequency distribution of channel complex thicknesses (n=15). 4.11d; Frequency distribution of channel element thicknesses (n=35). Data from this study is shown in solid grey bars. This is compared to data from (McHargue et al., 2010), subdivided into examples from well data (labelled Y. n=762) and outcrop (labelled X. n=72). This latter data has been normalised to a frequency maximum of 10 to better compare with data from this study.

for all complexes in the system = 51 m) and complexes Cr-12 to Cr-15 are above the average thickness (Figure 4.11a). An increase in the thickness of channel elements is also observed to mirror this trend (Figure 4.11a).

4.4.3 Biostratigaphic dating of the Finale section

In order to constrain the duration of the Finale channel system and the hierarchies within it, biostratigraphic dating was attempted using mudstone samples taken immediately adjacent to channel complex bodies (see appendix 3 for biostratigraphy report). Calcareous microfaunas were poorly preserved due to decalcification, however rare Miocene species were recovered. Radiolaria were more common although recovered samples were biased towards larger species. *Globorotalia sp. cf. siakensis* suggests an age no younger than the Mid-Miocene, while the presence of *Didymocyrtis cf. prismatica* (sampled adjacent to channel Cr-4) confirms the section to be older than end Burdigalian. Agglutinated benthonic foraminiferal assemblages also suggest deep water, low oxygen conditions during deposition.

4.5 Discussion

4.5.1 Seismic-scale depositional architectures

Mapping of channel forms within the Finale channel system shows 16 channel complexes which are organised into 2 channel complex sets. Similar hierarchies are reported from systems offshore West Africa (e.g Mayall et al., 2010) and the Kikgecit Formation of Turkey (Cronin et al., 2005a).

As described by Johannson et al. (1998) and Stow et al. (1999), the planforms of channel complexes are observed to be sinuous across a mudstone dominated slope with a local northeast dip. Furthermore, asymmetries are observed within channel complex cross sections (Cr-3, Cr-11 and Cr-15 in particular) with steep and deeply incised margins opposed by steep yet shallow margins. Such asymmetry within mappable channel forms is often interpreted to result from channel sinuosity (Jobe et al., 2010) whereby erosion is enhanced at the outer channel bend due to differential boundary shear stress from transiting flows (Jobe et al., 2010). Given the recognition of sinuous planforms and the variation in channel complex orientations recorded (Figures 4.1b and 4.4), sinuosity is a sensible interpretation for these geometries. The mapping of channel complex locations suggests that examples along the Pollina ridgeline are not correlatable through sinuosity as suggested by Stow et al. (1999) but represent successive younger channel complexes.

The Pollina ccs demonstrates a chaotic stacking pattern. Stacking is dominantly vertical, producing a channel complex belt 1.3 km less wide than the Capo Raisigerbi ccs. Within the Capo Raisigerbi ccs, an organised offset stacking is observed in which channel complexes migrate with a consistent southeast direction. This is coupled with a systematic change (and reversal) in palaeoflow orientations with younging (Figure 4.4). A combination of lateral migration (swing) with downslope migration (sweep) of sinuous channel complexes relative to the Finale section may produce such a combination. Each successive preserved outcrop of sinuous channel complex (e.g Cr-1 to Cr-8) would therefore represent a portion of downslope migrating channel in which channel orientation changes as the meander bend migrates past the section location. As recognised with the process based model of Peakall et al. (2000), levee confined sinuous channels tend to only undergo swing and not sweep. Incisionally confined channels in West Africa are however observed to undergo both downslope and lateral migration (Labourdette and Bez, 2010) with lateral confinement govern-

ing the proportion of each.

4.5.1.1 Entrenchment of channel complexes

Channel complexes are bound by a surface which clearly demonstrates truncation of beds immediately adjacent to the complex margin. In particular, channel complex Cr-3 reaches a thickness of ~90 m and is observed to truncate thin siltstones and sandstones interbedded with mudstones at the very top of the channel complex margin.

The width to depth ratio of channel complexes is estimated as 7:1 to ~3:1 which is high in comparison to reviewed examples of Clark and Pickering (1996) which include the Solitary channel from Tabernas (5:1) and the Ainsa 1 channel (28:1). Between channel complexes, featureless mudstones comprise <50% of stratigraphy (Figure 4.8a). Interbedded facies such as coarse grained massive sandstones (FA-3a, T_a) and isolated and incised channel elements up to 5 m thick are atypical of constructional levee environments. (Figure 4.8e) Channel complexes are therefore interpreted as entrenched within the slope and are classified as erosionally slope confined in the sense of Sprague et al. (2002). The Sicilide slope upon which the Finale channel system evolved can therefore be considered above grade, a style of channel typical of upper slope (Kneller, 2003; Cronin et al., 2005) and tectonically uplifting locations (e.g Mayall et al., 2005; Gee et al., 2006).

4.5.1.2 Scale and duration of the system

Biostratigraphic dating results obtained for this study give an early Miocene age, but do not allow for a higher resolution biozone differentiation. An early Miocene age range (e.g Aquitanian to end Burdigalian) represents a maximum 7 Myr duration (ICS International stratigraphic chart 2009). It has not been possible to establish a minimum age however. For the 650 m of stratigraphy at the Finale section an absolute minimum gross sedimentation rate of 93 m/Myr is established, which is considered extremely low in comparison to a compiled average for continental slope margin clinoforms of 500 m/Myr (Carvajal et al., 2009). It is therefore likely that this is a significant overestimation of duration. Using this compiled average, the Finale section could be expected to represent a ~1.3 Myr time interval.

The >4.6 km width and >650 m thickness of the Finale channel system suggests that it is similar in scale to outcrop examples from the Oligocene Gres du Champsaur Fm, France (Brunt and McCaffrey, 2007) and the proximal portion of the Cingoz formation, Turkey (Satur et al., 2007). In comparison to seismically imaged examples, the Pleistocene Benin-major Canyon (Deptuck et al., 2007), Niger Delta (Catterall et al., 2010), and examples from offshore west Africa (e.g Mayall et al., 2010) are similar in size. Such systems are typically interpreted as 3rd order low stand sequences (e.g 1-3 Myr), bound below and above by condensed sequences (including maximum flooding surfaces) (Mayall et al., 2010). Despite poor biostratigraphic control and an unknown system duration, the Finale Channel system provides a suitable scale outcrop analogue for seismic scale erosionally confined channel systems.

4.5.2 Channel element processes

A fairly consistent succession of facies is observed within channel elements. This comprises coarse grained massive sandstones and conglomerates (FA-1, 2c, 2d) deposited from high density debris flows and stratified turbidity currents, succeeded by stacked ungraded massive sandstones aggraded from quasi-steady turbidity currents (section 4.1).

Stacked beds of facies Fa-1a, 1b, 2c and 2d at the element base commonly drape the incisional surface and are laterally restricted either within the confines of an incisional thalweg where they are highly amalgamated, or in isolated beds apparently downlapping on to more planar sections of the element base. They represent coarse grained deposits from predominantly bypassing flows during the late waxing stage or early waning stage of the element and are similar to the S2 and S3 facies of Lowe (1982).

Massive ungraded sandstones (FA-2c), aggraded from quasi-steady turbidity currents (section 4.1), are the predominant facies within the upper non-thalweg confined part of channel elements. Beds span the entire channel element width with a tabular geometry, such that flow volumes were sufficient to fill a cross sectional areas of <500 m wide and 10's of metres thick. With a maximum channelised depth of 90 m (Cr-3a), flows traversing the entrenched channel complexes of the Finale system experienced a high degree of lateral confinement. Flows were therefore less able to overbank or laterally expand which may have promoted quasi-steady flow conditions. Stacked laminated sandstones (FA-3b), interbedded with massive ungraded sandstones, are interpreted to represent flow non-uniformity within a turbulent flow (e.g Kneller and McCaffrey, 2003). Producing deposits <2 m thick, such flows may be quasi steady over the life-time of the flow, with internal normally graded banding resulting from minor velocity surges produced at high frequency. In this respect, flows may be similar in duration and process to those which aggrade massive sandstones (FA-2b). The presence of velocity spikes in this context suggests a proximal location for the Finale section, in which flows have not had sufficient distance to evolve into a single waning surge (e.g (Kneller and McCaffrey, 2003). The incisional character of the Finale channel system also implies a steep slope gradient whereby flows would naturally be either quasi-steady, or else waxing if they had insufficient distance to reach a quasi steady condition. As a result, facies of the Bouma type are relatively rare.

Inclined bedsets identified in channel element Cr-5c (section 4.2.3) also evidence lateral migration of successive flows within the confines of the channel complex. They are interpreted as successive migration of an erosional chanel margin, with inclined and downlapping beds preserving the channel margin geometry. Beds downlap to the locally scoured base of the channel element such that they are a feature of the early fill phase of the channel element. The <4 m thickness within a 37 m thick channel element reveals flow being channelised at a scale below that of the channel element. Examples of lateral accretion deposits (LAD's) from both outcrop and seismic studies are associated with the preserved inner bend of a sinuous and laterally migrating channel form (Abreu et al., 2003; Arnott, 2007; Dykstra and Kneller, 2009). The consistent oblique up-channel dip of inclined bed sets from Cr-3 and Cr-5 reveals a local oblique-upslope migration, and is interpreted as recording the lateral migration (a combination of swing and sweep) of a sinous erosional channel form.

4.5.2.1 Heterogeneity and asymmetry

Asymmetry is commonly observed in channel elements. Incised thalwegs are observed laterally offset to both the channel complex thalweg and geographical centre. In channel complexes Cr-3, Cr-5, Cr-11, and Cr-15, the thalwegs of successive channel elements occur immediately adjacent to opposite sides of the channel complex margin. Their fill of coarse grained facies is therefore also laterally offset towards the channel complex margin (e.g Figures 4.5 and 4.6).

Rapid downslope changes in the gradient of the channel element floor are also observed (e.g Cr-3, figure 4.6a). Given their local, V to U shaped geometry, and fill of coarse grained facies in some

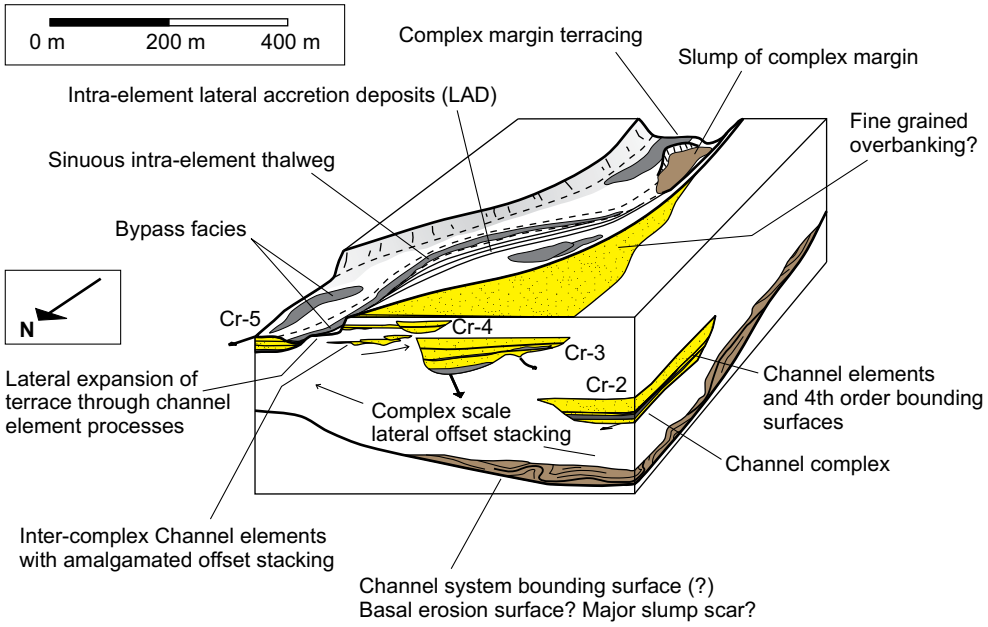

Figure 4.12.
A 3D schematic model of channel complexes Cr-2 to Cr-5 within the Capo Raisigerbi channel complex set (ccs) to demonstrate hierarchical relationships and their architectures. A bounding surface to the channel complex set is shown as is commonly interpreted from seismic examples of incised slope channel systems. The relationship between channel elements and complexes in terms of sinuosity and stacking is highlighted for complex Cr-5.

instances, they bear a strong similarity to channel element thalwegs observed in channel cross section. Such geometries preclude downslope orientated erosional processes and suggest that asymmetry in the location of a channel element thalweg results from sinuosity within the confines of the channel complex margin. Lateral accretion deposits in channel complexes Cr-3 and Cr-5 also represent migration of sinuous channel forms within the channel element. Commonly however, models of confined channel systems present vertically stacked channel elements (or channel storeys of Sprague et al. (2002)) with little lateral offset of facies or erosional thalweg (McHargue et al.; Sprague et al., 2005). Coarse grained deposits of facies FA-2b and 2c which drape the channel element base away from the thalweg thus record deposition from bypassing flows upon the terraced margin of the channel element rather than confined within the thalweg (Figure 4.12). In channel element Cr-3b, there are several locations of stacked coarse grained deposits filling incised depressions on the basal surface (e.g figure 4.7b). While unusual within the Finale section, this architecture suggests a braided style of channel floor morphology during the early fill phase and prior to deposition of massive sandstones.

Tabular massive sandstone beds within the upper part of channel elements do not display asymmetry however and suggest that sinuous channel geometries occur only during the excavation and early fill phases. Massive sandstones (FA-2b) which contain abundant mud clasts imbricated towards the channel margin (section 4.1) may therefore record flows which run directly towards the outer bank of a channel complex margin bend (e.g Dykstra and Kneller, 2009; Straub et al., 2008).

4.5.2.2 Impact upon Channel complex architecture

Channel element stacking patterns are almost entirely vertically dominated due to lateral confinement preventing migration of successive elements (Labourdette and Bez, 2010). Where significant asymmetry exists however (Section 4.5.2.1), the channel element thalweg occurs adjacent to the channel complex margin (i.e Cr-3a, Cr-5b, cr-11c, and Cr-15c. Figure 4.5; Section 4.5.2.1). In

this situation the process of channel element thalweg sinuosity during the incisional and early fill phases thus modifies the channel complex architecture. Where lateral (rather than vertical) stacking of successive elements occurs (Cr-5b, Cr-11c, and Cr-15c. Figure 4.5), the process of incising the element base similarly produces terracing within the channel complex margin (Figure 4.12).

Facies which contain large amounts (< 70% by volume) of mud clasts (e.g FA-1b, 2b and 2d) may result from such periods of expansion. In particular, mud clasts in coarse grained examples of massive ungraded sandstones (FA-2b) include a mud clast 1.5 m in diameter and imbricated angular mud clasts (Figure 4.3d) up to 0.3 m in length. Mud clasts in beds of mud and mud clast supported conglomerates (FA-1b) reach 1.2 m in length, while this facies is interpreted to represent flows similar to FA-1a (Poorly sorted pebble conglomerate) but modified through the entrainment of mud from the substrate. These facies occur interbedded within massive sandstones of the upper channel element fill, and also draping the channel element base. The incorporation of mud clasts through erosion and lateral expansion of the channel complex margin is a likely candidate for the origin of these mud clasts.

Channel complex margins are therefore a diachronous surface resulting from a combination of initial excavation of the channel complex, and incision during successive channel element formation. While channel complexes are the main mappable depositional element within the Finale section, processes which occur over the duration of channel elements are important in modifying their architecture.

4.5.3 Variations in the degree of slope incision

The characterisation of channel systems using a hierarchical methodology allows for a methodical comparison, both between depositional elements within the same system, and with depositional elements from different systems.

The thickness of Channel complexes and the elements within them have been measured through sedimentary logging and use of scaled photographs. Data on the thickness of similar architectural elements from other systems has been compiled by McHargue et al. (2010). Such measurements are complicated by factors including lack of outcrop 3-dimensionality, the location of well penetration within a channel complex body, and amalgamation of sandstone depositional elements such that channel element boundaries are unclear (McHargue et al., 2010). Within the Finale section, the main limiting factor for measurement has been the degree of exposure. To this end, the thickness data presented here (Table 4.2) is an underestimation where outcrop quality is insufficient to measure the full thickness.

Each of the hierarchies observed represent vertical cycles of incision and aggradation (waxing and waning) over increasing time frames and magnitudes (McHargue et al., 2010). As measured from the Finale channel system, the vertical impact of each hierarchy (and therefore each waxing-waning cycle) is expressed in terms of stratigraphic thicknesses; averaging ~16 m (channel element. See figure 4.11d), ~50 m (channel complex. See figure 4.11c), ~300 m (channel complex set) and >650m (channel system) respectively.

4.5.3.1 Channel elements compared to channel complexes

Channel complex thicknesses vary from 30 to 90 m (Figure 4.11c, tables 4.1 and 4.2). Considering that they are slope confined, the degree of slope incision is therefore highly variable. When viewed

in the context of the entire channel system, thicker channel complexes (e.g Cr-1, Cr-3, Cr-5, Cr-15) generally contain thicker channel elements (Figure 4.11b, section 4.4.2.4). Therefore where the magnitude of incision in the channel complex scale cycle is greater, the magnitude of the channel element scale cycle is similarly increased relative to the average.

Such a link may be explained by a waxing-waning cycle which occurs with a duration greater than that of a channel complex but less than that of the channel complex set. During waxing and increasing slope incision, the thickness of both the channel complex and the channel element are increased, and vice versa.

4.5.3.2 Temporal variations

For systems where erosion is the primary control upon element thickness, the depth of slope incision is strongly influenced by slope gradient (McHargue et al., 2010;Ferry et al., 2005; Pittet et al., 2000; Prather, 2000). When channel complex thicknesses are presented with younging (Figure 4.11a), complexes of the younger Pollina ccs are observed to increase in thickness with time. The thickness of channel elements also matches this trend.

The trend is observed to occur over ~6 complexes (Figure 4.11a) and may be estimated as a duration in the order of 360 Kyr to 1.2 Myr (e.g 16 complexes of equal duration within a 1-3 Myr 3rd order sequence). This combination of long duration and an impact upon several channel complexes suggests an increase in the magnitude of slope incision with time due to allocyclic forcing.

Several 3rd order eustatic sea level falls are recorded during the early Miocene (e.g Kominz et al., 1998; Van Sickel et al., 2004) which would serve to increase the source drainage area and lower storm wave base even if the shelf break was not exposed. Alternatively, a gradual steepening of the slope gradient may serve to increase slope incision. Ongoing encroachment of the accretionary prism at the far northern margin of the basin (Thomas et al., 2010) would serve to generate basin floor subsidence and may account for increasing slope gradients. The Finale channel system represents a progradational slope sequence however. Given local aggradation of 650 m of sediment, a slope gradient of 3° (for example) would mean a local slope progradation of ~10 km. Complexes at the section top are therefore relatively proximal to those lower in the section. If an appropriately concave slope profile existed, this would also serve to increase the local slope gradient with younging (pers. comm. Ben Kneller. 2011).

4.5.3.3 Channel element thickness frequency distribution and possible controls

Relatively few published studies quantativley compare channel systems given the complications which result from depositional hierarchies. Using a similar hierarchical classification as used for this study however, McHargue et al. (2010), reviewing a global catalogue of channel examples, calculated mean and median values of 13 m and 12 m for the thickness of channel complexes (their channel elements) from outcrop (n=72) and values of 10.7 m and 9.4 m for well examples (n=762). This is approximately the same range as that measured from channel elements for this study (Mean ~16 m and median of 12 m) and is presented for comparison in figure 4.11d.

These values represent minimum depths of incision considering measurement error, and that channel elements will have their thickness reduced through erosion from the subsequent channel element. Nevertheless, a frequency histogram of channel element thickness shows a strongly posi-

tively skewed distribution centred upon a mode of 12 m. This is remarkably similar to data (n=834) presented by McHargue et al. (2010) (Figure 4.11d). While the depth of incision is strongly influenced by slope gradient, this changes with downslope distance. Furthermore, the calibre of sediment, volume of flows and the nature of the substrate are important factors. It appears coincidental therefore that similar frequency distributions occur across many different systems. Increased preservation potential for less thick elements offers a further possibility, however we raise the question as to whether a fundamental process exerts a control upon the distribution of channel thicknesses.

Further work is required to test this distribution, however it can be speculated that were a limiting mechanism exist, it must create specific circumstances, namely: Channel element thicknesses must be 'forced' by creating a propensity to lower values in the range of 10-20 m; Thicker elements occur with decreasing frequency; All systems must be affected; The erosional effects of natural variability in initial flow volumes, slope gradients and grainsize distributions must be reduced.

Both climate variability and eustatic sea level fluctuations may fill these criterions, with a high frequency fluctuation forcing a waxing-waning cycle whose duration controls the magnitude of channel element incision. Milankovitch cyclicity as a driver of climate and eustatic sea level fluctuations (e.g Zachos et al., 1997) provides a possible candidate. Conversely, controls upon flow processes may provide a possible autogenic control. In particular, limits upon flow densities and consequent basal shear stress may serve to limit the amount of substrate incision.

4.6. Conclusions

A seismic scale slope confined channel system from the Numidian Flysch Formation of Sicily is described. The system demonstrates 3 internal orders of hierarchy comprising channel complexes (n=16) which contain nested channel elements (n=35) and are in turn organised in to 2 channel complex sets (Figure 4.12). The system provides a similar scale outcrop analogue to slope confined channel systems such as described from offshore West Africa.

Channel complexes up to 500 m in width and 90 m thick are entrenched within slope deposits. Within the Capo Raisigerbi channel complex set, complexes laterally offset stack and demonstrate a change in palaeoflow which may result from the downslope migration of low sinuosity meander bends. The younger Pollina channel complex set displays a disorganised stacking pattern. Asymmetry in the cross section geometry of complexes results from this sinuosity. Nested channel elements within the complexes predominantly stack vertically within the parent complex. Architectural asymmetry, in the form of thickness variations, occurs due to sinuosity of the incisional thalweg prior to filling of the element by massive ungraded sandstones, coarse grained massive sandstones, and thick normally graded sandstones. Thalweg confined lag deposits are therefore also commonly laterally offset from the thalweg and geographic centre of the channel complex. Where elements are asymmetric or are laterally stacked within the complex, channel element processes modify the architecture of the complex bounding surface with terracing.

Increasing slope entrenchment occurs with younging due to allocyclic forcing factors which may include basin floor subsidence and steepening of the slope due to encroachment of an accretionary prism at the northern edge of the basin. Thicker channel complexes also generally contain thicker channel elements suggesting a waxing-waning cycle not represented by a specific hierarchy of channel form. The frequency distribution of channel element thickness is strikingly similar to globally reviewed examples (McHargue et al., 2010). This distribution requires verification, but

suggests a fundamental control on their thickness. Such controls include allocyclic factors such as high frequency (4th to 5th order) climatic and/or eustatic fluctuations, and factors including practical limits to the density of flows or flow capacity. Hierarchical characterisations can therefore be usefully applied to outcrop systems to investigate the interaction between waxing-waning cycles of differing durations and magnitudes, and to gain a measure of the external controls placed upon the system, particularly where a detailed basin context is lacking.

References.

Abreu, V., Sullivan, M., Pirmez, C. and Mohrig, D., 2003. Lateral accretion packages (LAPs): an important reservoir element in deep water sinuous channels. Marine and Petroleum Geology, 20(6-8): 631-648.

Arnott, R.W.C., 2007. Stratal architecture and origin of lateral accretion deposits (LADs) and conterminuous inner-bank levee deposits in a base-of-slope sinuous channel, lower Isaac Formation (Neoproterozoic), East-Central British Columbia, Canada. Marine and Petroleum Geology, 24: 515-528.

Belayouni, H. et al., 2010. La Galite Archipelago (Tunisia, North Africa): Stratigraphic and petrographic revision and insights for geodynamic evolution of the Maghrebian Chain. Journal of African Earth Sciences, 56(1): 15-28.

Bouma, A.H., 1962. Sedimentology of some Flysch deposits;: A graphic approach to facies interpretation. 168 pp: Elsevier.

Brunt, R.L. and McCaffrey, W.D., 2007. Heterogeneity of fill within an incised channel: The Oligocene Gres du Champsaur, SE France. Marine and Petroleum Geology, 24: 529-539.

Campion, K.M. et al., 2000. Outcrop expression of confined channel complexes. Deep-water reservoirs of the world: SEPM, Gulf coast section, 20th annual Research Conference, 20th annual Research Conference: 127-50.

Carvajal, C., Steel, R. and Petter, A., 2009. Sediment supply: The main driver of shelf-margin growth. Earth-Science Reviews, 96(4): 221-248.

Catterall, V., Redfern, J., Gawthorpe, R., Hansen, D. and Thomas, M., 2010. Architectural style and quantification of a submarine channel-levee system located in a structurally complex area: Offshore Nile delta. Journal of Sedimentary Research, 80(11-12): 991-1017.

Cronin, B.T. et al., 2005a. Morphology, evolution and fill: Implications for sand and mud distribution in filling deep-water canyons and slope channel complexes. Sedimentary Geology, 179(1-2): 71-97.

Cronin, B.T., Celik, H., Hurst, A. and Turkmen, I., 2005b. Mud prone entrenched deep-water slope channel complexes from the Eocene of eastern Turkey. Geological Society, London, Special Publications, 244(1): 155-180.

Dasgupta, P., 2003. Sediment gravity flow - the conceptual problems. Earth-Science Reviews, 62(3-4): 265-281.

de Capoa, P., Di Staso, A., Guerrera, F., Perrone, V. and Tramontana, M., 2004. The age of the oceanic accretionary wedge and onset of continental collision in the Sicilian Maghrebian Chain. Geodinamica Acta, 17(5): 331-348.

de Capoa, P., Guerrera, F., Perrone, V., Serrano, F. and Tramontana, M., 2000. The onset of the syn-orogenic sedimentation in the Flysch Basin of the Sicilian Maghrebids: state of the art and new biostratigraphic constraints. Eclogae Geologicae Helvetiae, 93(1): 65-79.

Deptuck, M.E., Sylvester, Z., Pirmez, C. and O'Byrne, C., 2007. Migration-aggradation history and 3-D seismic geomorphology of submarine channels in the Pleistocene Benin-major Canyon, western Niger Delta slope. Marine and Petroleum Geology, 24: 406-433.

Dykstra, M. and Kneller, B., 2009. Lateral accretion in a deep-marine channel complex: implications for channellized flow processes in turbidity currents. Sedimentology, 56(5): 1411-1432.

Eschard, R., Albouy, E., Deschamps, R., Euzen, T. and Ayub, A., 2003. Downstream evolution of turbiditic channel complexes in the Pab Range outcrops (Maastrichtian, Pakistan). Marine and Petroleum Geology, 20(6-8): 691-710.

Ferry, J.-N., Mulder, T., Parize, O. and Raillard, S., 2005. Concept of equilibrium profile in deep-water turbidite system: effects of local physiographic changes on the nature of sedimentary

process and the geometries of deposits. Geological Society, London, Special Publications, 244(1): 181-193.

Guerrera, F., Martin-Martin, M., Perrone, V. and Tramontana, M., 2005. Tectono-sedimentary evolution of the southern branch of the Western Tethys (Maghrebian Flysch Basin and Lucanian Ocean): consequences for Western Mediterranean geodynamics. Terra Nova, 17(4): 358-367.

Hiscott, R.N., 1994. Loss of capacity, not competence, as the fundamental process governing deposition from turbidity currents. Journal of Sedimentary Research, 64(2a): 209-214.

Johansson, M., Braakenburg, N.E., Stow, D.A.V. and Faugeres, J.C., 1998. Deep-water massive sands: facies, processes and channel geometry in the Numidian Flysch, Sicily. Sedimentary Geology, 115(1-4): 233-265.

Kneller, B., 2003. The influence of flow parameters on turbidite slope channel architecture. Marine and Petroleum Geology, 20(6-8): 901-910.

Kneller, B.C. and Branney, M.J., 1995. Sustained High-Density Turbidity Currents and the Deposition of Thick Massive Sands. Sedimentology, 42(4): 607-616.

Kneller, B.C. and McCaffrey, W.D., 2003. The interpretation of vertical sequences in turbidite beds: The influence of longitudinal flow structure. Journal of Sedimentary Research, 73(5): 706-713.

Kominz, M.A., Miller, K.G. and Browning, J.V., 1998. Long-term and short-term global Cenozoic sea-level estimates. Geology, 26(4): 311-314.

Labourdette, R. and Bez, M., 2010. Element migration in turbidite systems: Random or systematic depositional processes? Aapg Bulletin, 94(3): 345-368.

Lowe, D.R., 1982. Sediment gravity flows; II, Depositional models with special reference to the deposits of high-density turbidity currents. Journal of Sedimentary Petrology, 52(1): 279-297.

Mayall, M., Jones, E. and Casey, M., 2006. Turbidite channel reservoirs - Key elements in facies prediction and effective development. Marine and Petroleum Geology, 23(8): 821-841.

Mayall, M. et al., 2010. The response of turbidite slope channels to growth-induced seabed topography. Aapg Bulletin, 94(7): 1011-1030.

McHargue, T. et al., Architecture of turbidite channel systems on the continental slope: Patterns and predictions. Marine and Petroleum Geology, In Press, Corrected Proof.

McHargue, T. et al., 2010. Architecture of turbidite channel systems on the continental slope: Patterns and predictions. Marine and Petroleum Geology, 28(3): 728-743.

Mulder, T. and Alexander, J., 2001. The physical character of subaqueous sedimentary density flows and their deposits. Sedimentology, 48(2): 269-299.

Navarre, J.-C. et al., 2002. Deepwater turbidite system analysis, West Africa: Sedimentary model and implications for reservoir model construction. The Leading edge, 21(11): 1132-1139.

Peakall, J., McCaffrey, B. and Kneller, B., 2000. A process model for the evolution, morphology, and architecture of sinuous submarine channels. Journal of Sedimentary Research, 70(3): 434-448.

Pedley, H.M., Cugno, G. and Grasso, M., 1992. Gravity slide and resedimentation processes in a Miocene carbonate ramp, Hyblean Platcau, southeastern Sicily. Sedimentary Geology, 79(1-4): 189-202.

Pescatore, T., Renda, P. and Tramutoli, M., 1987. Facies ed evoluzione sedimentaria del bacino Numidico nelle Madonie occidentale (Sicilia). Memorie-Societa Geological Italiana, 38: 297-316.

Pittet, B., Strasser, A. and Mattioli, E., 2000. Depositional seuences in deep-shelf envirionments: a response to sea-level changes and shallow-platform productivity (Oxfordian, Germany and Spain). Journal of Sedimentary Research, 70(2): 392-407.

Posamentier, H.W. and Kolla, V., 2003. Seismic geomorphology and stratigraphy of depositional elements in deep-water settings. Journal of Sedimentary Research, 73(3): 367-388.

Prather, B.E., 2000. Calibration and visualization of depositional process models for above-grade slopes: a case study from the Gulf of Mexico. Marine and Petroleum Geology, 17(5): 619-638.

Prélat, A., Hodgson, D.M. and Flint, S.S., 2009. Evolution, architecture and hierarchy of distributary deep-water deposits: a high-resolution outcrop investigation from the Permian Karoo Basin, South Africa. Sedimentology, 56(7): 2132-2154.

Riahi, S. et al., 2010. Stratigraphy, sedimentology and structure of the Numidian Flysch thrust belt in northern Tunisia. Journal of African Earth Sciences, 57(1-2): 109-126.

Satur, N., Hurst, A., Kelling, G., Cronin, B. and Gurbuz, K., 2007. Controlling factors on the character of feeder systems to a deep-water fan, Cingoz Formation, Turkey. Atlas of deep-water outcrops: AAPG Studies in Geology 56, CD-ROM, 28 p. (in T. H. Nilsen, R. D. Shew, G. S. Steffens, and J. R. J. Studlick, eds).

Shanmugam, G., 2000. 50 years of the turbidite paradigm (1950s-1990s): deep-water processes and facies models - a critical perspective. Marine and Petroleum Geology, 17(2): 285-342.

Speranza, F., Maniscalco, R. and Grasso, M., 2003. Pattern of orogenic rotations in central-eastern Sicily: implications for the timing of spreading in the Tyrrhenian Sea. Journal of the Geological Society, 160: 183-195.

Sprague, A.R. et al., 2005. Integrated slope channel depositional models: the key to successful prediction of reservoir presence and quality in offshore West Africa. CIPM, cuarto E-Exitep 2005, February 20-23 2005. Veracruz, Mexico.: 1-13.

Sprague, A.R. et al., 2002. The physical stratigraphy of deep-water strata; a hierarchical approach to the analysis of genetically related stratigraphic elements for improved reservoir prediction. In: Anonymous (Editor), AAPG annual convention with SEPM. American Association of Petroleum Geologists and Society of Economic Paleontologists and Mineralogists (AAPG). Tulsa, OK, United States. 2002.

Stow, D.A.V. and Johansson, M., 2000. Deep-water massive sands: nature, origin and hydrocarbon implications. Marine and Petroleum Geology, 17(2): 145-174.

Stow, D.A.V., Johansson, M., Braakenburg, N. and Faugeres, J.C., 1999. Deep-water massive sands: facies, processes and channel geometry in the Numidian Flysch, Sicily - reply. Sedimentary Geology, 127(1-2): 119-123.

Straub, K.M., Mohrig, D., McElroy, B., Buttles, J. and Pirmez, C., 2008. Interactions between turbidity currents and topography in aggrading sinuous submarine channels: A laboratory study. Geological Society of America Bulletin, 120: 368-385.

Thomas, M.F.H., Bodin, S., Redfern, J. and Irving, D.H.B., 2010. A constrained African craton source for the Cenozoic Numidian Flysch: Implications for the palaeogeography of the western Mediterranean basin. Earth-Science Reviews, 101(1-2): 1-23.

Van Sickel, W.A., Kominz, M.A., Miller, K.G. and Browning, J.V., 2004. Late Cretaceous and Cenozoic sea-level estimates: backstripping analysis of borehole data, onshore New Jersey. Basin Research, 16(4): 451-465.

Vanhouten, F.B., 1980. Mid-Cenozoic Fortuna Formation, Northeastern Tunisia - Record of Late Alpine Activity on North African Cratonic Margin. American Journal of Science, 280(10): 1051-1062.

Wezel, F.C., 1970. Numidian Flysch - an Oligocene - Early Miocene Continental Rise Deposit Off African Platform. Nature, 228(5268): 275-&.

Zachos, J.C., Flower, B.P. and Paul, H., 1997. Orbitally paced climate oscillations across the Oligocene/Miocene boundary. Nature, 388(6642): 567-570.

Chapter 5.

Sedimentology of the Numidian Flysch Formation in northern Tunisia.

Chapter 5. Sedimentology of the Numidian Flysch Formation in northern Tunisia

Abstract

The Oligo-Miocene Numidian Flysch Formation has a truly regional extent which is perhaps unique in ancient outcropping systems. Here, three sections are described from northern Tunisia, focussing upon lithofacies and depositional elements. All sections contain thick slope sequences, incised by entrenched channel complexes which are predominantly filled by massive ungraded sandstones. They are interpreted to represent upper slope environments where flows are quasi-steady and are inhibited from waning through confinement within channel complexes and relatively steep gradients. These lithofacies, depositional elements and depositional environments are remarkably similar to those described from sections in Sicily and Algeria. An above grade upper slope architecture is therefore a common feature across 1000 km of slope system. Controls upon the timing and style of deposition within the Numidian Flysch Formation are consequently interpreted to be regional, and include uplift of the North African Atlas chain at a time of wet climate, and progressive southwards encroachment of the accretionary prism which may serve continually increase slope gradients.

5.1. Introduction

The Numidian Flysch Formation has been the subject of much controversy regarding its provenance, depositional environment, and the origin of massive ungraded sandsones. It is an Oligo-miocene age formation which crops out over 2000 km within nappes of the Alpine aged fold and thrust belts of Spain, Morocco, Algeria, Tunisia, Sicily and mainland Italy (Wezel, 1970) (Figure 5.1). The formation produces gas in central Sicily, and oil seeps are common in northern Tunisia such that there has been much interest in offshore hydrocarbon potential. Deposits are subdivided into three sub-basins, with Tunisia forming the central, and deposits of Sicily and mainland Italy forming the easternmost Sicillide sub-basin (Thomas et al., 2010). Together they represent around 1000 km of slope deposits.

Studies of outcropping ancient submarine turbidite systems generally suffer from the effects of weathering and erosion. Unique examples including the Pab Formation of Pakistan (Eschard et al., 2003) and the Karoo basin fan systems (Hodgson et al., 2006) provide vast outcrop extent covering almost the entire fan system. Their characterisation however requires large multinational studies of many workers and industry support. In contrast, well mapped and understood turbidite basins such as those of the Italian Apennines and the Alps include many formations with differing controls (Mutti et al., 2009). The regional extent of Numidian Flysch Formation exposure is greater than all these examples and as such is fairly unique, providing a natural laboratory to study large scale variations in slope architecture and variability over a truly regional extent. Unfortunately, the controversies surrounding provenance of the clastic material, and in particular complications of reconstructing the slope architecture from dissected nappes, have meant that geologists have been unable to capitalise upon this unique aspect of the Numidian Flysch Formation (Thomas et al., 2010).

Here we describe three sections of the Numidian Flysch Formation from northern Tunisia (Figure 5.1). Three questions are addressed, namely: What depositional elements, lithofacies and dispositional environments are represented? Second, how does this compare with Numidian Flysch

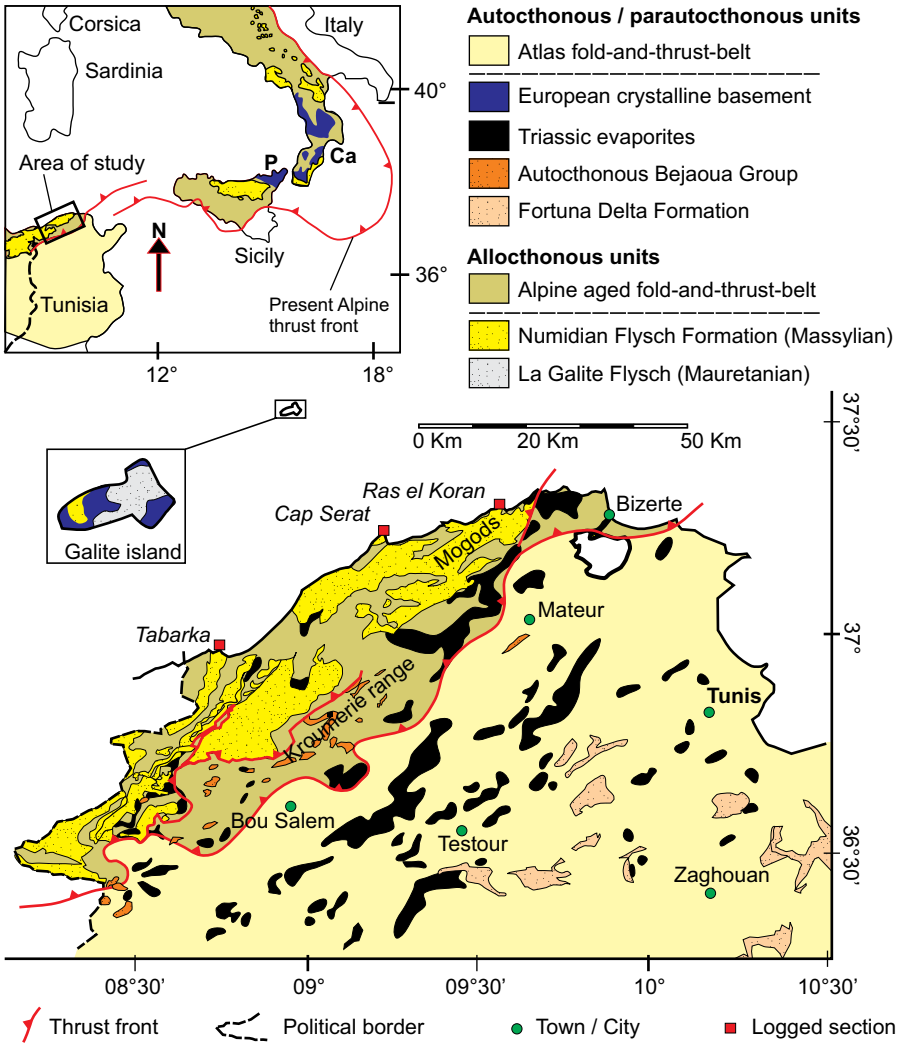

Figure 5.1.
Geological map of Tunisia and the studied areas. The extent of the Alpine aged and Atlas fold-and-thrust-belts are shown. Triassic evaporate extent is taken from Ben Slama et al. (2009). Detail of Galite island is taken from Belayouni et al. (2010). Other details are taken from the Tunisian geological map.

Formation sections from the adjacent Sicillide sub-basin? Lastly, what does this comparison tell us about the Numidian Flysch slope system over a regional scale?

5.2. Regional setting

The Oligo-Miocene Numidian Flysch Formation crops out in Spain, widely throughout North Africa, and in Sicily and southern Italy as part of the Alpine aged fold and thrust belt (Wezel, 1970) (Figure 5.1.). This discontinuous outcrop belt is over 2000 km in length and 10's of Kilometres in width. The Numidian Flysch Formation represents a broadly linear series of submarine fans deposited into the Mahgrebian Flysch Basin (MFB), a precursor basin to the western Mediterranean basin (de Capoa et al., 2004; Guerrera et al., 2005).

5.2.1 The Maghrebian Flysch Basin

The Maghrebian Flysch Basin (MFB) was a foreland basin remnant of the neo-Tethys ocean in the western portion of the present day Mediterranean Basin (Figures 5.1 and 5.2). The basin was bordered to the north by an active margin which consisted of a southward verging accretionary

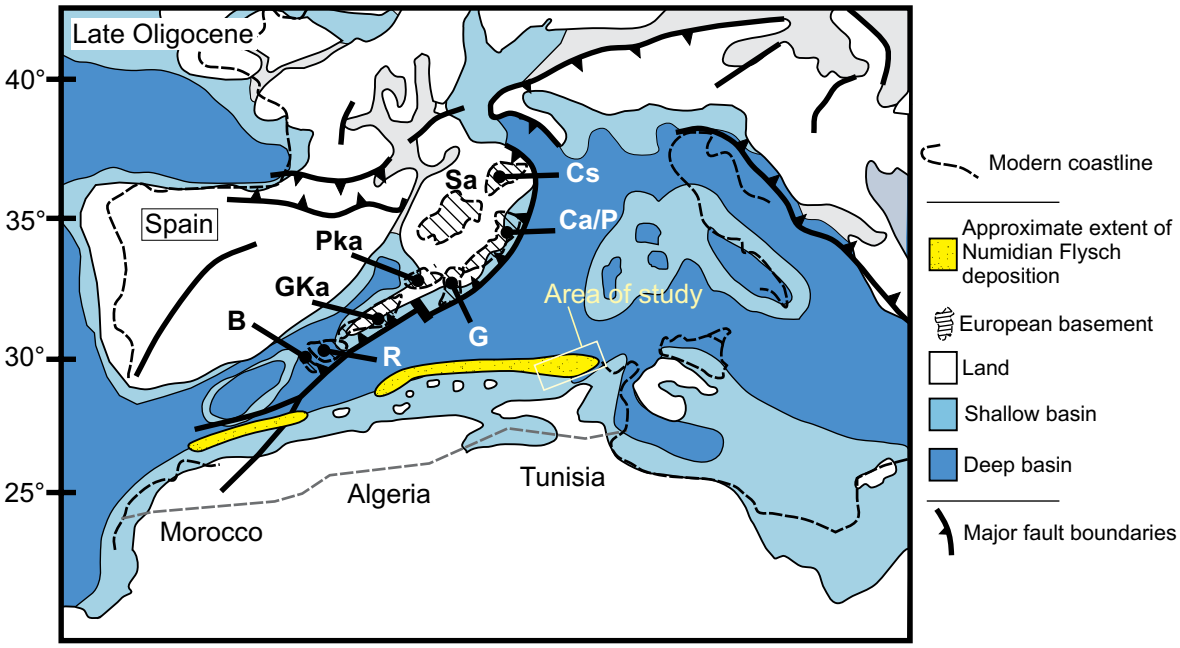

Figure 5.2.
Palaeogeographic reconstruction of the Maghrebian Flysch Basin (MFB) during the late Oligocene. Redrawn from (Thomas et al., 2010). The approximate location of the study area is shown.

prism, underlain by European crustal blocks which rode above northwards subducting oceanic crust (Golonka, 2004; Guerrera et al., 1993) (Figure 5.2.). To the south, the African margin formed a passive-margin to the basin. Based upon similar tectonostratigraphic evolutions, the MFB is divided into three sub-basins, comprising a western (Morocco and Spain), central (Algeria and Tunisia) and eastern basin (the Sicillide basin; Sicily and mainland Italy) (de Capoa et al., 2002; de Capoa et al., 2007; Thomas et al., 2010).

Throughout the MFB, African margin foreland sequences consist of thick Mesozoic to Cenozoic age platform carbonates and shallow marine clastic deposits (Thomas et al., 2010; their figure 4. Chapter 1 this thesis). Units derived from the northern margin consist of European derived crustal blocks (i.e the Kabylie, Galite, Peloritani and Calabrian blocks) transgressed by continental conglomerates, shallow marine limestones and very coarse grained turbidite sequences including canyon confined deposits (Bonardi et al., 1980; Gery, 1983; Mazzoleni, 1991).

Prolific deep marine clastic deposits also crop out, transgressing thick sections of basin mudstones but detached from crustal basement. Two distinct petrofacies are recognised, comprising an immature heterolithic series (Mauretanian deposits) and a quartzarenite Numidian series (Massylian deposits) (Belayouni et al., 2010; Guerrera, 1981; Guerrera et al., 1990; Guerrera et al., 1993) (Figures 5.1 and 5.2). The palaeogeographic relationship between these two series has been much debated but a regional review of all evidence (Thomas et al., 2010) concludes that the Mauretanian petrofacies was derived from European basement, and the Numdian petrofacies was derived from African basement. The Numidian Flysch Formation therefore represents the offshore portion of a regional drainage system on the Oligo-Miocene North African passive margin. The term flysch, applied to the Numidian Flysch Formation by Gottis (1953), remains as a result of the intense debate surrounding either a northern or southern provenance for Numidian Flysch Formation clastic material.

5.2.2 The Tunisian Numidian Flysch Formation

In Tunisia, the Numidian Flysch Formation crops out within the Alpine aged nappe belt in the north (Figure 5.1). The belt trends northeast, parallel to the Mediterranean coastline, decreasing in width from 30 km and trending offshore at Ras el Koran (Riahi et al., 2010; Wezel, 1969) (Figure 5.1). Nappes of Numidian Flysch deposits stack above deformed African foreland sequences which include upper cretaceous limestones, Palaeocene green marls (Dhahri and Boukadi, 2010) and Eocene mudstone – limestone alternations of the Bou Dabbous Formation (Klett, 2001). The latter formation represents a ramp setting with water depth increasing northwards. The foreland section is penetrated by Triassic salt structures, including diapirs and domes, which also crop out within a southwest trending diapir zone to the west of Tunis (Figure 5.1) (Jallouli et al., 2005).

The stratigraphy of the Numidian Flysch Formation consists of three members. The Zousa member is dominantly mudstones with interbedded sandstones, the Kroumeri member is sandstone rich, and the Babouche member is a 15 m thick sillexite series (Riahi et al., 2010). Glacon and Rouvier (1967) interpreted these members as vertically stacked (in that order) resulting in a formation greater than 2000 m thick. In recent studies however, biostratigraphic and palynological dating have demonstrated that these member are at least partly contemporaneous with the implication that they represent proximal to distal equivalents (Boukhalfa et al., 2009; Riahi et al., 2010; Torricelli and Biffi, 2001).

Contemporaneous to Numidian Flysch deposition, the Fortuna formation of eastern Tunisia (Figure 5.1) represents a large Oligocene to mid Miocene deltaic complex which fed sediment eastwards towards the Pelagian shelf (Vanhouten, 1980). Minor outcrops of the Bejaoua Group are also mapped close to, and underlying the Numidian thrust front (Figure 5.1). This group consists of Eocene to mid Miocene mudstone shelf deposits with interbedded glauconite sandstones, evidence of storm reworking, and stacked 30 m thick medium to pebbly sandstones of early Miocene age (Riahi et al., 2010).

On the Galite island deposits of Galite flysch crop out along with contemporaneous Numidian Flysch deposits, dated as early Miocene in age (Belayouni et al., 2010; Yaich, 1992) (Figure 5.1). They are immature micaceous mauretanian (European sourced) turbidites which occur also interbedded with Numidian (African sourced) petrofacies (Belayouni et al., 2010) and denote foredeep mixing of the two petrofacies.

As with all areas of Numidian Flysch research, the question of provenance has primarily focussed work upon the relationship between the Numidian Flysch Formation and underlying units of the African foreland. The role of the Fortuna delta has therefore been both proposed (Wezel, 1970) and disputed (Riahi et al., 2010; Yaich et al., 2000) as a sediment supplier to the Numidian slope system. In this respect, Tunisian deposits of the Numidian Flysch Formation are unique within the MFB, whereby contemporaneous foreland sequences are exposed and well dated (e.g Riahi et al., 2010). This has not been possible within deposits of the Sicillide sub-basin for example.

5.3. Study areas

Three areas have been studied in northern Tunisia (Figure 5.1). From west to east they are coastal cliff sections at Tabarka, Cap Serat, and Ras el Koran. All three are sections of the Kroumeri member (Boukhalfa et al., 2009) and have been dated by Torricelli and Biffi (2001). A west to east transect was chosen to allow for lateral variability to be assessed.

The **Tabarka section** is located on the 'castle' headland northwards of the harbour (Figure 5.1). The section is >1500 m thick and is early Oligocene in age (Toriccelli and Biffi, 2001). Repetition of palynological assemblages is interpreted as section repetition through thrust faulting (Toriccelli and Biffi, 2001). For this study, 190 m of section was logged.

The **Cap Serat section** is located on a northeastwards jutting promontory northwest of Sidi Ferdjani (Figure 5.1). Stratigraphy is exposed on both sides of the promontory, and the eastern side was logged, where a thickness of ~1400 m is recorded (Toricelli and Biffi, 2001). Palynological dating places the section as early Miocene (Toriccelli and Biffi, 2001). For the purposes of this study, 440 m of section was logged.

The final area is the easternmost outcrop of Numidian Flysch Formation in Tunisia, located at the **Ras el Koran** headland, 7 km northwest of Bechateur (Figure 5.1). Approximately 650 m of section is exposed (Toriccelli and Biffi, 2001), with dating confirming an early Miocene section, overthrust by a mid to late Oligocene section. 80 m of section was logged for this study, although its relation to dated stratigraphy is unknown.

5.4. Results

5.4.1 Density flow lithofacies

A range of lithofacies are recognised throughout the three study areas. They are described here using the density flow nomenclature of Dasgupta (2003) such that flows are grouped into; turbidity currents, hyperconcentrated flow, debris flow, and subaqueous grain flow, with increasing sediment to water ratio. They correspond to turbulent, transitional (between turbulent and plastic), laminar, and collisional flow characteristics respectively. Laminar debris flow deposits are subdivided into cohesive and noncohesive types based upon lithology, with noncohesive being equivalent to sandy debris flows of Shanmugam (1997). Figure 5.3 summarises the following lithofacies.

5.4.1.1 Massive ungraded beds (FA-1)

Massive ungraded beds (FA-1) contains deposits which are either ungraded or lack sedimentary structures. The finest grained deposits are massive poorly sorted mudstones (FA-1a) which form beds up to 8 m thick. Deposits vary between predominantly clastic (<40% mudstone) to mudstone rich (<95% mudstone) with a clastic fraction of silt to coarse sand and rare scattered pebbles (Figure 5.3a). No grading is observed however and bed bases are relatively planar. Mud clasts up to 0.4 m long and deformed blocks of coarse grained sandstone up to 0.4 m in width are present however, distributed throughout the bed (Figure 5.3a). With thicknesses of <8 m and large rafted sandstone blocks, a large volume flow with significant matrix strength is signified. As with FA-1a, the lack of grading and high mud content suggest laminar flow processes, such that a cohesive debris flow is interpreted.

Medium to coarse grained massive sandstones (FA-1b) represent a majority of the fill within stacked and amalgamated successions. Beds reach 18 m thick but are commonly <1.5 m thick (Figure 5.3b). Thinner beds of this facies (0.1 to 0.4 m thick) tend to be non amalgamated and occur interbedded with mudstones (Figure 5.3b). Outsize very coarse to gravel sized clasts can contribute <70 % of the bed volume. Mud clasts can also be numerous (Figure 5.3d). Bed bases are relatively planar and no grading is observed. Rare dewatering structures, large flutes up to 0.2 m in relief, and rare faint parallel lamination are observed, although other types of sedimen-

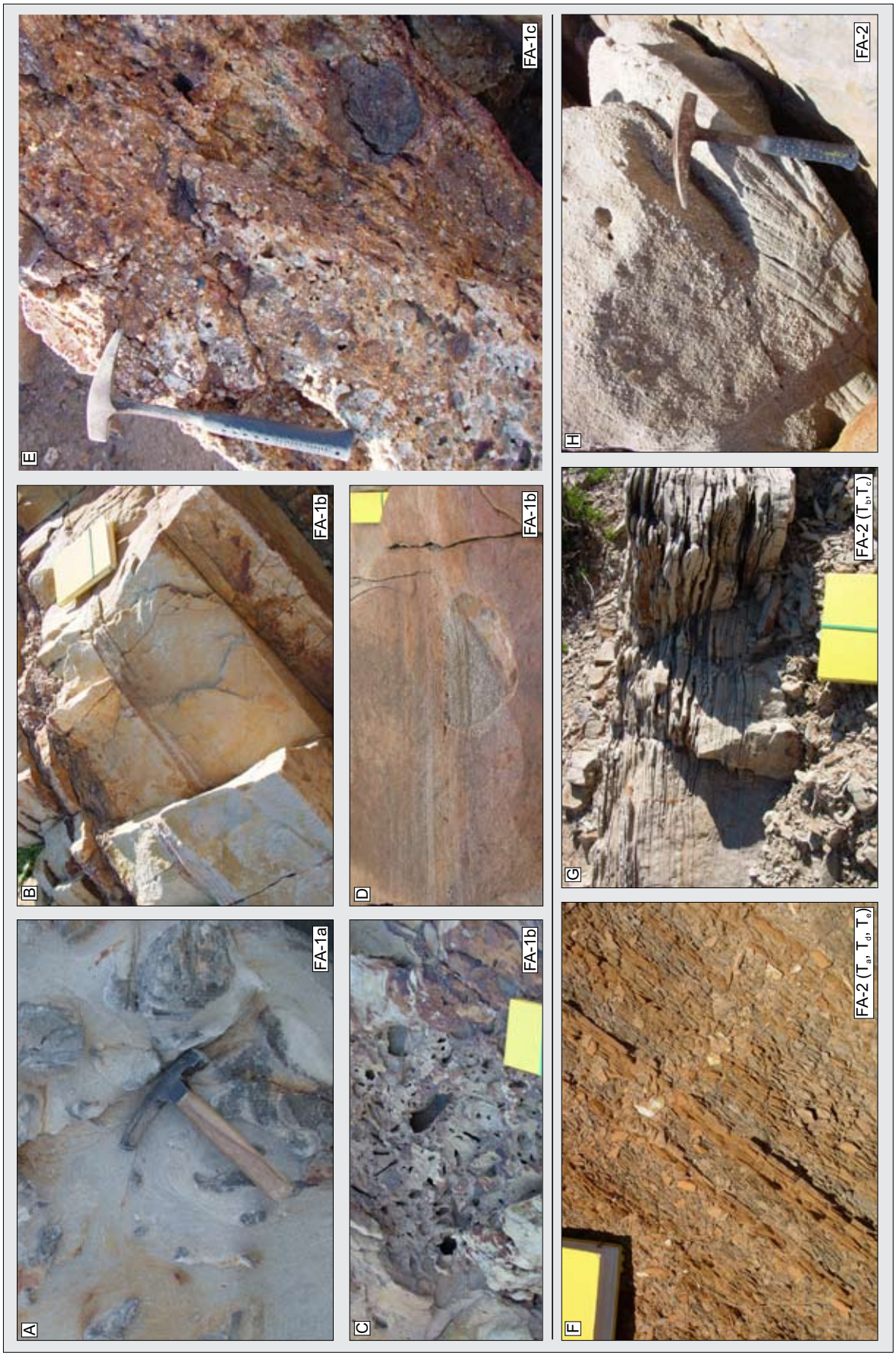

Figure 5.3.
Lithofacies of the Numidian Flysch Formation of northern Tunisia. 5.3a. massive poorly sorted mudstones (FA-1a). Cap Serat section. 5.3b. Medium to coarse grained massive sandstones (FA-1b) from the Cap Serat section. 5.3c. Medium to

Figure 5.3 continued..
coarse grained massive sandstones (FA-1b). Detail of mud clast rich portion. Cap Serat section. 5.3d. Medium to coarse grained massive sandstones (FA-1b). Detail of coarse grained scours. Tabarka. 5.3e. Poorly sorted pebble conglomerates (FA-1c). Cap Serat section. 5.3f. Thin to medium bedded siltstones and sandstones (FA-2a). Fine grained examples from Ras el Koran section. 5.3g. Thin to medium bedded siltstones and sandstones (FA-2a). Tb and Tc divisions. Cap Serat section. 5.3h. Thin to medium bedded siltstones and sandstones (FA-2a) with cross bedding. Cap serat section. 5.3i. Folded and truncated beds (FA-3a). A 10 m thick slump from the Cap Serat section. 5.3j. Discordant and irregular bedding (FA-3b). Large scale sand injectite from the Tabara section. Note circled geologist for scale. 5.3k. Discordant and irregular bedding (FA-3b). Small scale example of clastic dyke fed by a small channel. Ras el Koran section. 5.3l. Discordant and irregular bedding (FA-3b). The upper channel complex margin from Tabarka. Showing injections of mudstone into the channel body.

tary structures are absent. Gravel rich lenses are common, reaching 1 m thick with highly variable thicknesses (Figure 5.3c). Flutes indicate turbulence prior to deposition, although planar bed bases and the lack of grading is inconsistent with an unsteady waning turbidity current. A process similar to that proposed by (Kneller and Branney, 1995) is therefore interpreted, whereby a high sediment fallout rate occurs from a bypassing turbidity current and poorly sorted sands aggrade within a zone of hindered settling. This prevents both the traction of sediment and inhibits grading.
The coarsest such massive deposits are poorly sorted pebble conglomerates (FA-1c). Beds consist of rounded pebbles up to 20 mm in width, held within a poorly sorted matrix of silt to very coarse grained sand (Figure 5.3e). Beds reach 0.8 m thick with irregular and scoured bases. Mud clasts are numerous and reach 0.2 m long. The overall bed displays no grading or sedimentary structures. Substrate scouring results from turbulence at the flow front, while the coarse grainsize, lack of grading and poor sorting result from hyperconcentrated bedload processes, whereby a high sediment fallout rate prevents traction at the flow deposit interface. Deposition beneath a well stratified turbidity current is therefore interpreted.

5.4.1.2 Interbedded graded sandstones and siltstones (FA-2)

This lithofacies association refers to deposits which are normally graded and commonly contain tractional sedimentary structures. Thin to medium bedded siltstones and sandstones consist of deposits described by the Bouma classification scheme (Bouma, 1962). Beds consist of massive, laminated and rippled siltstones to coarse sandstones (Bouma T_b and T_c subdivisions respectively) interbedded with mudstones (hemipelagic mudstones and T_e) (Figure 5.3f and 5.3g). Rare beds with large scale cross beds reach 0.3 m thick with coarse grained sandstones (Figure 5.3h). Cross beds can show an aggradational architecture with foresets stacking vertically (Figure 5.3h). Packages reach 0.3 m in thickness and can be interbedded with massive graded sandstones (T_a). Bioturbation including *thallasinoides*, *palaeophycus*, *zoophycus* and *psammichnites* occur both on the top of sandstone beds and throughout mudstone caps (T_e) (Figure 5.4). Normal grading throughout, coupled with traction structures, indicates waning turbulent flow as described from the Bouma classification scheme (Bouma, 1962). Rare examples of large cross beds indicate very high flow velocities while a high angle of foreset climb (Figure 5.3h) also suggests high sedimentation rates from a strongly waning flow. These deposits are therefore interpreted as resulting from waning low density turbidity currents.

5.4.1.3 Discordant and terminating beds (FA-3)

A variety of complex bed geometries including abrupt terminations, cross cutting, and rapid dip changes are recognised throughout all sections.

Folded and truncated beds (FA-3a) occur in sections <10 m thick. Sections consist of mudstones interbedded with thin and non amalgamated sandstones (Figure 5.3i). The sandstone beds are folded, and may be truncated by other beds which cross cut at a high angle of dip. Where exposure allows, the folded section can be observed to unconformably overlie a relatively planar base of mudstones and thin sandstones. Conformable beds of similar facies can also be observed to truncate the folded beds at the section top such that folded sequences are bound below and above by undeformed stratigraphy.

This facies geometry indicates a discrete deformation event in which mudstones and interbedded sandstones are remobilised. Bed truncations suggests some that examples contain several episodes of remobilisation. A slump origin is therefore interpreted, with the latter examples represent-

ing a complex of slump bodies.

Discordant and irregular bedding (FA-3b) includes sandstones surrounded by structureless mudstones which have highly irregular thickness changes and often terminate over a few centimetres to 10's of metres. The beds are typically structureless and ungraded but may contain mud clasts. Beds can also dip at any angle ranging from the stratigraphic horizontal (e.g bed normal. Figure 5.3j) to perpendicular (Figure 5.3k). Folding of such beds is common, as are branching geometries whereby a bed splits into two or more separate ends.

These geometries are observed on two primary scales. Minor 'finger like' protrusions are common, reaching 0.1 m thick and projecting from the edges of large sandstone bodies including bedding and channel forms (Figure 5.3k and 3l). Larger beds reach several metres thick and can be traced for over 100 m (Figure 5.3j). They can show ramp-flat geometries and cross cut other conformable sandstone beds. In some examples, conformable bedding can be observed to become amalgamated laterally with discordant bedding (Figure 5.3j).

These beds are interpreted as clastic injectites which penetrate thick mudstone dominated suc-

Figure 5.4.
Ichnofossil traces from the Numidian Flysch Formation of northern Tunisia. 5.4a. 0.4 m long *siphonichnus* traces from the Tabarka section. 5.4b. Bedding plane of facies FA-2a from Cap Serat section containing: T; *Thallasinoides*. P; *Palaeophycus*. Z; *Zoophycus*. 5.4c. Bedding plane of facies FA-1b from Cap Serat section containing intense burrowing interpreted as *psammichnites*.

cessions. Vertically orientated geometries represent dyke style intrusions subsequently deformed through compaction and ptygmatic folding. Large horizontal beds represent sill intrusion.

5.4.2 Section descriptions

5.4.2.1 The Tabarka section

The Tabarka section is 190 m thick (Figure 5.5), running northeast along the coastline before turning south and inland (Figure 5.6). The section is broadly composed of two thick packages of amalgamated sandstones at the base and top of the logged section, separated by a more heterogeneous and mudstone rich section (Figure 5.5).

Amalgamated sandstone packages consist of stacked medium to coarse grained massive sandstones (FA-1b) and interbedded normally graded turbidite deposits (FA-2a).Coarse grained scours are common within the former facies and can be traced for several metres, reaching 0.5 m thick (Figure 5.3d). The upper amalgamated sandstone package (Figure 5.5. 133 to 156 m) is exposed at the most northerly headland where it is 24 m thick, and is observed to thin southwards due to an erosional base which truncates sandstone beds of the middle section (Figures 5.6 and 5.7a). Large flutes with amplitudes up to 0.4 m record a dominant palaeoflow towards the southeast at this locality (Figure 5.6). The thinning of the package therefore decreases approximately perpendicular to this orientation (Figure 5.6 and 5.7a). At the southern margin the contact between stacked sandstones to mudstones is observed (Figure 5.3l). The contact is observed to dip steeply towards the thicker northern end of the section. It is a discrete surface but is affected by minor injections of mudstones into the sandstones (Figure 5.3l).

Both lower and upper sandstone packages contain thin (<0.4 m thick) mudstone beds which can be interbedded with thin turbidite deposits (Figure 5.5. 12 and 143 m). Mudstone beds can also be erosionally truncated by massive sandstones (Figure 5.5. 13 m). To the south of the headland, a major incisional surface can also be seen to incise laterally within the sandstone package for around 80 m (Figures 5.6 and 5.7a), thereby amalgamating beds of coarse grained massive sandstone deposits.

The middle interval consists of 110 m of homogeneous mudstone interbedded with thin (0.1 m) to thick (4 m) sandstone beds and amalgamated packages of sandstones which reach 6 m thick (Figure 5.5, 23–115 m; and figures 5.6 and 5.7b). The interbedded sandstones are predominantly massive and ungraded (FA-1b) with relatively planar bases. Loading structures and dewatering pipes are also observed. Where amalgamated, they are bound by erosive bases with relief up to 3 m (Figure 5.5. 115 m) and scours with very coarse grained fill are present. Cohesive debrite deposits (FA-1a) are also present, both interbedded within mudstones and amalgamated within such packages. Intense bioturbation in the form of siphonichnus is common at specific intervals (Figure 5.4a) within the mudstones.

A broad range of bed geometries are observed within the middle section. Many folded and truncated sections indicate slumps up to 2 m thick. The section is however full of discordant beds which display a high dip angle with respect to the section (e.g Figure 5.6 and 5.7b). Beds are observed to cross cut bedding normal examples, and also show highly irregular thicknesses. These beds are interpreted as clastic injectite structures. In satellite images, they are observed to climb at typical angles of ~45-60° (Figure 5.6), although examples with ramp-flat geometries are more subtle in

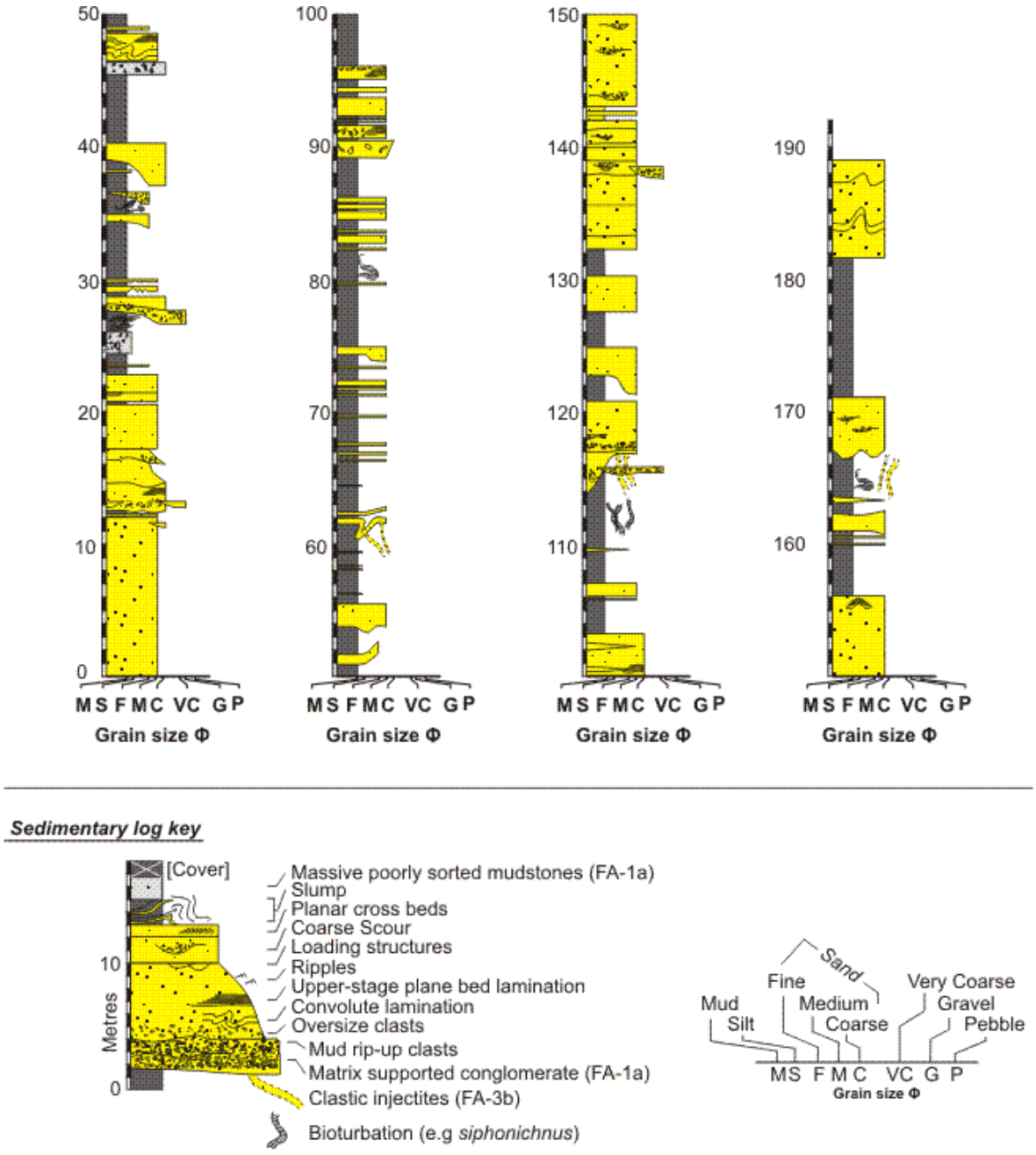

Figure 5.5.
Sedimentary log of the Tabarka section. See figure 5.6 for the logged route. A key for all sedimentary logs is shown below.

terms of their differences to normal depositional bedding (Figure 5.7b).

The geometry of the upper sandstone package suggests a channelised architecture which thickens northwards to >20 m and has a southeast orientated axis. Its base truncates beds of the mudstone dominated middle section and the channel is therefore bound by an erosional surface. While the degree of exposure does not allow characterisation of the lower sandstone package, the facies are very similar and it is considered likely that this is also a channel form.

The interruption of sandstone packages by thin mudstone beds, and also by a large scale erosional surface (the upper package) suggests that the channel form is more complex than a single homogeneous fill. In the case of the interchannel erosional surface, a switch from fill to bypass is recorded resulting from stacking of nested channels elements. This is commonly recognised in channel

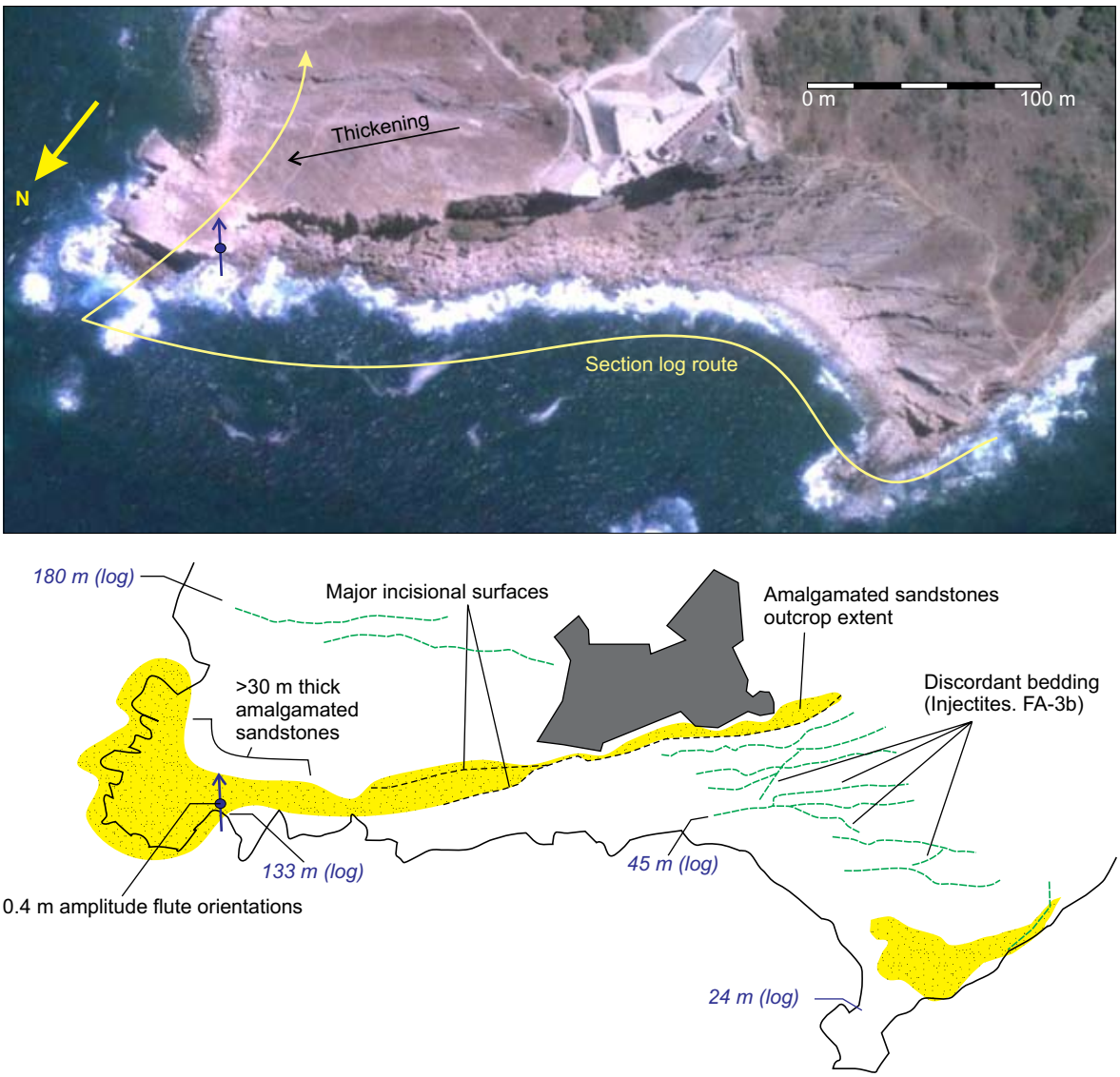

Figure 5.6.
A satellite photograph of the Tabarka section. The route of the sedimentary log is shown along with the extent of amalgamated sandstone outcrop. Major bedding surfaces are traced.

systems at both outcrop (Campion et al., 2003; Wild et al., 2005) and seismic (Mayall et al., 2006; Mayall et al., 2010). The larger channel form is therefore a channel complex consisting of stacked channel elements (sensu Campion et al., 2000; Sprague et al., 2005).

The middle section is defined by a network of clastic injection features. They intrude mudstones and interbedded sandstones which consist predominantly of massive ungraded deposits, minor channels and some slump deposits. These facies are atypical of levee successions and they are interpreted simply as slope deposits. The upper channel complex is therefore entrenched and slope confined rather than levee confined.

5.4.2.2 The Cap Serat section

The Cap Serat section is 430 m long (Figure 5.8) and runs southwards along the eastern coastline of the headland (Figure 5.9). Along the northern edge of the headland, sandstone packages can also be traced for several kilometres towards the west although these are inaccessible and have not been logged (Figure 5.9).

Figure 5.7.
Major architectural elements from the studies sections. 5.7a. The Tabarka headland showing amalgamated sandstones bound by an erosional surface. An internal erosion surface marking the base of a nested channel element is shown in white.

Figure 5.7 continued..
View looking east. 5.7b. The Tabarka middle section showing clastic injections through slope deposits. The white circle and arrows highlight injectites which climb up (or down) stratigraphy. View looking south. 5.7c. Ras el Koran section showing transition to upper, amalgamated sandstones section. The locations of figures 5.3f and 5.3k are shown. 5.7d. The upper section of Ras el Koran. Amalgamated sandstones are shown, separated by mudstones and a cohesive debris flow (FA-1a) and connected via small scale dykes (in white). An example of a large sandstone block within deposits of FA-1b is shown in white.

The log (Figure 5.8) predominantly records a fine grained succession of homogeneous mudstones and interbedded fine sandstones and siltstones (FA-2a). Rare beds of massive poorly sorted mudstones (FA-1a) reach 8 m thick. Four packages of amalgamated sandstones occur throughout the 430 m (Figure 5.8; 0-20 m, 180-195 m, 355-362 m, and 425 m), and are observed to thicken laterally. Massive sandstones (FA-2b) rich in oversize quartz clasts (<8 mm) and mud clasts are the predominant facies. Rare examples of cross bedded normally graded sandstones (FA-2a) also occur (Figure 5.3h). Bioturbation within packages includes thalassinoides, palaeophycus, zoophycus and beds of intense psammichnites traces (Figure 5.4).

Discordant bedding (FA-3a) is also common within fine grained successions (Figure 5.8, 69-92m). The thickest slump unit reaches 10 m (Figure 5.3i) and contains a single bed of poorly sorted pebble conglomerate (FA-1c) with an erosive base and large mud clasts within the matrix. Other examples contain beds which cross cut the bed-normal angle and show unpredictable lateral thickness variations. They are interpreted as clastic intrisions (FA-3b).

When viewed in satellite images (Figure 5.9), the northern edge of the headland contains prominent packages of sandstones which can be traced undeformed for up to 3 km. Towards the east, lenticular packages of sandstones are observed to reach <100 m thick and thin laterally, disappear-

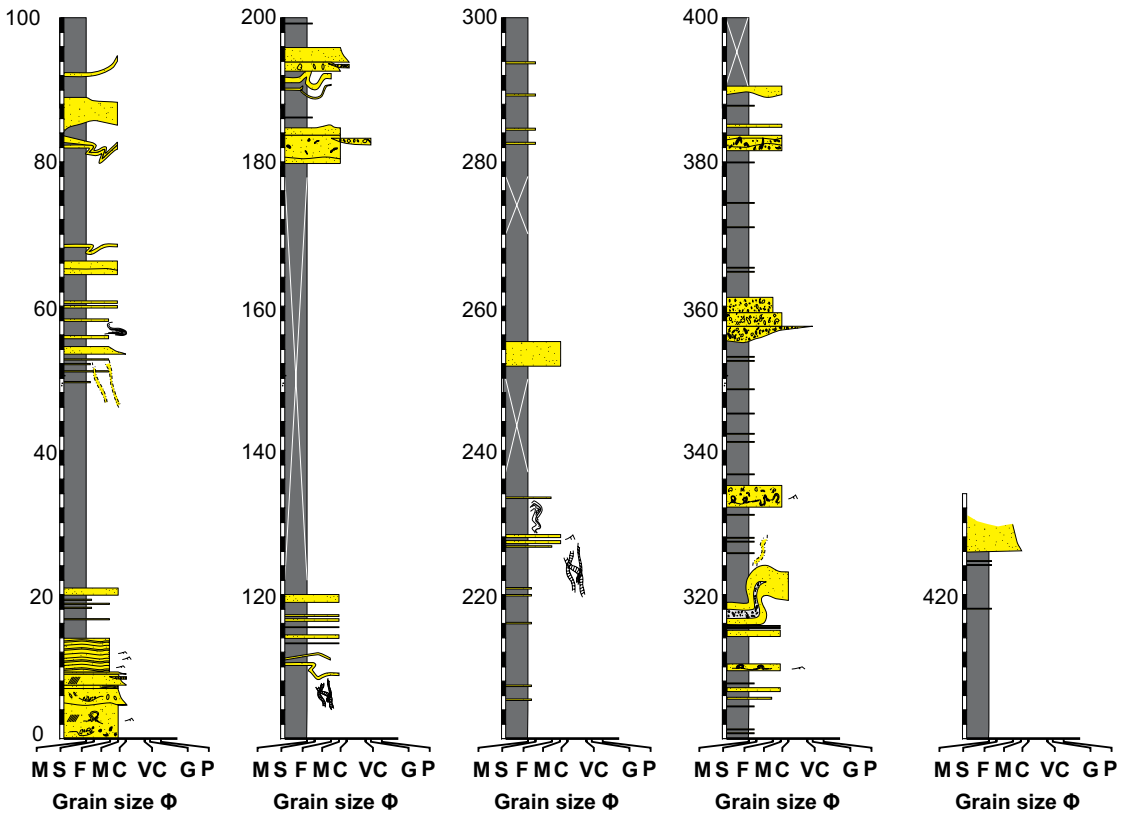

Figure 5.8.
Sedimentary log through the Cap Serat section. See figure 5.9 for log location. See figure 5.5 for sedimentary log key.

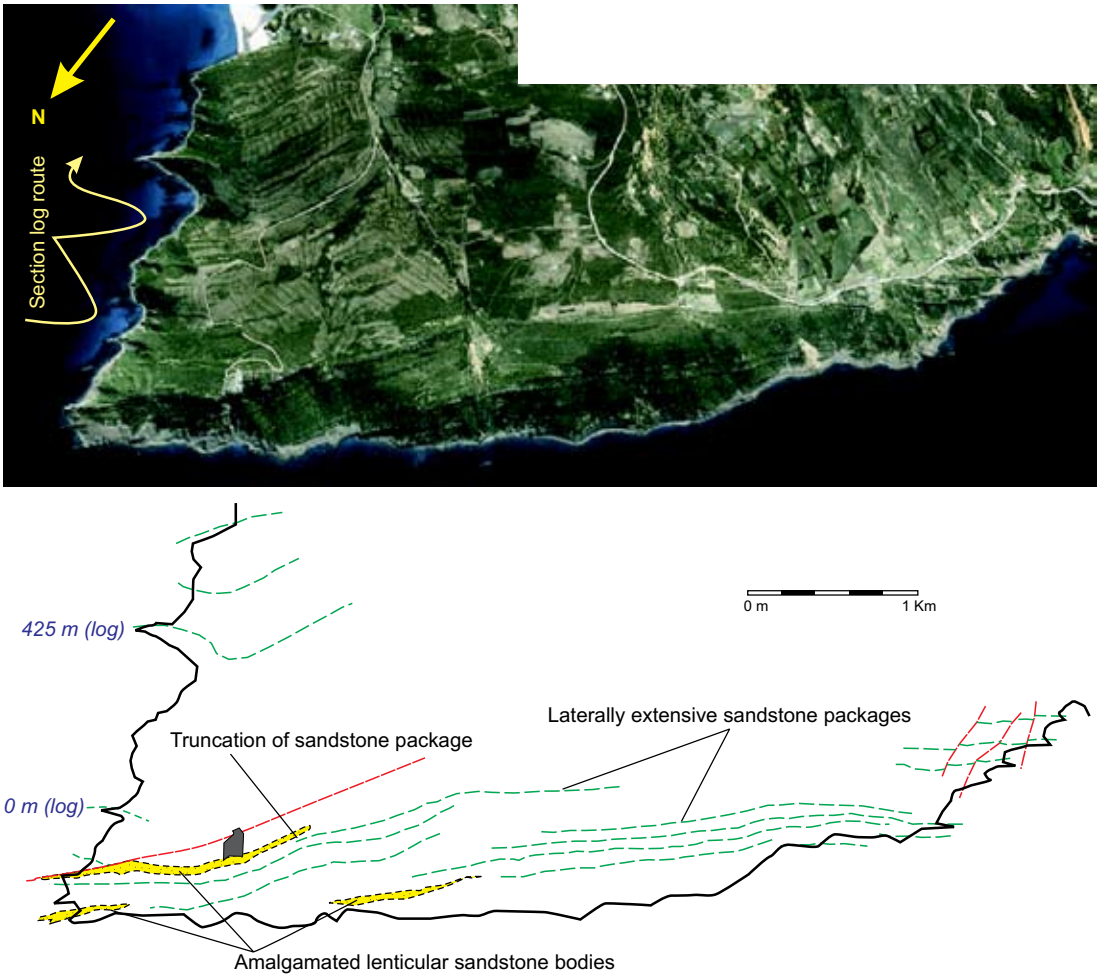

Figure 5.9.
A satellite photograph of the Cap Serat section. The route of the sedimentary log is shown along with the extent of amalgamated sandstone outcrops. Major bedding surfaces are traced.

ing over <1.2 km (Figure 5.9).

Overall, the Cap Serat section is dominantly fine grained with thin turbidites and hemipelagic mudstones while minor amalgamated packages which thicken laterally indicate channelization of flows. Slumping is also common. Sandstones packages observed in satellite images which pinch laterally and reach 100 m thick, indicate large channels however. Furthermore, the southernmost channel body is observed to truncate a laterally extensive sandstone package (Figure 5.9) suggesting that they are erosionally based.

5.4.2.3 The Ras el Koran section

The Ras el Koran section is 80 m thick (Figure 5.10). It broadly consists of a fine grained mudstone dominated section capped by an amalgamated sandstone package.

The lower fine grained section (Figure 5.10, 0-56 m) predominantly consists of mudstones interbedded with fine grained turbidites (FA-2a) including structureless siltstone T_a deposits which are capped by T_e deposits (Figure 5.3f). Ripples are fairly common in coarser grained deposits (T_c) as are parallel lamination (T_b) and some dewatering structures. Coarser grained deposits also contain mudclasts throughout the bed or concentrated at the bed top. Fine grained sandstones and silt-

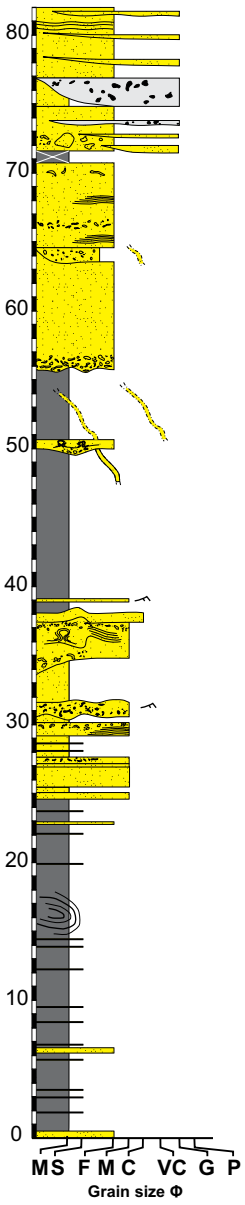

Figure 5.10.
Sedimentary log through the Ras el Koran section. See figure 5.5 for sedimentary log key.

stones are rarely observed to be folded in discrete packages interpreted as slumping (FA-3a). A single package of amalgamated sandstones reaches 3 m thick and shows some thickness variations (Figure 5.10, 25-38 m). Massive beds of sandstone are attached to these amalgamated packages and dip at a high angle to bedding, interpreted as clastic injection features (FA-3b) (Figure 5.4k)

The amalgamated sandstone package at the section top is >25 m thick and consists of stacked massive sandstone beds (FA-1b) (Figures 5.7c and 5.7d) The base of the package (Figure 5.7c) is incised into underlying mudstones and is full of mud clasts. Massive sandstones can contain scours with coarse grained fill and also horizons of mud clasts throughout. Large blocks of sandstone up to 0.4 m across occur within the base of one massive sandstone bed (Figure 5.7d). The package is interrupted by a 1.5 m thick mudstone and massive poorly sorted mudstone interval (Figure 5.10. 71 m and figure 5.7d). The lower and upper portions of the sandstone package are connected however via clastic intrusions which intrude through the mudstone interval (Figure 5.7d).

The amalgamated sandstone package shares many characteristics of channel fill, observed both within the Tabarka section and also from examples in the Karoo basin (Wild et al., 2005). The incised base, rich in mud clasts, is typical of lag deposits observed at channel bases (Hiscott, 1994; Mayall et al., 2006). The separation of the package in to two sections by a mudstone interval suggests that two or more phases of incision and fill occurred however, and the overall package likely represents a channel complex containing stacked channel elements (Campion et al., 2000; Sprague et al., 2005).

The fine grained section below is characterised by very fine grained turbidite deposits containing ripples and abundant mud clasts, and minor slumping. These features are contains common in levee environments (e.g Kane et al., 2007), although the lack of lateral control does not allow for confirmation of this.

5.5. Discussion

5.5.1 Depositional architectures

The three sections span three different times of Numidian Flysch Formation deposition, namely early Oligocene (Tabarka), early Miocene (Cap Serat) and mid Oligocene to early Miocene (Ras el Koran). Similar architectures and facies associations are recorded from each section however, while all three sections are interpreted as slope environments.

Channels are recognised in all sections. Where outcrop permits, channel complexes are interpreted, containing stacked nested channel elements. They range from >25 m (e.g Tabarka upper chan-

nel complex) to <100 m thick (Cap Serat) and up to >1.2 km in width. They are interpreted as slope confined and are bound by an erosional margin which truncates thin out-of-channel sandstones. In the lower part of the Ras el Koran section, the presence of fine grained rippled sandstones and siltstones with abundant mud clasts raises the possibility of levee deposits. These characteristics satisfy two of the three criterion set out by (Walker, 1985) who defines levee deposits as having a significant proportion of convolute lamination, mud clasts and ripples. While it is impossible to confirm this, the possibility of an aggradational levee confined channel system is raised.

Incisonally confined slope channels are typical of steep or uplifting slopes (e.g Kneller, 2003; Mayall et al., 2010). The channel complexes of Tabarka and Cap Serat are therefore likely proximal, above grade and upper slope examples. If Ras el Koran is interpreted as an aggradational channel environment, a lower below grade slope may be interpreted whereby low gradient slopes and low velocity flows are dominantly depositional and construct levees through overbanking (Pirmez and Imran, 2003; Posamentier and Kolla, 2003).

The presence of clastic intrusions is ubiquitous within the Numidian Flysch of Tunisia. Their relation to other depositional elements is highlighted at Tabarka where they occur laterally to a channel complex (e.g figure 5.6). Ptygmatic folding suggests early injection prior to substantial burial compaction. Parize and Beaudoin (1987) and Parize and Beaudoin (1988) document injections from the Tabarka section, suggesting that they are synsedimentary features produced as high density flows deposit within channels. In this interpretation, clastic material is forced into the muddy substrate under high pressure generated by rapid deposition. Throughout the sections studied here, clastic intrusions are observed to be sourced from amalgamated channel deposits rather than isolated interbedded sandstones (e.g figures 5.3k, 5.3l and 5.7d). At Tabarka, it is highly likely that the injectites are sourced from either the large upper channel complex and injected laterally along bedding planes, or from another channel complex towards the south which has been removed during emplacement. A shown by the margin of this channel complex, which is modified through injectites (Figure 5.3l), channel bodies are intimately associated with clastic injections. Figure 5.11 schematically demonstrates architectures of injections related to sand rich channel forms from the Vocontian basin of southern France (Parize and Fries, 2003). In the absence of further outcrop, these models

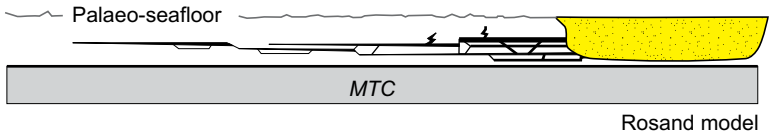

Figure 5.11.
A model for clastic injectite geometries associated with the Rosand channel from the Vocontian basin, southern France. Redrawn from Parize and Fries (2003).

represent a good analogue for Numidian Flysch injectite networks. Given that injectites at Tabarka reach 5 m thick, high resolution seismic surveys may also be capable of imaging them offshore from Tunisia. Furthermore, injectites which cross cut depositional bedding connect the lower and upper channel complexes at the Tabarka section, and are likely to be important features in relation to hydrocarbon prospectivity.

5.5.2 Density flow processes

The lithofacies documented demonstrate that a majority of flows are turbulent. Massive sandstones

indicate quasi-steady (e.g non waning) flow within both channel complex and slope environments. They represent a vast majority of deposits within channel complexes. Fine grained deposits resulting from waning turbidity currents are relatively rare within channel complexes however. A steep gradient upper-slope environment, as interpreted from the Tabarka and Cap Serat sections, is likely to minimise flow deceleration and prompt either waxing or quasi-steady flow conditions. Funnelling of turbidity currents into entrenched channel complexes may also aid with maintaining flow density and therefore flow velocity (e.g Straub and Mohrig, 2009).

Thick massive ungraded sandstone beds have been the subject of much discussion (Kneller and Branney, 1995; Shanmugam, 1997), in particular regarding whether deposits result from a single flow event or from amalgamation of several flow events. Beds aggrade from a flow which is quasi-steady over the life of the flow (sensu Kneller and Branney, 1995). Coarse grained scours within beds up to 8 m thick suggest however that the longitudinal flow structure is non uniform over short timescales, with velocity pulses resulting in mid-bed erosion and deposition of coarse grained deposits through changes in flow competence.

5.5.3 Comparisons with the Sicillide sub-basin

The depositional elements and lithofacies described here are very similar to those of the Sicilide basin (see chapters 3 and 4 this thesis). Deposits of the Sicillide basin are dated as early Miocene in Sicily and southern Italy (Carbone et al., 1987). As such they are approximately contemporaneous to the Cap Serat section described here.

In Sicily, Johansson et al. (1998) and work from chapter 4 (this thesis) describe large scale entrenched channel complexes which reach 500 m in width and 90 m thick. While entrenched channel complexes logged in Tunisia for this study are incomplete, examples observed in satellite images from Cap Serat (Figure 5.9) are of comparable scale (1.2 km wide and 100 m deep). The fill of the Sicillide channel complexes is dominantly massive ungraded medium to coarse grained sandstones in beds up to 8 m thick (Johansson et al., 1998). As with examples from Tabarka, they are interpreted as being deposited from quasi-steady turbidity currents within the confines of a channel. Similarly, flow non-uniformity is recognised, resulting in mid-bed scours at Tabarka, and repetitive grainsize banding within examples from northern Sicily (Chapter 4 this thesis). Coarser grained facies including poorly sorted pebble conglomerates (FA-1c, figure 5.3e) are equivalent to the poorly sorted pebble conglomerates (FA-1a) from Sicily (Chapters 3 and 4 this thesis) which are observed at the base of channel elements. While this facies is rare in Tunisia, it is more widely recognised in channels from Sicily. The only example logged in this study is from Cap Serat, which is similar in age to the channel complexes of northern Sicily.

As with the sections described here, channel complexes of northern Sicily are interpreted as proximal upper slope examples. In Sicily they are organised within a >650 m thick channel system, although outcrop does not allow for further context in Tunisian sections.

Slope deposits such as a majority of the Cap Serat section and the lower Ras el Koran section also share similar characteristics with sections of the Sicilide basin. They consist of mudstones interbedded with isolated massive sandstones, slumps and minor channel forms <5 m thick. All these features are recognised in sections from northern Sicily. The presence of 8 m thick cohesive debrite deposits at Cap Serat (FA-1a, figure 5.3a) is a unique facies however, and is not recognised within slope deposits of Sicily. They are however similar in character to a 200 m thick stacked section of

debris flow deposits described by (Carbone et al., 1987) from deposits of southern Italy. This facies likely represents collapse of muddy slope or shelf deposits prior to transport down the slope and as such is not diagnostic of a unique environment.

Clastic injectites, a common feature of northern Tunisia, are not as commonly recorded in the Sicilide basin. Parize and Beaudoin (1987) describe dykes and sills from Geraci in northern Sicily, although they are on a scale substantially less than observed at Tabarka. They also lack an exposed outcropping channel complex source.

Given the close similarities between the deposits of northern Tunisia with other Sicillide Numidian Flysch Formation deposits, it is reasonable to assume that controls upon slope architectures and lithofacies, including the slope gradient, rate of sediment supply and calibre of supplied sediment are governed by extensive and allocyclic regional controls. In particular, early Oligocene global climate cooling (and the establishment of permanent Antarctic ice sheets) corresponds to the onset of clastic deposition throughout North Africa (Benomran et al., 1987; Swezey, 2009) including the onset of Numidian Flysch deposition in Tunisia and Algeria (Thomas et al., 2010) and references therein). Oligocene to lower Miocene uplift of the Atlas chain throughout North Africa similarly coincides with the timing of deposition and likely increased the source area available (Thomas et al., 2010). Controls upon slope architectures may also have included basin floor subsidence through early Miocene encroachment of the accretionary prism. Given the similarities discussed across the Tunisian and Sicillide sections (~1000 km of slope), regional allogenic controls and not local or autogenic controls are responsible for the architectures observed.

Given this, deposits of Sicily, which contain more laterally extensive outcrops, may provide a useful and well matched analogue for northern Tunisia. Furthermore, the timing of events on the African foreland is much better understood in northern Tunisia than throughout the remainder of the Numidian Flysch outcrop belt, and an understanding of these events may prove useful in assessing the controls upon deposition throughout the remainder of the basin.

5.6. Conclusions

Three sections of the Numidian Flysch Formation in northern Tunisia demonstrate similar lithofacies and depositional elements and represent upper slope environments. Channel complexes are slope confined and are bound by an erosional master surface. They are entrenched into fine grained slope deposits of mudstones interbedded with isolated turbidite deposits and rare cohesive debrite deposits. Minor channels and slumps are widespread amongst such slope deposits.

Channel complexes reach 100 m thick and 1.2 km wide. They contain stacked channel elements whose fill is dominated by massive sandstones interbedded with thick graded sandstones. They represent deposits aggraded from quasi-steady turbidity currents, and the deposits of waning turbulent surge flows respectively. Very coarse grained scours which incise massive sandstone deposits result from flow nonuniformity and variations in flow capacity.

At Tabarka, a network of clastic injection features includes dykes, and beds which have a ramp-flat geometry and rapid lateral thickness variations. They are likely to be sourced from a >25 m thick channel complex and injected laterally into interchannel slope deposits during deposition or early burial. Their scale makes them an important factor in connectivity of different channel complexes which are potential hydrocarbon reservoirs offshore northern Tunisia.

The grainsizes, lithofacies and depositional architectures recognised in northern Tunisia are remarkably similar to those described from parts of the Sicilllide basin to the east. In particular, an upper slope and above grade environment, as interpreted here is also recognised in northern Sicily. Given these similarities observed over a regional extent, similar regional controls are interpreted to govern fan architectures. Furthermore, more extensively exposed deposits of Sicily should provide a useful and well matched analogue for northern Tunisia. Lastly, given that the timing of tectonic, eustatic, and climatic events on the African foreland are better understood in northern Tunisia than throughout the remainder of the basin, the Tunisian foreland is a key area to understand the controls upon Numidian Flysch Deposition throughout the entire Maghrebian Flysch Basin.

References.

Belayouni, H. et al., 2010. La Galite Archipelago (Tunisia, North Africa): Stratigraphic and petrographic revision and insights for geodynamic evolution of the Maghrebian Chain. Journal of African Earth Sciences, 56(1): 15-28.

Ben Slama, M.M., Masrouhi, A., Ghanmi, M., Ben Youssef, M. and Zargouni, F., 2009. Albian extrusion evidences of the Triassic salt and clues of the beginning of the Eocene atlasic phase from the example of the Chittana-Ed Djebs structure (N.Tunisia): Implication in the North African Tethyan margin recorded events, comparisons. Comptes Rendus Geoscience, 341(7): 547-556.

Benomran, O., Nairn, A.E.M. and Schamel, S., 1987. Sources and dispersal of mid-Cenozoic clastic sediments in the central Mediterranean region. In: F. Lentini (Editor), Atti del convegno su; Sistemi avanfossa-avampaese lungo la Catena Appenninico-Maghrebide. Memorie della Societa Geologica Italiana. Societa Geologica Italiana, Rome, Italy, pp. 47-68.

Bonardi, G. et al., 1980. Osservazioni sull'evoluzione dell'Arco Calabro-Peloritano nel Miocene inferiore: la Formazione di Stilo-Capo d'Orlando. Bollettino Della Societa Geologica Italiana, 99: 365-393.

Boukhalfa, K., Ismail-Lattrache, K.B., Riahi, S., Soussi, M. and Khomsi, S., 2009. Analyse biostratigraphique et sédimentologique des séries éo-oligocènes et miocènes de la Tunisie septentrionale : implications stratigraphiques et géodynamiques. Comptes Rendus Geosciences, 341(1): 49-62.

Bouma, A.H., 1962. Sedimentology of some Flysch deposits;: A graphic approach to facies interpretation. 168 pp: Elsevier.

Campion, K.M. et al., 2000. Outcrop expression of confined channel complexes. Deep-water reservoirs of the world: SEPM, Gulf coast section, 20th annual Research Conference, 20th annual Research Conference: 127-50.

Campion, K.M. et al., 2003. Outcrop expression of confined channel complexes. Bulletin of the South Texas Geological Society, 44(4): 13-36.

Carbone, S., Lentini, F., Sonnino, M. and De Rosa, R., 1987. Il flysch numidico di Valsinni (Appennino lucano)

Translated Title: The numidic flysch of Valsinni, Lucanian Apennines. Bollettino Della Societa Geologica Italiana, 106(2): 331-345.

Dasgupta, P., 2003. Sediment gravity flow - the conceptual problems. Earth-Science Reviews, 62(3-4): 265-281.

de Capoa, P., Di Staso, A., Guerrera, F., Perrone, V. and Tramontana, M., 2004. The age of the oceanic accretionary wedge and onset of continental collision in the Sicilian Maghrebian Chain. Geodinamica Acta, 17(5): 331-348.

de Capoa, P. et al., 2002. The Lower Miocene volcaniclastic sedimentation in the Sicilian sector of the Maghrebian Flysch Basin: geodynamic implications. Geodinamica Acta, 15(2): 141-157.

de Capoa, P., Di Staso, A., Perrone, V. and Zaghloul, M.N., 2007. The age of the foredeep sedimentation in the Betic-Rifian Mauretanian Units: A major constraint for the reconstruction of the tectonic evolution of the Gibraltar Arc. Comptes Rendus Geoscience, 339(2): 161-170.

Dhahri, F. and Boukadi, N., 2010. The evolution of pre-existing structures during the tectonic inversion process of the Atlas chain of Tunisia. Journal of African Earth Sciences, 56(4-5): 139-149.

Eschard, R., Albouy, E., Deschamps, R., Euzen, T. and Ayub, A., 2003. Downstream evolution of turbiditic channel complexes in the Pab Range outcrops (Maastrichtian, Pakistan). Marine and Petroleum Geology, 20(6-8): 691-710.

Gery, B., 1983. Age and Tectonic Situation of the Allochthonous Sedimentary Formations in Northern Grande Kabylie - an Example in the Djebel Aissa-Mimoun. Comptes Rendus De L Academie Des Sciences Serie Ii, 297(9): 729-&.

Glacon, G. and Rouvier, H., 1967. Precisions lithologies et stratigraphiques sur le “Numidien” de Kroumerie (Tunisie septentrionale). Bulletin De La Societe Geologique De France, 9(3): 410-417.

Golonka, J., 2004. Plate tectonic evolution of the southern margin of Eurasia in the Mesozoic and Cenozoic. Tectonophysics, 381(1-4): 235-273.

Gottis, C., 1953. Stratigraphie et tectonique du « flysch » numidien en Tunisie septentrionale. Compte Rendus Hebdomadaires des Seances de l’Academie des Sciences, Paris, 236: 1059-1061.

Guerrera, F., 1981. Turbiditic successions in Mauritanian and Numidian flyschs of Rif, Morocco Successions turbiditiques dans les flyschs mauretanien et numidien du Rif (Maroc). Revue De Geologie Dynamique Et De Geographie Physique, 23(2): 85-95.

Guerrera, F., Loiacono, F., Moretti, E. and Puglisi, D., 1990. The Numidian sequence and tectonics; a paleogeographic interpretation

La sequenza numidica nel suo contesto geotettonico; una proposta di ordine paleogeografico. Rivista Italiana Di Paleontologia E Stratigrafia, 96(2-3): 165-190.

Guerrera, F., Martin-Martin, M., Perrone, V. and Tramontana, M., 2005. Tectono-sedimentary evolution of the southern branch of the Western Tethys (Maghrebian Flysch Basin and Lucanian Ocean): consequences for Western Mediterranean geodynamics. Terra Nova, 17(4): 358-367.

Guerrera, F., Martinalgarra, A. and Perrone, V., 1993. Late Oligocene-Miocene Syn-/-Late-Orogenic Successions in Western and Central Mediterranean Chains from the Betic Cordillera to the Southern Apennines. Terra Nova, 5(6): 525-544.

Hiscott, R.N., 1994. Loss of capacity, not competence, as the fundamental process governing deposition from turbidity currents. Journal of Sedimentary Research, 64(2a): 209-214.

Hodgson, D.M. et al., 2006. Stratigraphic evolution of fine-grained submarine fan systems, Tanqua depocenter, Karoo Basin, South Africa. Journal of Sedimentary Research, 76(1-2): 20-40.

Jallouli, C. et al., 2005. Evidence for Triassic salt domes in the Tunisian Atlas from gravity and geological data. Tectonophysics, 396(3-4): 209-225.

Johansson, M., Braakenburg, N.E., Stow, D.A.V. and Faugeres, J.C., 1998. Deep-water massive sands: facies, processes and channel geometry in the Numidian Flysch, Sicily. Sedimentary Geology, 115(1-4): 233-265.

Kane, I.A., Kneller, B.C., Dykstra, M., Kassem, A. and McCaffrey, W.D., 2007. Anatomy of a submarine channel-levee: An example from Upper Cretaceous slope sediments, Rosario Formation, Baja California, Mexico. Marine and Petroleum Geology, 24: 540-563.

Klett, T.R., 2001. Total petroleum systems of the Pelagian Province, Tunisia, Libya, Italy, and Malta-The Bou Dabbous-Tertiary and Jurassic-Cretaceous Composite, USGS.

Kneller, B., 2003. The influence of flow parameters on turbidite slope channel architecture. Marine and Petroleum Geology, 20(6-8): 901-910.

Kneller, B.C. and Branney, M.J., 1995. Sustained High-Density Turbidity Currents and the Deposition of Thick Massive Sands. Sedimentology, 42(4): 607-616.

Mayall, M., Jones, E. and Casey, M., 2006. Turbidite channel reservoirs - Key elements in facies prediction and effective development. Marine and Petroleum Geology, 23(8): 821-841.

Mayall, M. et al., 2010. The response of turbidite slope channels to growth-induced seabed topography. Aapg Bulletin, 94(7): 1011-1030.

Mazzoleni, P., 1991. Porphyric rocks in the basal conglomerate from the Stilo-Capo d’Orlando

Formation
Le rocce profiriche nel conglomerato basale della formazione di Stilo-Capo d'Orlando. Memorie della Societa Geologica Italiana, 47: 557-565.
Mutti, E., Bernoulli, D., Lucchi, F.R. and Tinterri, R., 2009. Turbidites and turbidity currents from Alpine 'flysch' to the exploration of continental margins. Sedimentology, 56(1): 267-318.
Parize, O. and Beaudoin, B., 1987. Clastic Dikes in the Numidian Flysch (Tunisia, Sicily) - Their Relations with the Paleomorphology. Comptes Rendus De L Academie Des Sciences Serie Ii, 304(3): 129-134.
Parize, O. and Beaudoin, B., 1988. Clastic Dykes and Sills from Numidian Flysch (Sicily and Tunisia) - Sandy Injection Related to a High-Density Turbidity Deposit. Aapg Bulletin-American Association of Petroleum Geologists, 72(8): 1018-1018.
Parize, O. and Fries, G., 2003. The Vocontian clastic dykes and sills: a geometric model. Geological Society, London, Special Publications, 216. Subsurface Sediment Mobilization: 51-71.
Pirmez, C. and Imran, J., 2003. Reconstruction of turbidity currents in Amazon Channel. Marine and Petroleum Geology, 20(6-8): 823-849.
Posamentier, H.W. and Kolla, V., 2003. Seismic geomorphology and stratigraphy of depositional elements in deep-water settings. Journal of Sedimentary Research, 73(3): 367-388.
Riahi, S. et al., 2010. Stratigraphy, sedimentology and structure of the Numidian Flysch thrust belt in northern Tunisia. Journal of African Earth Sciences, 57(1-2): 109-126.
Shanmugam, G., 1997. The Bouma Sequence and the turbidite mind set. Earth-Science Reviews, 42(4): 201-229.
Sprague, A.R. et al., 2005. Integrated slope channel depositional models: the key to successful prediction of reservoir presence and quality in offshore West Africa. CIPM, cuarto E-Exitep 2005, February 20-23 2005. Veracruz, Mexico.: 1-13.
Straub, K.M. and Mohrig, D., 2009. Constructional canyons built by sheet-like turbidity currents: Observations from offshore Brunei Darussalam.Journal of Sedimentary Research, 79(1-2): 24-39.
Swezey, C.S., 2009. Cenozoic stratigraphy of the Sahara, Northern Africa. Journal of African Earth Sciences, 53(3): 89-121.
Thomas, M.F.H., Bodin, S., Redfern, J. and Irving, D.H.B., 2010. A constrained African craton source for the Cenozoic Numidian Flysch: Implications for the palaeogeography of the western Mediterranean basin. Earth-Science Reviews, 101(1-2): 1-23.
Torricelli, S. and Biffi, U., 2001. Palynostratigraphy of the Numidian Flysch of northern Tunisia (Oligocene-early Miocene). Palynology, 25: 29-55.
Vanhouten, F.B., 1980. Mid-Cenozoic Fortuna Formation, Northeastern Tunisia - Record of Late Alpine Activity on North African Cratonic Margin. American Journal of Science, 280(10): 1051-1062.
Walker, R.G., 1985. Mudstones and thin-bedded turbidites associated with the upper cretaceous Wheeler Gorge conglomerates, California - a possible channel-levee complex. Journal of Sedimentary Petrology, 55(2): 279-290.
Wezel, F.C., 1969. Lineamenti Sedimentologico Del Flysch Numidico Della Sicilia Nord-Orientale. Memorie Degli Instituti Di Geologia e Mineralogia Del L'Universita Di Padova, 26.
Wezel, F.C., 1970. Numidian Flysch - an Oligocene - Early Miocene Continental Rise Deposit Off African Platform. Nature, 228(5268): 275-&.
Wild, R.J., Hodgson, D.M. and Flint, S.S., 2005. Architecture and stratigraphic evolution of multiple, vertically-stacked slope channel complexes, Tanqua depocentre, Karoo Basin, South Africa. Geological Society, London, Special Publications, 244(1): 89-111.
Yaich, C., 1992. Dynamics of the Oligomiocene Detritic Facies of Tunisia. Journal of African Earth

Sciences, 15(1): 35-47.

Yaich, C., Hooyberghs, H.J.F., Durlet, C. and Renard, M., 2000. Stratigraphic correlation between the Numidian formation (North Tunisia) and Oligo-Miocene deposits of central Tunisia. Comptes Rendus De L Academie Des Sciences Serie Ii Fascicule a-Sciences De La Terre Et Des Planetes, 331(7): 499-506.

Chapter 6 .

Synthesis and final considerations.

Chapter 6. Synthesis and final considerations

The aim of this thesis was to re-evaluate the sedimentology of the Numidian Flysch Formation in light of current thinking. In particular, focussing upon downslope changes in lithofacies and fan architecture and the impact of intraslope topography. The four key questions which were posed at the beginning of the thesis and are required to answer this question, are revisited here and presented with relevant results from the previous chapters.

6.1. Returning to the key questions

Four key questions were presented in the introduction to this thesis and addressed through the four research chapters. The results are synthesised and discussed here.

6.1.1 Can the Numidian Flysch Formation provenance and basin setting be better constrained, so that Numidian Flysch fan architectures and their associated controls can be reconstructed?

6.1.1.1 Provenance and basin context of the Numidian Flysch Formation

The problem of provenance and basin setting has meant that little progress has been made on reconstructing Numidian fan architectures and the controls upon them. Chapter 1 represents an attempt to compile and discuss all the available evidence which is commonly used within this debate.

A review of the location of Numidian Flysch Formation nappes within the fold-and-thrust-belts of Spain, Morocco, Algeria, Tunisia, Sicily and southern mainland Italy clearly indicates that the Numidian Flysch Formation (Massylian flysch series) was deposited into the southern portion of the Mahgrebian Flysch Basin (MFB) while the Mauretanian flysch series was deposited into the northern portion of the basin. Furthermore, these two flysch series also contain distinct petrofacies. The Massylian (Numidian) series contains polycyclic quartz grains (<100%) while the Mauretanian series is lithic rich, immature and can contain volcaniclastic grains.

A distinction is also made in the zircon suites which each petrofacies contains. For Numidian sandstones, a source is required which contains Eburnian (~2 Ga) and PanAfrican (~600 Ma) age zircons but does not contain Hercynian (310 Ma) or Alpine (~50 Ma) aged zircons. Conversely, Mauretanian sandstones require a source with Hercynian age zircons (310 Ma) but none of Pan African (~600 Ma) or Eburnian (~2Ga) age. There is however only a single published examples of a zircon suite from the Mauretanian flysch series (Lancelot et al., 1977) and further studies are required to confirm this data.

Based upon these lines of evidence, two distinct source regions are required for these flysch series. Furthermore, the review covers deposits from the entire length of the MFB. The detrital zircon suite from the Numidian Flysch Formation matches well with a general ‘African basement signal’ which is observed in basement units across North Africa. The petrology is also very similar to the many units of sheet sandstones which cover much of North Africa. Conversely, the single Maure-

tanian detrital zircon suite matches with a general 'European basement signal', while the petrology matches with lithologies found within the basement blocks on the northern margin of the basin. The issue of palaeocurrent distribution is also discussed however and has been commonly used to constrain a European (northern) source. When viewed in context of complex deformations during basin closure, and foreland basin analogues, it is unlikely that they are representative of the original orientation that flow travelled. Furthemore, with an interpreted intraslope ponded basin within the deposits of Sicily (Chapter 3), flows would be expected to become reflected and deflected due to slope topography. This is observed in the palaeocurrents recorded from the Mt. Salici section. The presence of intraslope deformation throughout the MFB therefore provides an explanation for the widely variable palaeocurrents that are recorded in large studies such as Hoyez (1975) and Wezel (1969). A bulk of the available evidence reviewed consequently points to an African source with Numidian Flysch sandstones representing a further reworking of the polycyclic sandstones which cover much of North Africa.

The timing of Numidian deposition is also coincidental with a switch from carbonate to clastic deposition across North Africa. Described originally by Benomran et al. (1987), this depositional switch was recognised in the Sirte basin of Libya, the Tunisian foreland, the Pelagian platform and the Hyblean plateau (southern Sicily). Benomran et al. (1987) chose to group the Numidian Flysch Formation within this list and suggested that a major eustatic sea level fall coupled with Alpine tectonic movements was responsible. The more recent review of Swezey (2009) also recognises a change from carbonate to clastic deposition in Mauritania, Senegal, Algeria (the Tindouf , Souara, Tademait, Taoudenni Lullemmed and Chotts basins), northern Chad, northeast Libya, and northern Egypt (Figure 6.1a). Swezey (2009) correlates the timing of clastic deposition to Atlas uplift throughout North Africa, and also the onset of permanent glaciations in Antarctica at the beginning of the Oligocene, marking the onset of global icehouse conditions (Figure 6.1b). A clear precedent therefore exists for the Numidian Flysch Formation to represent clastic shedding from North Africa, representing simply an offshore continuation of this regional evolution.

6.1.1.2 Controls upon regional deposition

The location of Numidian Flysch deposition is regional in scale, and therefore requires a regional event to initiate deposition. As reviewed in chapter 1, the timing of Numidian Flysch deposition is contemporaneous with uplift of the Atlas fold-and-thrust-belt throughout North Africa. The earliest deposition of Numidian Flysch sandstones, in Tunisia and Gibraltar also matches the onset of the Oligocene global cooling event. This matches the conclusions of Swezey (2009) when reviewing sedimentation across North Africa (Chapter 1 figure 1.13, and this chapter figure 6.1b). While evidence is scant, the studies presented in chapter 1 point to North Africa being a much wetter environment than prior to the Oligocene, and it is during this time that the palaeo Nile (Sudan and Egypt) and Eoshabi (Algeria) river systems were established. A combination of Atlas uplift coupled with a wetter climate is therefore concluded as the main driver on Numidian Flysch deposition over this regional extent.

6.1.2 What lithofacies and depositional elements are recognised within deposits of the Numidian Flysch Formation (with emphasis placed on Sicily and Tunisia)?

6.1.2.1 Lithofacies of the Numidian Flysch Formation

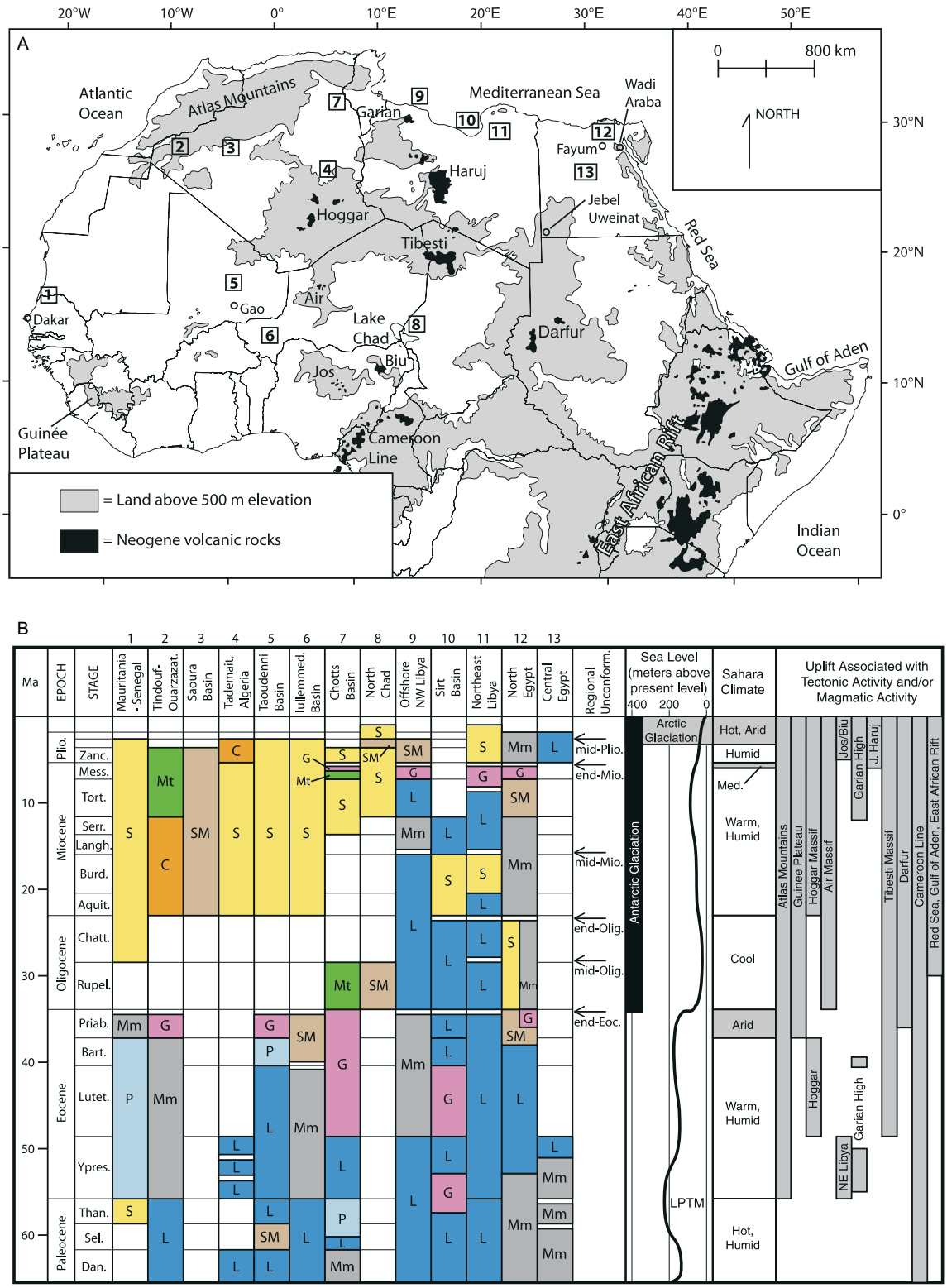

Figure 6.1.

North Africa Cenozoic stratigraphy, taken from (Swezey, 2009). 6.1a. Map of North Africa highlighting the areas studied by (Swezey, 2009) significant exposures of African basement (e.g the Hoggar), and the area of Atlas uplift. Numbers correspond to stratigraphic summary logs in figure 6.1b. 6.1b. Stratigraphic summary logs across North Africa highlighting the switch from carbonate to clastic depsotion in the Oligocene and Miocene. Major tectonic events, climate, and eustatic sea level are shown to highlight controls upon deposition.

Within the study areas of Sicily and Tunisia, lithofacies can broadly be combined within four associations based upon character. These are; massive ungraded deposits, graded structured deposits, hybrid deposits, and deformed deposits.

6.1.2.1.1 Massive ungraded deposits

Massive ungraded deposits include conglomerates in which pebbles are held within a poorly sorted matrix, and massive gravels to siltstones. Thick beds (>18 m thick in Tabarka, Tunisia) are commonly amalgamated within channel complex bodies. Thin examples (<1 m thick) are however generally interbedded with mudstones and occur within interchannel areas and lobe environments. Most facies of this association demonstrate deposition from a turbidity current, evidenced through fluting, substrate erosion and entrainment of mudclasts, traction and imbrication of clasts and pebbles, and some top-only normal grading. Two mechanisms are interpreted, namely deposition through high density bedload processes which result in traction affected deposits, and suspension dominated deposition from high density quasi-steady turbidity currents (e.g Kneller and Branney, 1995). Poorly sorted massive deposits which are mud dominated show no evidence of deposition through turbidity current processes and are interpreted as laminar flow deposits from cohesive debris flows.

Within proximal settings such as the entrenched channel complexes of Finale (Sicily), Tabarka, and Cap Serat (Tunisia), gravel filled scours and lenses of mud clasts are common within massive ungraded deposits. They are interpreted to represent flow non uniformity, whereby velocity fluctuations produce fluctuations in flow competence. This results in localised and short lived incisions through flow waxing, and deposition of coarse grained clasts during flow waning, which were previously bypassing the location. Kneller and McCaffrey (2003) suggest this process as being more common in proximal settings where flows have not had sufficient downslope distance to evolve into a single waning surge event.

6.1.2.1.2 Graded and structured deposits

Graded and structured sandstones and siltstones represent the second major lithofacies association. They include facies of the Bouma classification scheme (Bouma, 1962). They are mainly observed in lobe environments and not within channel complexes and are interpreted to be deposited from waning tubidity currents in relatively unconfined settings.

A rare facies within the Finale channel system is a graded bed which includes grainsize banding over mm to cm thicknesses (FA-3b, chapter 3). Complex vertical grainsizes are interpreted to represent flow non-uniformity and as with coarse grained scours within massive sandstones (section 1.2.1.1) this process is considered to be indicative of proximal environments (Kneller and McCaffrey, 2003). This lithofacies, as with massive ungraded deposits which display this character are similarly only observed within upper slope entrenched channel systems.

6.1.2.1.3 Hybrid deposits

A variety of hybrid flow deposits (sensu Haughton et al. (2009) are also observed, mainly within the Mt. Salici section, interpreted as the most distal environment described within this thesis. Linked debrites, a turbidity current which partitions and generates a co-genetic debris flow, are increasingly being recognised in lobe environments (e.g the Karoo basin (Hodgson, 2009) and the Britannia field, North Sea (Haughton et al., 2003)) and occur in small numbers within the Mt. Salici middle subdivision. Within the upper subdivision, interpreted as a channel lobe transition zone, a single 8 m thick section of banded slurry flow deposits (facies type H2 from Haughton et al., 2009) are

interpreted. They form from flows which are intermediate between laminar and fully turbulent and require a relatively high degree of mud (Haughton et al., 2009). These facies have not been interpreted in northern Tunisia. However, given the high degree of similarity between Sicilian and Tunisian deposits (e.g the high proportion of ungraded massive sandstones) it could be expected that hybrid facies are present in distal sections of northern Tunisia, such as those of the Zousa member.

A single variety of hybrid flow is interpreted from the Finale section. Beds of mud dominated poorly sorted conglomerates are similar in character to the cleaner (silt to coarse sandstone dominated) pebble conglomerates with the exception of large mud clasts (1.2 m long) and large volumes of mud within the matrix. It is interpreted that erosion and entrainment of substrate mud during bedload transport beneath a turbidity current can result in a cohesive debris flow.

6.1.2.1.4 Deformed and discordant deposits

Deformed deposits include slumps and clastic injectite features. Slumps are recognised within both upper and lower slope channel elements and lobe fringe environments. Within channel elements they tend to occur within marginal areas as with the Karsa section (Sicily) where they occur away from the channel complex axis and consist of thin bedded sandstones interbedded with mudstones representing collapse of the channel margin. In lobe environments, similar thin bedded and fine grained sandstones represent lobe fringe deposits and minor instability within them.

Clastic injectites are a ubiquitous feature of northern Tunisia and are intimately associated with channel complexes. A combination of vertical dyke intrusion, horizontal sill type intrusion, and stepped beds are recorded. In Mt. Salici, minor dykes connect stacked lobe axis deposits which are otherwise separated by interlobe mudstones and interbedded thin sandstones. At Tabarka, a network of large clastic intrusions connects two channel complex bodies which are separated from each other by over 100 m vertically and ~300 m laterally.

6.1.2.2 Depositional elements of the Numidian Flysch Formation

In Sicily, the Finale, Karsa, and Mt. Salici sections are respectively interpreted as an upper-slope; lower slope; and low gradient basin floor environments respectively. According to the slope model of Mutti and Ricci Lucchi (1978) these represent upper, mid and outer fan locations respectively based upon their facies, stacking patterns and depositional architectures. In Tunisia, the Tabarka, Cap Serat, and Ras el Koran sections are also interpreted as upper slope. Lower slope and basin floor deposits were not observed, although Riahi et al. (2010) have interpreted lobes within the mudstone rich Zousa member. Within these environments, a range of depositional elements are interpreted.

6.1.2.2.1 Entrenched slope channel complexes

Channel complexes are observed within both Tunisia and Sicily. Well exposed examples are observed to truncate beds in interchannel areas. Interchannel areas in both Finale and Tabarka also show no evidence for levee construction, and channel complexes are characterised as slope confined and entrenched. Channel complexes reach 500 m wide in Sicily and 1200 m wide in Tunisia, and reach 90-100 m thick in both countries. channel elements are commonly observed to be stacked within channel complexes. They comprise a generally repeatable progression of facies which overlie an erosional base. Their fill consists of coarse grained bedload deposits which fill incised thalwegs of the basal surface, overlain by stacked massive sandstone and interbedded normally graded sandstones, both deposited from suspension sedimentation.

In Finale (Sicily) where exposure is greater than Tunisia, channel complexes are observed to be slightly sinuous, and are offset stacked with either a systematic or chaotic trend. The geometry of channel complexes can be asymmetric which results from complex sinuosity. Non-vertical stacking of channel elements within the parent complex (e.g lateral stacking of channel elements), and sinuosity of the channel element thalweg within the confines of the channel complex also result in asymmetric complexes however.

Given that coarse grained bedload deposits tend to fill channel element thalwegs, this also results in an asymmetry of facies distribution. Where multiple thalweg geometries occur within a single channel element, a braided type of channel floor morphology results. Rare lateral accretion deposits are also recognised downlappping onto the channel element base. They may represent either lateral migration of the element thalweg, or possible lateral migration of bar type features.

6.1.2.2.2 Aggradationally stacked slope channel complexes

This depositional element is only interpreted from the Karsa section in northern Sicily. Channel complexes are over 1.2 km in width, and are vertically stacked to a thickness of >600 m, with increasing amalgamation to the north. This culminates in a sandstone axis at the north of the section and a change from channel complex margin to axis is interpreted. The opposing stacked channel complex margins have been removed during emplacement however. The thickness of individual channel complexes is unknown given the degree of vertical amalgamation, although channel complex margins are recorded with a maximum measured thickness of 30 m and visual estimates reach 80 m thick. Within the channel complex axis, nested channel elements are observed and also large scale slumping. Channel complex fill consists predominantly of massive ungraded sandstones and interbedded normally graded sandstones. Small scale slumping is observed towards their margins which is interpreted as channel element margin collapse.

Exposure does not allow for characterisation of fine grained sediments to the south, although aggradationally stacked channel complexes require levee construction in order to continually confine transiting flows. They would therefore be expected to flank the outcropping channel complex margins to the south.

6.1.2.2.3 Mass transport complexes

Mass transport complexes (MTC) are observed within a majority of sections at a variety of scales. They occur in mudstone dominated slope deposits (e.g Cap Serat), lobe environments, and within channel complexes.

Packages of deformed and folded thin beds of sandstone are interbedded with mudstones. Truncations of folded beds indicate several episodes of deformation. At the Karsa section (Sicily), aggradationally stacked slope channels overlie a >25 m thick MTC which can be traced for >700 m at the base of the section. This is interpreted as large scale mass wasting of the slope, which may have played a role in capturing and possible ponding flows at this locality. In slope deposits, MTC’s are observed up to 10 m thick at Cap Serat (Tunisia).

6.1.2.2.4 Channel lobe transition zone

The CLTZ is a zone linking a channel mouth with a depositional lobe, typically at a break of slope, in which rapid deceleration, thickening, and lateral spreading of flows scours the sea floor, often inferred as a hydraulic jump. Coarse grained sediments are typically recognised in long-wavelength

sediment waves and transverse bedforms (Kenyon et al., 1995), while shallow cores from the Rhone CLTZ contained well sorted medium to coarse sands (Wynn et al., 2002). High backscatter acoustic facies, recorded from side-scan sonar data of the Rhone and Agadir CLTZ's, are also interpreted to represent coarse grained (sandy) sediments (Wynn et al., 2002). There are relatively few outcrop studies which describe and interpret a CLTZ in ancient systems.

The upper subdivision of the Mt. Salici section is interpreted as a channel lobe transition zone. The zone can be traced for over 1 km laterally and is around 80 m thick. It consists almost exclusively of amalgamated stacked massive granular sandstones and coarse grained turbidites, deposited within large scours. The large percentage of poorly sorted granular sandstones suggests that coarse grained bedload was being deposited from bypassing turbidity currents as predicted by flume experiments including Garcia and Parker (1989) and Garcia (1993) who calculated a drop in bed shear stress, and deposition of coarse grained bedload immediately downslope of a gradient change. Flows therefore underwent a loss of competence and sediment was dumped. Banded slurry flows are also interpreted but represent a small percentage of deposits. Channel lobe transition zones from modern systems reach 10's of kilometres across and include individual scours up to 2.5 km in width (Wynn et al., 2002). At Mt. Salici, the location is likely a consequence of intraslope deformation.

6.1.2.2.5 Depositional lobes

Lobes are interpreted from the Mt. Salici middle subdivision. They have also been interpreted from western Sicily (Pescatore et al., 1987), southern mainland Italy (Carbone et al., 1987) and the zousa member of Tunisia (Riahi et al., 2010).

They consist of predominantly of fine grained turbidity current deposits showing normal grading, ripples (T_c) and upper stage plane beds (T_b), and are interbedded with mudstones. Other facies include fine to medium grained massive unstructured sandstones, linked debrites and cohesive debris flow deposits. Coarsening upwards cycles are recognised, with fine grained sections capped by lobe axis channels. Lobe axis deposits consist of amalgamated coarse grained turbidites within low aspect ratio channels. The sequence represent progradation of individual lobes from fringe to axis environments. Contrary to the other depositional elements described, waning turbidity currents are the primary depositional mechanism within lobe environments, resulting from a low gradient basin floor.

6.1.2.2.6 Intraslope ponded basin

At Mt. Salici, a progression from large channels (levee confined?) to stacked lobes to a channel lobe transition zone is interpreted. This is unlikely to result from a progradational sequences due to the large slope gradient changes implicated, high variability in palaeocurrents which indicate flow reflection from topographic relief, and an increasing in mud cap thickness in relation to coarser grained turbidite deposits. An intraslope ponded basin is considered likely, resulting from syn-depositional slope uplift.

Intraslope ponded basins are recognised from topographically complicated slopes including the Gulf of Mexico, Angola, and the North Sea such that they can be considered a relatively 'normal' slope condition. They are also interpreted from ancient outcropping turbidite systems including several basins from the Alps (Sinclair, 1992; Sinclair, 1997) but may be relatively under-represented in comparison to modern systems.

The scale of an intraslope ponded basin at Mt. Salici in Sicily is unknown and key pieces of evidence including onlap of lobes to a slope, and intraformational unconformaties, are lacking. The total section thickness is around 1800 m thick however, which is comparable to the thickness of the Auger field from the Gulf of Mexico, a ponded to bypass succession resulting from salt migration (Prather, 2000; Prather et al., 1998).

6.1.3 Following from questions 1 and 2, can conclusions be drawn about slope and fan architectures within the Numidian Flysch Formation?

6.1.3.1 Fan architecture

Entrenched slope channel complexes are interpreted from the Finale section of Sicily, and all three sections of Tunisia. They are a commonly recognised depositional element, and similar architectures are described from Numidian Flysch studies in Algeria (Laval, 1992; Vila et al., 1995). They are a depositional element recognised in upper slope environments from offshore West Africa, including from areas of tectonically uplifting slopes (Mayall et al., 2010) (Figure 6.2). This reduces the slope gradient below an equilibrium value based upon the average volume and sediment character of transiting flows, prompting flows to incise and become confined by lateral slope deposits (Kneller, 2003; Mayall et al., 2010). Their common interpretation throughout the Maghrebian Flysch Basin suggests however that they are a likely consequence of an above grade upper slope environment which is common to modern slope systems.

Aggradationally stacked channels are observed in the Karsa section of Sicily. They represent a below grade slope environment in which channels aggrade into available accommodation space

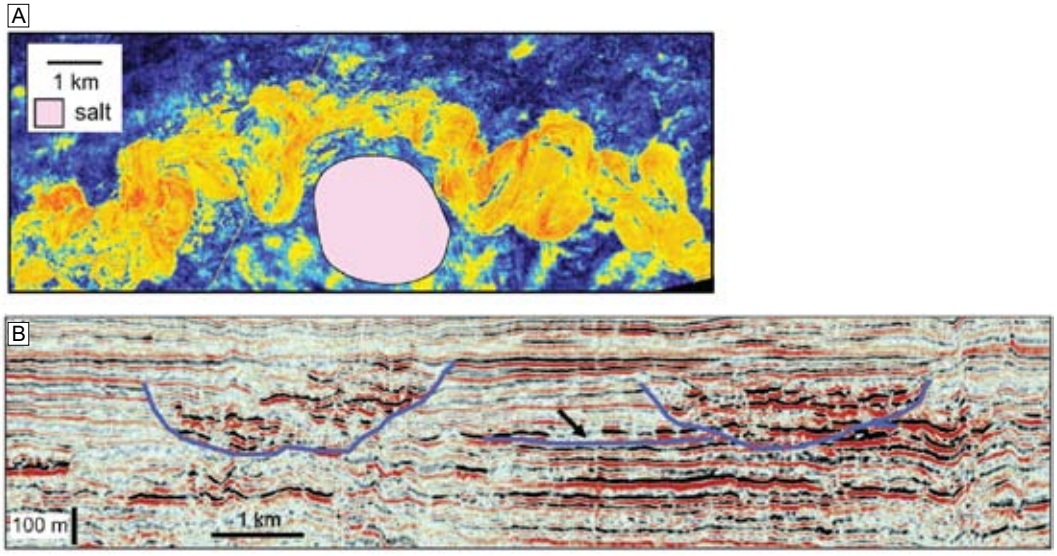

Figure 6.2.
Entrenched, slope confined channel complexes from offshore West Africa. Figure taken from Mayall et al, (2010). 6.2a. Seismic RMS amplitude extraction showing the sinuous architecture of channel complexes. Downslope orientation is to the left, while complexes show deflection around an uplifting salt diapir (pink). Bright colours are high amplitudes (e.g likely to be sandstones), cool colours are low amplitudes (e.g likely to be mudstones). 6.2b. A seismic line cross section through two large channel complexes. They are wider than thicker than examples observed from the Numidian Flysch, however their architectures (steep margins, flat bottoms and terracing) is similar. The purple line denotes the erosional complex base. A large overbank splay like feature is highlighted by the black arrow. This is similar to thick sandstone bodies which are truncated by channel complex Cr-5 from the Finale channel system, Sicily. Interpretation is taken from Mayall et al, (2010).

(Kneller, 2003). As such a lower slope environment is typically interpreted, where slope gradient decreases and flows reduce in velocity, prompting overbanking and levee construction (Kane et al., 2007; Pirmez and Imran, 2003).

Lobes and a channel lobe transition zone are interpreted from the Mt. Salici section (Sicily) and their context within an intraslope ponded basin is discussed. The Mt. Salici section evidences significant gradient changes with younging and as such the section represents slope and basin floor settings. Intraslope basins have not been discussed within previous Numidian Flysch Formation studies and provide a new way to interpret the complexity observed, both in placing stratigraphic sections within the context of the slope system, and the wide variation in recorded palaeocurrent orientations.

According to classic models of slope turbidite systems, these sections may be interpreted as upper slope, lower slope and basin floor environments (Mutti and Ricci Lucchi., 1978, Richards et al., 1998) and placed as a simple downslope palaeogeographic trend. In Sicily, this trend occurs from northwest to southeast. The sections in Sicily have not been correlated for this study however due to low resolution dating and lack of marker beds.

With the interpretation of an intraslope ponded basin at Mt. Salici this downslope trend is further complicated. However, given the lack of substantial sandstone outcrops elsewhere within Sicily and previous work which similarly interprets a southeast proximal to distal trend (e.g Faugeres et al., 1992), confidence is established that a Numidian Flysch fan axis is being recorded. Figure 6.3 develops a model which incorporates the depositional elements observed and their interpreted environments, and the relationship between them. Sections described therefore are not correlated and are described here as case studies within this Numidian Flysch fan. A question remains regarding the African provenance and an apparent contradiction with the palaeogeographic trend towards the southeast. This is addressed below in section 6.1.3.3.

6.1.3.1.1 Mechanisms for slope deformation

Triassic salt structures are known to have been active within the foreland and shelf of northern Tunisia (refs). In the present day they reach the coastline in the north (see chapter 4 figure 4.1) and are imaged in seismic data from offshore northern Tunisia. They are also known to have been active during the Oligocene and Miocene, and to have extruded onto the sea floor (Ben Slama et al., 2009; Vila et al., 2002). They represent a possible mechanism to generate intraslope deforma-

Figure 6.3. (following page)
Final conceptual model of the depositional elements interpreted from the Numidian Flysch Formation during this study (incorporating both Sicily and Tunisia). Annotation and representative scales are shown. Three environments are shown in a downslope trend (e.g downslope is towards the bottom left of the figure) along with the percentages of lithofacies recorded from each environment. From right to left the environments are: 6.3a. Upper slope environment; containing entrenched channel complexes which display offset stacking and internally nested channel elements. The Numidian Flysch Formation is shown transgressing Oligocene platform carbonates of the Panormide domain as is the case in northern Sicily (Carbone et al., 1990). 6.3b. Lower slope environment with aggradationally stacked channel complexes as interpreted at the Karsa section (Sicily). The 600 m thick section is shown incising a large mass transport complex. Levees are shown (as are required in an aggradationally stacked channel system) although they have not been observed at outcrop. 6.3c. Intraslope ponded basin as interpreted from the Mt. Salici section, Sicily. The model is shown during deposition of the upper subdivision where bypass of the ponded basin occurs. Deformation of the slope is shown to occur via Triassic evaporate intrusion although this is speculative (see section 6.1.3.1.1). 6.3d. The approximate positions of these environments are shown schematically on a downslope profile according to the slope equilibrium model of Kneller (2003). Entrenched channel complexes record a slope profile which is above equilibrium (negative accommodation space). Aggradational channel complexes record a slope profile below the equilibrium profile (positive accommodation space).

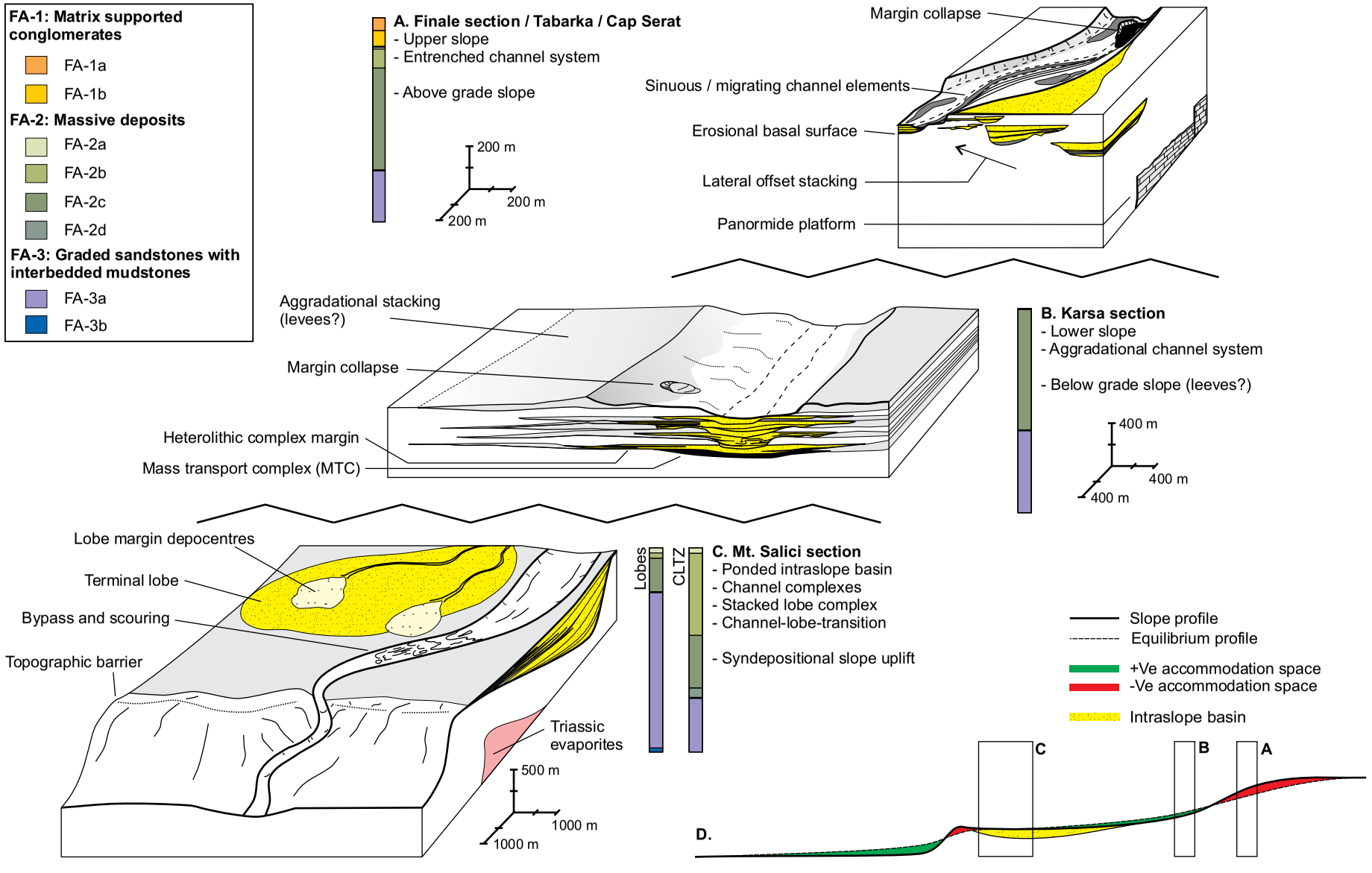
FA-1: Matrix supported conglomerates
FA-1a
FA-1b
FA-2: Massive deposits
FA-2a
FA-2b
FA-2c
FA-2d
FA-3: Graded sandstones with interbedded mudstones
FA-3a
FA-3b
A. Finale section / Tabarka / Cap Serat
- Upper slope
- Entrenched channel system
- Above grade slope
200 m
200 m
200 m
Margin collapse
Sinuous / migrating channel elements
Erosional basal surface
Lateral offset stacking
Panormide platform
Aggradational stacking (levees?)
Margin collapse
Heterolithic complex margin
Mass transport complex (MTC)
B. Karsa section
- Lower slope
- Aggradational channel system
- Below grade slope (leeves?)
400 m
400 m
400 m
Lobe margin depocentres
Terminal lobe
Bypass and scouring
Topographic barrier
Triassic evaporites
500 m
1000 m
1000 m
Lobes
CLTZ
C. Mt. Salici section
- Ponded intraslope basin
- Channel complexes
- Stacked lobe complex
- Channel-lobe-transition
- Syndepositional slope uplift
Slope profile
Equilibrium profile
+Ve accommodation space
-Ve accommodation space
Intraslope basin
C
B
A
D.

tion as occurs in the Gulf of Mexico (e.g Prather, 2000) and offshore Angola (Gee and Gawthorpe, 2006; Gee et al., 2007) (Figure 6.4). In these examples, salt driven tectonics produces ponded intraslope basins which are interpreted to show a fill to spill evolution as is interpreted from the Mt. Salici section.

Gravitational collapse of the slope sediment wedge upon a basal decollement may also provide an alternative mechanism. With ongoing encroachment of the orogenic wedge from the north, oversteepening of the slope is a likely consequence from the resulting basin floor subsidence, and would likely lead to gravitational collapse as the slope equilibrium is re-established. Such slope collapse is recognised from the Amazon fan (Reis et al., 2010). Thrust faulting within the collapsing wedge produces a series of ponded basins bound by both blind and emergent thrust fault tips. Thick debris flow deposits are located immediately downslope of the headwall scarp within some basins (Reis et al., 2010). Similar processes of slope collapse and “strong basin deformation” are interpreted by Carbone et al. (1987) to account for 200 m thick debris flow deposits (13% of stratigraphic thickness) within the Numidian Flysch Formation of Valsinni, southern Italy. Slope steepening from encroachment of the accretionary prism is also interpreted as a likely mechanism to account for increased slope incision with younging which is observed within the Finale channel system (chapter 4).

Given the similar Oligocene-Miocene tectonic histories throughout North Africa, a topographically complex slope may be a reasonable model for the rest of the basin.

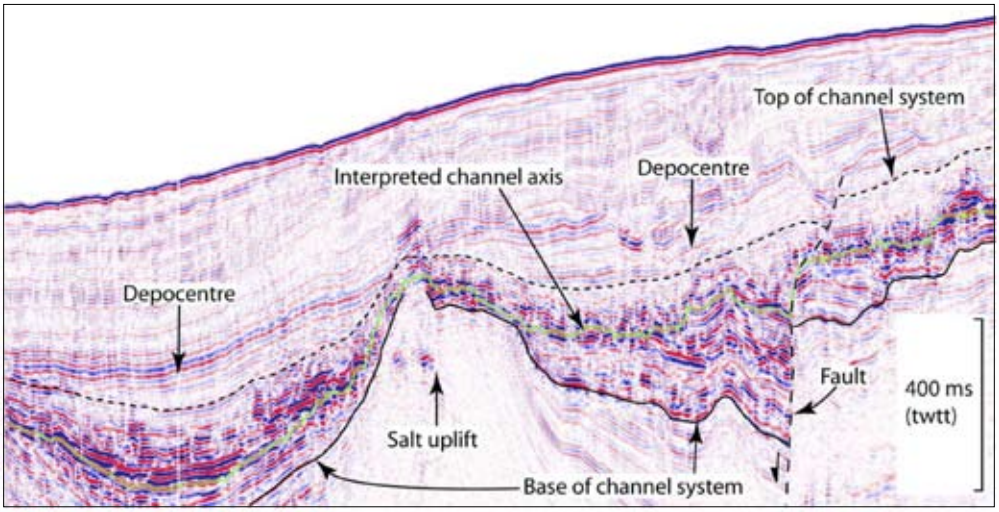

Figure 6.4.
Seismic line from offshore Angola taken from Gee and Gawthorpe, (2006) (their interpretation). Uplifting salt is shown to generate a topographically complex slope with ponded basins.

6.1.3.1.2 Connection of the fan to the foreland

Linking the Numidian Flysch Formation with the foreland has been problematic, and has in part generated the provenance controversy described above (Chapter 1, section 1.1.1). Vila et al. (1995) describes an Oligocene aged Numidian Flysch channel incised into African Tellian foreland sequences from Algeria and suggest that this represents a proximal sediment delivery route into the basin. The sections described within this thesis from both Sicily and Tunisia are also interpreted as upper slope entrenched channel systems. Fans within modern environments however typically contain a single large canyon which transitions downslope to a channelised system. These include the Zaire fan (Babonneau et al., 2002), the Ebro canyon offshore Spain (Bertoni and Cartwright,

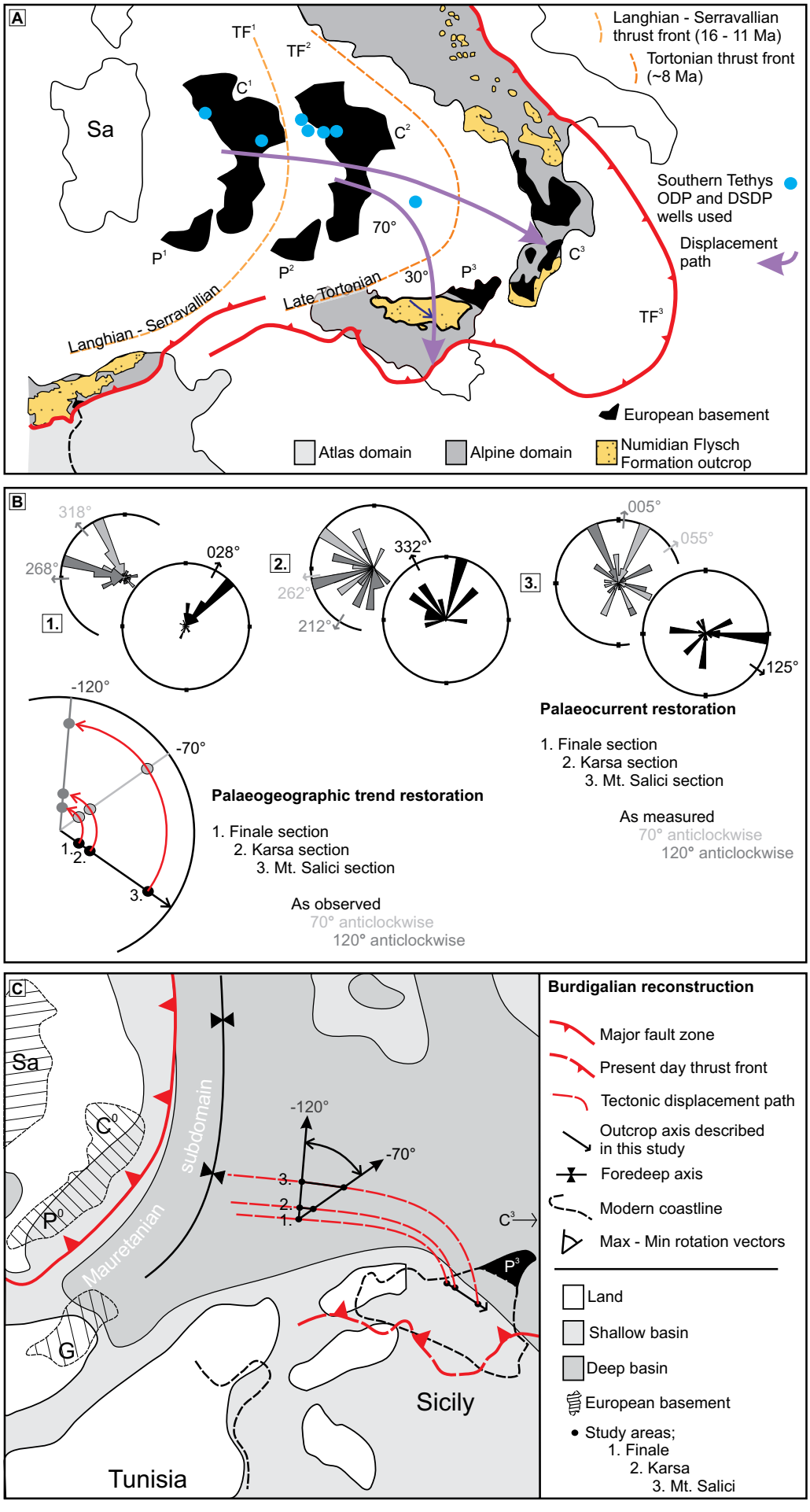
A
Langhian - Serravallian thrust front (16 - 11 Ma)
Tortonian thrust front (~8 Ma)
Sa
TF1
TF2
TF3
C1
C2
C3
P1
P2
P3
70°
30°
Late Tortonian
Langhian - Serravallian
Southern Tethys ODP and DSDP wells used
Displacement path
European basement
Atlas domain
Alpine domain
Numidian Flysch Formation outcrop
B
318°
268°
028°
1.
332°
262°
212°
2.
005°
055°
125°
3.
-120°
-70°
1.
2.
3.
Palaeogeographic trend restoration
1. Finale section
2. Karsa section
3. Mt. Salici section
As observed
70° anticlockwise
120° anticlockwise
Palaeocurrent restoration
1. Finale section
2. Karsa section
3. Mt. Salici section
As measured
70° anticlockwise
120° anticlockwise
C
Sa
C0
P0
G
subdomain
Mauretanian
-120°
-70°
3.
2.
1.
C3
P3
Sicily
Tunisia
Burdigalian reconstruction
Major fault zone
Present day thrust front
Tectonic displacement path
Outcrop axis described in this study
Foredeep axis
Modern coastline
Max - Min rotation vectors
Land
Shallow basin
Deep basin
European basement
Study areas;
1. Finale
2. Karsa
3. Mt. Salici

Figure 6.5. (Previous page)
Schematic palaeogeographic reconstruction of the Numidian Flysch fan axis described from Sicily in chapters 3 and 4 (shown by dark blue arrow): 6.5a; Published data on the timing and position of the accretionary prism thrust front and associated nappes, based upon palaeomagnetic data and taken from Speranza et al. (2003). P=Peloritani block (European basement block); Ca=Calabrian block (European basement block); TF=thrust front of accretionary prism. [1]= Langhian-Serravallian; [2]= Late Tortonian; [3]=Present day position. Sa=Sardinia. 6.5b; Restored rotations of palaeocurrents and the palaeogeographic trend from Sicily (fan axis described in chapters 3 and 4). Palaeocurrents are shown as recorded, and 'back rotated' by 70° (a minimum value based upon data from Monaco and De Guidi, 2006; Oldow et al., 1990; Somma, 2006; Speranza et al., 2003) and 120° (a maximum value based upon data taken from Oldow et al., 1990). The southeast palaeogeographic trend of the fan axis as interpreted in Sicily is also shown 'back rotated' by these values. 6.5c; A final reconstruction. The fan axis is shown back rotated and restored towards the northwest based upon data from figures 6.5a and 6.5b. A north to northeast downslope orientation results, dependant on which values of 'back rotation' are used.

2005) and the Monterey fan (e.g Paull et al., 2005). Canyons associated with Numidian Flysch sandstones have not been described on the North African margin, and here their possibility is explored.

Throughout proximal study areas of Sicily there is no evidence for significant erosional topography upon the platform carbonates which underlie the Numidian Flysch Formation. Furthermore, widespread petrographic analyses of Numidian Flysch sandstones throughout the MFB routinely describe a compositionally mature quartzarenite (Thomas et al., 2010) with no evidence for substantial extraformational carbonate or dolomite clasts. A canyon, were it to exist would therefore not have incised into underlying formations.

While canyons are a common feature of modern submarine fans given the current highstand and geologically recent glacial-maximum, models of submarine fans also include ramp systems, whereby a shallow gradient connects the uppermost submarine fan to shallow marine environments (see Richards et al., 1998). A submarine ramp environment with no significant shelf break is indeed recorded within the Bou Dabbous Formation of northern Tunisia, representing an Eocene carbonate ramp succession (El Euchi et al., 2000) prior to Numidian Flysch clastic deposition. The detachment and lateral eastwards allocthony of Numidian Flysch nappes from contemporaneous shallow water deposits, and the latter's subsequent burial by nappes of the MFB, do not allow for confirmation of this model however. If a canyon was indeed incisional into Meso-Cenozoic carbonate platform deposits of the African foreland, it could be expected to lie to the west of Sicily within the Sicily straight, at the northern edge of the Tunisian or pelagian platforms. 2D seismic lines from this area indicate southeast verging nappes of Miocene flysch deposits overlying Mesozoic to Miocene platform carbonates as is observed in northern Sicily (Catalano et al., 1995).

6.1.3.3 Placing the results within a basin context

The Numidian Flysch Formation is constrained by provenance to have been deposited in a passive margin setting (e.g not an active subduction related margin). An approximately south to north palaeogeographic trend therefore results. This contrasts however with a northwest to southeast downslope trend recognised in Sicily (chapter 3). The palaeocurrents recorded are highly variable with very different mean orientations recorded for each study area (including Tunisia). Given also the discussion above regarding provenance and analogue foreland basins, the use of palaeocurrents to determine a downslope trend is considered unsafe.

Published data on the evolution of the foreland fold-and-thrust-belt throughout the basin shows large horizontal rotations of the nappes and their basement during emplacement (Figure 6.5a). In Sicily, clockwise rotations of 70° are recorded using palaeomagnetic data (Monaco and De Guidi,

2006; Oldow et al., 1990; Somma, 2006; Speranza et al., 2003) while a palinspastic reconstruction of basement domains by Oldow et al. (1990) (Figures 1.5 and 1.6 in the chapter 1) suggests a clockwise rotation of 120° since the late Miocene (Figure 6.5b). This is coupled with a long range allocthonous transport which is also recognised using palaeomagnetic data from Sicily (Speranza et al., 2003) (Figure 6.5a).

Figure 6.5c attempts to schematically reconstruct the approximate location of the downslope trend recognised in Sicily, which is towards the southeast, based upon these constraints. Restoring the sections towards the Northeast, based upon the data of Speranza et al. (2003) (Figure 6.5a) places the sections to the north of the Tunisian coastline. When horizontal rotations are taken into account (Figure 6.5b and 6.5c), a consequent downslope trend towards the north or northeast results (dependent on which value of rotation is used). This is not perpendicular to the North African margin but runs slightly axially to the basin (Figure 6.5c). Matching these restored rotations to the palaeocurrent data (Figure 6.5b) also fails to match the palaeocurrent data to this northern trend.

The Numidian Flysch Formation of southern mainland Italy had a less rotated nappe transport but was still transported to the southeast (Speranza et al., 2003). These deposits, regardless of their deposition location would have been to the north of those in Sicily and Tunisia and would have lacked a distinct foreland other than that which was proximal to deposits in Sicily and Tunisia. The Ionian oceanic basin formed a separate basin to the east, and with Italian deposits dated as early to mid Miocene, the central portion of the MFB had already closed with continental collision from the early Miocene onwards (chapter 1). Flows are therefore constrained to have been sourced from an area between the Galite block (where the Galite Flysch and Numidian Flysch deposits are also dated as early Miocene in age (Belayouni et al., 2010) and the Pelagian shelf (Figure 6.5c). Interpreted as lobes (Carbone et al., 1987), the southern Italy sections of Numidian Flysch Formation are therefore interpreted as distal equivalents of the Sicilian deposits. As constrained within chapter 1, closure of the eastern portion of the MFB occurred in an eastwards direction. It can be speculated that this generated an east or northeastwards tilting basin axis, contributing to long run-out turbidity currents which culminated in the deposits of southern Italy.

The observed southeast palaeogeographic trend in Sicily can therefore be restored, via published structural data, to a northerly trend and matched to the both the African provenance and the location of Italian sections (Figure 6.5). This provides further confidence that the observed downslope trend (Figure 6.3) is genuine, given that that it has been impossible to correlate the sections using biostratigraphy.

6.1.4 What can the slope processes recorded within the Numidian Flysch Formation contribute to the wider discussion about deep marine sedimentology, particularly given its unique regional extent?

There are several characteristics identified which may be of interest regarding other deep marine studies.

6.1.4.1 The relationship between channel system hierarchies

Channel hierarchies are commonly recognised within studies of submarine channel systems. Several methods are used, and in particular applied to seismically imaged systems from offshore West Africa (Campion et al., 2000; Mayall et al., 2006; Sprague et al., 2005). They represent an attempt by oil exploration companies to formalise nomenclature in deep marine channel systems and asses heterogeneity. It is rare however that the interaction between the different hierarchies, and the impact of this interaction upon what is observed in seismic data is assessed. Hierarchies are also rarely quantified in terms of thickness and width. McHargue et al. (2010) has made a preliminary attempt at this which is discussed in chapter 4.

Characterisation of the seismic scale (5.7 km wide) Finale channel system (Sicily shows that it is organised into 3 hierarchical levels, comprising; 2 channel complex sets, 16 channel complexes, and 36 channel elements. Mappable channel complexes reach 500 m wide and 90 m thick and are also seismic in scale (e.g capable of being imaged by a standard industry seismic survey).

Channel elements are bound by a basal erosion surface and generally stack to form channel complexes. They show a progression of incision and bypass from coarse grained stratified flows, to fill with aggrading massive sandstones interspersed with waning turbidite deposits. Lateral expansion of the channel element width produces terracing within the complex margin, and has the capacity to alter flow rheology through incorporation of large mud volumes. Asymmetry observed at the channel complex scale results from sinuosity of channel element thalwegs which become offset from the thickest part of the complex. Non vertical stacking of channel elements, while rare, also increases the width of the channel complex. Channel elements which are typically subseismic, are therefore important factors in governing the geometry of seismic scale architectures. This has implications for reservoir heterogeneity at the sub-seismic scale, and also with ancient ourcropping channel complexes which are asymmetric, a characteristic which is often attributed to sinuosity.

Both channel-complexes and elements thicken with younging within the Finale channel system, indicating increased entrenchment through allocyclic forcing. The frequency distribution of channel-element thicknesses (n=35) also shows a positive skew centred around 12m, in agreement with data from examples of McHargue et al. (2010) (n=834). Many factors effect depth of erosion including slope gradient, location and sediment calibre. Given the statistically significant number of data points presented however, it seems likely that there is a fundamental (global) control upon the thickness of channel elements within all systems. An answer is not presented here, however the magnitude of high frequency eustatic cycles (e.g in relation to Milankovitch cyclicity) and a theoretical flow density maximum are two possibilities. Further work is required to clarify this relationship. Nevertheless, quantifying channel depositional hierarchies is useful, particularly in providing a measure of allocyclic controls where they are poorly understood.

6.1.4.2 Slope topography and its effect upon transiting flows

The impact of slope topography upon flow process and subsequent deposits is largely theoretical, with conceptual models such as Kneller (2003) and Kneller and McCaffrey (2003).

A significant downslope facies variability is recorded within the Numidian Flysch Formation of Sicily. Proximal entrenched channel complexes are composed predominantly of very coarse grained bedload deposits and massive ungraded sandstones from quasi steady turbidity currents. In contrast, lobes are dominated by strongly waning flow conditions, and the deposition of normally graded sandstones. Slope gradient, as to be expected, seems therefore to be extremely important in the

style of deposition. Steep proximal slopes inhibit flow waning (over the duration of the flow but not on short timescales) while low gradient basin lobe environments allow strong flow waning.

The change between these end members occurs between the lower slope and basin floor environments. Channel lobe transition zones (CLTZ) are an important feature which indeed separate lower slopes from basin floor environments due to a change in slope gradient (Wynn et al., 2002). They are an important factor in topographically complex slopes systems, are not commonly described in outcrop studies of turbidite systems. Cornamusini (2004) identified a CLTZ from the Macigno Costiero turbidite system in the Northern Apennines of Italy. Facies consist of thin-bedded pebble beds, massive pebbly sandstones and cross-stratified sandstones (their facies association 2; Coarse grained sandstones) characterised by amalgamation surfaces and scours. Boiano (1997) finds similar irregular and scoured coarse-grained sandstones and granule conglomerates in a CLTZ interpreted from the Gorgoglione Flysch Formation of the Italian Apennines. The coarse grained facies described from these studies are similar to Facies FA-2c and 2b from this study, which are the dominant lithofacies recorded.

Similar depositional architectures and lithofacies are therefore recorded within the Numidian Flysch Formation of Sicily and other ancient CLTZ examples. Its role in modifying transiting density flows is relatively unknown, with much discussion centred upon the role of hydraulic jumps. (Ito, 2008) for example finds erosion of the substrate in a CLTZ from the Otadai Formation, Japan, in which turbidity currents incorporate mud clasts and transform to debris flows. At Mt. Salici, a loss of capacity is interpreted to accompany flow deceleration such that massive ungraded sandstones fill scours. This alters the remaining flows substantially, reducing the median grainsize and contributing further to flow deceleration. The remainder flow then bypasses to the lobe with a strongly waning velocity profile. Many modern CLTZ examples such as the Agadir, Rhone and Valencia fans (Kenyon et al., 1995; Morris et al., 1998) contain the architectures described from ancient examples, but are relatively fine grained in comparison. Flows have therefore been interpreted to dump sediment downslope of a scour zone produced by a hydraulic jump. Wynn et al. (2002) discuss that variations in flow volume and density, which vary with each successive flow, will cause the location of the CLTZ to migrate up and downslope accordingly. Outcrop studies which can characterise CLTZ over a sufficient area may provide answers to some of these issues.

6.2. Implications for hydrocarbon exploration

As described in the introduction (Introduction section 1.1.3.1), the Numidian Flysch Formation produces gas in Sicily, and contains seeps and direct hydrocarbon indicators in Tunisia. The following findings are considered of importance to future exploration.

6.2.1 Trap types

Based upon this work, the most prolific large scale depositional element are upper slope entrenched channel systems. Given their scale (<100 m thick, 1200 m in width, <4 km in length) they represent reservoirs of substantial volume. In northern Sicily their lateral extent is limited by truncation through thrust faulting. Furthermore, examples in both northern and central Sicily (Sperlinga) are contained in nappes with a hanging wall anticline geometry. Structural trapping, bound by low angle thrust faults are therefore likely to be the most abundant mechanism.

Ponded basin successions provide the opportunity for stratigraphic trapping. Depositional lobes,

which are several kilometres in extent and pinch out gradually into mudstone dominated successions, are unlikely to be preserved completely given the restricted size of nappes. They are therefore unlikely to represent the opportunity for stratigraphic trapping. Nevertheless, syn-depositional intraslope deformation decreases net to gross with younging (as at Mt. Salici) and is likely to form thick fine grained sucessions which provide an effective cap to ponded lobe reservoirs. Onlap to intraslope highs similarly provides rapid pinch out of lobe bodies on to fine grained slope successions as with the Auger field, Gulf of Mexico (Prather et al., 1998). The potential for stratigraphic traps is therefore increased.

6.2.2 Connectivity of potential reservoirs

Networks of clastic injectites, particularly in Tunisia, provide multiple pathways between channel complex bodies as observed at Tabarka. Similarly, abundant minor injectites at the Mt. Salici section vertically connect >16 lobes within a 580 m section. Ptygmatic folding indicates early stage injections, prior to substantial burial. It is unlikely therefore highly that injectites cross thrust faults which date from late Miocene to Pliocene.

Entrenched channel complexes are also connected laterally though truncation of inter channel sandstones and minor channelforms which become amalgamated with channel element fill. Within the Finale channel system, complexes Cr-3 and Cr-5, separated laterally by 400 m of slope sediments, are likely to be connected via beds of massive sandstone and turbidites up to 5 m thick. In Sicily, injectites are less common, and vertical connectivity of potential channel complex reservoirs is likely to be less affected.

Within channel complexes however, the stacking of channel elements creates substantial heterogeneity. Channel element bases, particularly where high relief is present, reduce heterogeneity and amalgamate massive sandstones from successive elements both laterally and vertically. The impact of cohesive debris flows which reach several metres thick and are potential vertical flow baffles, is therefore reduced. Where channel element bases are not high relief, thin mudstone beds can separate channel elements, as at Tabarka (Tunisia). They are likely to be laterally continuous, although insufficient exposure is present to test this. If a channel element thalweg is present, mudstones are likely to be incised and their impact on vertical connectivity will be reduced.

6.2.3 Potential source rocks

Studies of Numidian Flysch Formation mudstones cite low total organic carbon contents. An unexplored possibility however lies with the Monterey excursion. Dated as 17 to 13.5 Ma (early to mid Miocene), the Monterey event was a positive carbon isotope excursion which correlates with the end of a global warm period and the start of an expansion of the Antarctic ice sheet (Jacobs et al., 1996). The event has been studied in the western Mediterranean within platform and ramp carbonate environments (Jacobs et al., 1996). In comparison, organic rich mudstones deposited during oceanic anoxic events during the Toarcian and Silurian represent major source rocks globally (Baudin et al., 1990; Luening et al., 2000).

This event is relatively late in comparison to the sections studied here, although the youngest age of the 1800 m thick Mt. Salici section is unknown. A 5 m thick ‘jet black’ mudstone layer at the top of the middle subdivision is unique in the sections studied, and the Monterey event represents a distinct possibility. The Numidian Flysch Formation of southern mainland Italy reached mid Miocene and the Monterey event is likely to be present within the sections described by Carbone et al.

(1987). Further attempts at dating the Numidian Flysch Formation are crucial to establish whether the Monterey event is important or not.

6.3. Final comments and future recommendations

The scale of the Numidian Flysch Formation is perhaps unique in deep marine outcropping successions. Its scale, which is greater than the width of the Gulf of Mexico and greater than the length of the Angolan margin, provides an opportunity to evaluate the controls on fan deposition at a truly regional scale. In order to exploit this opportunity however several issues must be tackled.

The issue of provenance, which has hampered understanding of the basin context, needs to be resolved in order to progress. The results of chapter 1, published in the journal Earth Science Reviews, provide a fairly robust argument for a constrained African source. The debate however continues with nine papers published since 2007 which argue for both European and African sources. Perhaps what is required are further studies of detrital zircon suites from both the Numidian Flysch Formation, and various Mauretanian Flysch formations. If these continue to show significantly different signatures which match the significantly different basement zircon suites of European and African terrains, then perhaps the issue of provenance can finally be resolved.

Dating of Numidian sections is also an issue, such that correlation with confidence remains problematic. It is difficult to see how this can be resolved but perhaps palynology and radiolaria may provide the best option given the large amount of decalcification within mudstone samples. Carbon, Oxygen and Strontium isotopes may also provide a useful tool to aide correlation in the future and evaluate climatic and eustatic controls. Correlations of Numidian dating and isotope stratigraphy with data from the foreland will therefore be a key development in correlation and assessing allogenic controls (assuming that an African source is accepted within the community).

Lastly, further work is required to test and further develop the concept of ponded basins in the Numidian Flysch Formation throughout the basin. As discussed above, the idea of topographically complex slope systems provides a new way of interpreting the complexity which is commonly observed in the Numidian, including palaeocurrents which have caused much concern since the 1960’s.

References.

Babonneau, N., Savoye, B., Cremer, M. and Klein, B., 2002. Morphology and architecture of the present canyon and channel system of the Zaire deep-sea fan. Marine and Petroleum Geology, 19(4): 445-467.

Baudin, F. et al., 1990. Distribution of organic matter during the Toarcian in the Mediterranean Tethys and Middle East. In: Y. Huc (Editor), Depostion of Organic Facies. AAPG Studies in Geology, pp. 73-92.

Belayouni, H. et al., 2010. La Galite Archipelago (Tunisia, North Africa): Stratigraphic and petrographic revision and insights for geodynamic evolution of the Maghrebian Chain. Journal of African Earth Sciences, 56(1): 15-28.

Ben Slama, M.M., Masrouhi, A., Ghanmi, M., Ben Youssef, M. and Zargouni, F., 2009. Albian extrusion evidences of the Triassic salt and clues of the beginning of the Eocene atlasic phase from the example of the Chitana-Ed Djebs structure (N.Tunisia): Implication in the North African Tethyan margin recorded events, comparisons. Comptes Rendus Geoscience, 341(7): 547-556.

Benomran, O., Nairn, A.E.M. and Schamel, S., 1987. Sources and dispersal of mid-Cenozoic clastic sediments in the central Mediterranean region. In: F. Lentini (Editor), Atti del convegno su; Sistemi avanfossa-avampaese lungo la Catena Appenninico-Maghrebide. Memorie della Societa Geologica Italiana. Societa Geologica Italiana, Rome, Italy, pp. 47-68.

Bertoni, C. and Cartwright, J., 2005. 3D seismic analysis of slope-confined canyons from the Plio–Pleistocene of the Ebro Continental Margin (Western Mediterranean). Basin Research, 17(1): 43-62.

Boiano, U., 1997. Anatomy of a siliciclastic turbidite basin: The Gorgoglione Flysch, Upper Miocene, southern Italy: Physical stratigraphy, sedimentology and sequence-stratigraphic framework Sedimentary Geology, 107(3-4): 231-262.

Bouma, A.H., 1962. Sedimentology of some Flysch deposits;: A graphic approach to facies interpretation. 168 pp: Elsevier.

Campion, K.M. et al., 2000. Outcrop expression of confined channel complexes. Deep-water reservoirs of the world: SEPM, Gulf coast section, 20th annual Research Conference, 20th annual Research Conference 127-50.

Carbone, S., Lentini, F., Sonnino, M. and De Rosa, R., 1987. Il flysch numidico di Valsinni (Appennino lucano)

Translated Title: The numidic flysch of Valsinni, Lucanian Apennines. Bollettino Della Societa Geologica Italiana, 106(2): 331-345.

Carbone, S., Catalano, S., Grasso, M., Lentini, F. and Monaco, C., 1990. Carta Geologica Della Sicilia Centro-Orientale (1: 50,000)

Catalano, R., Infuso, S. and Sulli, A., 1995. Tectonic History of the Submerged Maghrebian Chain from the Southern Tyrrhenian Sea to the Pelagian Foreland. Terra Nova, 7(2): 179-188.

Cornamusini, G., 2004. Sand-rich turbidite system of the Late Oligocene Northern Apennines foredeep: physical stratigraphy and architecture of the 'Macigno costiero' (coastal Tuscany, Italy). Geological Society, London, Special Publications, 222(1): 261-283.

El Euchi, H., Troudi, H., Tremolieres, P., Boubaker, H. and Rourou, A., 2000. Field trip guidebook; fractured carbonate reservoirs in central-northeast Tunisia. ETAP's Memoir Series. Enterprise Tunisienne d'Activites Petrolieres (ETAP), Tunis, Tunisia, 26 pp.

Faugeres, J.C., Broquet, P., Duee, G. and Imbert, P., 1992. Sedimentary Record of Volcanic and Paleocurrent Events in the Numidian Sandstones of Sicily - the Tuffites and Contourites of Karsa. Comptes Rendus De L Academie Des Sciences Serie Ii, 315(4): 479-486.

Garcia, M. and Parker, G., 1989. Experiments on hydraulic jumps in turbidity currents near a canyon-fan transition. Science, 245(4916): 393-396.

Garcia, M.H., 1993. Hydraulic jumps in sediment-driven bottom currents. Journal of Hydraulic Engineering-Asce, 119(10): 1094-1117.

Gee, M.J.R. and Gawthorpe, R.L., 2006. Submarine channels controlled by salt tectonics: Examples from 3D seismic data offshore Angola. Marine and Petroleum Geology, 23(4): 443-458.

Gee, M.J.R., Gawthorpe, R.L., Bakke, K. and Friedmann, S.J., 2007. Seismic geomorphology and evolution of submarine channels from the Angolan continental margin. Journal of Sedimentary Research, 77(5-6): 433-446.

Haughton, P., Davis, C., McCaffrey, W. and Barker, S., 2009. Hybrid sediment gravity flow deposits - Classification, origin and significance. Marine and Petroleum Geology, 26(10): 1900-1918.

Haughton, P.D.W., Barker, S.P. and McCaffrey, W.D., 2003. 'Linked' debrites in sand-rich turbidite systems - origin and significance. Sedimentology, 50(3): 459-482.

Hodgson, D.M., 2009. Distribution and origin of hybrid beds in sand-rich submarine fans of the Tanqua depocentre, Karoo Basin, South Africa. Marine and Petroleum Geology, 26(10): 1940-1956.

Hoyez, B., 1975. Dispersion du materiel quartzeux dans les formations aquitaniennes de Tunisie septentrionale et d' Algerie nord-orientale. Bulletin - Societe Geologique de France, 25(6): 1147-1156.

Ito, M., 2008. Downfan transformation from turbidity currents to debris flows at a channel-to-lobe transitional zone: The lower Pleistocene Otadai Formation, Boso Peninsula, Japan. Journal of Sedimentary Research, 78(9-10): 668-682.

Jacobs, E., Weissert, H., Shields, G. and Stille, P., 1996. The Monterey event in the Mediterranean; a record from shelf sediments of Malta. Paleoceanography, 11(6): 717-728.

Kane, I.A., Kneller, B.C., Dykstra, M., Kassem, A. and McCaffrey, W.D., 2007. Anatomy of a submarine channel-levee: An example from Upper Cretaceous slope sediments, Rosario Formation, Baja California, Mexico. Marine and Petroleum Geology, 24: 540-563.

Kenyon, N.H., Millington, J., Droz, L. and Ivanov, M.K., 1995. Scour holes in a channel-lobe transition zone on the Rhone Cone. Atlas of deep water environments: architectural style in turbidite systems: 212-215.

Kneller, B., 2003. The influence of flow parameters on turbidite slope channel architecture. Marine and Petroleum Geology, 20(6-8): 901-910.

Kneller, B.C. and Branney, M.J., 1995. Sustained High-Density Turbidity Currents and the Deposition of Thick Massive Sands. Sedimentology, 42(4): 607-616.

Kneller, B.C. and McCaffrey, W.D., 2003. The interpretation of vertical sequences in turbidite beds: The influence of longitudinal flow structure. Journal of Sedimentary Research, 73(5): 706-713.

Lancelot, J., Reille, J.L., Wezel, F.C., 1977. Etude morphologique et radiochronologique de zircons détritiques des flyschs "numidien" et "gréso-micacé". Bulletin De La Societe Geologique De France 7 (19), 773–780.

Laval, F., 1992. Gravity Depositional Systems and Sedimentary Megasequence of the Numidian Flysch Formation, North and East of the Grande Kabylie Massif (Algeria). Geodinamica Acta, 5(4): 217-233.

Luening, S., Craig, J., Loydell, D.K., Storch, P. and Fitches, B., 2000. Lower Silurian "hot shales" in North Africa and Arabia; regional distribution and depositional model. Earth-Science Reviews, 49(1-4): 121-200.

Mayall, M., Jones, E. and Casey, M., 2006. Turbidite channel reservoirs - Key elements in facies prediction and effective development. Marine and Petroleum Geology, 23(8): 821-841.

Mayall, M. et al., 2010. The response of turbidite slope channels to growth-induced seabed topography. Aapg Bulletin, 94(7): 1011-1030.

McHargue, T. et al., 2010. Architecture of turbidite channel systems on the continental slope: Patterns and predictions. Marine and Petroleum Geology, 28(3): 728-743.

Monaco, C. and De Guidi, G., 2006. Structural evidence for Neogene rotations in the eastern Sicilian fold and thrust belt. Journal of Structural Geology, 28(4): 561-574.

Morris, Kenyon, Limonov and Alexander, 1998. Downstream changes of large-scale bedforms in turbidites around the Valencia channel mouth, north-west Mediterranean: implications for palaeoflow reconstruction. Sedimentology, 45(2): 365-377.

Mutti, E. and Ricci Lucchi, F., 1978. Turbidites of the northern Apennines: introduction to facies analysis. International Geology Review, 20(2): 125 - 166.

Oldow, J.S., Channell, J.E.T., Catalano, R. and D, A.B., 1990. Contemporaneous thrusting and large-scale rotations in the western Sicilian fold and thrust belt. Tectonics, 9(4): 661-681.

Paull, C.K., Mitts, P., Ussler, W., Keaten, R. and Greene, H.G., 2005. Trail of sand in upper Monterey Canyon: Offshore California. Geological Society of America Bulletin, 117(9-10): 1134-1145.

Pescatore, T., Renda, P. and Tramutoli, M., 1987. Facies ed evoluzione sedimentaria del bacino Numidico nelle Madonie occidentale (Sicilia). Memorie-Societa Geological Italiana, 38: 297-316.

Pirmez, C. and Imran, J., 2003. Reconstruction of turbidity currents in Amazon Channel. Marine and Petroleum Geology, 20(6-8): 823-849.

Prather, B.E., 2000. Calibration and visualization of depositional process models for above-grade slopes: a case study from the Gulf of Mexico. Marine and Petroleum Geology, 17(5): 619-638.

Prather, B.E., Booth, J.R., Steffens, G.S. and Craig, P.A., 1998. Classification, lithologic calibration, and stratigraphic succession of seismic facies of intraslope basins, deep-water Gulf of Mexico. Aapg Bulletin-American Association of Petroleum Geologists, 82(5): 701-728.

Reis, A.T. et al., 2010. Two-scale gravitational collapse in the Amazon Fan: a coupled system of gravity tectonics and mass-transport processes. Journal of the Geological Society, 167(3): 593-604.

Riahi, S. et al., 2010. Stratigraphy, sedimentology and structure of the Numidian Flysch thrust belt in northern Tunisia. Journal of African Earth Sciences, 57(1-2): 109-126.

Richards, M., Bowman, M. and Reading, H., 1998. Submarine-fan systems - I: characterization and stratigraphic prediction. Marine and Petroleum Geology, 15(7): 689-717.

Sinclair, H.D., 1992. Turbidite sedimentation during Alpine thrusting: the Taveyannaz sandstones of eastern Switzerland. Sedimentology, 39(5): 837-856.

Sinclair, H.D., 1997. Tectonostratigraphic model for underfilled peripheral foreland basins: An Alpine perspective. Geological Society of America Bulletin, 109(3): 324-346.

Somma, R., 2006. The south-western side of the Calabrian Arc (Peloritani Mountains): Geological, structural and AMS evidence for passive clockwise rotations. Journal of Geodynamics, 41(4): 422-439.

Speranza, F., Maniscalco, R. and Grasso, M., 2003. Pattern of orogenic rotations in central-eastern Sicily: implications for the timing of spreading in the Tyrrhenian Sea. Journal of the Geological Society, 160: 183-195.

Sprague, A.R. et al., 2005. Integrated slope channel depositional models: the key to successful prediction of reservoir presence and quality in offshore West Africa. CIPM, cuarto E-Exitep 2005, February 20-23 2005. Veracruz, Mexico.: 1-13.

Swezey, C.S., 2009. Cenozoic stratigraphy of the Sahara, Northern Africa. Journal of African Earth

Sciences, 53(3): 89-121.

Thomas, M.F.H., Bodin, S., Redfern, J. and Irving, D.H.B., 2010. A constrained African craton source for the Cenozoic Numidian Flysch: Implications for the palaeogeography of the western Mediterranean basin. Earth-Science Reviews, 101(1-2): 1-23.

Vila, J.M. et al., 1995. The Sandy Uppermost Oligocene Channel and the Miocene of Sidi-Affif Area in Their East Algerian Structural Setting - the Saharan Origin of the Numidian and the Calendar of the Miocene Overthrusts. Comptes Rendus De L Academie Des Sciences Serie Ii, 320(10): 1001-1009.

Vila, J.M., Ghanmi, M., Youssef, M.B. and Jouirou, M., 2002. The submarine “salt glaciers” of northeastern Maghreb (Algeria and Tunisia), and the US Gulf Coast passive continental margins: Comparisons, special look on the composite “salt glaciers” illustrated by the Fedj el Adoum structure (northwestern Tunisia), and global review. Eclogae Geologicae Helvetiae, 95(3): 347-380.

Wezel, F.C., 1969. Lineamenti Sedimentologico Del Flysch Numidico Della Sicilia Nord-Orientale. Memorie Degli Instituti Di Geologia e Mineralogia Del L’Universita Di Padova, 26.

Wynn, R.B., Kenyon, N.H., Masson, D.G., Stow, D.A.V. and Weaver, P.P.E., 2002. Characterization and recognition of deep-water channel-lobe transition zones. Aapg Bulletin, 86(8): 1441-1462.

Appendices.

Appendix 1.

Thomas et al. (2010)

M. F. H. Thomas, S. Bodin, and J. Redfern. 2010. Comment on ‘European provenance of the Numidian Flysch in northern Tunisia’ by Fildes et al. (2010). Terra Nova, Vol 22, No. 6, 501–503

Terra Nova

COMMENT

doi: 10.1111/j.1365-3121.2010.00967.x

Comment on 'European provenance of the Numidian Flysch in northern Tunisia' by Fildes *et al.* (2010)

M. F. H. Thomas,[1] S. Bodin[1,2] and J. Redfern[1]

[1]*North Africa Research Group, School of Earth, Atmospheric and Environmental Sciences, The University of Manchester, Williamson Building, Oxford Road, Manchester M13 9PL, UK;* [2]*Present address: Institute for Geology, Mineralogy and Geophysics, Ruhr-University Bochum, Universitätsstrasse 150, D-44801 Bochum, Germany*

Fildes *et al*. (2010) provide a valuable contribution and much needed data regarding the problem of Numidian Flysch provenance. However, when viewed in the context of previously published data, we believe the evidence better supports an African than a European provenance as interpreted in their study.

The Oligocene–Miocene Numidian Flysch is a suite of deep-marine sandstones with a quartz-rich petrofacies. It crops out within the Alpine thrust belt of North Africa, extending into Spain, Sicily and Italy. It was deposited in a foreland basin bordered to the south by the North African passive margin and to the north by an active margin consisting of European crustal blocks called the AlKaPeCa domain.

The addition of new data by Fildes *et al*. (2010) enables much discussion, and here we focus on the interpretation of their detrital zircon data when integrated with previous studies and viewed in a regional context.

Detrital zircon geochronology

Detrital zircons provide a valuable tool for the identification of sediment provenance, dependent upon the quality and quantity of zircon dating from potential source regions. As Fildes *et al*. (2010) make clear, there have been previous attempts to characterise the Numidian Flysch detrital zircon suite. In these studies, zircon dates of 1.35 Ga ± 60 Ma and 1.83 Ga ± 100 Ma (Lancelot *et al*., 1977) and 1.75 Ga ± 100 Ma (Gaudette *et al*., 1975) have been attained, and were interpreted as a signature typical of African basement, being similar to ages recorded in the Algerian Hoggar. Within the same study of Lancelot *et al*. (1977), immature-micaceous flysch deposits (the Troina-Tusa Flysch Fm) from northern Sicily, which were deposited coevally with the Numidian Flysch, show Permo-Carboniferous age zircons (290–310 Ma), which Lancelot *et al*. (1977) suggested as a European affinity. These two contrasting petrofacies are mirrored in Alpine nappes throughout North Africa, resulting in two flysch zones termed the Mauretanian and Massylian subdomains, characterised by immature and ultramature petrofacies respectively (see De Capoa *et al*., 2007). In Tunisia, these subdomains are represented by the immature Galite Flysch Fm (Mauretanian subdomain), which is juxtaposed against the coeval ultramature Numidian Flysch (Massylian subdomain) on the Galite archipelago (Belayouni *et al*., 2010).

The study of Fildes *et al*. (2010) obtained zircon dates of 514 ± 19 and 550 ± 28 Ma from the Numidian Flysch of Tunisia and Sicily respectively, which are considerably younger than dates reported by previous studies, and are interpreted as characteristic of a European source. Their evidence for this is that Rb–Sr dating of mica (Bossiere and Peucat, 1986) from the Kabylie basement block (part of the European AlKaPeCa domain, now accreted to northern Algeria) yielded dates of *c*. 505 Ma. Their conclusion is therefore a European provenance for the Numidian Flysch sandstones. We suggest that a thorough review of basement zircon chronology (excluding other radioisotope dating methods) from both African and European terranes reveals an alternative interpretation.

A review of published zircon ages from African basement, presented in histogram format, reveals that Cambrian and Precambrian ages are common. Dates of 450–600 Ma and *c*. 2 Ga correspond to the Pan-African and Eburnian orogenic events respectively (e.g. Ennih *et al*., 2002). The European basement blocks from the AlKaPeCa domain (the northern, European margin of the basin) reveal a distinctly different signature, with peak frequencies around 25–40 Ma (Eocene–Oligocene), 300 Ma (Permo-Carboniferous) and only rare dates between 450 and 650 Ma (Cambrian to Neoproterozoic) (e.g. Peucat *et al*., 1996). These dates correspond to the Alpine, Hercynian and Pan-African events respectively. Example frequency distributions are demonstrated in Fig. 1 using data from the African Hoggar basement block of southern Algeria (Bertrand *et al*., 1986; Paquette *et al*., 1998), in comparison with examples from the European Kabylie block of northern Algeria (Peucat *et al*., 1996; Hammor *et al*., 2006). Similar results for the African basement are found within the West African craton, Hoggar and Tibesti massifs and East African craton, while ages recorded for the European Kabylie block are consistent with results from across the AlKaPeCa domain (including the Peloritan and Calabrian blocks). A more comprehensive review of basement-terrain zircon suites is provided in Thomas *et al*. (2010).

The zircon ages characterised by Fildes *et al*. (2010) (514 ± 19 and 550 ± 28 Ma) are therefore recognised in both European and African

Correspondence: Mr Myron Francis Hubert Thomas, Earth, Atmosphere and Environmental Sciences, The University of Manchester, Rm. 1.62, The Williamson Building, Manchester M13 9PL, UK. Tel.: +44(0)161 275 7679; fax: +44(0)161 306 9361; e-mail: myron.thomas@manchester.ac.uk

Comment Terra Nova, Vol 22, No. 6, 501–503

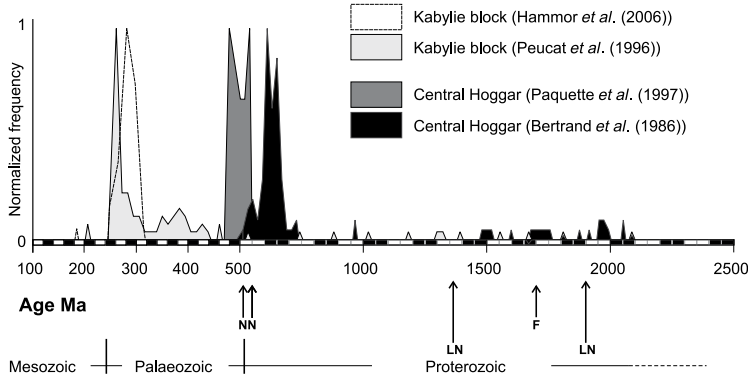

Fig. 1 A frequency histogram comparing zircon ages from the European Kabylie block of northern Algeria and the Hoggar area of southern Algeria. New detrital zircon ages from Fildes *et al.* (2010) are shown with short arrows; N for Numidian Flysch ages, F for the Fortuna Delta age. Long arrows (LN) show Numidian Flysch detrital zircon ages obtained by Lancelot *et al.* (1977).

basement blocks; however, considering their frequency distributions, an African source is statistically far more likely (Fig. 1). Furthermore, a typical Kabylie-sourced signature (European) should record mostly Hercynian age zircons, with some Alpine and rare Pan-African ages. In contrast, zircon studies from the Numidian Flysch have not recorded Hercynian (Permo-Carboniferous) age zircons. This Kabylie signature is, however, similar to that of the immature Troina-Tusa Flysch Fm of Sicily (Lancelot *et al.*, 1977) suggesting that it has a northern provenance rather than the Numidian Flysch. This implies that immature flysch deposits of the Mauretanian subdomain are sourced from European blocks such as the Kabylies, while the ultramature Numidian Flysch petrofacies is sourced from African terrains. Further characterisation of the detrital zircon suites of immature Mauretanian deposits throughout the entire Alpine chain is, however, required to clarify the relationship of this flysch subdomain to the northern and southern margins of the basin.

Fildes *et al.* (2010) also compare these results with dates of 1.698 Ga ± 67 Ma which they obtained from the autocthonous Fortuna Delta of Tunisia, long suggested as a possible Numidian Flysch sediment route from North Africa (e.g. Yaich *et al.*, 2000). Theses ages are significantly older than their Numidian Flysch data, such that it is suggested they rule out the Fortuna Delta, and thereby North Africa, as a possible source region. These Fortuna Delta dates are, however, in reasonable agreement with Numidian Flysch zircon data of Lancelot *et al.* (1977) from Sicily (Fig. 1). However, given the widespread occurrence of Numidian Flysch throughout North Africa, it may be unhelpful to focus solely upon the Fortuna Delta as a possible sediment input route, given that analogue foreland basins show sediment can travel significant distances along basin strike. Even if an African provenance is interpreted, problems raised by Yaich *et al.* (2000) and Fildes *et al.* (2010) would appear to rule it out.

Implications of the detrital zircon results

Our interpretation is that detrital zircon data from Fildes *et al.* (2010), supported by previous studies, point strongly towards an African source. Discussion is therefore required as to why other data such as palaeocurrents do not always support this conclusion.

Palaeocurrent data presented by Fildes *et al.* (2010, fig. 4) point to a fairly uniform southwards flow direction. However, datasets of previous authors from Sicily, Tunisia and Algeria often show different and contrasting results, which include northward flow directions (e.g. Hoyez, 1975). This inconsistency has undoubtedly been one of the main causes of the provenance debate. Horizontal rotations may have had a significant impact on palaeocurrent orientations during structuration. Indeed, field observations in Tunisia show the thrust-belt strike to vary by up to 50°, while nappes in Sicily are shown by palaeomagnetic studies to have rotated by up to 70° during emplacement (Thomas *et al.*, 2010 and references therein). Furthermore, palaeoflow within analogue foreland basins appears to be highly complex and is commonly orientated parallel to basin strike rather than parallel to the dipslope (Thomas *et al.*, 2010 and references therein). A simple northward or southward orientation may therefore be unlikely.

Finally, given that zircon studies strongly point to an African source, finding Numidian sediment input paths on the North African margin is indeed a challenge. Laval (1992) suggested a possible main sediment input in central Algeria; however, the emplacement of Alpine nappes upon the African foreland coupled with a forebulge unconformity means that contemporaneous fluvial and shallow-marine sediments are commonly missing or poorly understood.

Summary

The data provided by Fildes *et al.* (2010) are very welcome and a valuable addition to the literature. We suggest, however, that their detrital zircon data, which is dominated by Pan-African and Eburnian but no Hercynian ages, strongly favours an African rather than a European source when compared with zircon suites from the Kabylie block and other basement terrains. An African

Terra Nova, Vol 22, No. 6, 501–503 Comment

provenance is also in agreement with previous detrital zircon studies of the Numidian Flysch from Sicily and Gibraltar.

Given the consensus of these studies, further discussion is required as to why palaeocurrent orientations often offer contrasting results. Characterising the detrital zircon suites of immature flysch deposits from the Mauretanian subdomain and establishing the relationship between them and the Numidian Flysch will also be important factors in reconstructing basin architecture. Thomas *et al*. (2010) present a further discussion of these issues within the context of the western Mediterranean basin.

References

Belayouni, H., Brunelli, D., Clocchiatti, R., Brunelli, D., Clocchiatti, R., Di Staso, A., Hassani, I.E.E.A.E., Guerrera, F., Kassaa, S., Ouazaa, N.L.M., Manuel, M.M., Serrano, F. and Tramontana, M., 2010. La Galite Archipelago (Tunisia, North Africa): stratigraphic and petrographic revision and insights for geodynamic evolution of the Maghrebian Chain. *J. Afr. Earth Sci.*, **56**, 15–28.

Bertrand, J.-M., Michard, A., Boulier, A.-M. and Dautel, D., 1986. Structure and U/Pb geochronology of central Hoggar (Algeria): a reappraisal of its Pan-African evolution. *Tectonics*, **5**, 955–972.

Bossiere, G. and Peucat, J.J., 1986. Structural evidence and Rb-Sr, Ar-39-40 mica ages relationships for the existence of an Hercynian deep crustal shear zone in Grande Kabylie (Algeria) and its Alpine reworking. *Tectonophysics*, **121**, 277–294.

De Capoa, P., Di Staso, A., Perrone, V. and Zaghloul, M.N., 2007. The age of the foredeep sedimentation in the Betic-Rifian Mauretanian Units: a major constraint for the reconstruction of the tectonic evolution of the Gibraltar Arc. *C. R. Geosci.*, **339**, 161–170.

Ennih, N., Laduron, D., Greiling, R.O., Errami, E., de Wall, H. and Boutaleb, M., 2002. Pan-African overprint on Eburnian granitoids at the northern boundary of the West African Craton, Zenaga Inlier, central Anti-Atlas, Morocco. *J. Afr. Earth Sci.*, **32**, 677–693.

Fildes, C., Stow, D., Riahi, S., Soussi, M., Patel, U., Milton, A.J. and Marsh, S., 2010. European provenance of the Numidian Flysch in northern Tunisia. *Terra Nova*, **22**, 94–102.

Gaudette, H.E., Hurley, P.M. and Lajmi, T., 1975. Source area of the Numidian flych of Tunisia as suggested by detrital zircon ages. In: *The Geological Society of America 1975 annual meetings (7th September. Boulder, Colorado). Abstracts with programs*, **7**(7), 1083–1084.

Hammor, D., Bosch, D., Caby, R. and Bruguier, O., 2006. A two-stage exhumation of the Variscan crust: U-Pb LA-ICP-MS and Rb-Sr ages from Greater Kabylia, Maghrebides. *Terra Nova*, **18**, 299–307.

Hoyez, B., 1975. Dispersion du materiel quartzeux dans les formations aquitaniennes de Tunisie septentrionale et d' Algerie nord-orientale. *Bull. Soc. Geol. France*, **25**, 1147–1156.

Lancelot, J., Reille, J.L. and Wezel, F.C., 1977. Etude morphologique et radiochronologique de zircons détritiques des flyschs 'numidien' et 'gréso-micacé'. *Bull. Soc. Geol. France*, **7**, 773–780.

Laval, F., 1992. Gravity depositional systems and sedimentary megasequence of the Numidian Flysch Formation, North and East of the Grande Kabylie Massif (Algeria). *Geodin. Acta*, **5**, 217–233.

Paquette, J.L., Caby, R., Djouadi, M.T. and Bouchez, J.L., 1998. U-Pb dating of the end of the Pan-African orogeny in the Tuareg shield: the post-collisional syn-shear Tioueine pluton (Western Hoggar, Algeria). *Lithos*, **45**, 245–253.

Peucat, J.J., Mahdjoub, Y. and Drareni, A., 1996. U-Pb and Rb-Sr geochronological evidence for late Hercynian tectonic and Alpine overthrusting in Kabylian metamorphic basement massifs (northeastern Algeria). *Tectonophysics*, **258**, 195–213.

Thomas, M.F.H., Bodin, S., Redfern, J. and Irving, D.H.B., 2010. A constrained African craton source for the Cenozoic Numidian Flysch: implications for the palaeogeography of the western Mediterranean basin. *Earth Sci. Rev.*, **101**, 1–23.

Yaich, C., Hooyberghs, H.J.F., Durlet, C. and Renard, M., 2000. Stratigraphic correlation between the Numidian formation (North Tunisia) and Oligo-Miocene deposits of central Tunisia. *C. R. Acad. Sci. II a Sci. Terre Planetes*, **331**, 499–506.

Received 22 March 2010; revised version accepted 15 August 2010

Appendix 2.

Stow et al. (2010)

Dorrik Stow, Christine Fildes, Sami Riahi, Mohamed Soussi, Urval Patel, J. Andy Milton and Stuart Marsh. 2010. Reply to comment on ‘European provenance of the Numidian Flysch in northern Tunisia’. Terra Nova, Vol 22, No. 6, 504–505

Terra Nova

REPLY

doi: 10.1111/j.1365-3121.2010.00966.x

Reply to comment on 'European provenance of the Numidian Flysch in northern Tunisia'

Dorrik Stow,[1] Christine Fildes,[2] Sami Riahi,[3] Mohamed Soussi,[3] Urval Patel,[4] J. Andy Milton[5] and Stuart Marsh[6]

[1]*Institute of Petroleum Engineering, Heriot-Watt University, Edinburgh EH14 4AS, UK;* [2]*School of Environment, University of Auckland, Private Bag 92012, Auckland, New Zealand;* [3]*Geology Department, Faculty of Science, University of Tunis, Tunis, Tunisia;* [4]*Core Laboratories, Redhill, Surrey RH1 2LW, UK;* [5]*National Oceanography Centre, Southampton SO14 3ZH, UK;* [6]*Anadarko (Algeria) Company LLC, 1 Harefield Road, Uxbridge UB8 1YH, UK*

The Numidian Flysch is a major sedimentary succession that straddles the two distinct tectonic plates of Africa and Eurasia. Its accumulation during parts of the Oligocene and Miocene epochs represents an important phase in the tectonic development of the region, marked by basin formation and active sedimentary fill during the continued closure of the Tethys Seaway. It reservoirs a producing gas field in the subsurface of Sicily and is the subject of active oil exploration offshore in the western Mediterranean region. However, it is a complex succession and there are many questions remaining, including that of its ultimate provenance.

In our recent paper (Fildes *et al*., 2010), we presented new data on the Numidian Flysch of northern Tunisia and argued that these provided good evidence for an original European provenance. The data were certainly preliminary in nature, with more analyses currently in progress, and there is clearly still room for debate. We therefore welcome the comment on our paper by Thomas *et al*. (2010a), based on previously published zircon geochronology data. We further acknowledge their excellent and more substantial review recently published (Thomas *et al*., 2010b), which also promotes an African provenance for the Numidian Flysch.

However, having carefully considered their review of the literature on zircon dating, we are inclined to maintain our interpretation of a northern (European) provenance. We take this opportunity, therefore, to reinforce our earlier arguments, to introduce some new data and to propose further lines of research that we suggest will produce fruitful results in the future.

Correspondence: Professor Dorrik Stow, Institute of Petroleum Engineering, Heriot-Watt University, Edinburgh EH14 4AS, UK. Tel.: +44 (0)7887 870309; fax: +44 (0)131 451 3173; e-mail: dorrik.stow@pet.hw.ac.uk

Combined evidence

As with most areas of geology, the best and most reliable interpretations are made by considering *multiple* datasets rather than one alone. In this case, the combination of evidence we believe is very strong and includes the following.

Palaeogeographic reconstruction

All tectonic reconstructions place the Numidian Flysch basin (or series of basins) somewhere between Europe and North Africa. We know from previous biostratigraphic studies and from our own recent work (Riahi *et al*., 2010a; 2010b) that the principal sedimentary fill took place from about 35 to 20 Ma, and that final thrust emplacement was around 15 Ma. It is reasonable to assume that, during this time, the basin was moving southwards in front of the European crustal block (the so-called AlKaPeCa domain) – let us say at a relatively slow average rate of spreading/emplacement of 2–3 cm year^{-1}. This would therefore result in a net southward movement of between 400 and 600 km over a 20 Ma period. Such a distance is similar to the maximum width of the western Mediterranean Sea today, so that at least the *early* basin fill would have been a long way from any African supply system.

It is possible that as convergence continued and the Numidian Basin approached northern Africa, there would have been potential for additional supply from an African source during the *late* stages of basin fill. However, as the foredeep portion of the foreland basin is occupied by an immature Mauritanian Flysch system of similar age, the Numidian Flysch should have been confined to the backdeep (or back-bulge) region to the north of a fore-bulge high. Both the fore- and back-bulge areas of foreland basins are typically of shallow-water affinity and unlikely, therefore, to be depositional sites for a thick succession of deep-water turbidites.

Coastal barrier

Other work is currently underway at the University of Tunis on the equivalent-age rocks immediately south of the Numidian Flysch thrust front in northern Tunisia. These are represented by: (i) coarse-grained, mineralogically immature siliciclastics of the fluvial–deltaic Fortuna Formation (as mentioned in Fildes *et al*., 2010); (ii) shallow-marine carbonates of various lithofacies; and (iii) minor glauconitic sandstones of shallow-marine affinity. Locally, the carbonate and glauconitic sandstones appear to have accumulated on a relative tectonic high (perhaps the fore-bulge region mentioned above) and therefore to have acted as an effective barrier to sediment supply from the Fortuna delta. Of course, we accept the proposition of Thomas *et al*. (2010a,b) that supply to the Numidian Flysch basin could have been in part longitudinal, from further to the west for example.

Terra Nova, Vol 22, No. 6, 504–505

Fluvio-deltaic supply

There is little doubt that the volume of sediment represented by the Numidian Flysch formation, even that of northern Tunisia alone, requires prolonged input from a major sediment supply route – presumably one or more fluvio-deltaic systems. The *only* one known from northern Africa is the Fortuna system, which is why it has been implicated as the principal supply route by proponents of a North African provenance. However, the combined data presented (above and below) militate against the Fortuna, as accepted by Thomas *et al.* (2010a,b). They therefore invoke lateral supply from Algeria in the west and assume that all evidence of the major fluvio-deltaic supply system has been removed by subsequent erosion. This seems to us to be an unnecessarily complex explanation.

Palaeocurrent directions

The data we presented are difficult to ignore completely and represent a compilation of our own observations and those reported in the literature. They very dominantly show a north–south directed supply route. Certainly there are local variations from this norm, exactly as one would expect in any sedimentary system – indeed, we might have anticipated a still more diverse pattern. Large-scale uniform rotation of the entire emplaced succession, by at least 50 degrees as proposed by Thomas *et al.* (2010b), once again seems unnecessary. An irregular-shaped thrust front as observed in the field is entirely normal in complex emplacement terranes and does not necessarily imply rotation of individual parts.

Petrographic and heavy-mineral data

Highly quartz-rich sandstone assemblages, such as the Numidian Flysch, are notoriously difficult to work with from a provenance perspective but, conversely, are likely to form excellent reservoirs in the subsurface. The heavy-mineral assemblage has a high proportion of ziron–rutile–tourmaline (a high ZRT index). Both these characteristics at first sight point towards a very mature sandstone provenance, perhaps involving several cycles of erosion and deposition – the ancient African craton, therefore, seemed the perfect match to many early workers. However, more careful scrutiny revealed a significant proportion of polycrystalline strained quartz grains, together with a suite of accessory heavy minerals all indicative of a medium–high grade metamorphic source. Furthermore, around 80% of zircon grains were relatively large, euhedral, prismatic crystals. None of these facets is conducive to an origin through poly-cycling. We freely admit that the evidence is not, however, unequivocal.

Zircon geochronology

The arguments put forward by Thomas *et al.* (2010a) focus almost entirely on the zircon dates we obtained and their comparison with others from the literature. Our dates of 500–550 Ma for the Numidian Flysch from Tunisia and Sicily are consistent with metamorphic ages found in *both* European and African basement blocks – this much we accept. We then argue that the collective additional evidence favours a European provenance, whereas Thomas *et al.* (2010a) favour an African source and then attempt to variously explain away the converse data.

Summary

We are very pleased to see that the Numidian Flysch debate is open. The best way forward will be to gather much additional evidence from many more *new* samples across the length and breadth of the Numidian Flysch succession as well as from potential source regions in Europe and Africa. Both zircon geochronology and zircon morphology are likely to yield important results for the provenance debate. There is much further work still to be carried out on Numidian Flysch sedimentology, part of which is nearly completed for Tunisia (Stow *et al.*, 2009; Riahi, 2010b). As far as we are aware, much more is still open for study across northern Africa, but we should welcome correspondence from any others already engaged in such studies. Furthermore, in our view, the Numidian Flysch was most likely to have been deposited in a series of separate and partly separated basins along the length of the orogenic belt. Distinguishing these basins is an equally important task with considerable significance for hydrocarbon prospects.

References

Fildes, C., Stow, D., Riahi, S., Soussi, M., Patel, U., Milton, A.J. and Marsh, S., 2010. European provenance of the Numidian Flysch in northern Tunisia. *Terra Nova*, **22**, 94–102.

Riahi, S., Soussi, M., Bou Khalfa, K., Ben Ismail-Lattrache, K., Stow, D.A.V., Khomsi, S. and Bedir, M., 2010a. Stratigraphy, sedimentology and structure of the Numidian Flysch thrust belt in northern Tunisia. *J. Afr. Earth Sci.*, **57**, 109–129.

Riahi, S., 2010b. *The Oligo-Miocene Numidian Flysch of northern Tunisia*. Unpubl. PhD Thesis, Tunis Univ. Tunis.

Stow, D.A.V., Riahi, S., Soussi, M., Fildes, C., Patel, U., Marsh, S. and Johansson, M. 2009. *Reservoir Characteristics of Deepwater Massive Sandstones: Case Studies from the Numidian Flysch and Mediterranean Region*. Abstract AAPG Annual Meeting, Denver, June 2009, Abstr. Vol. p. 208.

Thomas, M.F.H., Bodin, S. and Redfern, J., 2010a. Comment on: European provenance of the Numidian Flysch in northern Tunisia. *Terra Nova*, **22**, 501–503.

Thomas, M.F.H., Bodin, S., Redfern, J. and Irving, D.H.B., 2010b. A constrained African craton source for the Cenozoic Numidian Flysch: implications for the palaeogeography of the western Mediterranean basin. *Earth Sci. Rev.*, **101**, 1–23.

Received 12 July 2010; revised version accepted 15 August 2010

Appendix 3.

Numidian Flysch Formation biostratigraphy report.

Report commissioned from the British Geological Survey. Author Ian Wilkinson.

British Geological Survey
NATURAL ENVIRONMENT RESEARCH COUNCIL

Microfossils from the Numidian Flysch of Sicily (Miocene)

Commercial Report CR/09/020

BRITISH GEOLOGICAL SURVEY

COMMERCIAL REPORT CR/09/020

Microfossils from the Numidian Flysch of Sicily (Miocene)

I.P. Wilkinson

.

Keywords

Foraminifera, radiolaria, Miocene, Sicily.

Bibliographical reference

WILKINSON, IP. 2011. Microfossils from the Numidian Flysch of Sicily (Miocene). *British Geological Survey Commercial Report*, CR/09/020. 4pp.

.

Keyworth, Nottingham British Geological Survey 2011

BRITISH GEOLOGICAL SURVEY

The full range of our publications is available from BGS shops at Nottingham, Edinburgh, London and Cardiff (Welsh publications only) see contact details below or shop online at www.geologyshop.com

The London Information Office also maintains a reference collection of BGS publications, including maps, for consultation.

We publish an annual catalogue of our maps and other publications; this catalogue is available online or from any of the BGS shops.

The British Geological Survey carries out the geological survey of Great Britain and Northern Ireland (the latter as an agency service for the government of Northern Ireland), and of the surrounding continental shelf, as well as basic research projects. It also undertakes programmes of technical aid in geology in developing countries.

The British Geological Survey is a component body of the Natural Environment Research Council.

British Geological Survey offices

BGS Central Enquiries Desk

Tel 0115 936 3143 Fax 0115 936 3276

email enquiries@bgs.ac.uk

Kingsley Dunham Centre, Keyworth, Nottingham NG12 5GG

Tel 0115 936 3241 Fax 0115 936 3488
email sales@bgs.ac.uk

Murchison House, West Mains Road, Edinburgh EH9 3LA

Tel 0131 667 1000 Fax 0131 668 2683
email scotsales@bgs.ac.uk

Natural History Museum, Cromwell Road, London SW7 5BD

Tel 020 7589 4090 Fax 020 7584 8270
Tel 020 7942 5344/45 email bgslondon@bgs.ac.uk

Columbus House, Greenmeadow Springs, Tongwynlais, Cardiff CF15 7NE

Tel 029 2052 1962 Fax 029 2052 1963

Forde House, Park Five Business Centre, Harrier Way, Sowton EX2 7HU

Tel 01392 445271 Fax 01392 445371

Maclean Building, Crowmarsh Gifford, Wallingford OX10 8BB

Tel 01491 838800 Fax 01491 692345

Geological Survey of Northern Ireland, Colby House, Stranmillis Court, Belfast BT9 5BF

Tel 028 9038 8462 Fax 028 9038 8461

www.bgs.ac.uk/gsni/

Parent Body

Natural Environment Research Council, Polaris House, North Star Avenue, Swindon SN2 1EU

Tel 01793 411500 Fax 01793 411501
www.nerc.ac.uk

Website www.bgs.ac.uk
Shop online at www.geologyshop.com

Contents

TABLES

Summary

This report summarises the foraminifera and radiolaria recovered from a suite of samples from the Sicilian Numidian Flysch. Calcareous microfaunas were poorly preserved due to decalcification, but rare Miocene species were recovered. Radiolaria were more common in this deep water deposit, and although biased towards the larger species, an Early Miocene age can be assigned to the assemblages.

1 Introduction

Sixteen samples were examined for calcareous microfossils in order to determine a biostratigraphical position for the Numidian Flysch in Sicily. The samples and a summary of the microfossils found are shown in Table 1.

Original sample number	BGS sample number	Planktonic foraminifera	Benthonic calcareous foraminifera	Benthonic agglutinated foraminifera	Radiolaria	Fish debris	Barren samples
C1	MPA 58320	very rare	very rare		common	very rare	
C3	MPA 58321				rare		
BL4	MPA 58322						barren
BL5	MPA 58323		rare				
G1	MPA 58324				rare		
P1	MPA 58325			rare			
P4	MPA 58326		very rare		frequent		
P5	MPA 58327				rare		
P8	MPA 58328				very rare		
P9	MPA 58329			very rare			
P10	MPA 58330						barren
P11	MPA 58331				rare		
P13	MPA 58332				rare		
P16	MPA 58333			very rare	rare		
P18	MPA 58334						barren
P21	MPA 58335			rare			

Table 1. Microfossils recovered from a suite of samples from the Numidian Flysch of Sicily

2 Methods

The samples of mudstone and sandy mudstones were registered into the BGS system, each being given a unique identifier (MPA58320-58335). The samples were crushed to 5 mm and soaked in white spirit, before being washed through 75 micron sieves. When the water flowing through the sieve ran clean, each sample was transferred to a saucepan, covered with water and a quantity of sodium hexametaphosphate and brought to the boil. The samples were then washed through the

sieve again and finally placed into a petri-dish to dry in a warm drying cabinet. The dry, disaggregated samples were then packaged into plastic bags ready for examination.

Examination was made using a Wild M7 binocular microscope and specimens observed were transferred from the residue into slides using a 000 sable brush and identified.

3 Microfossils

The samples were prepared in order to extract calcareous microfossils. However, all samples showed that decalcification had taken place and the few foraminifera recovered were generally indeterminate, although agglutinated foraminifera were better preserved (Table 1). Radiolaria were more common in the samples, their siliceous skeletons being better able to survive. Only the larger radiolaria were present in the prepared residues, the sub-75 micron specimens being lost during processing.

Microfossil (radiolaria [r]; foraminifera [f]) assemblages recorded were as follows (vr= very rare; r= rare; f= frequent):

MPA 58320 Remarks: common radiolaria, very rare foraminifera, very rare fish debris

[r] *Didymocyrtis cf. prismatica* (Haeckel,1887)	vr
[r] *Cenosphaera riedeli* Blueford 1982	f
[r] *Spongodiscus* sp. cf. *Spongodiscus klingi* Caulet 1986	r
[f] *Globorotalia sp. cf. siakensis* (partially decalcified)	vr
Decalcified, indeterminate benthic foraminifera	vr

MPA 58321 Remarks: rare radiolaria

[r] *Cenosphaera riedeli* Blueford 1982	r
[r] *Spongodiscus* sp. cf. *Spongodiscus klingi* Caulet 1986	vr

MPA 58322 Remarks: Barren

MPA 58323 Remarks: benthonic foraminifera,

[f]?*Cibicides* spp. (decalcified)	r

MPA 58324 Remarks: rare radiolaria

[r] *Didymocyrtis cf. prismatica* (Haeckel,1887)	vr
[r] *Cenosphaera riedeli* Blueford 1982	r
[r] *Spongodiscus* sp. cf. *Spongodiscus klingi* Caulet 1986	r

MPA 58325 Remarks: benthonic agglutinated foraminifera

[f] *Glomospira gordialis* (Jones & Parker, 1860)	r
[f] *Reticulophragmium acutidorsatum* (Hantken, 1868)	vr
[f] *Recurvoides* sp.	r
[f] *Ammodiscus* "*cretaceus*"	vr
[f] *Trochammina* sp.	vr
[f] *Sacammina* sp. cf. *S.sphaerica*	vr

MPA 58326 Remarks: very rare foraminifera and frequent radiolaria

[r] *Didymocyrtis cf. prismatica* (Haeckel,1887)	vr
[r] *Cenosphaera riedeli* Blueford 1982	f
[r] *Spongodiscus* sp. cf. *Spongodiscus klingi* Caulet 1986	r

Radiolaria sp.	vr
Indeterminate moulds of benthic foraminifera	r

MPA 58327 Remarks: rare radiolaria. Sandy sample with occasional glauconite grains

[r] *Spongodiscus* sp. cf. *Spongodiscus klingi* Caulet 1986	r

MPA 58328 Remarks: very rare radiolaria

[r] *Spongodiscus* sp. cf. *Spongodiscus klingi* Caulet 1986	r

MPA 58329 Remarks: very rare agglutinated foraminifera

[f] *Recurvoides* sp.	vr

MPA 58330 Remarks: barren

MPA 58331 Remarks: rare radiolaria

[r] *Cenosphaera riedeli* Blueford 1982	r
[r] *Spongodiscus* sp. cf. *Spongodiscus klingi* Caulet 1986	r

MPA 58332 Remarks: rare radiolaria

[r] *Cenosphaera riedeli* Blueford 1982	r

MPA 58333 Remarks: rare radiolaria, rare foraminifera

[r] *Cenosphaera riedeli* Blueford 1982	r
Recurvoides sp.	r

MPA 58334 Remarks: barren

MPA 58335 Remarks: rare radiolaria, rare agglutinated foraminifera

[r] *Cenosphaera riedeli* Blueford 1982	r
[f] *Recurvoides* sp.	vr
[f] *Ammodiscus* "*cretaceus*"	r
[f]*Bathysiphon* sp. (fragment)	vr

4 Biostratigraphical conclusions

The absence of identifiable hyaline benthonic foraminifera and near absence of planktonic species make biostratigraphical conclusions difficult. The moderately diverse planktonic foraminiferal assemblage noted by Moretti et al. (1991) in the Numidian sequence of eastern Tell, Algeria, was not found. The single specimen of partially decalcified *Globorotalia sp. cf. siakensis* suggests an age no younger than the Mid-Miocene. Iaccarino (1985) shows its extinction towards the top of the Serravallian, having first appeared in the Palaeogene. However, neither the *Globigerinita dissimilis/Globigerinoides altiaperturus* Zone of Bizon et al. (1979) nor the *Globigerinoides altiaperturus/Catapsydrax dissimilis* Subzone of the *Globoquadrina dehiscens/C. dissimilis* Zone of Iaccarino (1985) recognised by Moretti et al. (1991) could not be confirmed.

The agglutinated benthonic foraminiferal assemblages (notably MPA 58325 and MPA 58335) are similar to those recorded by Moretti et al. (1991) from the Numidian sequence of Algeria. They are typical of the Oligocene to Miocene, but their long ranges prevent biostratigraphical conclusions. The faunas of MPA 58325 and MPA 58335 suggest deeper water, low oxygen condition during deposition.

The largest part of the microfossil assemblages comprise radiolaria. Being siliceous, they have not suffered from the decalcification of the foraminifera, but as the samples were prepared for foraminifera and ostracods (using 75-micron sieves), only the larger species are recorded here. *Cenosphaera riedeli* is the most numerous species in the suite of samples examined, but *Spongodiscus* sp. cf. *klingi* can be found in many of the samples. Both species are of Miocene age. However the presence of *Didymocyrtis cf. prismatica* in MPA 58320 58324 and 58326 suggests a stratigraphical position within the Early Miocene as it disappears from the record below the top of the Burdigalian (Nigrini and Sanfilippo, 2001; Web site: Radiolaria.org/Miocene). Althoough only very rare, damaged specimens (spines are reduced to stubs) were found, they are considered stratigraphically important.

No stratigraphically significant differentiation could be recognised between assemblages throughout the succession and it is concluded that all can be placed within the Early Miocene.

.

References

BIZON, G, MULLER, C, BORSETTI, AM, CAULET, JP, GERSONDE, R, D'ONOFRIO, S and SOKAC, A. 1979. Report of the weorking group on Micropalaeontology. Ann. Géol. Pays Hellén, 3, 1335-1364.

BLUEFORD, JR. 1982. Miocene actinommid radiolaria from the equatorial Pacific. Micropaleontology, 28, 189-213.

IACCARINO, S. 1985. Mediterranean Miocene and Pliocene planktic foraminifera. In: Bolli, HM, Saunders, JB and Perch-Nielsen, K (eds) Plankton Stratigraphy, 283-314 [Cambridge University Press].

MORETTI, E, COCCIONI, R, GUERRERA, F, LAHONDÈRE, J-C, LOIACONCONO, F and PUGLISI, D. 1991. The Numidian Sequence between Guelma and Constantine (Eastern Tell, Algeria). Terra Nova, 3, 153-165.

NIGRINI, C and SANFILIPPO, A. (compilers) 2001.Cenozoic Radiolarian stratigraphy for low and middle latitudes with descriptions of biomarkers and stratigraphically useful species. Ocean Drilling Program, Technical Note 27 [Online], http://www-odp.tamu.edu/publications/tnotes/tn27/index.html

Appendix 4.

Numidian Flysch Formation (Sicily) sample list

Sample list of all samples from Sicily.

Sample code	location X	Location Y	Section / Locality	Sample type
Ka15	37/56/35.657 N	14/8/57.755 E	Karsa	Sand/Consolidated
Ka14	37/56/35.657 N	14/8/57.755 E	Karsa	Sand/Consolidated
Ka13	37/56/35.657 N	14/8/57.755 E	Karsa	Coarse Sand/Consolidated
Ka12b	37/56/35.657 N	14/8/57.755 E	Karsa	Sand/Consolidated
Ka12a	37/56/35.657 N	14/8/57.755 E	Karsa	Sand/Consolidated
Ka11	37/56/35.657 N	14/8/57.755 E	Karsa	Sand/Consolidated
Ka10	37/56/35.657 N	14/8/57.755 E	Karsa	Sand/Consolidated
Ka9	37/56/35.657 N	14/8/57.755 E	Karsa	Mud/Loosely consolidated
Ka8	37/56/35.657 N	14/8/57.755 E	Karsa	Mud/unconsolidated
Ka7	37/56/35.657 N	14/8/57.755 E	Karsa	Sand/Consolidated
Ka6	37/56/35.657 N	14/8/57.755 E	Karsa	Mud/unconsolidated
Ka5	37/56/35.657 N	14/8/57.755 E	Karsa	Sand/Consolidated
Ka4	37/56/35.657 N	14/8/57.755 E	Karsa	Sand/Consolidated
Ka3b	37/56/35.657 N	14/8/57.755 E	Karsa	Sand/Consolidated
Ka3a	37/56/35.657 N	14/8/57.755 E	Karsa	Sand/Consolidated
Ka2	37/56/35.657 N	14/8/57.755 E	Karsa	Mud/unconsolidated
Ka1	37/56/35.657 N	14/8/57.755 E	Karsa	Sand/Consolidated
Ka(2)1	37/56/55.7 N	14/8/56.3 E	Karsa 2 (lower)	Mud/Loosely consolidated
Ka(2)2a	37/56/55.7 N	14/8/56.3 E	Karsa 2 (lower)	Sand/Consolidated
Ka(2)2b	37/56/55.7 N	14/8/56.3 E	Karsa 2 (lower)	Sand/Consolidated
Ka(2)2c	37/56/55.7 N	14/8/56.3 E	Karsa 2 (lower)	Sand/Consolidated
Ka(2)3	37/56/55.7 N	14/8/56.3 E	Karsa 2 (lower)	Silt/sand/mud loosely consolifated
Ka(2)4	37/56/55.7 N	14/8/56.3 E	Karsa 2 (lower)	Mud/unconsolidated
Ka(2)5	37/56/55.7 N	14/8/56.3 E	Karsa 2 (lower)	Mud/Loosely consolidated
Pf-F1	38/1/43.096 N	14/08/40.848 E	Finale channel system, complex Cr-5	Coarse Sand/Conglomerate, Consolidated
Pf-F1	38/1/43.096 N	14/08/40.848 E	Finale channel system, complex Cr-5	Coarse Sand/Conglomerate, Consolidated
Pf-F1b	38/1/43.096 N	14/08/40.848 E	Finale channel system, complex Cr-5	Crumbly conglomerate
Pf-F2	38/1/43.096 N	14/08/40.848 E	Finale channel system, complex Cr-5	Muddy Conglomerate, reasonably consolidated
Pf-F2b	38/1/43.096 N	14/08/40.848 E	Finale channel system, complex Cr-5	Muddy Conglomerate, reasonably consolidated
Pf-F3	38/1/43.096 N	14/08/40.848 E	Finale channel system, complex Cr-5	Coarse Sand, Consolidated
Pf-F4a	38/1/43.096 N	14/08/40.848 E	Finale channel system, complex Cr-5	Sand/Consolidated
Pf-F4b	38/1/43.096 N	14/08/40.848 E	Finale channel system, complex Cr-5	Sand/Consolidated
Pf-F5	38/1/43.096 N	14/08/40.848 E	Finale channel system, complex Cr-5	Sand/Consolidated
Pf-F5	38/1/43.096 N	14/08/40.848 E	Finale channel system, complex Cr-5	Sand/Consolidated
Pf-F5	38/1/43.096 N	14/08/40.848 E	Finale channel system, complex Cr-5	Sand/Consolidated
PF-1	38/01/35.769 N	14/08/45.8 E	Finale channel system, complex Cr-5	Sand/Consolidated
PF-2	38/01/35.769 N	14/08/45.8 E	Finale channel system, complex Cr-5	Sand/Consolidated
Pf-IC1	38/01/35.769 N	14/08/45.8 E	Finale channel system (interchannel, Cr-4 and Cr-5)	Sand/Consolidated
Pf-IC2	38/01/35.769 N	14/08/45.8 E	Finale channel system (interchannel, Cr-4 and Cr-5)	Mud/unconsolidated
Pf-IC3	38/01/35.769 N	14/08/45.8 E	Finale channel system (interchannel, Cr-4 and Cr-5)	Mud/unconsolidated
Pf-IC4	38/01/35.769 N	14/08/45.8 E	Finale channel system (interchannel, Cr-4 and Cr-5)	Sand/Consolidated
Pf-IC4	38/01/35.769 N	14/08/45.8 E	Finale channel system (interchannel, Cr-4 and Cr-5)	Mud/Loosely consolidated
Pf-IC5 Base	38/01/35.769 N	14/08/45.8 E	Finale channel system (interchannel, Cr-4 and Cr-5)	Sand/Consolidated
Pf-IC5 Top	38/01/35.769 N	14/08/45.8 E	Finale channel system (interchannel, Cr-4 and Cr-5)	Sand/Consolidated
Pf-IC6	38/01/35.769 N	14/08/45.8 E	Finale channel system (interchannel, Cr-4 and Cr-5)	Sand/Consolidated
Pf-IC7	38/01/35.769 N	14/08/45.8 E	Finale channel system (interchannel, Cr-4 and Cr-5)	Mud/Loosely consolidated
Pf-IC8	38/01/35.769 N	14/08/45.8 E	Finale channel system (interchannel, Cr-4 and Cr-5)	Mud/unconsolidated
Pf-IC9	38/01/35.769 N	14/08/45.8 E	Finale channel system (interchannel, Cr-4 and Cr-5)	Mud/Loosely consolidated
Pf-IC10	38/01/35.769 N	14/08/45.8 E	Finale channel system (interchannel, Cr-4 and Cr-5)	Sand/Consolidated
P1	37°59'41.07"N	14° 8'45.99"E	Pollina village	External
A1	38/0/40.96 N	14/05/55.53 E	Ambroggio River	Sand/Concolidated
A1b	38/0/40.96 N	14/05/55.53 E	Ambroggio River	Sand/Concolidated
A2	38/0/40.96 N	14/05/55.53 E	Ambroggio River	Sand/Concolidated
A3	38/0/40.96 N	14/05/55.53 E	Ambroggio River	Sand/Concolidated
A5	38/0/41.914 N	14/5/56.837 E	Ambroggio autostrada	Sand/Concolidated
A6	38/0/41.914 N	14/5/56.837 E	Ambroggio autostrada	Sand/Concolidated
A7	38/0/41.914 N	14/5/56.837 E	Ambroggio autostrada	Sand/Concolidated
A8	38/00/31.460 N	14/05/51.33 E	Ambroggio autostrada	Mud/unconsolidated
A8b	38/00/31.460 N	14/05/51.33 E	Ambroggio autostrada	Sand/Concolidated

A9	38/00/31.460 N	14/05/51.33 E	Ambroggio autostrada	Mud/unconsolidated
A9b	38/00/31.460 N	14/05/51.33 E	Ambroggio autostrada	Sand/Concolidated
A10	38/00/31.460 N	14/05/51.33 E	Ambroggio autostrada	Mud/unconsolidated
A10b	38/00/31.460 N	14/05/51.33 E	Ambroggio autostrada	Sand/Concolidated
A11	38/00/31.460 N	14/05/51.33 E	Ambroggio autostrada	Mud/unconsolidated
A11b	38/00/31.460 N	14/05/51.33 E	Ambroggio autostrada	Sand/Concolidated
A12	38/00/34.839 N	14/05/52.310 E	Ambroggio autostrada	Mud/unconsolidated
A12b	38/00/34.839 N	14/05/52.310 E	Ambroggio autostrada	Sand/Concolidated
A13	38/00/36.995 N	14/05/52.914 E	Ambroggio autostrada	Mud/unconsolidated
A13b	38/00/36.995 N	14/05/52.914 E	Ambroggio autostrada	Sand/Concolidated
A14	38/00/36.995 N	14/05/54.350 E	Ambroggio autostrada	Mud/unconsolidated
A14b	38/00/36.995 N	14/05/54.350 E	Ambroggio autostrada	Sand/Concolidated
M1	37/55/57.61 N	14/21/43.74 E	Mistretta south	Sand/Concolidated
M2	37/55/57.61 N	14/21/43.74 E	Mistretta south	Sand/Concolidated
M3	37/55/57.61 N	14/21/43.74 E	Mistretta south	Sand/Concolidated
G1	37/51/53.36 N	14/09/21.78 E	Geraci Siculo	Sand/Concolidated
G2	37/51/54.97 N	14/09/20.22 E	Geraci Siculo	Sand/Concolidated
S1	37/46/16.16 N	14/21/05.87 E	Sperlinga	Sand/crumbly
S2	37/45/44.52 N	14/21/24.08 E	Sperlinga	Sand/crumbly
S3	37/45/58.29 N	14/21/53.94 E	Sperlinga	Sand/crumbly
CDR1	37°45'40.86"N	14°24'24.98"E	Contrada di Romano	Sand/crumbly
CDR2	37°45'40.86"N	14°24'24.98"E	Contrada di Romano	Sand/crumbly
CDR3	37/45/39.41 N	14/24/22.18 E	Contrada di Romano	Sand/crumbly
IBM 1	37/53/21.782 N	14/11/9.492 E	3.7 Km NE of Karsa	Mud/unconsolidated
IBM 2a	37°53'40.44"N	14°10'35.92"E	4 Km N of Karsa	Mud/unconsolidated
IBM 2b	37°53'40.44"N	14°10'35.92"E	4 Km N of Karsa	Mud/unconsolidated
IBM 2c	37°53'40.44"N	14°10'35.92"E	4 Km N of Karsa	Mud/unconsolidated
IBM 2d	37°53'40.44"N	14°10'35.92"E	4 Km N of Karsa	Mud/unconsolidated
IBM 2e	37°53'40.44"N	14°10'35.92"E	4 Km N of Karsa	Mud/unconsolidated

Appendix 5.

Numidian Flysch Formation (Tunisia) sample list

Sample list of all samples from Tunisia.

Sample code	Latitude	Longitude	Section / Locality	Sample type	Member
T1	36/57/46.5 N	8/45/24.21 E	Tabarka	Coarse sand/consolidated	Kroumerie
TM1	36/57/46.5 N	8/45/24.21 E	Tabarka	Mud/fissile	Kroumerie
T7	36/57/46.5 N	8/45/24.21 E	Tabarka	Clast rich Sand/consolidated	Kroumerie
T2	36/57/46.5 N	8/45/24.21 E	Tabarka	Sand/consolidated	Kroumerie
TM2	36/57/46.5 N	8/45/24.21 E	Tabarka	Mud/fissile	Kroumerie
T3	36/57/46.5 N	8/45/24.21 E	Tabarka	Sand/consolidated	Kroumerie
T4	36/57/46.5 N	8/45/24.21 E	Tabarka	Sand/consolidated	Kroumerie
TM3	36/57/46.5 N	8/45/24.21 E	Tabarka	Mud/fissile	Kroumerie
TM4	36/57/46.5 N	8/45/24.21 E	Tabarka	Mud/fissile	Kroumerie
TM5	36/57/46.5 N	8/45/24.21 E	Tabarka	Mud/fissile	Kroumerie
T5	36/57/46.5 N	8/45/24.21 E	Tabarka	Sand/consolidated	Kroumerie
T6	36/57/46.5 N	8/45/24.21 E	Tabarka	Muddy sand/crumbly	Kroumerie
TM6	36/57/46.5 N	8/45/24.21 E	Tabarka	Silty mud/fragile	Kroumerie
T7	36/57/46.5 N	8/45/24.21 E	Tabarka	Sand/consolidated	Kroumerie
T8	36/57/46.5 N	8/45/24.21 E	Tabarka	Clast rich Sand/consolidated	Kroumerie
T9	36/57/46.5 N	8/45/24.21 E	Tabarka	Sand/consolidated	Kroumerie
B1	36/49/383 N	8/58/625 E	Babouche	Sillexite	Babouche term
B2	36/49/383 N	8/58/625 E	Babouche	Mud/fissile	Babouche term
B3	36/49/383 N	8/58/625 E	Babouche	Granular sand/consolidated	Not Numidian
BM1	36/49/383 N	8/58/625 E	Babouche	Mud/fissile	Not Numidian
B4	36/49/383 N	8/58/625 E	Babouche	Sand/Consolidated	Not Numidian
B5	36/49/383 N	8/58/625 E	Babouche	Fine sand/Consolidated	Not Numidian
B6	36/49/383 N	8/58/625 E	Babouche	Fine sand/Consolidated	Not Numidian
B7	36/49/383 N	8/58/625 E	Babouche	Fine sand/Consolidated	Not Numidian
Z1	36/51/531 N	9/2/284 E	Jebel el Gassa	Mud/soft but consolidated	Zousa
Z2	-	-	Jebel el Gassa	Sand/reasonable consolidated	Zousa
Z3			Jebel el Gassa	Sand/reasonable consolidated	Zousa
CS1	37/14/349 N	009/13/122 E	Cap Serat	Coarse sand/Consolidated	Kroumerie
CS2	37/14/349 N	009/13/122 E	Cap Serat	Sand/Consolidated	Kroumerie
CS3	37/14/349 N	009/13/122 E	Cap Serat	Sand/Consolidated	Kroumerie
CS4	37/14/349 N	009/13/122 E	Cap Serat	Sand/Consolidated	Kroumerie
CS5	37/14/349 N	009/13/122 E	Cap Serat	Sand/Consolidated	Kroumerie
CS6	37/14/349 N	009/13/122 E	Cap Serat	Sand conglomerate/Consolidated	Kroumerie
CS7	37/14/349 N	009/13/122 E	Cap Serat	Sand/Consolidated	Kroumerie
CS8	37/14/349 N	009/13/122 E	Cap Serat	Sand/Consolidated	Kroumerie
CS9	37/14/349 N	009/13/122 E	Cap Serat	Sand/Consolidated	Kroumerie
CS10	37/14/349 N	009/13/122 E	Cap Serat	Sand/Consolidated	Kroumerie
CS11	37/14/349 N	009/13/122 E	Cap Serat	Sand/Loosely consolidated	Kroumerie
CSM1	37/14/349 N	009/13/122 E	Cap Serat	Mud/unconsolidated	Kroumerie
CSM2	37/14/349 N	009/13/122 E	Cap Serat	Mud/unconsolidated	Kroumerie
K2	37/20/265 N	9/40/315 E	Ras el Koran	Sand/Consolidated	Kroumerie
K3	37/20/265 N	9/40/315 E	Ras el Koran	Sand/Reasonable consolidated	Kroumerie
K4	37/20/265 N	9/40/315 E	Ras el Koran	Sand/Reasonable consolidated	Kroumerie
K5	-	-	Ras el Koran	Sand/Reasonable consolidated	Kroumerie

Appendix 6.

Point counting data for Numidian Flysch Formation sandstones

QFL point counting data (Quartz;Lithic;Feldspar) and Qm:QP (Monocrystalline Quartz:Polycrystalline Quartz). See Appendix 3 and 4 for sample locations and context.

		Totals Q, L, F					% Q, L, F		
	Sample	**Qt**	**Lt**	**Ft**	**total**		**Qt%**	**Lt%**	**Ft%**
Sicily external	29/ab/002	437.0	11.0	0.0	448.0		97.5	2.5	0.0
	29/ab/002 (stained)	475.0	14.0	1.0	490.0		96.9	2.9	0.2
	29/ab/003	471.0	6.0	0.0	477.0		98.7	1.3	0.0
	28/pr/001	406.0	10.0	0.0	416.0		97.6	2.4	0.0
	28/pr/003	473.0	1.0	0.0	474.0		99.8	0.2	0.0
	28/pr/003	466.0	6.0	0.0	472.0		98.7	1.3	0.0
	28/pr/002	300.0	25.0	5.0	330.0		90.9	7.6	1.5
	29/pr/002	304.0	27.0	1.0	332.0		91.6	8.1	0.3
	18/pf/001	326.0	37.0	0.0	363.0		89.8	10.2	0.0
	Ka4	316.0	3.0	3.0	322.0		98.1	0.9	0.9
	Ka(2)2a	429.0	1.0	0.0	430.0		99.8	0.2	0.0
	G1	476.0	0.0	0.0	476.0		100.0	0.0	0.0
	IBM	212.0	0.0	1.0	213.0		99.5	0.0	0.5
Sicily mixed successions	M1	500.0	0.0	2.0	502.0		99.6	0.0	0.4
	M3	486.0	0.0	1.0	487.0		99.8	0.0	0.2
Sicily internal	30/cdr/001	440.0	42.0	0.0	482.0		91.3	8.7	0.0
	30/cdr/001 (stained)	406.0	8.0	2.0	416.0		97.6	1.9	0.5
	CDR3	334.0	0.0	0.0	334.0		100.0	0.0	0.0
	S1	255.0	0.0	9.0	264.0		96.6	0.0	3.4
	S3	371.0	0.0	7.0	378.0		98.1	0.0	1.9
Tunisia	T4	329.0	0.0	0.0	329.0		100.0	0.0	0.0
	CS1	413.0	1.0	0.0	414.0		99.8	0.2	0.0
	Z3	0.0							
	K2 (ras el Koran)	385.0	9.0	0.0	394.0		97.7	2.3	0.0

	Sample	Qm total	Qp total	Q total		Qm %	Qp %
Sicily external	29/ab/002	349.00	88.00	437.00		79.86	20.14
	29/ab/002 (stained)	377.00	98.00	475.00		79.37	20.63
	29/ab/003	151.00	320.00	471.00		32.06	67.94
	28/pr/001	393.00	13.00	406.00		96.80	3.20
	28/pr/003	411.00	62.00	473.00		86.89	13.11
	28/pr/003	413.00	53.00	466.00		88.63	11.37
	28/pr/002	288.00	12.00	300.00		96.00	4.00
	29/pr/002	297.00	7.00	304.00		97.70	2.30
	18/pf/001	233.00	93.00	326.00		71.47	28.53
	Ka4	279.00	37.00	316.00		88.29	11.71
	Ka(2)2a	375.00	54.00	429.00		87.41	12.59
	G1	394.00	82.00	476.00		82.77	17.23
	IBM	208.00	4.00	212.00		98.11	1.89
Sicily mixed successions	M1	346.00	37.00	383.00		90.34	9.66
	M3	295.00	41.00	336.00		87.80	12.20
Sicily internal	30/cdr/001	437.00	3.00	440.00		99.32	0.68
	30/cdr/001 (stained)	397.00	9.00	406.00		97.78	2.22
	CDR3	184.00	150.00	334.00		55.09	44.91
	S1	228.00	27.00	255.00		89.41	10.59
	S3	362.00	9.00	371.00		97.57	2.43
Tunisia	T4	297.00	32.00	329.00		90.27	9.73
	CS1	290.00	123.00	413.00		70.22	29.78
	Z3	0.00	0.00	0.00			
	K2 (ras el Koran)	369.00	16.00	385.00		95.84	4.16

Appendix 7.

X-Ray diffraction results

A selection of results from Sicily and Tunisia. Run time is 2 hours.

Ab001 (Ambroggio, Sicily) - Mudstones

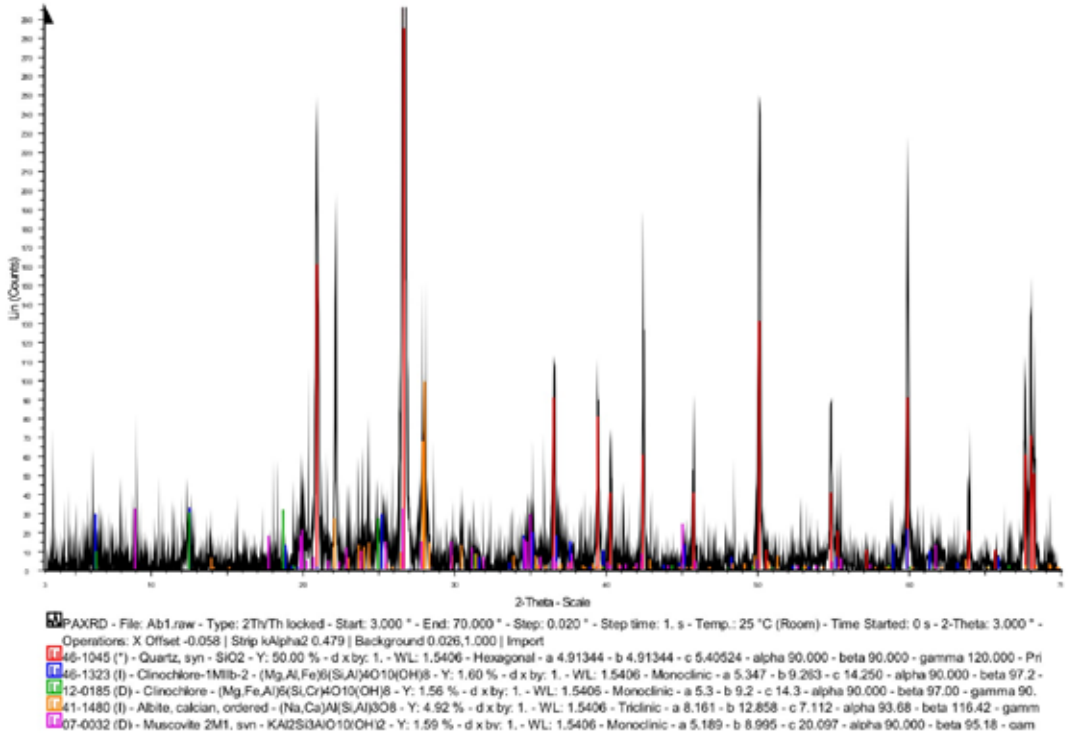

IBM-1 (Geraci, Sicily) - Mudstones

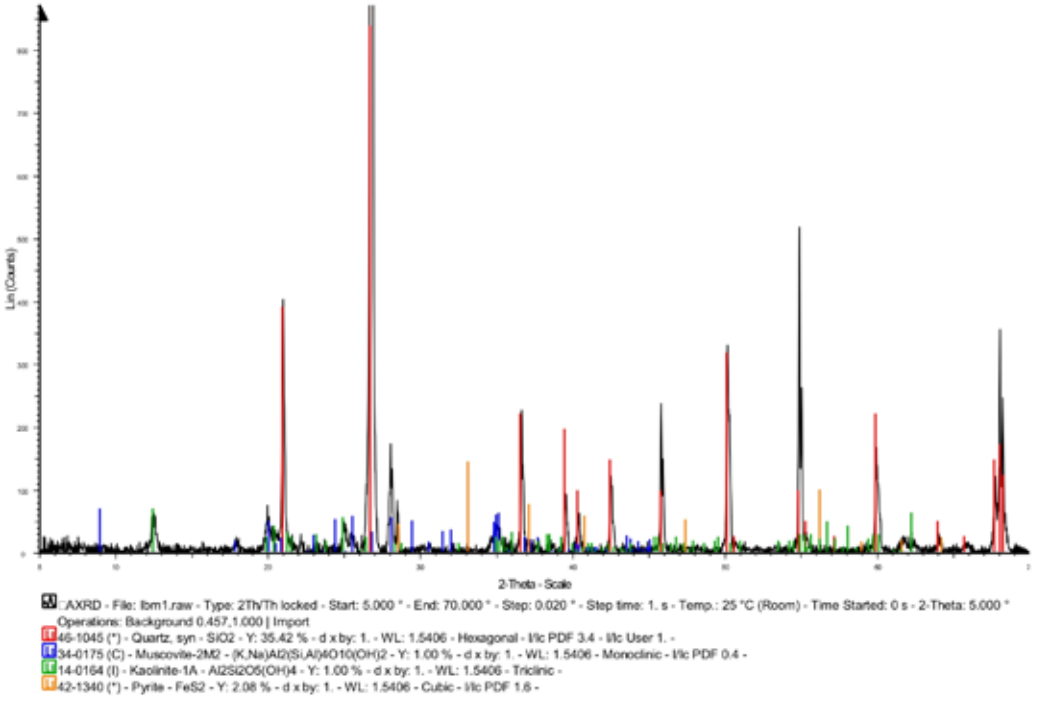

Ka-4 (Karsa section, Sicily) - Coarse sandstones

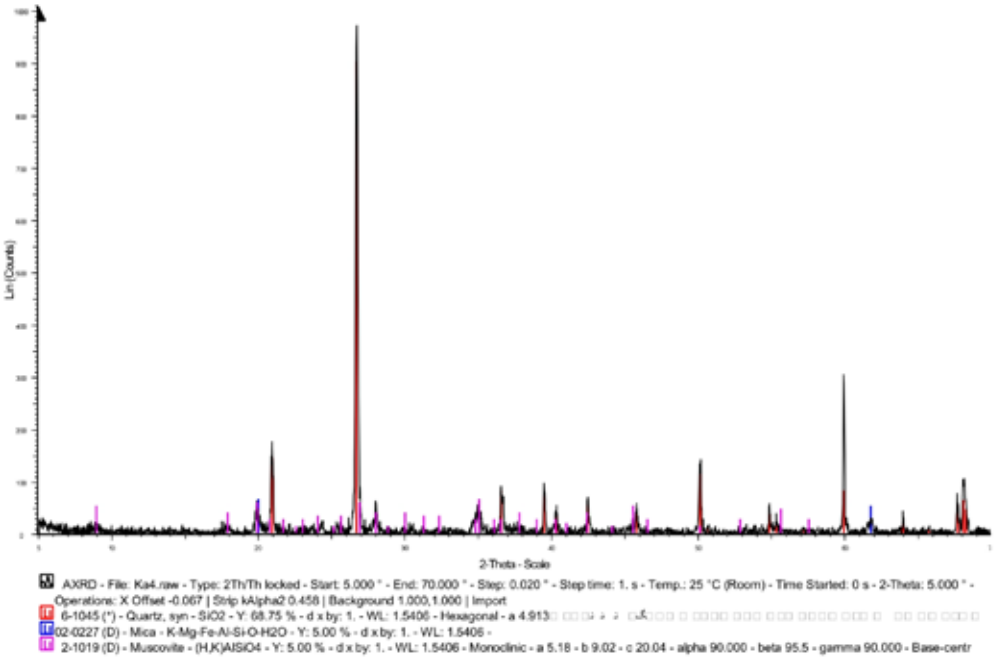

M-1 (Mistretta Sicily) - Coarse sandstones

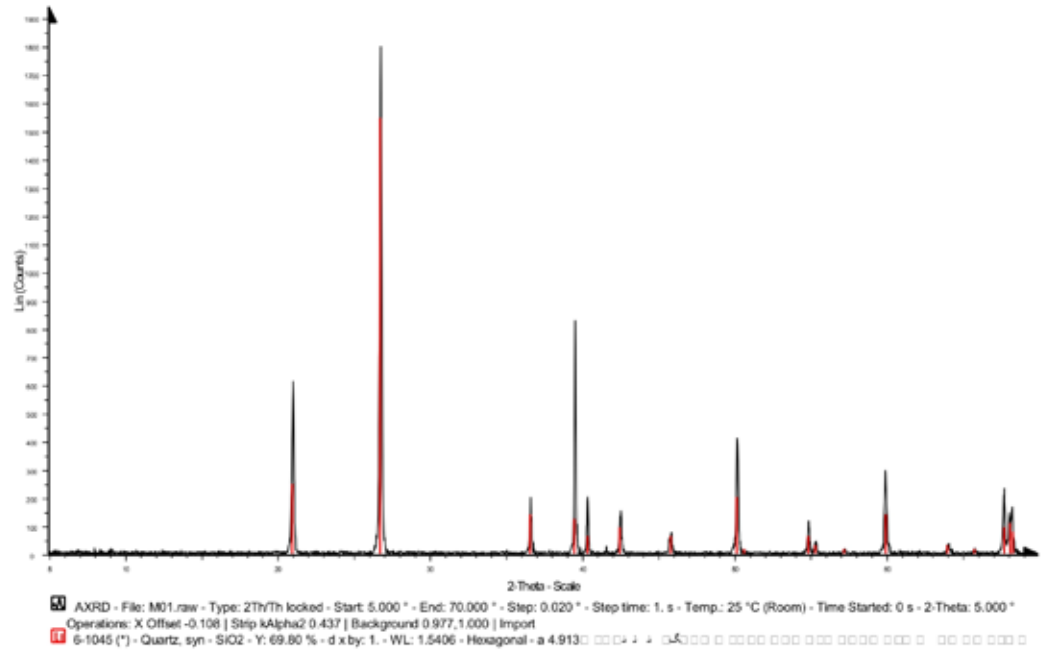

S-1 (Sperlinga, Sicily) - Fine sandstones

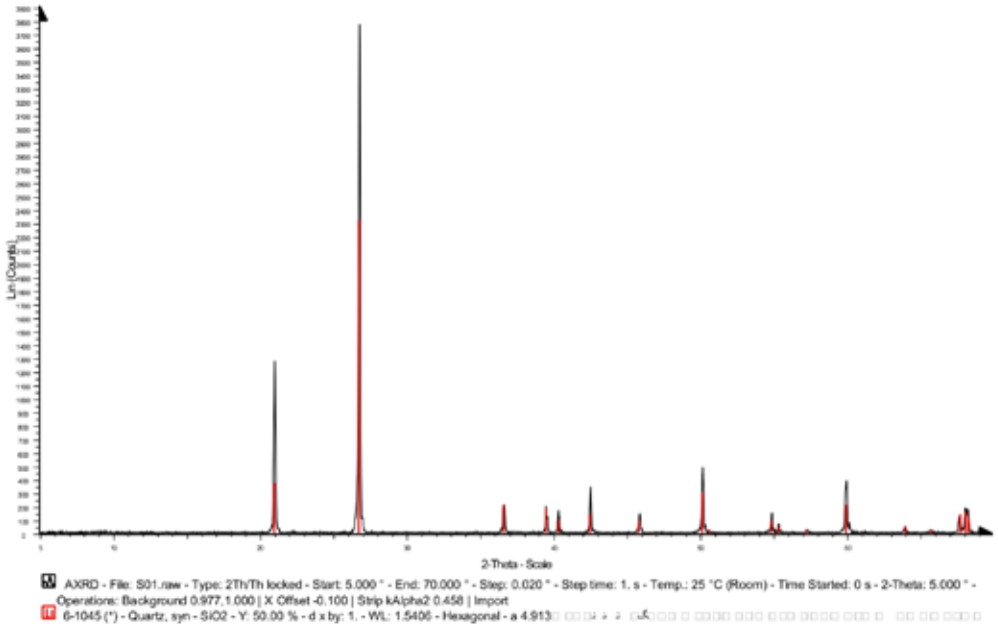

CDR-1 (Contrada di Romano, Sicily) - Fine sandstones

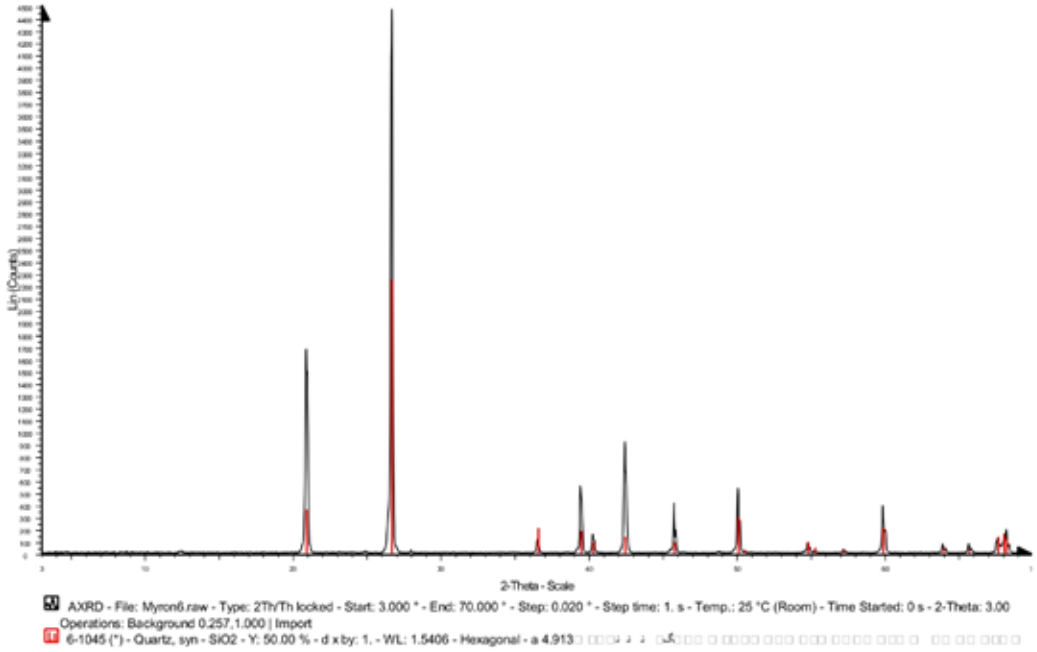

TM-3 (Tabarka, Tunisia) - Mudstones

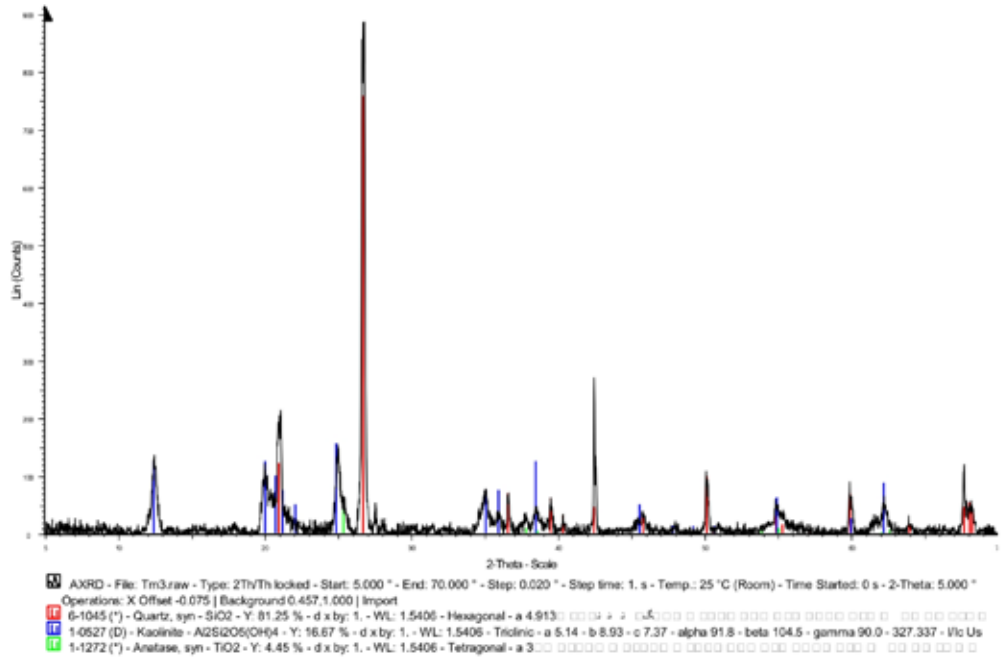

T-4 (Tabarka, Tunisia) - Coarse sandstones

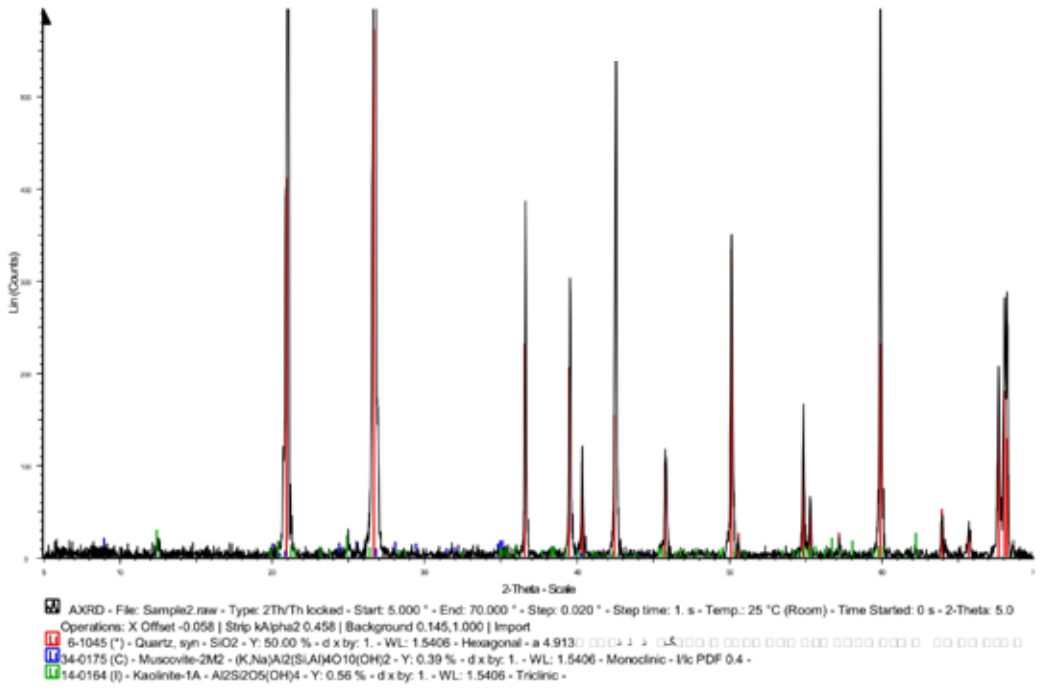

Z-1 (Jebel el Gassa, Tunisia) - Mudstone

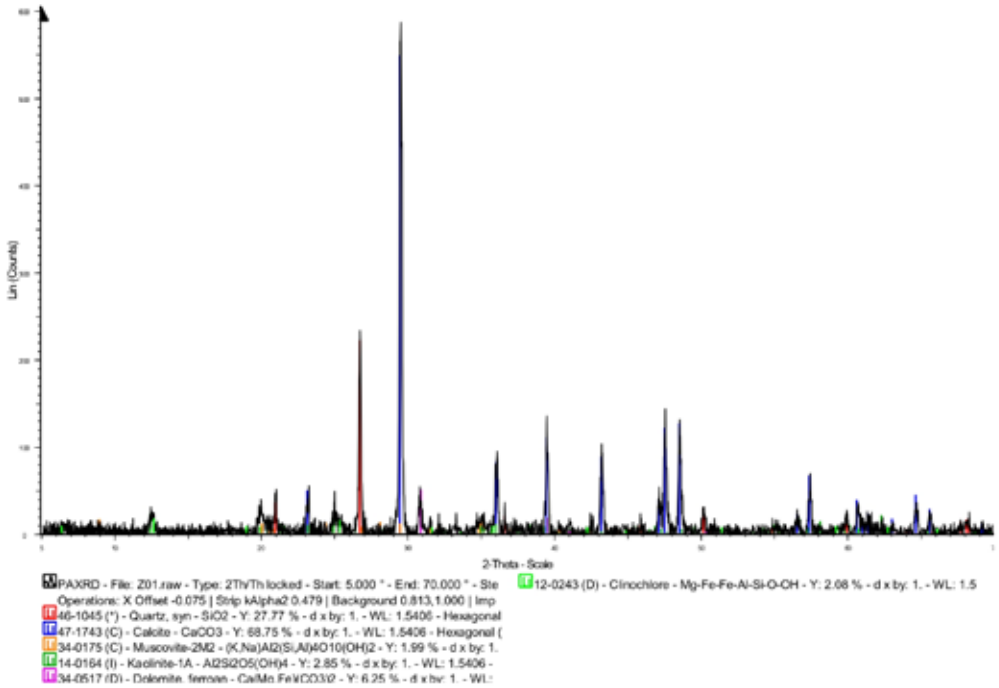

B-2 (Babouche village, Tunisia) - Claystone

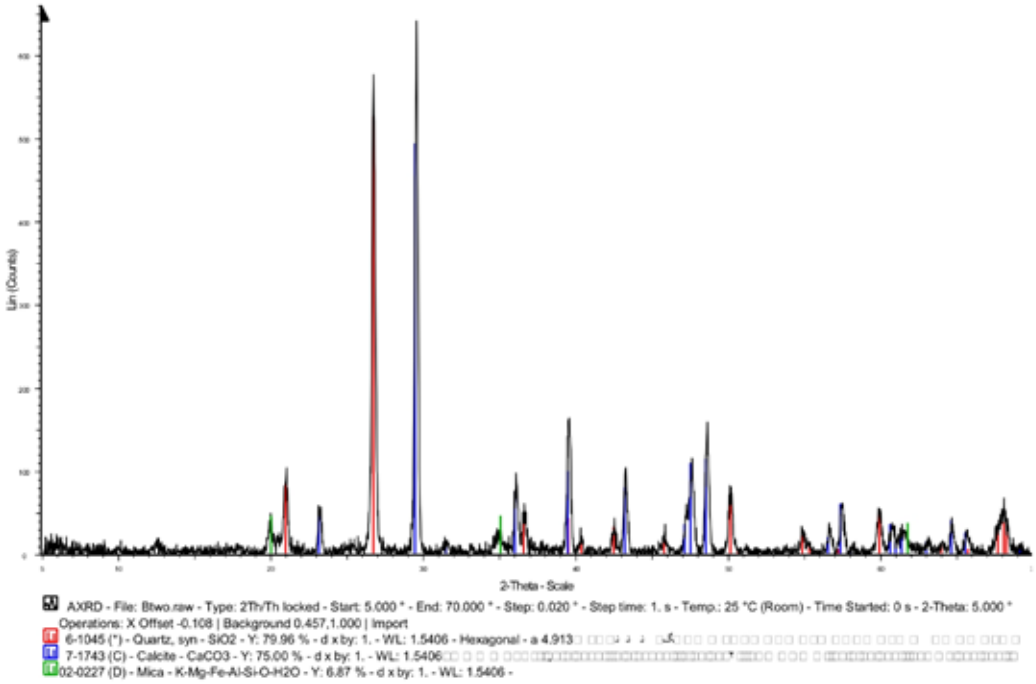

Appendix 8.

Thin section photomicrographs

A selection of results from Sicily and Tunisia highlighting similarities and rare exceptions.

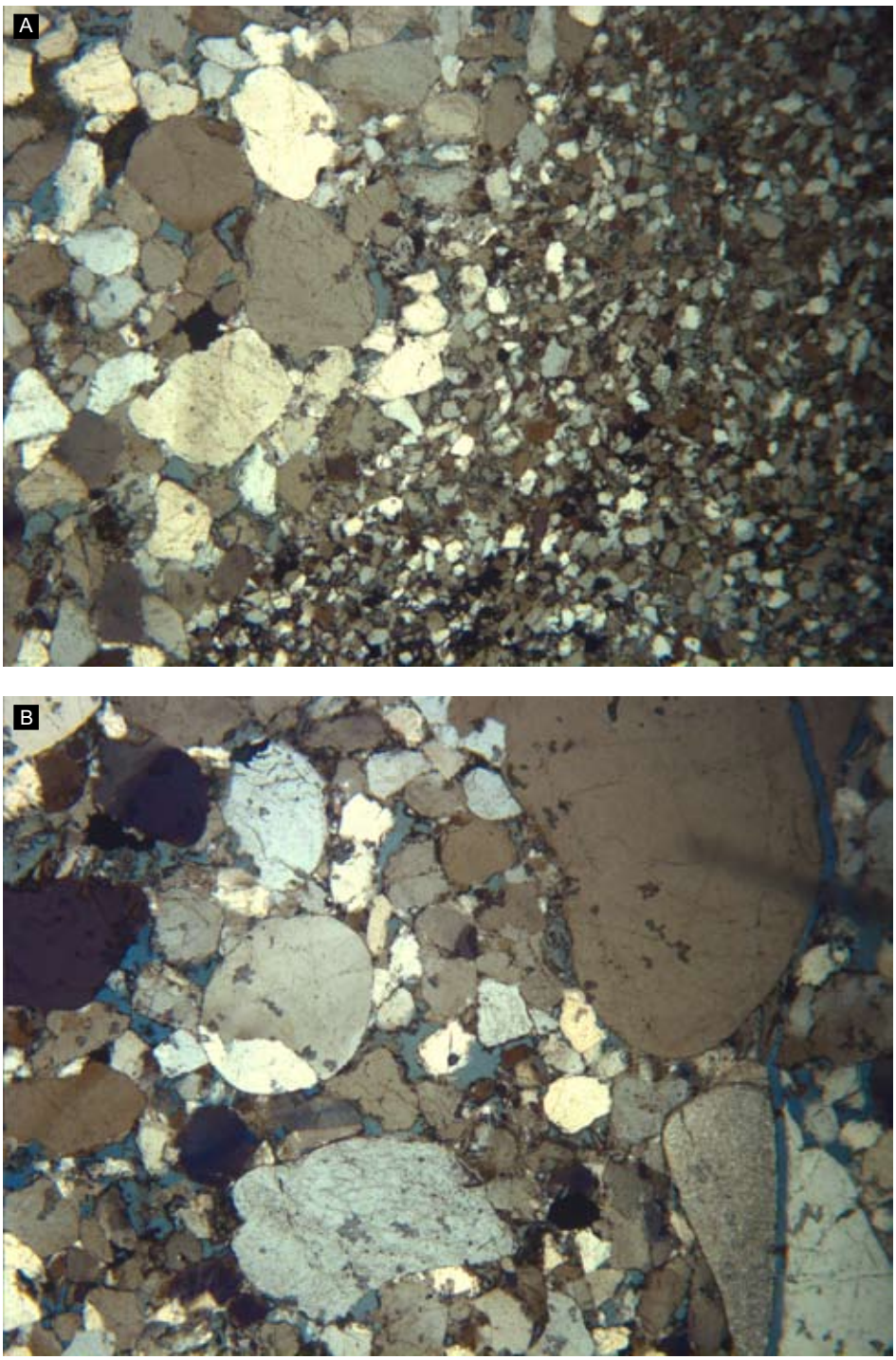

Sample 29/PF/001
A and B. Coarse grained sandstone from channel complex Cr-5, Sicily.

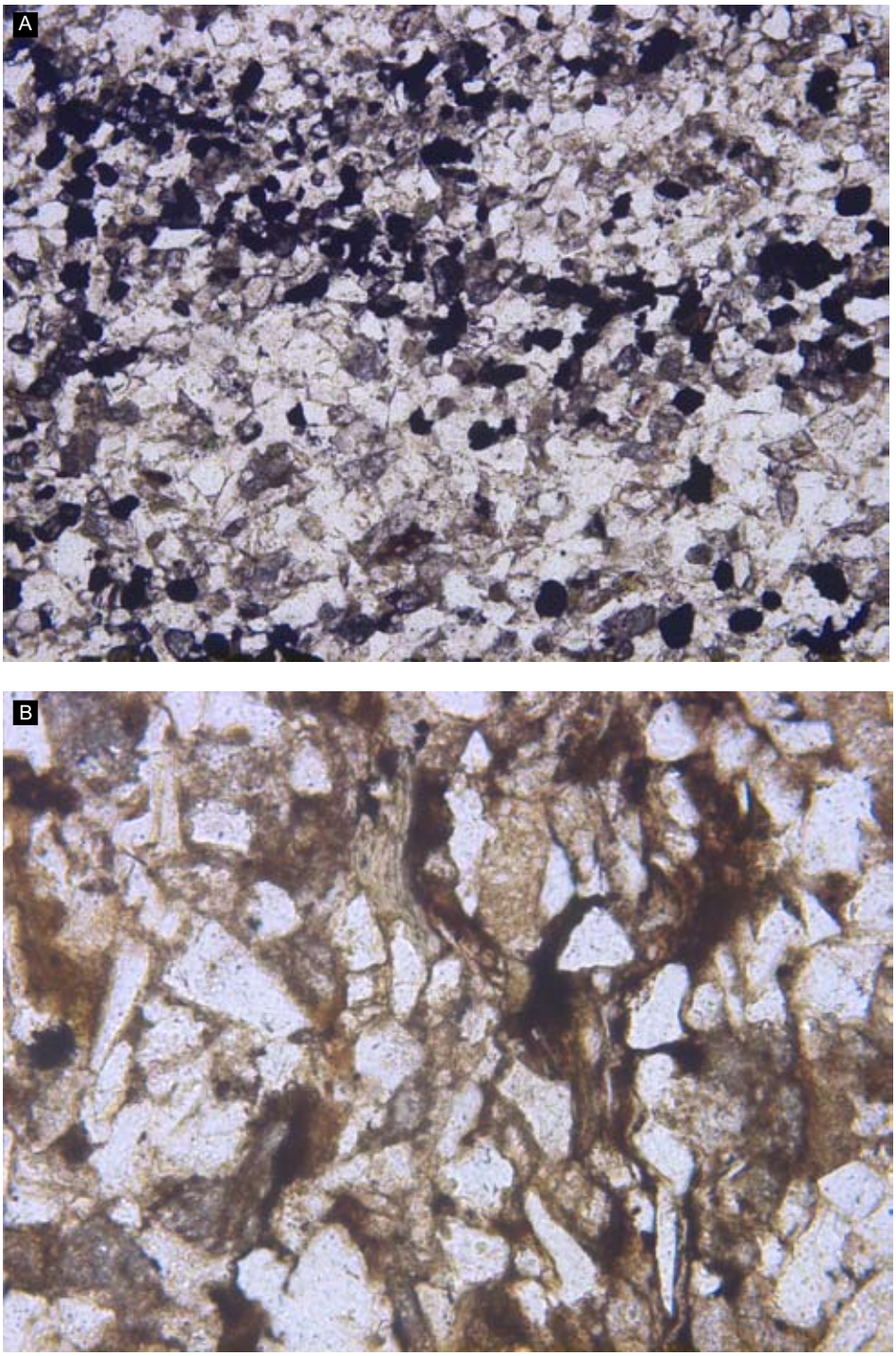

Sample 29/Ab-001

A. Fine grained sandstone from Ambroggio channel complex, Ambroggio, sicily. Abundant small mud rip up clasts occur. View is time 10 magnification.

Sample 29/!b-001

B. Times 20 magnification view of same sample. Note kaolinite within pore spaces and rare calcite crystals.

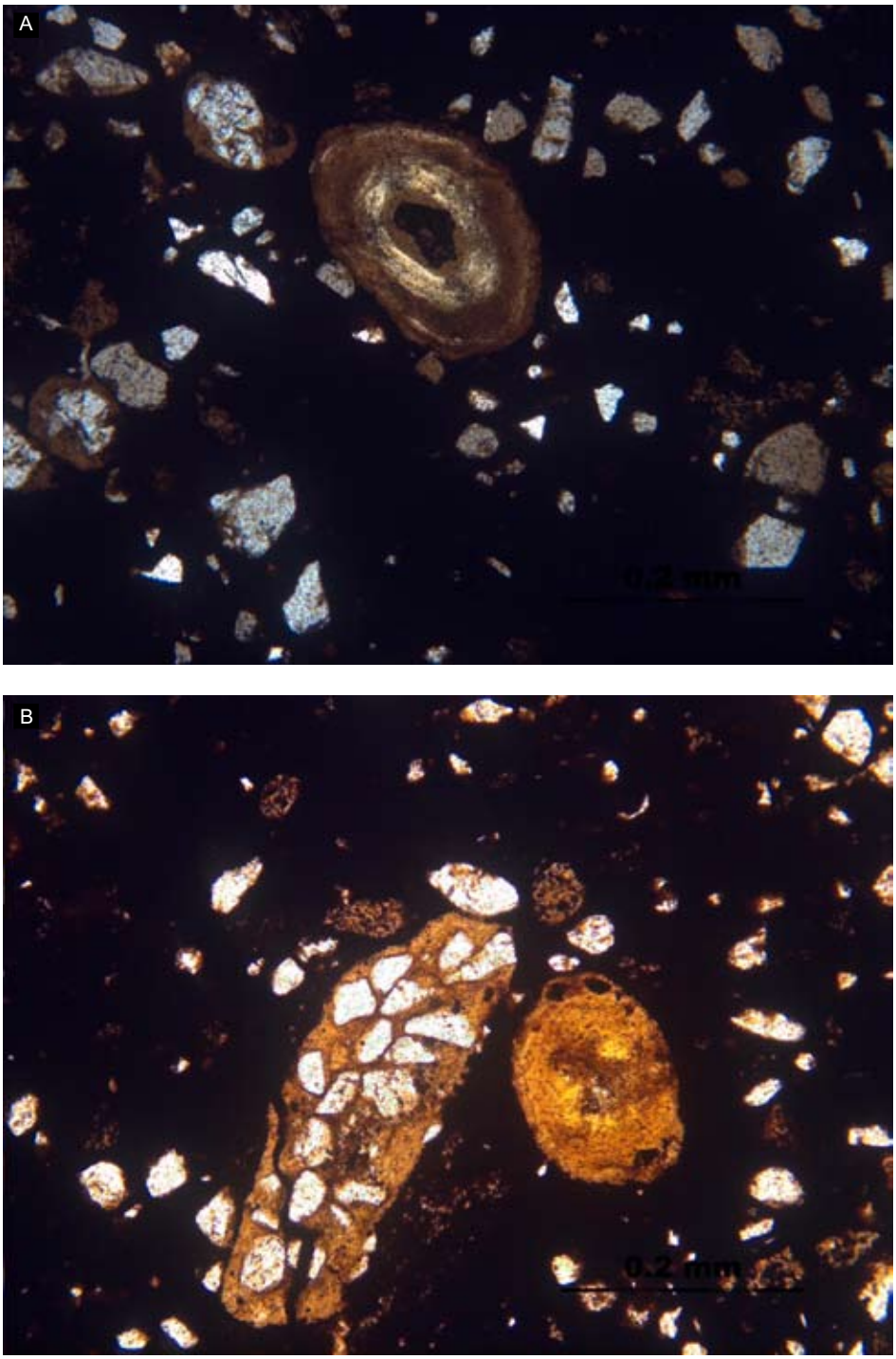

A. Sample Ka-8
Mudstone from the top of the Karsa section, Sicily. The thin section shows fish remains within a rounded phosphorous pellet. This denotes winnowing of the sea floor and very low sedimentation rates.

B. Sample Ka-8
Mudstone from the top of the Karsa section, Sicily. Section shows winnowed rounded phosphorous pellets which are armoured with quartz grains.

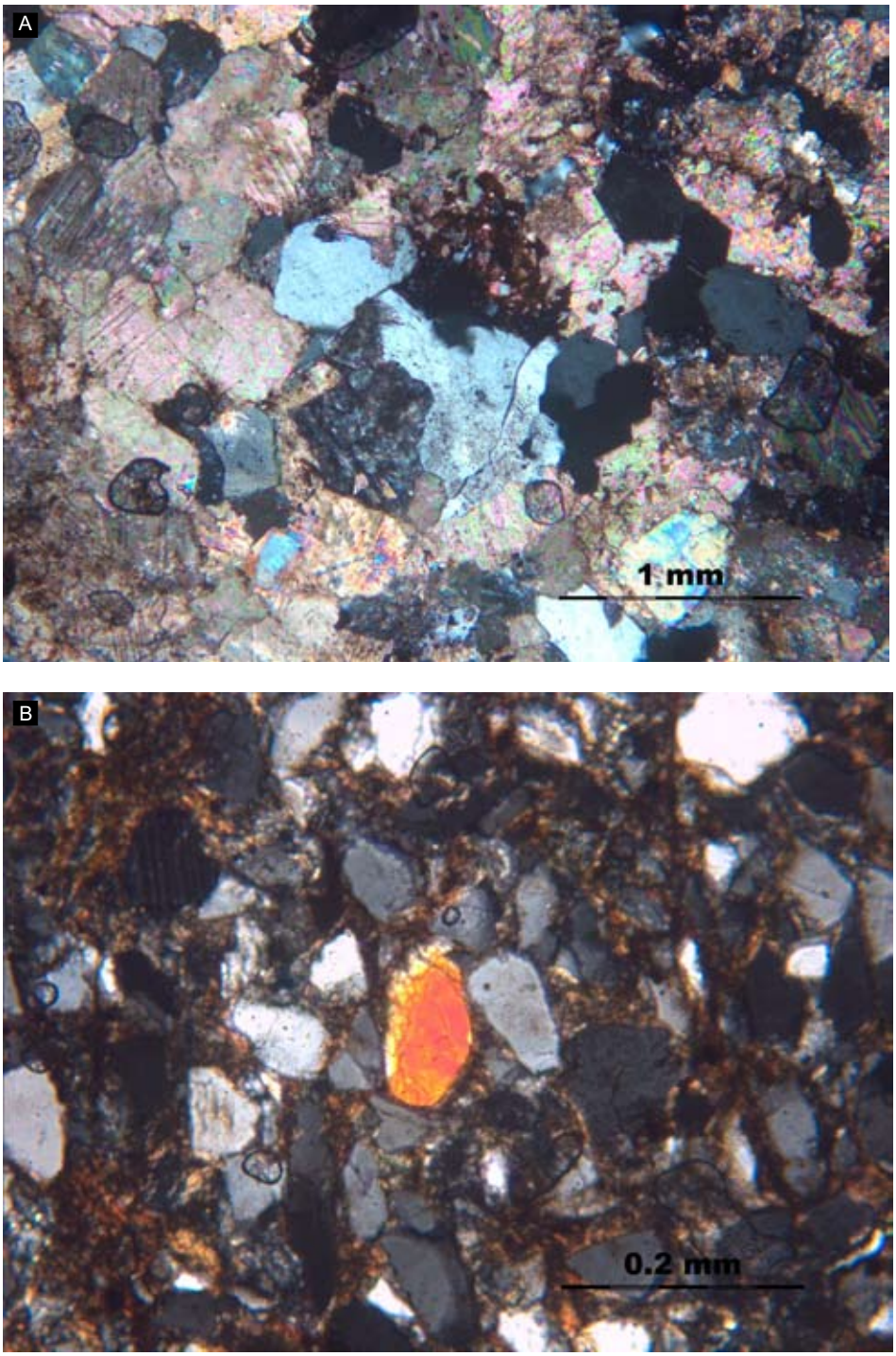

A. Sample Ka-1
Coarse grained sandstone from Karsa, Sicily. Contains locally abundant muscovite.

B. Sample Ka-1
Fine grained sandstone from Karsa, Sicily. A single clast of epidote is present in the centre. Pore spaces are full of clays.

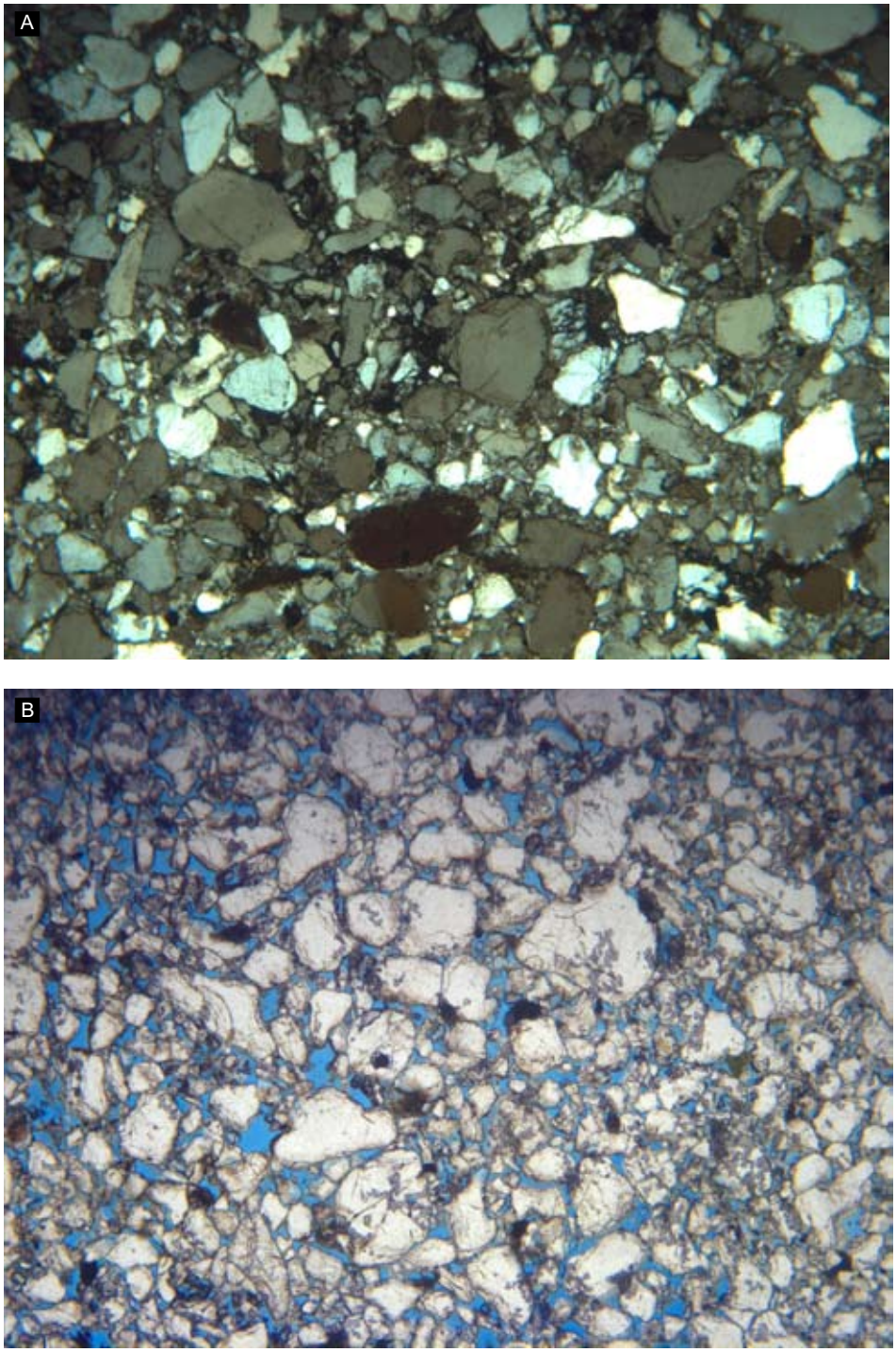

A. Sample 30/CDR/001
Fine grained sandstone with well rounded clasts from Contrada di Romano, central Sicily. View is x10 magnification.

B. Sample 30/CDR/001
Fine grained sandstone with well rounded clasts from Contrada di Romano (Same view as above), central Sicily. View is x10 magnification. Blue staining denotes high porosity.

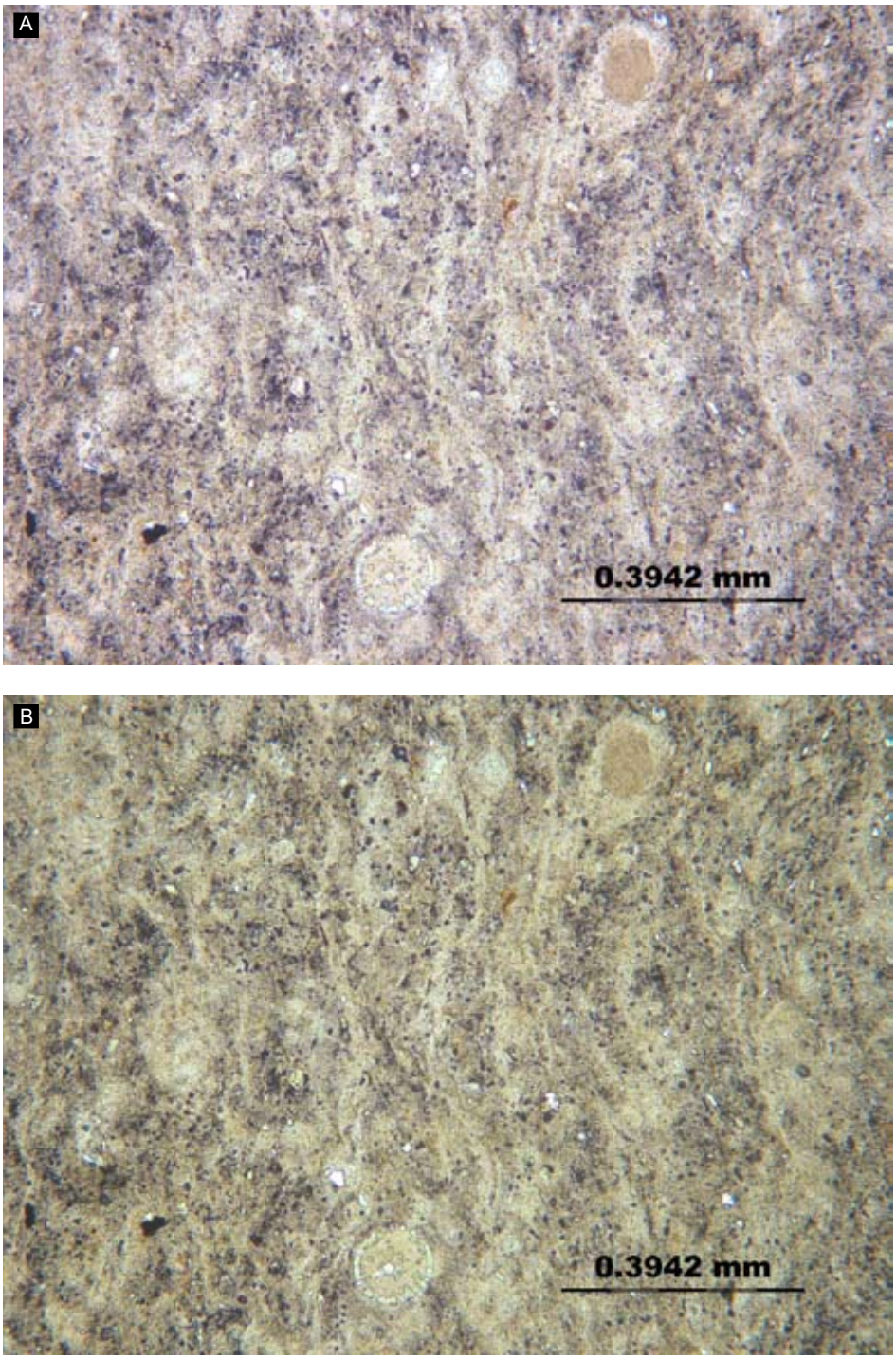

A. Sample B1
Claystone from the Babouche member of northern Tunisia. Note small quartz grains and foraminifera.

B. Sample B1
Claystone from the Babouche member of northern Tunisia. Note small quartz grains and foraminifera. Same view as above, with crossed polars.

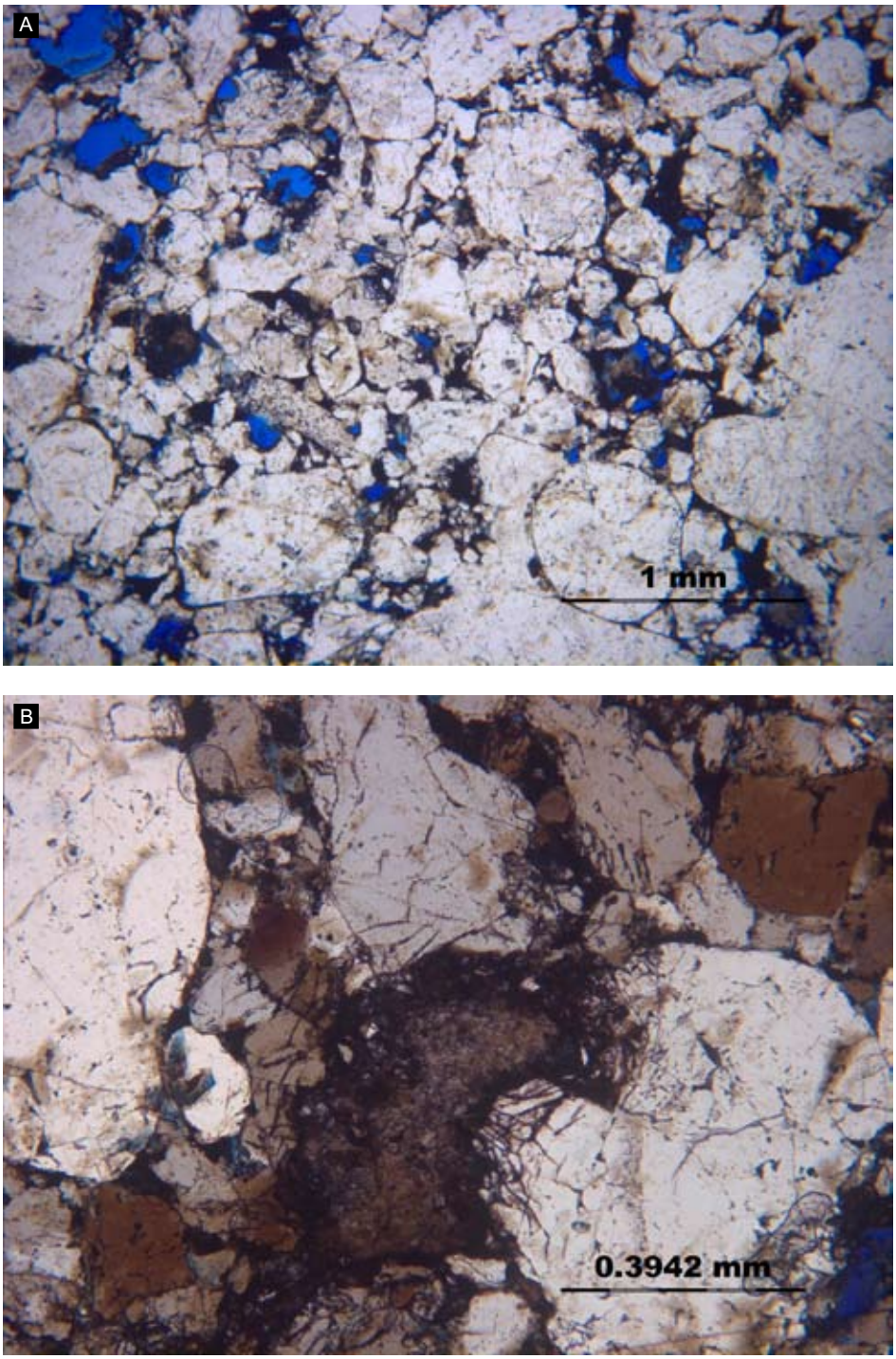

A. Sample T4
Coarse grained sandstone from Tabarka, Tunisia. Note rounded grains and intergranular porosity shown with blue staining.

B. Sample T4
Coarse grained sandstone from Tabarka, Tunisia. Note rounded grains and intergranular porosity shown with blue staining. There is some pressure dissolution between grain contacts and clay within pore spaces.

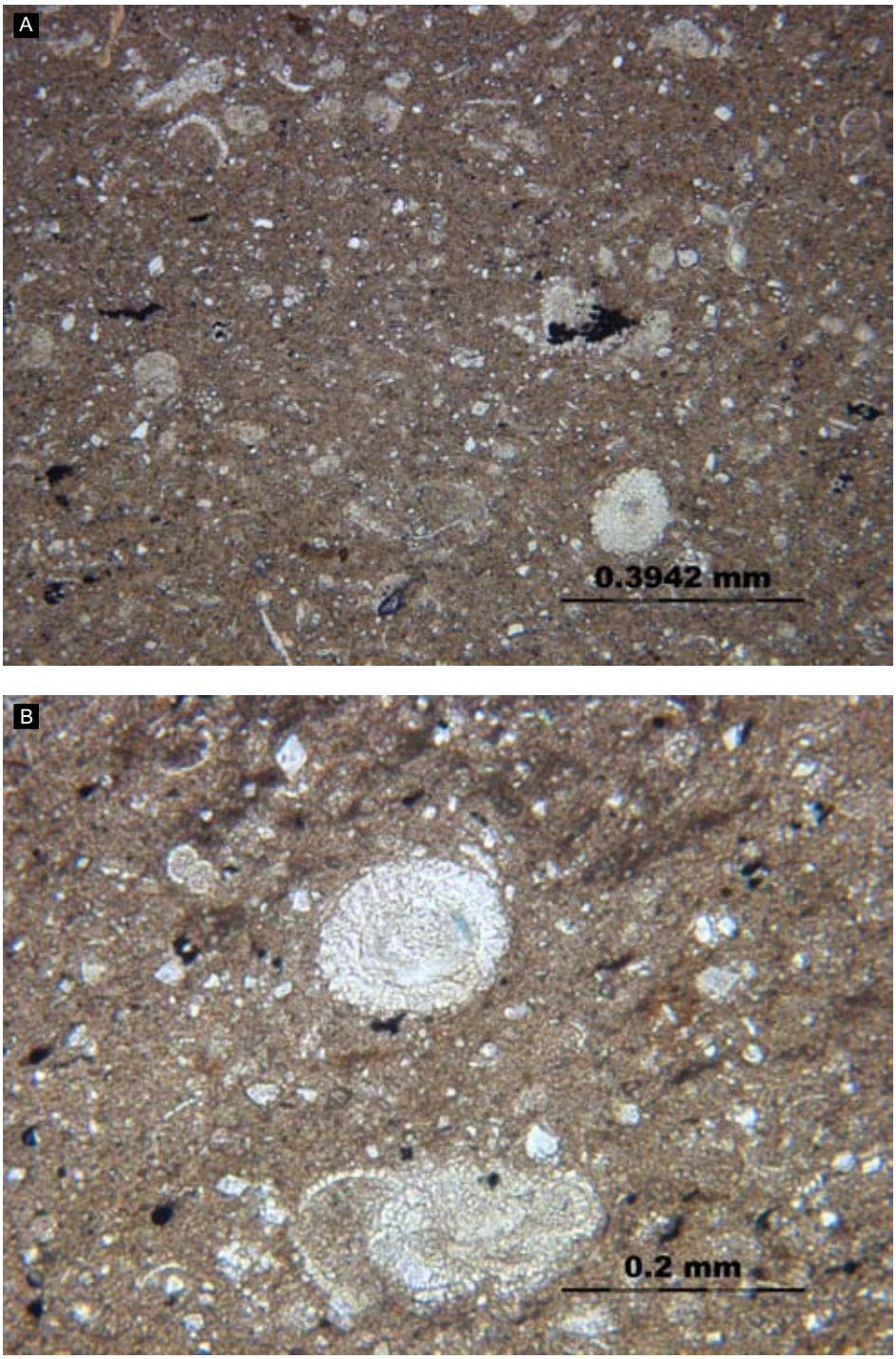

A. Sample Z1
Mudstone sample from Jebel el Gassa, Tunisia. Sample contains abundant foraminifera and small quartz grains.

B. Sample Z1
Mudstone sample from Jebel el Gassa, Tunisia. Agglutinated foraminifera and small quartz grains are present.

Appendix 9.

Lithofacies quantification

The calculated percentages from each major study area based upon bed numbers and not bed thickness. The lithofacies presented correspond to those used in chapter 3.

	FA-1a	FA-1b	FA-2a	FA-2b	FA-2c (<1 m)	FA-2c (>1 m)	FA-2d	FA-3a	FA-3b	Total values
Mt. Salici (mid subdivision-Lobes)	0	0	14	14	81	11	0	420	11	**551**
%	0.00	0.00	2.54	2.54	14.70	2.00	0.00	76.23	2.00	**100.00**
Mt.Salici (upp subdivision)	0	18	10	68	63	6	0	75	0	
Mt.Pellegrino (upp subdivision)	0	18	1	60	36	0	20	33	0	
CLTZ total	0	36	11	128	99	6	20	108	0	**408**
%	0.00	8.82	2.70	31.37	24.26	1.47	4.90	26.47	0.00	**100.00**
Karsa section	0	0	0	0	89	10	0	64	0	
Pollina river section	0	0	1	0	24	15	0	30	0	
Midfan total	0	0	1	0	113	25	0	94	0	**233.00**
%	0.00	0.00	0.43	0.00	48.50	10.73	0.00	40.34	0.00	**100.00**
Cr-2	0	0	3	0	10	3	0	24	0	
Cr-8 (log 1)	0	0	0	0	9	5	0	5	0	
Cr-8 (log 2)	0	0	0	0	12	5	0	3	0	
Cr-9	0	0	1	5	21	2	0	21	0	
Cr-1 (log 1)	0	4	0	7	6	2	0	3	0	
Cr-1 (log 2)	0	3	0	6	9	2	0	11	0	
Cr-5	18	15	0	4	52	18	0	6	0	
Cr-3	5	7	0	12	20	7	0	19	0	
Channel system total	23	29	4	34	139	44	0	92	0	**365.00**
%	6.30	7.95	1.10	9.32	38.08	12.05	0.00	25.21	0.00	**100.00**

	Bouma total	Ta	Tb	Tc	Td	Te
Mt. Salici (mid subdivision-Lobes)	420	356	51	40	6	15
%	% of total	84.76	12.14	9.52	1.43	3.57
Mt.Salici (upp subdivision)						
Mt.Pellegrino (upp subdivision)						
CLTZ total	108	63	14	1	0	0
%	% of total	58.33	12.96	0.93	0.00	0.00
Karsa section						
Pollina river section						
Midfan total	94	48	10	6	0	0
%	% of total	16	17	15	0	9
Cr-2	92	23	3	3	0	0
Cr-8 (log 1)		5	0	0	0	0
Cr-8 (log 2)		3	0	0	0	0
Cr-9		12	9	1	0	0
Cr-1 (log 1)		3	0	0	0	0
Cr-1 (log 2)		0	7	4	0	0
Cr-5		3	0	3	0	0
Cr-3		19	8	0	0	0
Channel system total		68	27	11	0	0
%	% of total	73.91	29.35	11.96	0.00	0.00

Appendix 10.

Geological map of northern Sicily. Redrawn from Wezel (1969)

The first attempt to map the Numidian Flysch Formation of northern Sicily, and published in a substantial work;

Wezel, F.C., 1969. Lineamenti Sedimentologico Del Flysch Numidico Della Sicilia Nord-Orientale. Memorie Degli Instituti Di Geologia e Mineralogia Del L'Universita Di Padova, 26.

This paper is difficult to obtain and the quality of reproduction is poor. It is therefore reproduced here for posterity.

Geological Map of the northern Nebrodi and Madonie mountains, Sicily.
Redrawn from F.C Wezel 1970 (mem, Soc, Geol, It, 9 (1970), 225-280.

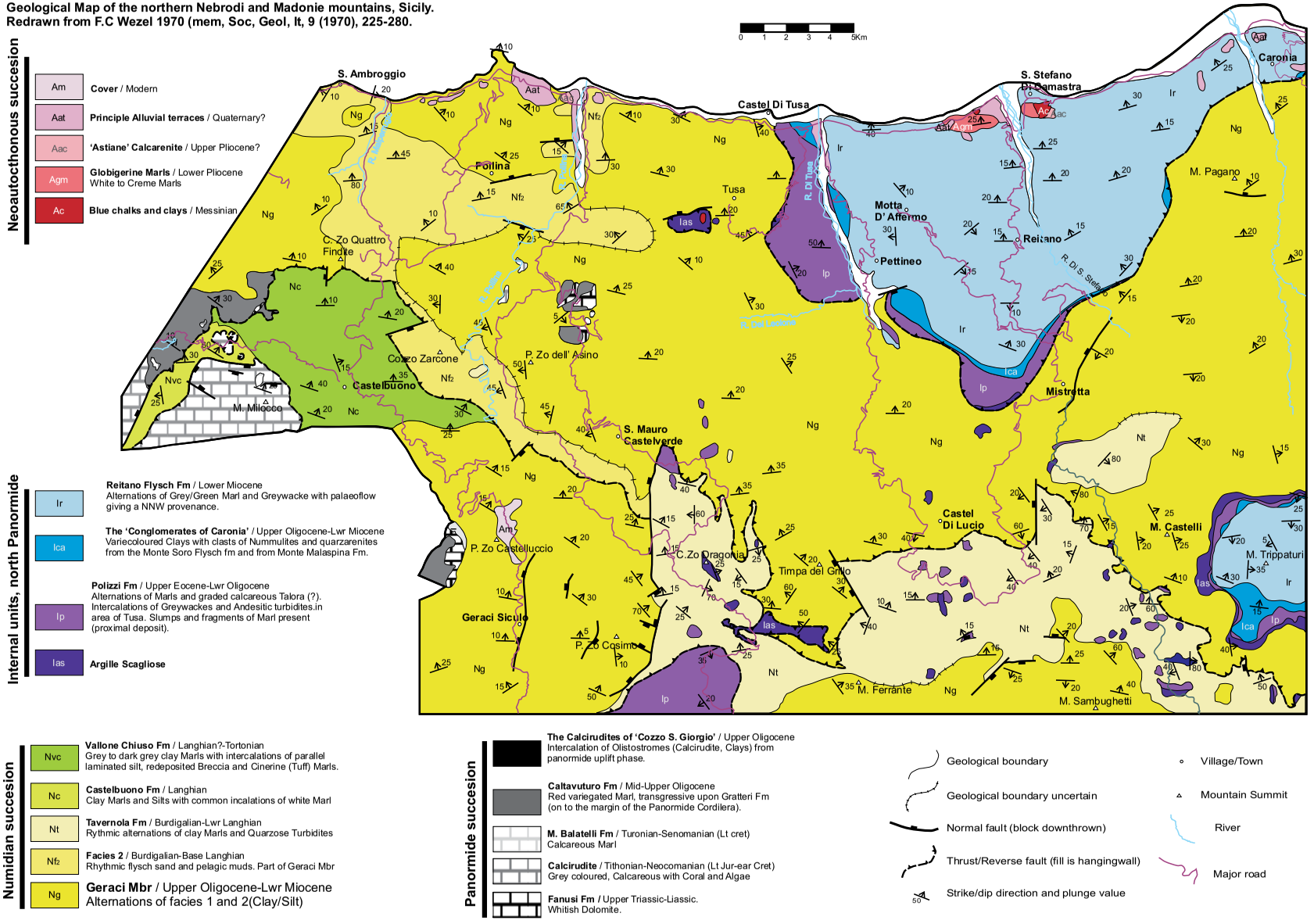

Appendix 11.

Geological maps of Sicily. Created for this study

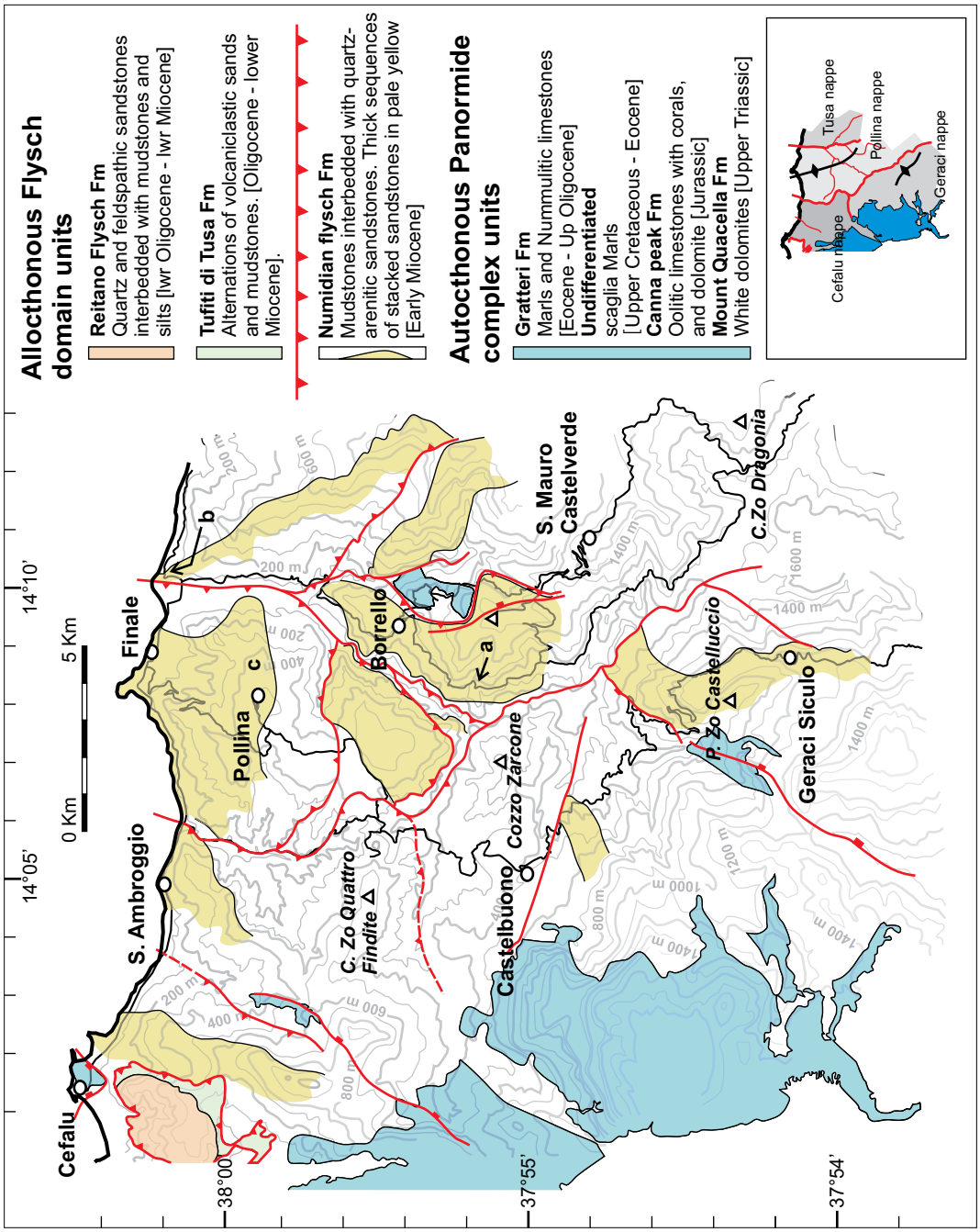

Geological map of northern Sicily

The area east of Cefalu was mapped for this study in order to better constrain the stratigraphy in light of poor biostratigraphic resolution. The results are presented here.

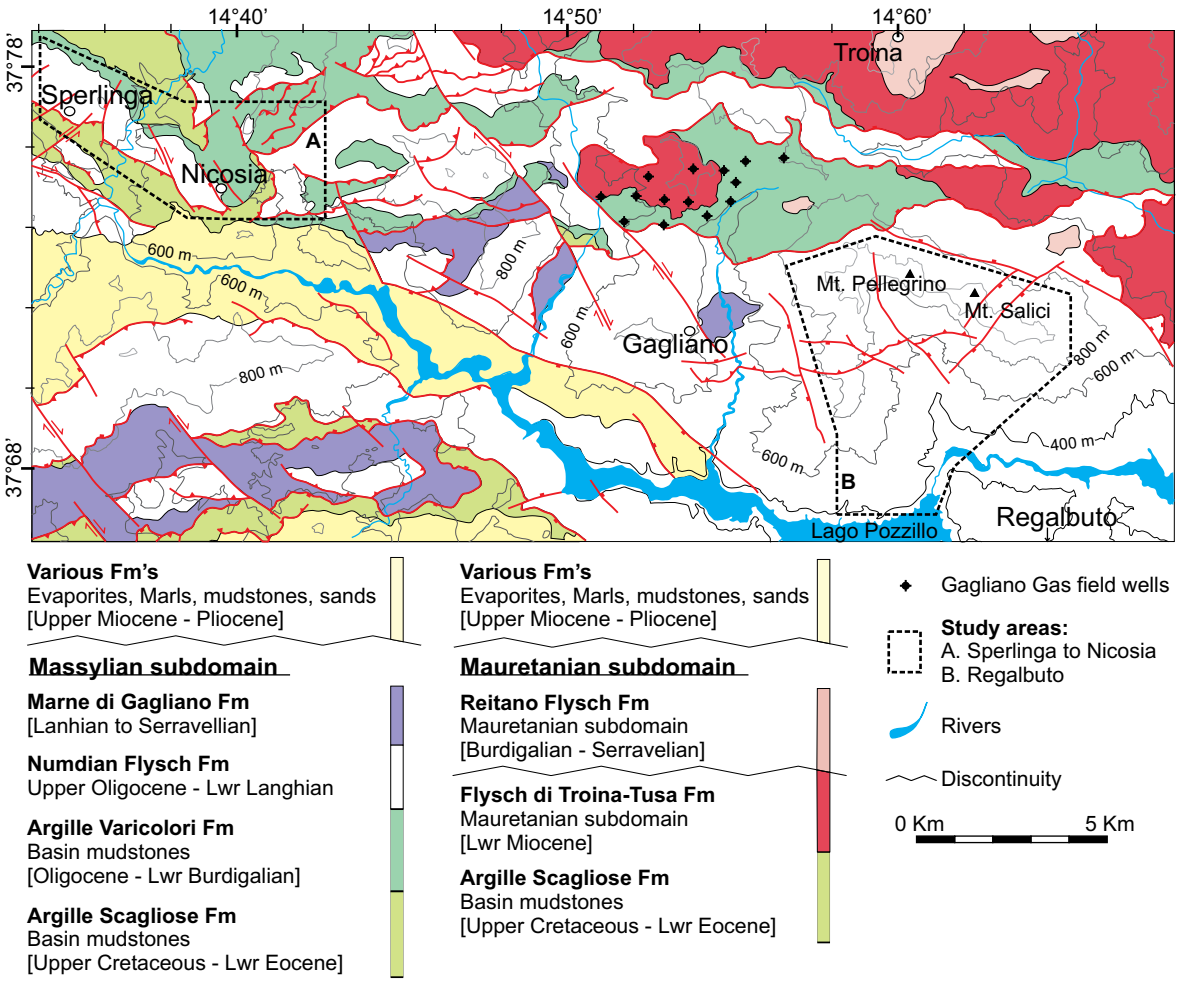

Geological map of central Sicily

Covering the study areas of Sperlinga, Contrada di Romano (area A) and Mt. Salici (Area B), this map is redrawn from Lentini et al. (1974).

Lentini, F., Vezzani, L., Carveni, P., Copat, B. and Grasso, M., 1974. Carta Geologica della Madonie (Sicilia Centro - Settentrionale) (1:50,000). Instituto di Geologia dell'Universitá di Catania.

Appendix 12.

An overview of Geraci Siculo, northern Sicily

Geraci Siculo is a small town which rests upon a ridgeline of Numidian Flysch Sandstones (see geological map of northern Sicily, Appendix 11). The section is of interest, but insufficient work was carried out to fully characterise the area within a chapter of this thesis. An overview section panoramic photograph, overlaid interpretation and sedimentary logs are therefore presented here.

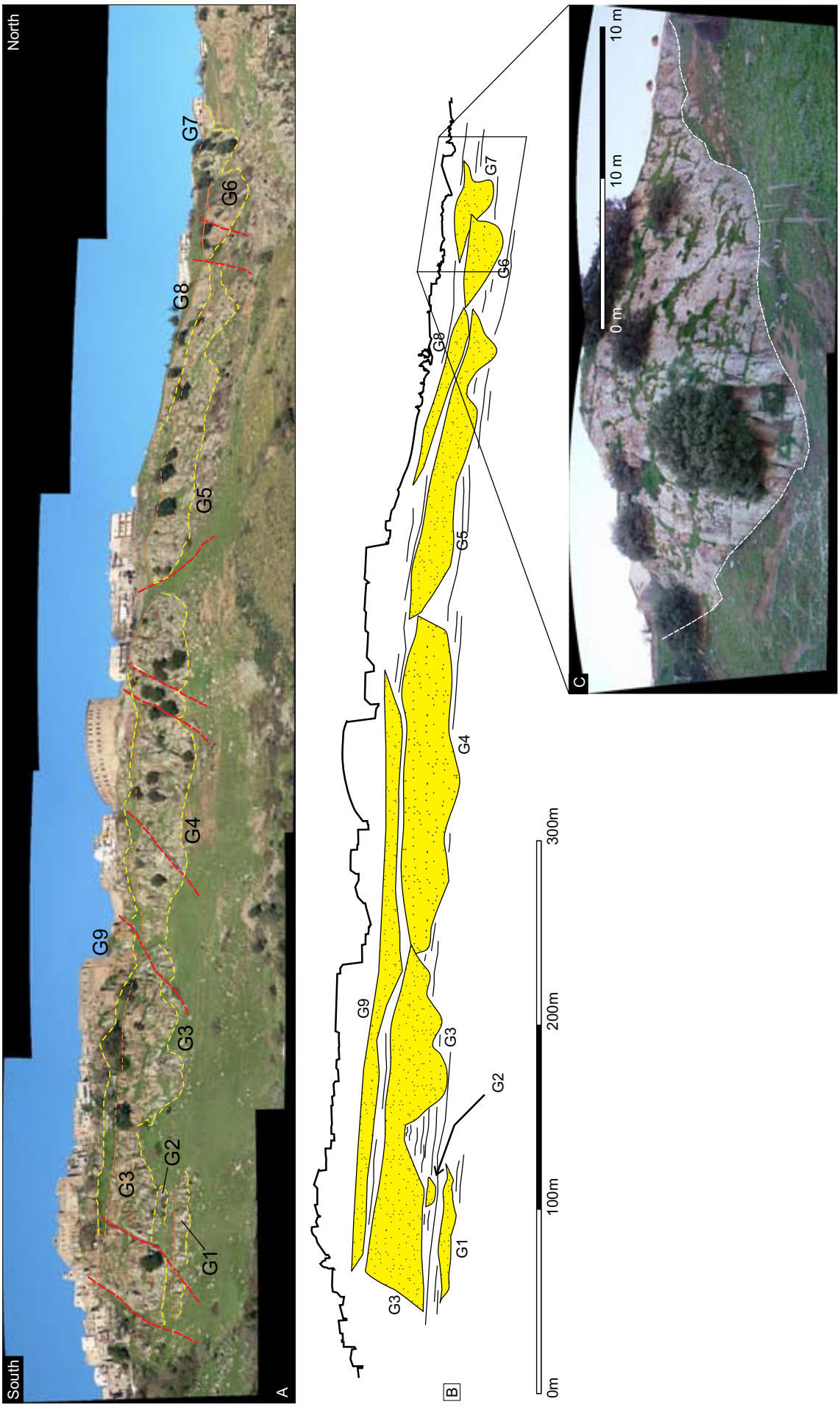
North
South
A
G1
G2
G3
G3
G9
G4
G5
G8
G6
G7
B
G1
G3
G2
G3
G9
G4
G5
G8
G6
G7
0m
100m
200m
300m
C
0 m
10 m
10 m

Previous page

A. Photographic pan of the Geraci Siculo ridgeline with major sandstone packages highlighted. Major channel forms are labelled G1 to G9. B. Interpretation of the Geraci Siculo ridgeline based upon the photographic panorama. A mutli-storey channel system is interpreted consisting of channels with a very high aspect ratio. Note geometries (e.g G3 and G5) with very high relief of the basal erosion surface which suggest lateral amalgamation of seperate channel forms. C. An image of channelform G7.

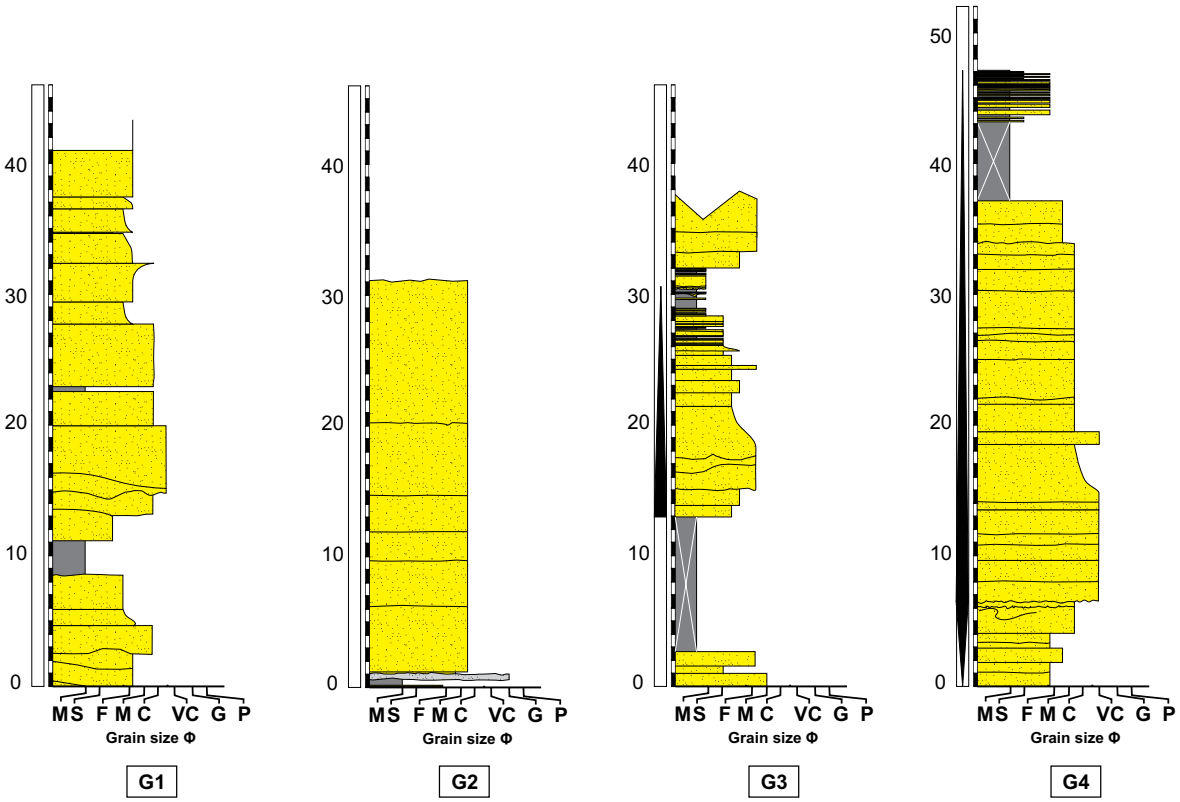

Sedimentary logs from the Geraci Siculo ridgeline

Sedimentary logs through channelforms G1 to G4. Massive sandstones (FA-2c according to the lithofacies scheme of chapter 3, this thesis) are the dominant lithofacies. Normally graded turbidites are relativley rare but are observed within the margins of the channel forms (e.g log G3).

Brief summary

The section has not been fully characterised, however the geometries observed bear some similarities to modern gullies which occur at the shelf break along the eastern seaboard of the United States. This is highlighted as a possible interpretation, however more work is required to confirm or dispute this idea.

Appendix 13.

Mt. Pellegrino sedimentary log

This log shows the upper subdivision of the Mt. Salici section in central Sicily (an interpreted channel lobe transition zone). The section is laterally equivalent to that shown in chapter 3 of this thesis (figure 3.12 and 3.15) and it is likely that the mudstone section at 17 m height (this log) is equivalent to the mudstone section at 607 m in figure 3.15a.

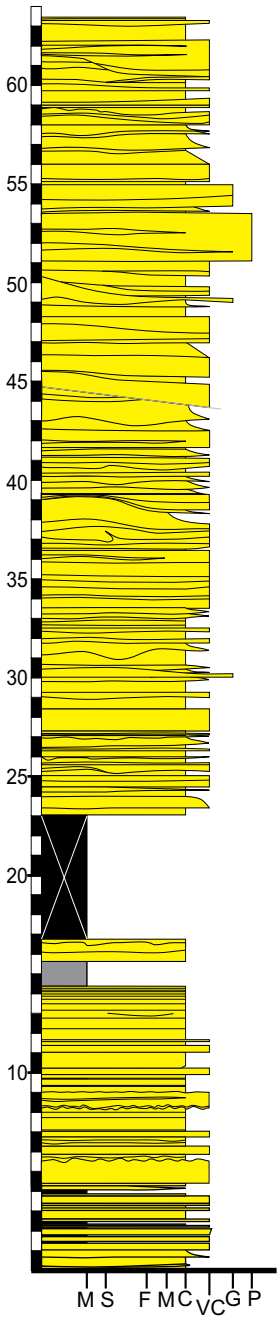
60
55
50
45
40
35
30
25
20
10
M S
F M C
VC
G P

Appendix 14.

Karsa section bed thickness graph

This graph plots bed thickness against sequential bed number. Fining and thinning upwards trends are interpreted within the Karsa section (chapter 3) and this graph demonstrates upwards bed thinning motifs. The section covered in this figure is the same as shown in Figure 3.9c (chapter 3).

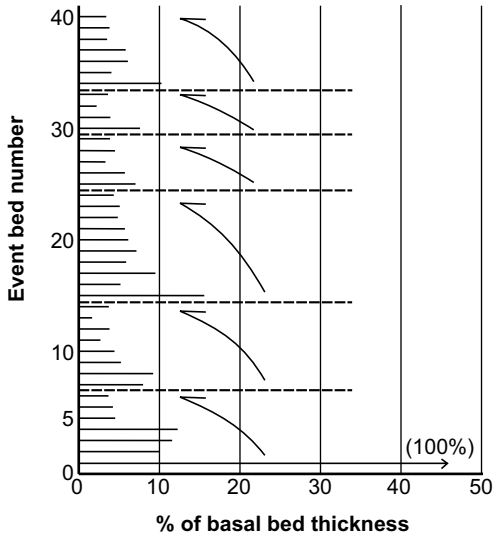
Event bed number
40
30
20
10
5
0
0
10
20
30
40
50
(100%)
% of basal bed thickness